Integrating Traditional and Close Range Photogrammetric Bathymetric Reconstructions to Enhance Predictions of Fish Abundance and Distribution on the NSW Coast

Thesis submitted in fulfillment of the requirements for the degree of Doctor of Philosophy

School of Life and Environmental Sciences
Faculty of Science
The University of Sydney

Daniel Richard Pygas

September 2023

Acknowledgments

This thesis was possible due to the substantial previous efforts undertaken by the NSW DPI (Fisheries), the former Office of Environment and Heritage (OEH), National Parks and Wildlife Service (NPWS) and Australian Field Robotics Centre and The University of Sydney. Thanks go to Tim Ingleton, Melanie Coleman, Hamish Malcomb, David Haristi, Nader Boutros, Lachlan Tooyey, Augustine Porter and numerous other researchers for collecting, processing and sharing the datasets included in this thesis and providing invaluable advice regarding its use.

Special thanks to my supervisors; Dr. Will Figueira and Dr Renata Ferrari for their time, guidance, and patience. Most importantly for taking a chance and allowing me to embark on this work.

Bathymetric data used in Chapters 3, 4 and 5 was also partly sourced Australia's Integrated Marine Observing System (IMOS) – IMOS is enabled by the National Collaborative Research Infrastructure Strategy (NCRIS). It is operated by a consortium of institutions as an unincorporated joint venture, with the University of Tasmania as Lead Agent.

Attribution

Chapter 2 of this thesis is published as: Pygas, D. R., Ferrari, R., & Figueira, W. F. (2020). Review and meta-analysis of the importance of remotely sensed habitat structural complexity in marine ecology. *Estuarine, Coastal and Shelf Science*, 235. https://doi.org/10.1016/j.ecss.2019.106468. I designed the study, analysed the data and wrote the drafts of the manuscript.

Abstract

The physical structure of marine habitat is a key determinant of the distribution and abundance of marine biota. Physical structure mediates key abiotic and biotic resources, environmental gradients and ecological processes that together determine habitat suitability at local and broad spatial scales. Metrics of habitat structural complexity (structural complexity) provide surrogates of these otherwise often difficult and expensive to measure components of habitat suitability. These metrics are used widely in marine ecology to explore and model the mechanisms underpinning observed distributions and abundance. 'Traditional' methods of deriving bathymetric reconstructions (e.g., multibeam echosounder and optical techniques) currently allow the capture of bathymetric reconstructions and derivation of such metrics over spatial extents far greater than initial *in-situ* methods. Associated model predictions of species distributions and abundance are used to inform marine spatial planning, management and conservation.

Photogrammetry, or structure from motion, is a more recent method used to create bathymetric reconstructions from overlapping imagery. Photogrammetry represents several potential improvements over traditional bathymetric reconstruction methods, including much finer resolutions, a more realistic 3D mesh surface, and derivation of novel mesh-based metrics. However, the greater cost of collecting photogrammetric compared to traditional bathymetric reconstruction data requires careful consideration be given to its implementation, and whether the purported benefits to marine research are worth the additional cost. \.The primary aim of this thesis is to objectively assess the potential for photogrammetry to improve predictions of marine biota abundance and distribution. This is achieved in **Chapter 2** through a quantitative literature review of previous studies to identify key metrics of structural complexity and key considerations when deriving these metrics. The adoption of photogrammetric metrics also adds to an ever-expanding suite of metrics available to marine researchers, which is rationalised in **Chapter 3** through a systematic exploration of correlations and relationships among metrics. The resulting predictor dataset is used in **Chapter 4** to identify which fish species and trophic-mobility groups traditionally and / or photogrammetrically derived metrics provide the best performing predictors. Finally, **Chapter 5** evaluates a method of achieving some of the improved performance of otherwise local-scale photogrammetric metrics over broad-spatial scales typical of traditionally derived metrics.

To my knowledge this thesis undertakes the most comprehensive comparison of the relative performance of traditionally (resolution 5 m to 240 m) and close range

photogrammetric (resolution 0.03 m to 2.4 m) derived metrics of structural complexity when modelling and predicting the distribution and abundance of fish on the eastern coastline of Australia (total 791 km^2 across Solitary Islands, Port Stephens and Batemans Bay). It describes solutions to key emerging methodological challenges associated with integrating local-extent (625 m^2) photogrammetric data with the broad-extent (100s km^2) data requirements of marine spatial prioritisation. It also advances marine ecological research by identifying species and groups of fish for which photogrammetric metrics are particularly important, less important, and those for which the combination of photogrammetric and traditional methods provide the best outcomes. Collectively, these findings greatly advance the understanding of structural complexity, its role in marine ecology, and how researchers and managers can use this knowledge to benefit future marine research, management and conservation.

First, **Chapter 2** reviews the latest research on the use of traditional bathymetric reconstructions and metrics used to predict marine biota worldwide. The quantitative meta-analysis identified the relative performance of common metrics and indicated the most well-known of which, such as surface-rugosity, may not always be the best performing. Importantly, the key requirement of including multiple resolutions and spatial extents when deriving metrics was identified, along with several other considerations key to the effective use of these metrics in marine ecological research. **Section 3** explores the relationships between metrics derived from three types of bathymetric reconstructions commonly used in the scientific literature. This systematic examination reduced a dataset of over 2,000 predictors to one of less than 100 predictors, whilst simultaneously maximising the information on structural complexity captured. Three discrete groups of structural complexity were also identified, capturing gross-complexing (a measure of total complexity present), orientation (related to the direction a surface is facing) and curvature (capturing discrete features such as ridges, valleys and other concave and convex surfaces). The relative sensitivity of these metrics to changing resolution and extent allowed further rationalisation of these large datasets. The substantial reduction in redundant information and time to derive such metrics provided a predictor dataset more appropriate to common statistical modelling techniques and far more suited to informing applied research and management.

The relative performance of metrics derived from traditional (multibeam and LIDAR) and photogrammetric bathymetric reconstructions was assessed in **Section 4**. Photogrammetric metrics contributed to the best performing final Generalized Additive Model (GAM) of abundance of 22 of the 35 fish species and 10 of the 15 trophic-mobility groups. On average,

combined photogrammetric and traditional metric models explained a third more of the variability in fish abundance compared to models based either method separately. The findings confirmed substantial synergism from combining traditional broad-scale and coarse-resolution and local-scale and fine-resolution photogrammetric metrics. However, the transfer of such benefits to broad-scale spatial prioritisation is hindered by the relative cost, per unit area, of photogrammetric data collection. **Section 5** describes and validates a novel method of mitigating this hinderance. Broad-extent photogrammetric metrics are extrapolated or 'engineered' from metrics derived from traditional bathymetric reconstructions and their performance evaluated using a fish dataset independent from Chapter 4. Of the 50 fish species and groups considered, the variance of 26 was explained best by species distribution models (SDMs) based solely or partly on these engineered metrics. This method offers potential for enhancing predictive models of species distributions using photogrammetric metrics over the broad spatial extents required for marine spatial planning and conservation.

Overall, these findings help confirm the purported benefits to marine research, management and conservation associated with photogrammetry and derived metrics. Photogrammetric metrics would likely improve predictions of the distribution and abundance of most fish, and most likely other marine biota, in southeastern Australia and worldwide. The use of engineered metrics would also allow greater model performance and prediction to be translated to broad-extents required by marine spatial prioritisation and management. The combined results of **Sections 4** and **5** also further confirm previous findings on the response of fish to structural complexity, reinforcing the importance of traditional metrics for planktivores and of photogrammetric metrics for predators. Planktivores respond more strongly to variability in larger components of structural complexity apparently linked with its influence on visibility of approaching piscivores. Bottom dwelling predators respond more to variability in finer resolution structural complexity, likely related to its ability to capture prey benthic abundance and availability of refuge from piscivores. Importantly also, these findings indicate that while photogrammetric metrics often provide better model performance, for some fish species and groups, traditional metrics are more important. Future studies should seek to combine these methods wherever possible and avoid reliance on either method in isolation. Overall, these findings substantially advance the field of remote sensing of marine environments and ecosystems, spatial science and marine ecology at local (100s m^2) to broad (100s km^2) spatial extents.

Contents

1 Chapter 1 - General Introduction 15

1.1 Habitat Structural Complexity 15

1.2 Measuring Habitat Structural Complexity and its Influence on Marine Biota 17

1.2.1 In-Situ Studies 17

1.2.2 Traditional Remote Sensing 18

1.2.3 Photogrammetry 20

1.3 Thesis Aims 23

1.4 Data Chapter Structure 26

1.4.1 Chapter 2 26

1.4.2 Chapter 3 27

1.4.3 Chapter 4 27

1.4.4 Chapter 5 28

1.5 Study Area 28

1.6 Appendices 34

2 Chapter 2 - Review and Meta-analysis of the Importance of Remotely Sensed Habitat Structural Complexity in Marine Ecology 36

2.1 Summary 36

2.2 Introduction 37

2.3 Methods 38

2.3.1 Study Selection 38

2.3.2 Measures of Complexity 38

2.3.3 Study Focus and Broad Performance 38

2.3.4 Predictor Performance 40

2.4 Results 41

2.4.1 Study Focus and Broad Performance 41

2.4.2 Predictor Performance 44

2.5 Discussion 47

2.5.1 Predictor Performance 47

2.5.2 Why are measures of complexity often-poor predictors? 53

2.6 Conclusion 63

3 Chapter 3 - Optimising the Derivation of Habitat Structural Complexity Metrics from Rock reef Environments 67

3.1 Summary 67

3.2 Introduction 68
3.3 Methods 70
3.3.1 Approach 70
3.3.2 Bathymetry Reconstructions 71
3.3.3 Metrics of Structural Complexity 75
3.3.4 Correlations among Metrics 79
3.3.5 Role of Extent and Resolutions 80
3.4 Results 82
3.4.1 MBLI Raster 82
3.4.2 AUV Raster 89
3.4.3 AUV Mesh 93
3.5 Discussion 97
3.5.1 Relationships Among Metrics 97
3.5.2 Spatial Scale 102
3.6 Conclusion 103
4 Chapter 4 - Synergism of Photogrammetric and Traditional Remote Sensing in Predicting Fish Abundance 106
4.1 Summary 106
4.2 Introduction 107
4.3 Methods 110
4.3.1 Study Area 110
4.3.2 Bathymetric Data 110
4.3.3 Fish Data 111
4.3.4 Data Analysis 113
4.4 Results 117
4.4.1 Model Performance 117
4.4.2 Fish-Structural Complexity Relationships 122
4.5 Discussion 127
4.5.1 Metric and Dataset Performance 127
4.5.2 Behavioral and Ecological Linkages 129
4.5.3 Planning and Management Considerations 132
4.6 Conclusion 136
4.7 Appendices 137

5 Chapter 5 - Bridging the Gap Between Photogrammetry and Traditional Remote Sensing Methods to Improve Predictions of Fish Distributions 143

5.1 Summary 143

5.2 Introduction 144

5.3 Methods 146

5.3.1 Approach 146

5.3.2 Study Area 146

5.3.3 Bathymetry and Benthic Cover Data 148

5.3.4 Fish Data 149

5.3.5 Statistical Methods 150

5.4 Results 154

5.4.1 Predictor Engineering 154

5.4.2 Species Distribution Models 154

5.5 Discussion 168

5.5.1 Predictor Engineering 168

5.5.2 Engineered Predictor Performance 170

5.5.3 Patterns in Fish Responses 171

5.5.4 Fish Distributions 173

5.6 Conclusion 174

5.7 Appendices 176

6 Chapter 6 - Overall Discussion 185

6.1 Summary of Findings 185

6.2 Quantifying structural complexity 186

6.3 Performance of Traditional vs Photogrammetry Methods 190

6.4 Fish responses to structural complexity 190

6.5 Limitations and Further Research 197

6.6 Conclusions and Recommendations 198

7 References 202

Tables

Table 1-1 Summary of main differences between traditional and photogrammetric methods of deriving metrics of structural complexity..... 23

Table 2-1 Measures of habitat structural complexity and other associated environmental variables used as predictors of the distribution of marine biota in remote sensing studies included in Section 2. 39
Table 2-2 Approaches to deriving metrics of complexity from DEMs 58
Table 2-3 Findings of studies with an a-priori aim of investigating the role of spatial scale (i.e., resolution or spatial extent) on the modelling of the distribution of marine biota using measures of habitat structural complexity. See Table 2-1 for explanation of predictors (measures of complexity). 60
Table 3-1 Metrics of structural complexity derived from raster-based datasets. Mean and SD calculated for each raster-based metric. For further detail see text. 76
Table 3-2 Metrics of structural complexity derived from the mesh-based dataset. For further detail see text. 77
Table 3-3 Resolutions and extents over which each metric was derived. Numbers in cells indicate the number of metrics derived at that resolution and extent. Blank cells indicate extent x resolution combinations for which metrics were not derived (when resolutions ≥ 10 m were not an even number multiple of the extent). 78
Table 3-4 Summary of metric correlations and identity of those metrics that are retained. Coloured shading indicates groups of correlated metrics identified when resolution and extent are considered. Purple and yellow shading represents the AspEast and complexity groupings, respectively. Blank cells indicate where a metric was not retained. 85
Table 3-5 Final models of MBLI Raster metrics identifying the number and identity of uniquely important resolutions and extents required to explain the optimal proportion of variability in metric values. For each metric, the optimal number of resolutions / extents is equal to those identified by the model terms plus one, where the additional resolution/extent may be any of those not included in the model terms. Res – resolution and Ext = extent over which metrics were derived (m). 86
Table 3-6 Summary of AUV Raster metric correlations and identity of those metrics that are retained (Yes). Green shading indicates the '*curvature grouping*' and blue / red the '*complexity grouping*' (albeit not all pairs of metrics within the 'complexity grouping' were directly highly correlated). Blank cells indicate where a metric was not retained. 91
Table 3-7 Final models of AUV Raster metrics identifying important resolutions required to explain the greatest proportion of variability in metric values. Res – resolution over which metrics were derived (m). 92
Table 3-8 Summary of metric correlations and identity of those metrics that are retained. Coloured shading indicates groups of correlated metrics identified when resolution and extent are considered. 95
Table 3-9 Final models of AUV Mesh metrics identifying the number and identity of uniquely important resolutions required to explain the optimal proportion of variability in metric values. For each metric, the optimal number of resolutions is equal to those identified by the model terms plus one, where the additional resolution may be any of those not included in the model terms. Res – resolution over which metrics were derived (m). .. 96
Table 4-1 Metrics of structural complexity retained for each dataset and used to model fish abundance. Metric values are the mean, except where standard deviation (Std) is identified. 112
Table 4-2 Number of predictors and models used per fish response. For the identity of the predictors see Table 4-1. Only predictors with correlation <0.28 r were included in potential models. 114
Table 4-3 Best performing models of fish species / trophic-mobility groups for each dataset and dataset combination indicating the predictor and the resolution (Res.) and extent (window length) (Ext.) over which it was derived. Species targeted (T) by recreational /

commercial fishers or of conservation significance (C) also included. Results for all species and groups are provided in Appendix 3-3. 123
Table 4-4 Identify of the dataset(s) that would provide the best quality model (identified using AICc) and the greatest predictive performance (identified using dev. Exp.) for each species and group. dataset providing greater predictive performance only identified if this was greater than the best quality model. 135
Table 5-1 Metrics (mean value, unless identified as standard deviation = std) of structural complexity and benthic cover included in this study. AUV metrics and benthic cover quantified at an extent of approximately 625 m^2 and MBLI metrics at 900 m^2. Resolution (m) = Res. (m). Native resolution of mesh = 0.03 m to 0.07 m (ResNative). 148
Table 5-2 Brief descriptions of the machine learning methods used to model and predict engineered structural complexity predictors. 151
Table 6-1 Summary of best models identified for each fish species and groups in Sections 4 and / or 5. The overall response indicates if model performance was best using only MBLI Raster (Obligate MBLI), photogrammetric (AUV Mesh and / or AUV Raster) (Obligate AUV), combined MBLI Raster and photogrammetric (combined) in each Chapter (Combined), combined in Section 4 and either MBLI Raster (Facultative MBLI) or photogrammetric (Facultative AUV) in Section 5, or using MBLI Raster in one chapter but photogrammetric in the other (Divergent). 191
Table 6-2 Summary of the form of responses of fish species and groups to metrics of structural complexity in Sections 4 and 5. Only species and groups that provided the best performing models and that were examined in detail in each chapter are presented. Responses consist of preference for positive (Pos.), negative (Neg.), intermediate (Int.) and extreme (Ext.) values of the metric. 193

Figures

Figure 1-1 Summary of thesis background, structure, key data and the associated key questions and outcomes examined by each data chapter. 25
Figure 1-2 a) Overview of the three study locations: b) Solitary Islands, c) Port Stephens and d) Batemans Bay on the New South Wales Coastline on the east coast of Australia. Circles represent availability of photogrammetric, benthic biota or fish data. 30
Figure 1-3 Study sites near a) South Solitary Island to Split Solitary Island and b) Offshore Bundageree Head in the Solitary Islands 31
Figure 1-4 Study sites near a) Broughton Island and b) Shark Island in the Port Stephens 32
Figure 1-5 Study sites near a) Bawley Point to South Durras, b) Lilli Pilli to Burrewarra Point and c) Congo to Potato Point in Batemans Bay 33
Figure 2-1 Biotic group focus of remote sensing studies that examine the role of habitat structural complexity. Corals include deep/cold water (7 studies) and tropical (1 study) taxa. 42
Figure 2-2 Model performance (mean% deviance / variance explained ± SE) a) among biota groups and b) among response levels. Numbers outside and inside parenthesis indicate number of studies and number of models, respectively. Different letters indicate significant differences at $P < 0.001$. Mobile inverts and benthic infauna were not modelled due to small sample size. 43
Figure 2-3 Use of measures of complexity and other predictors among taxonomic group. See Table 2-1 for explanation of measures of complexity. 44
Figure 2-4 Mean standardised rank scores ($Rs_{1\text{-}10}$) (±SE) for predictors for models a) all taxa, b) fish and c) sessile invertebrates. Numbers outside and inside parenthesis indicate number

of studies and number of models, respectively. See Table 2-1 for explanation of measures of complexity. 45
Figure 2-5 Relationship type (positive, negative, otherwise significant (e.g., significant non-linear relationship or directionality not applicable) and non-significant) reported between predictors and various response variables when a) all models are combined and for models of b) fish and c) sessile invertebrates. Directionality not applicable for orientation, other complexity, geographic, habitat, backscatter and management. See Table 2-1 for explanation of measures of complexity. 46
Figure 2-6 The complexity of each of these habitats (a to d) measured using rugosity would be the same, however, they differ in other aspects of complexity including diversity (i.e., a vs c) and spatial arrangement (b vs d) of elements. 57
Figure 3-1 Graphical representation of the three datasets and derived metrics / predictors. For AUV Mesh, the native resolution was the default range of triangle side length (0.03 m to 0.07 m) output from the mesh generation workflow. When converting AUV Mesh to AUV Raster, the finest AUV Raster resolution was set at 0.1 m to ensure creation of a contiguous raster with no missing data. 72
Figure 3-2 Process of deriving AUV Mesh, AUV Raster and benthic cover metrics and predictors from the AUV surveys 73
Figure 3-3 Correlations among MBLI metrics when partitioned among extents and resolutions. Red and blue shading indicates negative and positive correlation, respectively, and the numbers inside the shading the Pearson's correlation coefficient r. 83
Figure 3-4 Correlation (r) values (y axis) calculated between pairs of MBLI metrics when extent and resolution (cell side length) was considered. Colours indicate resolutions and x axis the extents. Dots indicate the correlation r value between the metrics for each extent and resolution combination and the lines the fitted locally weighted running line smoother (LOESS). 84
Figure 3-5 Frequency of uniquely important resolutions and extents identified for MBLI metrics .. 87
Figure 3-6 Mean values of metrics derived at a) resolutions and b) extents. Solid red circles indicate the uniquely important resolutions / extents identified by selected parsimonious models. Open red circles indicate the resolution / extent selected to represent all remaining non-uniquely important metrics. Note, only 10 extents were included in the modelling..... 88
Figure 3-7 Correlations among AUV Raster metrics when partitioned among resolutions. Red and blue shading indicates negative and positive correlation, respectively, and the numbers inside the shading the Pearson's correlation coefficient r. 90
Figure 3-8 Frequency of uniquely important resolutions and extents identified for AUV Raster metrics. 92
Figure 3-9 Mean values of AUV Raster metrics derived at each resolution. Solid red circles indicate the uniquely important resolutions identified by selected parsimonious models. Open red circles indicate the resolution selected to represent all remaining non-uniquely important metrics. 93
Figure 3-10 Correlations among AUV Mesh metrics a) for all metrics at native resolution and b) for those metrics derived over multiple resolutions. Red and blue shading indicates negative and positive correlation, respectively, and the numbers inside the shading the Pearson's correlation coefficient r. 94
Figure 3-11 Frequency of uniquely important resolutions and extents identified for AUV Mesh metrics. 96
Figure 3-12 Mean values of AUV Raster metrics derived at each resolution. Solid red circles indicate the uniquely important resolutions identified by selected parsimonious models. Open red circles indicate the resolution selected to represent all remaining non-uniquely important metrics. 96

Figure 3-13 Important extents (orange shading) and resolutions (blue shading) identified for each of the MBLI Raster metrics retained (bold type with correlated metrics in brackets) following examination of correlations (green shading indicates important extend and resolution at that scale). 104
Figure 3-14 Important resolutions (blue shading) identified for each of the AUV Raster metrics retained (bold type with correlated metrics in brackets) following examination of correlations. 105
Figure 3-15 Important resolutions (blue shading) identified for each of the AUV Mesh metrics retained (bold type with correlated metrics in brackets) following examination of correlations. 105
Figure 4-1 Metric performance based on relative importance. Results are averaged across all extents and resolutions considered for each metric (see Table 4-1) Symbol colours indicate the source of each metric. Bathymetry was sourced from MBLI Raster but was considered separately. 118
Figure 4-2 Relative importance of datasets in modelling fish species and functional group abundance determined a) by the rate (numbers above bars indicate number of models) final models were retained in favour of the null model (random effect of location) and b) by the average deviance explained by final models aggregated across all species / groups. 118
Figure 4-3 Deviance explained by the best performing model for each dataset (selected using AICc) for fish species and trophic-mobility groups relative to that explained by MBLI Raster. For full final model results see Appendix 4-3. Note that the overall best performing model select using AICc and considering the parsimony principle did not always explain the greatest deviance. Negative and positive x axis labels indicate smaller or greater, respectively, deviance explained by dataset and dataset combinations relative to that explained by MBLI Raster alone. 120
Figure 4-4 Venn diagram identifying the source of predictors included in the overall best performing model of fish species and trophic-mobility group abundance based on model selection using AICc. 121
Figure 4-5 PCA based on deviance explained by best final models for each dataset and dataset combination. PCA axis based on deviance values transformed to sum to 1 for each species / groups and then centered. This accentuates relative differences in deviance explained between dataset(s) rather than absolute differences. 122
Figure 4-6 Partial dependance plots from best performing GAM models of fish species abundance identifying the marginal effect of the predictor on the response identified as the smooth (s) function of the predictor. Numbers associated with predictors refer to resolution (Res) and extent (Ext) over which the predictor was derived. Circles represent partial residuals coloured by location. Shaded area represents the standard error of the fitted function. 125
Figure 4-7 Partial dependance plots from best performing GAM models of fish species abundance identifying the marginal effect of the predictor on the response identified as the smooth (s) function of the predictor. Numbers associated with predictors refer to resolution (Res) and extent (Ext) over which the predictor was derived. Circles represent partial residuals coloured by location. Shaded area represents the standard error of the fitted function. 126
Figure 5-1 Flowchart displaying the key data, steps and outputs of the modelling undertaken in this chapter. 147
Figure 5-2 Proportion of variance explained (on x-axis) by a) ML models of AUV metrics (on y-axis) and b) GAM models of benthic cover (i.e., prevalence) (on y-axis) based on MBLI Raster predictors (colours-coded bars). For AspEast and AspNorth, the maximum contribution across the two resolutions considered is presented. 155

Figure 5-3 PCA plot based on the variance explained (Var. Exp.) by each set of predictors for fish species. PCA axis based on scaled and centered R2 values averaged across all train-test repeats. 156
Figure 5-4 PCA plot based on the variance explained (Var. Exp.) by each set of predictors for fish trophic-mobility groups. PCA axis based on scaled and centered R2 values averaged across all train-test repeats. 157
Figure 5-5 Model performance averaged across a) different sets of predictors and b) averaged across species / trophic-mobility groups and c) the difference in variance explained by engineered AUV Raster, AUV Mesh and benthic cover predictions relative to the variance explained by the MBLI Raster predictors. 158
Figure 5-6 Variance explained my ML models of fish a) species and b) trophic-mobility group abundance. Variance explained by models based on engineered (engin.) AUV Mesh, AUV Raster and Benthic Cover predictors and MBLI Raster & all engineered predictors expressed relative to the variance explained solely using MBLI Raster (green bars). Specie and groups ordered by top to bottom according to variance explained solely using MBLI Raster. 159
Figure 5-7 Species distribution models for a) Snapper and b) blackspot goatfish based on MBLI Raster predictors (top) and AUV Mesh (bottom) predictors. Model domain (MD) was the range of abundance values in the fish dataset. 162
Figure 5-8 Relative importance of predictors included in random forest models of fish abundance and associated partial dependance plots (PDPs) of the three most important metrics of complexity. Positive and minus signs indicate overall relationships with depth, easting and northing. 166
Figure 6-1 Major groups of structural complexity derived from raster-based DEMs. Orange and green shading indicate groups of correlated gross complexity and orientation metrics, respectively. Metrics indicated by * were not included in this thesis but were grouped according to (Wilson *et al.*, 2007a). 188

Glossary of Common Acronyms

Term	Definition
AIC	Akaike information criterion
AICc	Akaike information criterion corrected for small sample size
Australian Centre for Field Robotics	ACFR
AUV	Automated underwater vehicle
AUV Mesh	3-Dimensional (3D) Mesh based bathymetric reconstruction derived using photogrammetric structure from motion techniques
AUV Raster	Raster based bathymetric reconstruction derived from photogrammetry by converting the AUV Mesh surface to 2.5 D raster surface
Bathymetric Dataset	AUV Mesh, AUV Raster and / or MBLI Raster
BTM	Benthic Terrain Modeler
DEM	Digital elevation model, typical refers to raster based bathymetric reconstructions.
GAM	Generalised Additive Modeling
GLM	Generalised Linear Modeling
Gross complexity (also referred to as terrain variability)	A component of complexity consisting of the metrics surface-rugosity, slope, terrain-ruggedness, and the variability in these metrics and all metrics of curvature.
IMOS	Integrated Marine Observing System
LIDAR	Light Detection and Ranging
Linear-rugosity	2D measure of seafloor terrain variability typically measured *in-situ* by SCUBA diver using a chain and tape. May also be derived virtually from a mesh or raster bathymetric model. Calculated as the ratio of convoluted measure (chain) to the linear distance between start and finish (tape).
MBES	multibeam echo-sounding
MBLI Raster	Raster based 2.5 D bathymetric reconstruction derived from combining contiguous traditional multibeam echo-sounding and LIDAR surveys
ML	Machine Learning
MPA	Marine Protected Area
NSW	New South Wales
OEH	NSW Office of Environment and Heritage
PCA	Principal components analysis
PCR	Principal components regression
PLSR	Partial Least Squares Regression
Photogrammetric metrics	Metrics of structural complexity derived from AUV Mesh and AUV Raster
Terrain variability (also referred to as gross complexity)	A component of complexity consisting of the metrics surface-rugosity, slope, terrain-ruggedness, and the variability in these metrics and all metrics of curvature.
Traditional metrics	Metrics of structural complexity derived from MBLI Raster
SDM	Species Distribution Model
SfM	Structure from Motion
Surface Rugosity	3D measure of seafloor terrain variability calculated as the ration of the convoluted 3D surface area to 2D planar area.
TIN	Triangular irregular network

1 Chapter 1 - General Introduction

1.1 Habitat Structural Complexity

Habitat structural complexity (structural complexity) describes the physical three-dimensional abiotic and biotic surface with which organisms interact directly. It represents a place of attachment for sessile biota, refuge for mobile biota, and various biotic and environmental resources. In doing so, structural complexity mediates ecological mechanisms that shape the distribution and abundance of biota across seascapes. Structural complexity has been long acknowledged as a driver of biotic composition. Early studies have linked the response of birds (Macarthur & Macarthur, 1961; Roth, 1976), rodents (Rosenzweig & Winakur, 1969), insects (Murdoch *et al*., 1972) and lizards (Pianka, 1967) with measures of structural complexity. In their review terrestrial vegetation structure, (Davies & Asner, 2014) demonstrated how its vertical component (e.g., canopy cover, height) was a strong determinant of flying vertebrate, non-flying mammal, and invertebrate assemblages. Seventeen of 23 avian studies, 2 of 3 bat studies, all 8 non-flying mammal and all 8 invertebrate studies examined found a relationship between the biotic response (e.g., diversity and abundance) and structural complexity. Various explanatory mechanisms were suggested, including the role of canopy structure in providing niche space, influencing environmental variables such as temperature and solar radiation and influencing flying and hunting efficacy. Plant structural complexity may also influence arthropods via mediation of microclimate and volatile chemicals used by these organisms to locate their food (Randlkofer *et al*., 2010).

Structural complexity provides similar functional roles in marine as in terrestrial environments. The biogenic structure of coral reefs supports ecosystem biodiversity and productivity, as does tree structural complexity in terrestrial environments (Calders *et al*., 2020). Links between organisms and structural complexity are also expected to be stronger in marine than in terrestrial environments. Tokeshi & Arakaki, (2012) identified two characteristics of the marine environment that strengthen these relationships: the drag exerted on organisms by a water medium and the predominance of particle feeding generalists (suspension-feeders, deposit feeders, grazers of microalgae, etc.). The protection afforded by underwater physical structure would be particularly influential, directly affecting the degree of sheer stress and habitat suitability, biodiversity, and abundance of biota. The availability of suspended particulate food and the presence of biota would also be directly related to structural complexity and its mediating effect on local and broad-scale hydrodynamic flow. In the terrestrial environment, habitat choice is likely more strongly

associated with the presence of food, rather than physical structure and how this may influence food availability directly.

Fish studies undertaken on coral reefs represent most studies on the influence of structural complexity in the marine environment (Graham & Nash, 2013). Structural complexity exerts influence on fish (and other biota) by mediating predator-prey interactions and prey capture efficacy, niche space on complex reefs, the number and variety of refuges from predation, density-dependent competition, and limiting environmental variables such as strong currents (Almany, 2004a; Harman *et al*., 2003; Komyakova *et al*., 2013; Scharf *et al*., (2006). Other important pluralistic processes likely include selection of complex habitat by settling larvae, post settlement migration to complex habitats, and the active selection of complex habitat by juveniles and adults. Increased surface area in complex habitats also provides a greater number of shelter sites and area for attachment of prey invertebrates and algae (Luckhurst & Luckhurst, 1978). The influence of structural complexity is itself complex, and structural complexity may not always be positively correlated with fish community responses, including coral reef fish abundance (Mccormick, 1994). When included with other habitat-based predictor variables, such as coral cover, depth, or distance to shore, it may also not be the most powerful predictor (Brokovich *et al*., 2006; Newman *et al*., 2015). The relative importance of structural complexity may also vary with the life stage of fish and may influence the time of ontogenetic habitat shifts (Almany, 2004b).

Fewer studies have involved biota other than fish, though equality influential relationships with structural complexity and algae and invertebrates would be expected Margiotta *et al*., (2016) found a positive correlation between oyster shell structural complexity and the density of oyster sprat and the density and size of crabs. Structural complexity was also important for the settlement and habitat preferences of sponges, corals, and gastropods (Beck, 2000; Carleton & Sammarco, 1987; Russ, 1980). It is likely that sessile fauna responds, perhaps more strongly, to structural complexity via its influence on the availability of substratum for attachment and local hydrology (Bell & Barnes, 2000), the latter influencing seabed sheer stress and the availability of suspended food particles. In one of the few studies that examined fish and sessile invertebrates concurrently (Rees *et al*., 2014), only the later were found to be associated with structural complexity.

1.2 Measuring Habitat Structural Complexity and its Influence on Marine Biota

1.2.1 In-Situ Studies

Before structural complexity can be related to fish and other biota, it must first be quantified in the environment. Early observational marine studies quantified structural complexity *in-situ*, either qualitatively using visual assessment of the presence of flat sand, reef, boulders etc., visual scoring complexity using an ordinal categorical scale (Jennings *et al*., 1996) or otherwise quantitatively, most commonly by fitting a metal chain to the contours of the seafloor, known as the 'chain and tape' method (Brokovich *et al*., 2006; Harman *et al*., 2003; Luckhurst & Luckhurst, 1978; Mumby & Wabnitz, 2002; Risk, 1972). Though see other, less common quantitative methods of measuring structural complexity *in-situ* (Dustan *et al*., 2013; Lazarus & Belmaker, 2021 Nanami & Nishihira, 2002; Wilson *et al*., 2007b). The ratio of chain length to linear seabed distance provides a measure of complexity often known as linear-rugosity, a ratio of 1 indicating a low complexity flat surface and a ratio greater than 1 a surface of increasing complexity. Linear-rugosity provides a useful predictor of coral reef biota abundance, with Graham & Nash, (2013) reporting an overall (72% of 140 studies) positive effect of increasing linear-rugosity on various fish, invertebrate and coral responses, as well as on ecosystem services such as tourism and shoreline protection. Their quantitative meta-analysis using data from 150 sites across the Indo-Pacific and Caribbean indicated a significant positive correlation between linear-rugosity and fish density and biomass and coral cover, and a significant negative correlation with algae cover and sea urchin density. The efficacy of linear-rugosity as a predictor was linked to its surrogacy relationship with niche space and number of refuges, which explained why more fish were found on complex reefs.

While linear-rugosity provides a useful measure of structural complexity, it is relatively coarse as it does not discriminate between different components of structural complexity present in the marine environment (Knudby *et al*., 2007). Other observational studies that measure more discrete (compared to linear-rugosity) components of structural complexity have linked fish community metrics with coral colony abundance (Harborne *et al*., 2011), coral growth form (Gratwicke & Speight, 2005b; Mellin *et al*., 2007) and the height and number of associated refuges (Harborne *et al*., 2012). In particular, Roberts & Orrmond, 1987) found that the number of refuges of three different sizes explained 77% of the variance in coral reef fish abundance. Experimental studies that manipulated natural and artificial habitats have provided further insight into the components of structural complexity that influence fish. Several of these studies provided direct support for the number and size of

refuges in influencing fish abundance and species richness (Almany, 2004b; Gratwicke & Speight, 2005a; Gregor & Anderson, 2016; Hixon & Beets, 1993; Lingo & Szedlmayer, 2006). Not surprisingly, increased refuge density was associated with greater fish abundance (Almany, 2004b; Hixon & Beets, 1993), though refuge availability may not always a limiting factor (Lingo & Szedlmayer, 2006; Robertson & Sheldon, 1979). The size of refuge was also important for prey fish survivability (Hixon & Beets, 1993; Lingo & Szedlmayer, 2006), with refuges more similar in size to prey species better able to exclude larger bodied predatory species (Gratwicke & Speight, 2005a) and reduce predator maneuverability (Gregor & Anderson, 2016). Refuge variety was also associated with greater numbers of fish and fish species on artificial reefs, with small grunts (*Haemulon* spp.), beaugregory damselfish (*Stegastes leucostictus*) and Atlantic trumpetfish (*Aulostomus maculatus*) each preferring uniquely complex habitat (Gratwicke & Speight, 2005a).

Several other measures of structural complexity developed originally for use in terrestrial environments have been adopted in marine ecology. Many capture discrete components of structural complexity, such as steep and flat terrain, valleys, ridges, and the direction in which terrain is facing. They are just as easily derived from seafloor DEMs and used to predict the abundance and distribution of marine biota. The adoption of these metrics alongside advancement in methods of deriving bathymetric reconstructions has allowed greatly increased the use of structural complexity to predict and understand the distribution of marine biota over far greater areas than achievable using *in-situ* methods such as linear-rugosity. Associated data processing and analytical methods are now also at a stage where hypothesis linking structural complexity and its functional role in marine (and terrestrial) environments can be formally tested (Calders *et al*., 2020).

1.2.2 Traditional Remote Sensing

The development of methods in capturing bathymetric reconstructions using remote sensing techniques, primarily hydroacoustic side-scan sonar and multibeam echo sounding (multibeam) (one of the earliest examples by Moravec & Elfes, (1985), Light Detection and Ranging (LIDAR) and satellite optical imaging has been influential to the use of structural complexity metrics in marine ecological research. In this thesis remote sensing is used to refer to such traditional methods of deriving bathymetric reconstruction and newer photogrammetric methods (**Section 1.2.3**). However, remote sensing more broadly refers to the use of any reflected radiation to obtain physical information of an area or surface. In their 2011 review, Brown *et al*., (2011) identified almost 140 benthic mapping studies based

on acoustic methods undertaken since 1997. This included 102, 32 and 23 that mapped the habitat of epifauna / flora, infauna and / or fish, respectively, over distances up to and over 10 km. Most studies derived metrics from raster DEMs to model the abundance and / or distribution of marine biota. One of the most common metrics, surface-rugosity, is the ratio of convoluted surface area to planar area (Parravicini *et al*., 2006; Wedding *et al*., 2008) and the equivalent to linear-rugosity but based on 2D planar area rather than linear distance. Along with other originally terrestrial, these are derived over a range of spatial extents (up to several kilometers) and resolutions from 0.5 m (Coleman *et al*., 2016; Dolan *et al*., 2008) to 200 m cell size (Knudby *et al*., 2010; Rengstorf *et al*., 2013) much greater than that achievable using *in-situ* methods. It is noted that the resolution of the multibeam (5 m) and LIDAR (2 m) bathymetric reconstructions used in this thesis were combined to provide a 5 m resolution bathymetric reconstruction. This is within the range of resolutions considered by previous studies, though finer resolutions were considered in some previous studies. This has been considered when interpreting the findings of this thesis analyses, associated limitations, and directions for future research.

The utility of these remotely sensed metrics as predictors, in comparison to *in-situ* methods such as linear-rugosity, relates to their correlation with important resources and environmental gradients that drive the abundance and distribution of species across broad-scales (Guisan & Zimmermann, 2000) far greater than achievable using *in-situ* methods. Surrogacy relationships between structural complexity metrics and these drivers allow the modelling and prediction of species responses in marine ecology (Anderson *et al*., 2009; Hirst, 2008; Huang *et al*., 2014; McArthur *et al*., 2010) and make key contributions to species conservation, marine resource management, more precise stock assessments and Marine Protected Area (MPA) design and assessment (Rees *et al*., 2018; Ward *et al*., 1999), of which require accurate and spatially explicit information on species distributions often unobtainable using direct sampling. Species distribution models (SDMs) are a common tool used to incorporate variation in several metrics derived over various spatial extents and resolutions to predict the distribution of fish for such purposes (Ferrari, Malcolm, Neilson, *et al*., 2018).

Although the advancement in marine ecological research and management provided by remotely sensed metrics of structural complexity has been vast, there are limitations. First, while the spatial extent of hydroacoustic and LIDAR surveys can be substantial (up to 100s km^2) the resolutions (generally 0.5 m or greater) are relatively coarse relative to the body size of most marine biota of interest (Luckhurst & Luckhurst, 1978; Roberts & Ormond,

1987). Thus, while derived metrics capture important processes operating at coarser resolutions over broad extents, they have limited capacity to capture process and resources influencing habitat suitability and species abundance at sub-metre resolutions, at large or small spatial extents. As numerous observational and experimental studies have demonstrated and as summarised above, the ability to capture structural complexity at fine resolutions commensurate with the density and potential the type and shape of habitat refuges, for example, represents a substantial advancement in predicting species' abundance and distribution. Secondly, 2.5D raster-based DEMs derived from traditional remote sensing provide a relatively poorer approximation of the true 3D structure of the seafloor. Although raster-based bathymetric reconstructions capture variation in height, they do not capture surfaces beyond vertical (and therefore are sometimes referred to as 2.5D). Beyond vertical surfaces capture important features such as overhangs, caves, tabular corals and other such complex 3D structure. These features have ecological relevance (Kerry & Bellwood, 2015) and if not captured, model and predictive performance could be hindered, particularly for biota closely associated with these features.

1.2.3 Photogrammetry

More recent advances in remote sensing are now addressing many of the limitations of traditional methods. Photogrammetry is a method used to construct 3D models of physical objects and environments from overlapping photographic images. Also referred to as structure from motion (SfM), this technique is undergoing rapid development as a tool to capture 3D models of the seafloor. The 3D models usually consist of triangulated irregular networks (TINs) of points (or vertices) connected by lines that partition geographic space into contiguous, non-overlapping triangles (Bhargava *et al*., 2013). Photogrammetry and derived 'mesh-based' bathymetric reconstructions have several advantages over those based on rasters, including greater resolution, the reduction of redundant reconstructed bathymetric data (for example where the rate of change in depth is relatively small) and the ability to capture novel metrics (e.g., surfaces beyond vertical) alongside mesh-based equivalents of traditional metrics, such as surface-rugosity and slope (Aston *et al*., 2022). Early photogrammetry studies described the methodological process and associated accuracies in mesh models of reef patches accurate to a few centimeters (Friedman *et al*., 2012; Johnson-Roberson *et al*., 2010) and coral colonies on the order of millimeters (Ferrari *et al*., 2016a; Figueira *et al*., 2015; Helmholz *et al*., 2016; Storlazzi *et al*., 2016). The fine resolutions associated with photogrammetry are more suited to exploring how individual biota respond to their immediate habitat (and how associated species-habitat relationships

influence local abundance and distribution). Traditionally, mechanisms operating over these resolutions have been explored using *in-situ* metrics such as linear-rugosity. Photogrammetry expands the fine resolutions achievable using *in-situ* methods to much greater spatial extents (albeit not to the extents possible using traditional remote sensing) to explore fish refuge use on coral reefs, anthropogenic, disease and other influences on coral reef structure, and fish habitat use.

Indeed, photogrammetry has facilitated an expansion of research into the role of structural complexity in marine ecology (Ferrari *et al*., 2022). Examples include using photogrammetry to better understand the role of corals as shelter for reef fish (Urbina-Barreto *et al*., 2021), the effect of marine traffic on coral reef structure (Chen & Dai, 2021), measure sponge growth (Olinger *et al*., 2019), and coral growth / erosion (Ferrari *et al*., 2017) and disease induced tissue loss in corals (Combs *et al*., 2021). Derived metrics of structural complexity have also been related to benthic cover and coral bleaching (Ferrari *et al*., 2016b). Fish studies include the use of bathymetric-range (albeit derived from stereo-imagery, not SfM) to model fish abundance in the Pilbara region of Western Australia (Collins *et al*., 2017), use of viewshed and refuge density to model damselfish abundance in the Caribbean (González-Rivero *et al*., 2017) and surface-rugosity, bathymetric-range, RMS variation (variation of values from plane of best fit) and kurtosis (analogous to raster curvature metrics), along with cover of benthic biota and substratum identified from the orthomosaic, to model fish assemblages structure, diversity species richness and biomass in the Philippines (Bayley *et al*., 2019). Outside the tropics, mesh-based surface-rugosity was used to model fish abundance in the Mediterranean (Monfort *et al*., 2021), surface-rugosity and viewshed to explore fish habitat use in eastern temperate Australia (Taylor & Figueira, 2021), and surface-rugosity and slope to model fish abundance in the Solitary Islands in eastern sub-tropical Australia (Ferrari, Malcolm, Byrne, *et al*., 2018).

Several studies have also converted photogrammetrically derived meshes to raster-based bathymetric reconstructions. Such procedures provide a method of obtaining metrics commonly derived from rasters with demonstrated predictive performance, but at the finer resolutions achievable using photogrammetry. This included the successful prediction of cold-water cover and diversity and fish abundance around 850 m deep in the North Atlantic (Price *et al*., 2019a) and fish species richness and abundance in Hawaii (Fukunaga, Kosaki, *et al*., 2020). Streit *et al*., (2021) derived slope and surface-rugosity from rasters converted from meshes, though these metrics were not correlated with lemon damselfish (*Pomacentrus moluccensis*) and green chromis (*Chromis viridis*) territory size (live coral

cover and body size were more important). In a novel approach, Carlot *et al*., (2020) predicted raster-based rugosity (again, converted from meshes) using abiotic and biotic measures of benthic cover including rubble, macroalgae and corals. Reductions in predicted rugosity values reconstructed from historic benthic cover data were able to be linked to previous disturbance events from crown of thorns and cyclones. Although not considered in this thesis, photogrammetry surveys can also provide contiguous orthorectified photographic mosaics of the seafloor from which complimentary data on abiotic and biotic benthic cover can be quantified. Typically, such data is not collected alongside traditional remote sensing (multibeam, LIDAR and satellite methods), and derived bathymetric reconstructions generally do not have imagery associated with them.

As with traditional methods of capturing bathymetric reconstructions (e.g., MBES and LIDAR), photogrammetry-based methods have limitations (**Table 1-1**). Per unit area of seafloor coverage, they are more time-intensive than traditional remote sensing methods. In most cases at shallower depths, images used to create the meshes are collected on snorkel or using SCUBA, limiting spatial coverage requiring additional logistical needs associated with people being in the water. Although images may be collected using Automated Underwater Vehicles (AUVs) (Ferrari *et al*., 2016b; Ferrari, Malcolm, Byrne, *et al*., 2018), this requires substantial hardware, automated piloting, and surface support. The decision to include traditional and / or photogrammetric based remote sensing methods in studies will need to balance the increased cost of photogrammetry against this smaller area of coverage, the potential benefits that may be associated with it, and the area under consideration as part of the research question. Although covering greater spatial extents than *in-situ* methods, photogrammetric survey extents are smaller than that required to adequately inform large scale spatial prioritisation as part of conservation and management efforts, for example identification of marine use and no fishing zones. When structural complexity has been used with such goals in mind, the spatial extents tend to be large. For example, 1.8 km^2 and spatial-temporal closure measures for parrotfish in Brazil (Roos *et al*., 2015), 200 km of abalone fisheries managed coastline in southern Australia (Jalali *et al*., 2015) and assessing yellowtail kingfish (*Seriola lalandi*) no-take zone performance within a 3,500 km^2 MPA in eastern Australia (Rees *et al*., 2018).

Clearly, while photogrammetry can enhance understanding of ecological mechanisms operating at local scales, as costs of data collection increase at broader scales, the ability to make informed choices regarding the cost-benefit of photogrammetry becomes

Table 1-1 Summary of main differences between traditional and photogrammetric methods of deriving metrics of structural complexity.

Component	Traditional Methods	Photogrammetric Methods
Data collection methods	Methods include multibeam echosounder (MBES) and other hydroacoustic methods from watercraft, Light Detection and Ranging (LIDAR) from aircraft, and satellite-based imaging. Excludes in-situ methods of capturing data, such as diver surveys using chain and tape methodology.	Collection of multiple overlapping images of the seabed using still photography or extraction of still images from videos collected using SCUBA divers or AUVs / ROVs.
Bathymetric reconstruction	Typically 2.5D raster-based surfaces (e.g., MBLI Raster).	3D TIN mesh-based models (e.g., AUV Mesh) or 2.5D rasters created from mesh models (e.g., AUV Raster)
Maturity of Technology	Multiple and established technologies with history of applications in ecology over several decades.	Application of photogrammetric to map marine environment is relatively new, though undergoing rapid advancement in technology and usages.
Maximum spatial extent	Typically up to several hundred square kilometers. Satellite imaging could potentially provide data far more than this.	From sub-m^2 to potentially 10,000s m^2. Typically 10s m^2 to 100s m^2 using divers and underwater ROVs / AUVs. Greater spatial extents could be achieved using ROVs / AUVs and aerial drones.
Minimum resolution	Typically 0.5 m to 100s m, though as fine as at least 0.25 has been reported.	Smaller extents can be modelled at sub-millimetre resolutions. Though at typical spatial extents resolutions tend be on centimetre to 10s of centimetres scales.
Relative advantages	Can provide bathymetric reconstructions over much larger spatial extents.	Can provide much finer resolutions, potentially much better at capturing ecologically ecological and environmental drivers of marine biota abundance and distribution. Allows derivation of novel metrics of structural complexity from 3D mesh, as well as traditional metrics.
Relative disadvantages	Resolutions achievable are generally coarser. More restricted number of metrics of structural complexity can be derived from 2.5D raster surfaces.	Cost per unit area of spatial extent much greater.

increasingly important. Although many studies are adopting mesh-based metrics of structural complexity to model fish, we still lack the knowledge to assess the benefits to predictive performance associated with this method and metrics compared to traditional methods. This is of need because any enhanced predictive performance associated with photogrammetry would come at an additional cost of field data collection and processing, with photogrammetric data likely to be more expensive to collect per unit area than traditional data for the foreseeable future.

1.3 Thesis Aims

The primary aim of this thesis, summarised in **Figure 1-1**, is to objectively assess the potential for photogrammetry to improve predictions of marine biota (in this case fish on the southeastern coast of Australia) abundance and distribution compared to established traditional remote sensing methods (in this case, multibeam and LIDAR). This knowledge

will help facilitate the adoption of photogrammetry as a further remote sensing method and identify circumstances where the increased cost is worthwhile. To my knowledge, no other study has attempted such a broad- and multi-scale, systematic and *a-priori* attempt at assessing the relative and combined performance of photogrammetric and traditionally derived metrics of structural complexity as predictors of marine biota abundance and distribution. Many previous studies have used traditionally (reviewed in Chapter 2) and more recently photogrammetrically (summarised in **Section 1.2.3**) derived metrics to model the abundance and / or distribution of marine biota, often considering multiple spatial scales (see summary for traditional metric base studies in **Table 2-3** in Chapter 2). However, none have combined the three methods of metric derivation (traditionally derived raster-based metrics, photogrammetrically derived mesh-based metrics, and metrics derived from rasters following conversion from meshes) to compare their performance or inform further research.

This primary objective is supported by the aims of the individual data chapters:

- Chapter 2 undertakes a quantitative review and metanalysis of similar previous marine ecology studies with the aim of identifying common metrics of structural complexity, their relative predictive performance, and the important factors to consider when deriving these metrics.
- Chapter 3 systematically explores relationships between metrics and the important role of spatial scale in structuring these relationships. The aim is to identify a reduced but predictor dataset that optimises information on structural complexity captured whilst minimising the number of metrics and effort required to capture this information.
- Chapter 4 compares the predictive performance of the reduced predictor datasets when modelling the abundance of fish species and trophic-functional groups. The aim was to identify for which species and groups traditional and / or photogrammetrically derived metrics provide greatest predive performance, potential synergy between these metrics, and, thus, inform future studies considering the use of photogrammetric methods.
- Chapter 5 uses a novel method of engineering otherwise local-scale photogrammetrically derived metrics across the broad-spatial scales typical of traditionally derived metrics. The aim is to improve predictions of fish abundance and distribution over broad spatial extents currently unachievable using photogrammetric data collection methods.

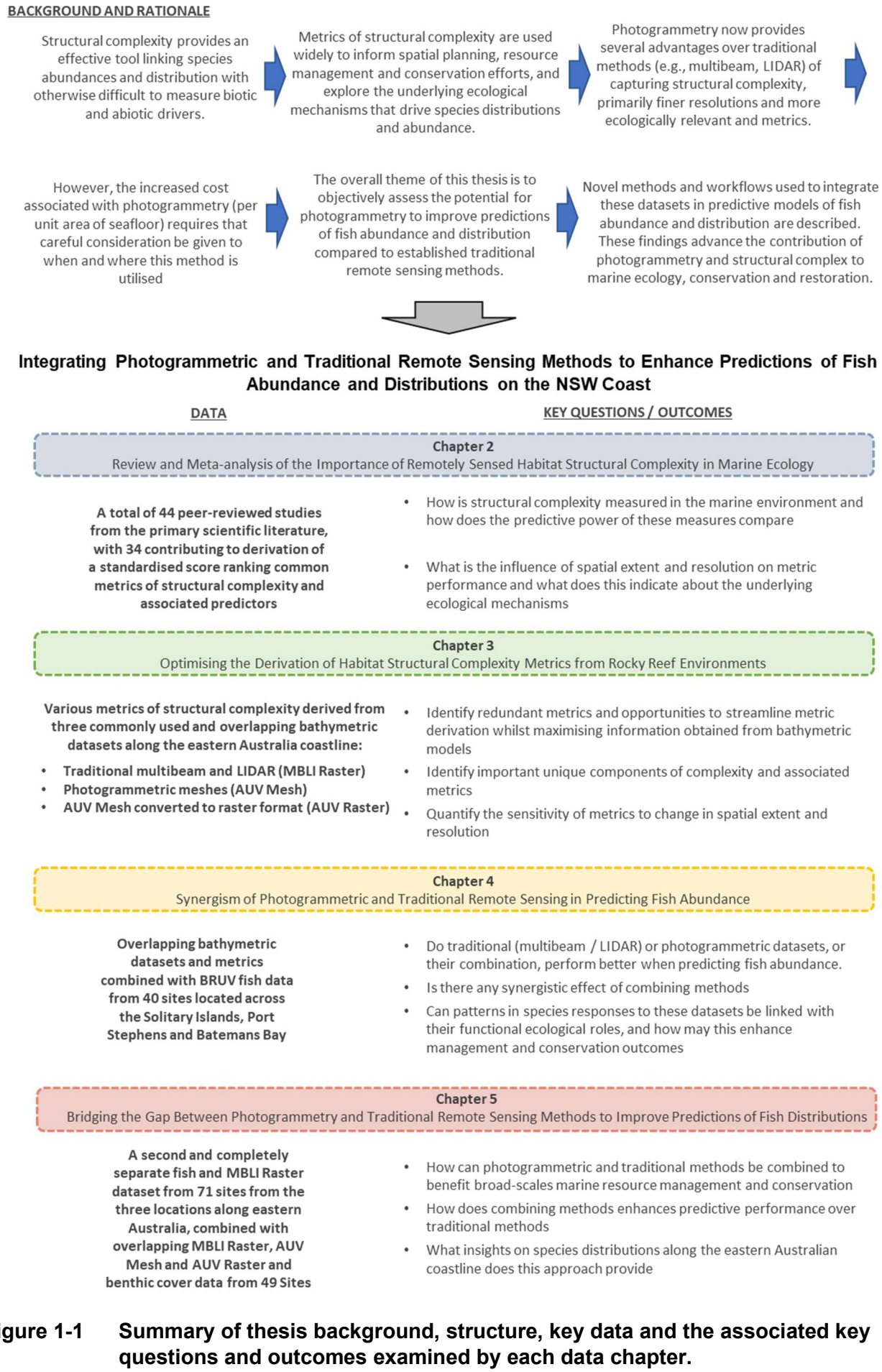

Figure 1-1 Summary of thesis background, structure, key data and the associated key questions and outcomes examined by each data chapter.

Such an assessment is made possible by the availability of overlapping multibeam / LIDAR, photogrammetry and fish data sets from several locations along the NSW coastline in southeastern Australia. This offers a unique opportunity to undertake this assessment for a range of fish species. It also allows methods to be explored that could enhance predictive performance in areas of the coastline where photogrammetry data does not currently exist. This will improve the understanding of fish ecology along 500 km of the Australian coastline and improve conservation and management outcomes that rely on accurate information of fish abundance and distribution across large spatial extents. This thesis describes methods and workflows that can be used to help integrate different datasets in predictive models of fish abundance and distribution and identifies species and functional groups where integration is likely to be most effective in enhancing predictive performance. Findings and methods presented here will advance the fields of marine ecology, conservation and restoration.

1.4 Data Chapter Structure

1.4.1 Chapter 2

Many studies have used traditional remote sensing and derived metrics of structural complexity to model the prevalence, abundance and distribution of a range of marine biota worldwide. However, until now there has been little attempt to synthesise the findings of these studies to inform the best approach to integrating traditional and photogrammetric methods. This chapter undertakes a literature review and meta-analysis of studies that have used traditional remote sensing to create bathymetric reconstructions of the seafloor, derived measures of structural complexity, and used these to predict the abundance and distribution of marine biota. It identifies the most common metrics, their relative predictive performance and performance of related habitat and geographic based variables and identifies common analytical methods and the influence of spatial extent and resolution on metric performance. The findings guide the derivation of metrics from the bathymetric reconstructions examined in this thesis and provide an improved understanding of the key role of spatial extent and resolution in structing variability in metric values and the form and direction of associated biotic responses. The findings are supported by development of a new rank-based scoring assessment that allows comparison of the relative performance of various metrics across the disparate studies included in the review. This review was not restricted to fish, the type of traditional remote sensing, or geographic location and the findings have relevance well outside this thesis.

This chapter is already published as: Pygas, D. R., Ferrari, R., & Figueira, W. F. (2020). Review and meta-analysis of the importance of remotely sensed habitat structural complexity in marine ecology. *Estuarine, Coastal and Shelf Science*, 235. https://doi.org/10.1016/j.ecss.2019.106468

1.4.2 Chapter 3

Metrics of structural complexity may be summarised in various ways (e.g., mean, variation, range) and derived over a range of spatial extents and resolutions any of which could have unique ecological relevance, with the findings of Chapter 2 identifying how marine biota may respond to metrics derived over multiple discrete spatial scales, often with different forms of response. However, such metric diversity soon results in large and often highly correlated predictor datasets that can hinder data handling and common statistical modelling techniques. This chapter describes methods of optimising large metric datasets extracted from traditional (multibeam and LIDAR) and photogrammetric bathymetric reconstructions, each combining varying spatial extents, resolutions, and associated metrics of complexity. A reduced dataset of less than 100 predictors is identified from over 2,000 initial candidate predictors. This reduced dataset is far more suitable for common statistical modelling methods whilst simultaneously maximising the amount of retained information on the structure of the seafloor. The dataset reduction is done in a systematic and objective way that also maximises the interpretability of the retained metrics. It provides useful information on the relative sensitivities of various metrics to changes in extent and resolution and helps to identify and confirm key groupings or related metrics of structural complexity that guides their use in later **Sections** and in other studies.

1.4.3 Chapter 4

To assist future studies considering the inclusion of photogrammetric metrics as predictors of fish abundance and distribution, an objective assessment of their relative performance alongside metrics derived from traditional remote sensing is needed. The reduced predictor dataset from Chapter 3 is used to identify the combination of metrics that provides the greatest predictive performance of fish species and trophic-mobility group abundance along 500 km of the southeastern Australian coast. The primary aim is to identify which single dataset, one from traditional remote sensing and two from photogrammetric survey, or combination provides the greatest predictive power. This allows informed decisions based on the expected costs and benefits to predictive performance associated with photogrammetric metrics. Also, on situations where they should replace or otherwise

be included alongside traditionally derived metrics, or when traditional methods are the preferred approach. Chapter 4 also investigates whether combining predictors across different datasets provides improved predictions compared with any dataset in isolation. The presence of such synergistic effects would have important considerations for further studies that aim to predict fish abundance and distributions.

1.4.4 Chapter 5

Chapter 4 identified many fish species and groups for which photogrammetric metrics improved model performance. While these models help to better understand local-scale mechanistic drivers of abundance, their contribution to broad-scale spatial prioritisation, manage and conservation will for the foreseeable future remain limited due to the expense of collecting photogrammetric data. Methods of combining these datasets are required to allow management decisions that rely on broad-scale predictors to also benefit from improved model performance associated with photogrammetric metrics. Chapter 5 develops a novel method of combining the enhanced predictive performance associated with photogrammetry with the broad-scale coverage achievable using traditional methods. Rather than further expensive photogrammetry data collection, pseudo-photogrammetry metrics are 'engineered' from the traditional multibeam and LIDAR bathymetric reconstruction and derived metrics. This is done using modelled relationships between metrics from areas of overlapping traditional and photogrammetric bathymetric reconstructions. Species distribution models (SDMs) based on the engineered and traditional metric are created for fish species and trophic-mobility groups using common machine learning methods and their predictive performance assessed. Maps from SDMs are compared to identify if including the engineered photogrammetric metrics provide additional insight into fish distributions compared to traditional reconstructions and metrics. The findings indicate those species and groups for which engineered metrics enhance broad-scale predictive performance where photogrammetry data otherwise does not exist. This enhanced performance is achieved at a fraction of the cost of collecting photogrammetry data in the field, with potential for improved management and conservation outcomes on the NSW coast.

1.5 Study Area

Figure 1-2 provides an overview of the three study locations and sites included in this these and along southeastern Australian coastline and consisting of the Solitary Islands (**Figure 1-3**), Port Stephens (**Figure 1-4**) and Batemans Bay (**Figure 1-5**). The coloured

bathymetric raster layer represents combined multibeam / LIDAR bathymetric data (MBLI Raster) used in **Sections 3**, **4** and **5**.Further information on these datasets is provided in the respective **Sections**. A full list of the sites included in this thesis, associated data and which chapter(s) these data appear in is provided in **Appendix 1-1**. As identified in **Section 0**, these sites were not chosen *a-priori*, but were included in this thesis due to the apparently unique availability of key bathymetric and fish data.

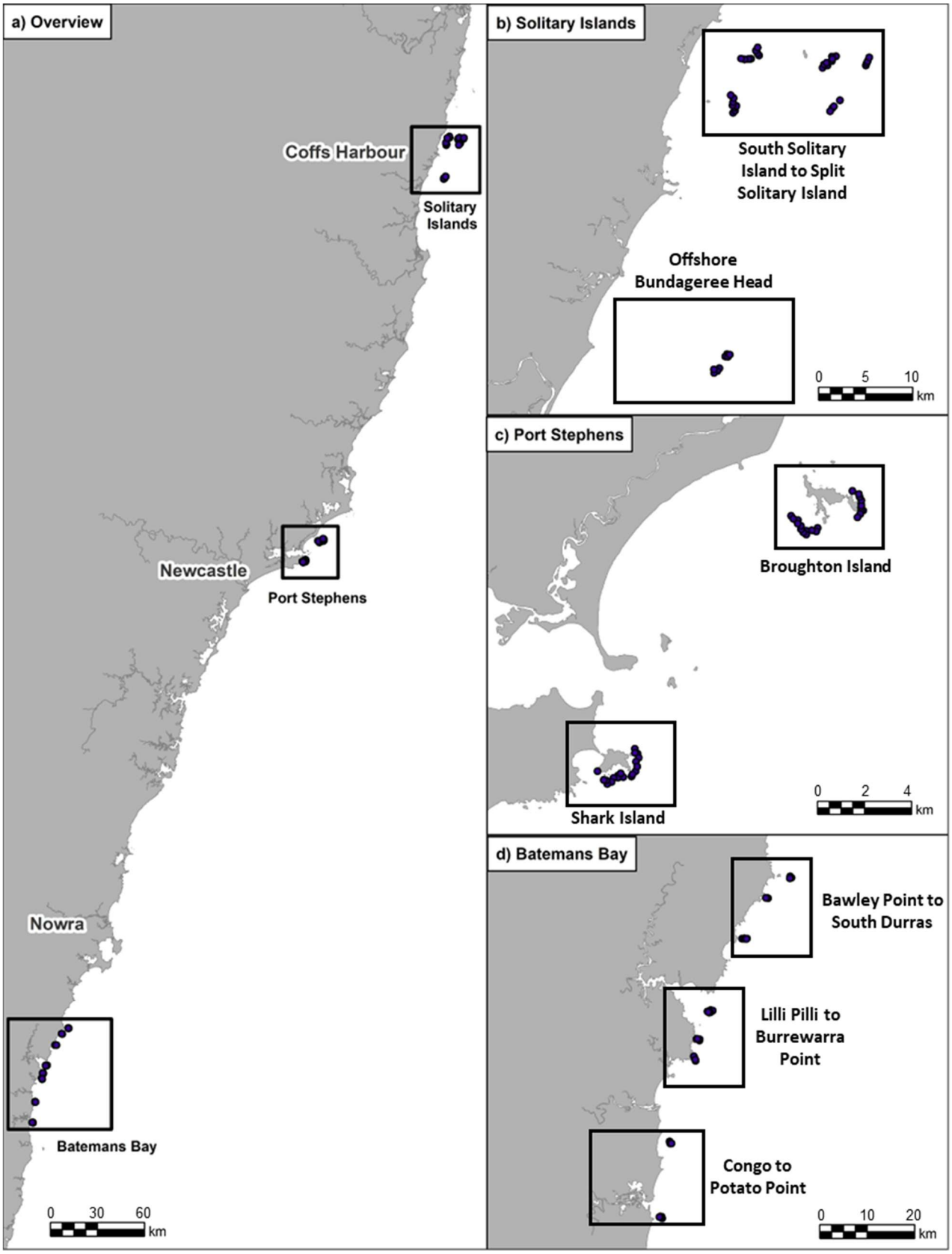

Figure 1-2 **a) Overview of the three study locations: b) Solitary Islands, c) Port Stephens and d) Batemans Bay on the New South Wales Coastline on the east coast of Australia. Circles represent availability of photogrammetric, benthic biota or fish data.**

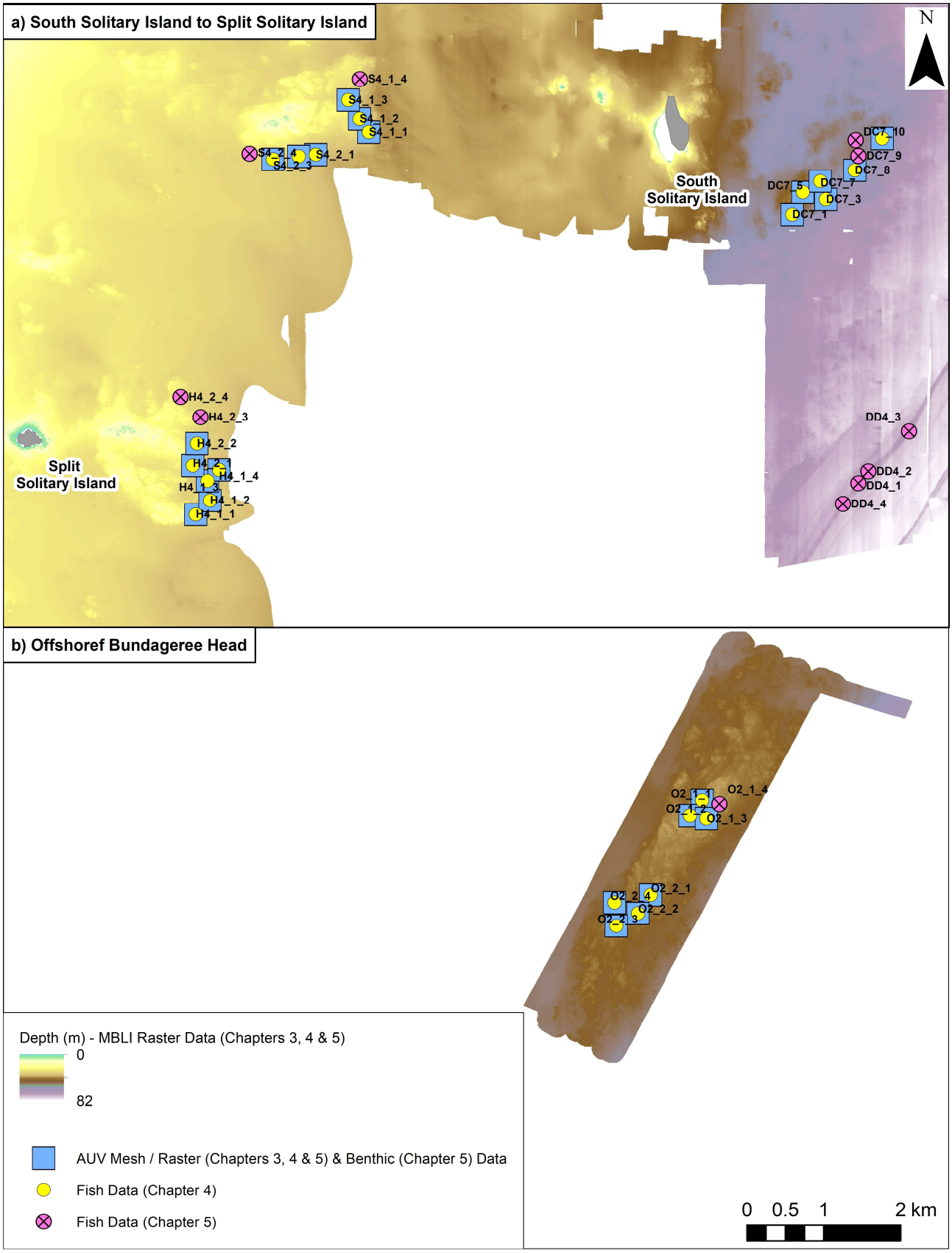

Figure 1-3 Study sites near a) South Solitary Island to Split Solitary Island and b) Offshore Bundageree Head in the Solitary Islands

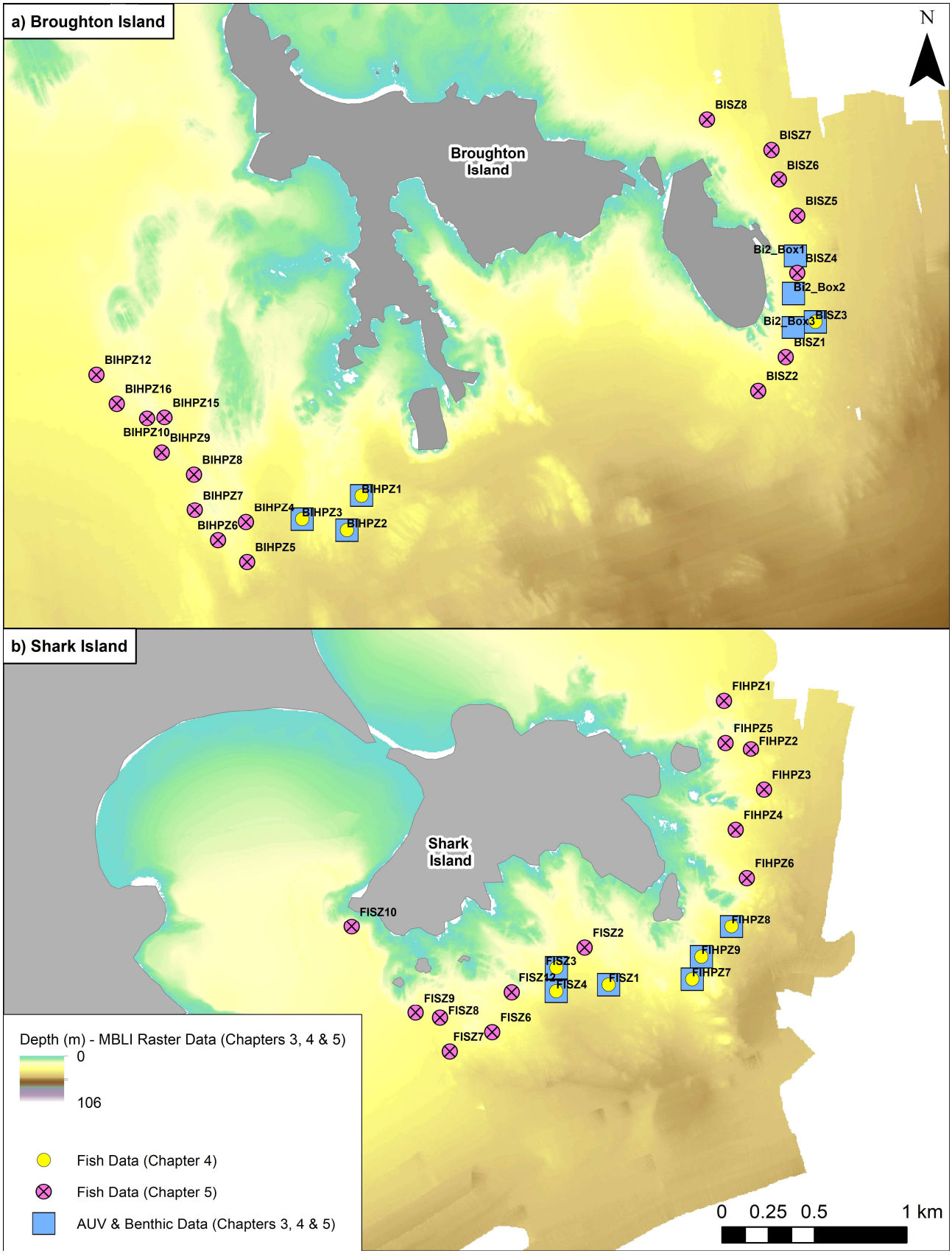

Figure 1-4 Study sites near a) Broughton Island and b) Shark Island in the Port Stephens

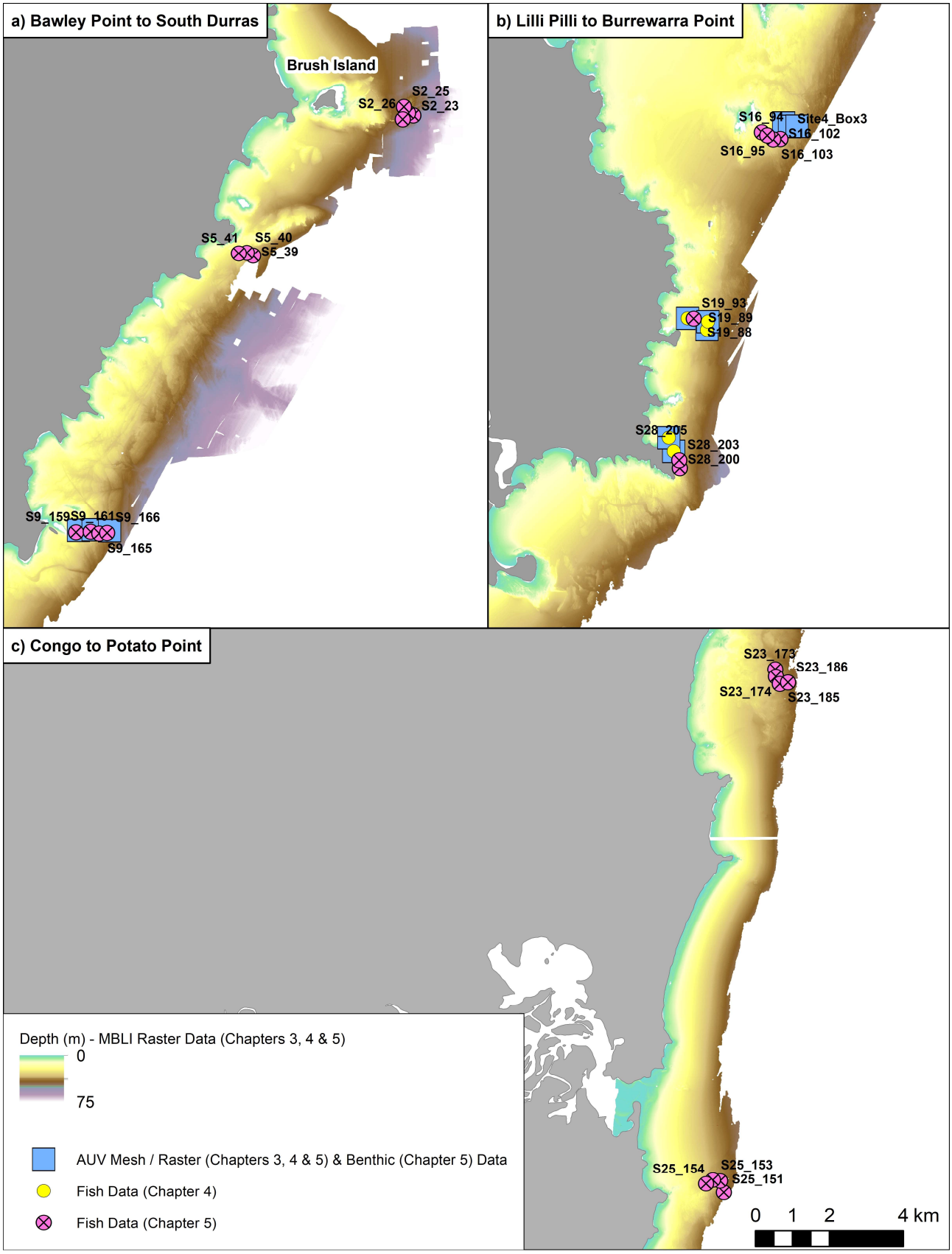

Figure 1-5 Study sites near a) Bawley Point to South Durras, b) Lilli Pilli to Burrewarra Point and c) Congo to Potato Point in Batemans Bay

1.6 Appendices

Appendix 1-1 Details of all sites included in this thesis and the Chapter(s) (Chp.) for which they provide data.

Site	Location	Latitude	Longitude	Bathymetric Data	Biotic Data	Chp 3	Chp 4	Chp. 5
BISZ3	Port Stephens	-32.624568	152.339510	MBLI and Photogram.	Fish	Y	Y	Y*
Bi2_Box1	Port Stephens	-32.621352	152.338385	MBLI and Photogram.	Benthic	Y	N	Y*
Bi2_Box2	Port Stephens	-32.623192	152.338254	MBLI and Photogram.	Benthic	Y	N	Y*
Bi2_Box3	Port Stephens	-32.624853	152.338237	MBLI and Photogram.	Benthic	Y	N	Y*
BIHPZ1	Port Stephens	-32.632885	152.313255	MBLI and Photogram.	Fish and Benthic	Y	Y	Y*
BIHPZ2	Port Stephens	-32.634585	152.312395	MBLI and Photogram.	Fish and Benthic	Y	Y	Y*
BIHPZ3	Port Stephens	-32.634032	152.309813	MBLI and Photogram.	Fish and Benthic	Y	Y	Y*
DC7_1	Solitary Islands	-30.214000	153.283778	MBLI and Photogram.	Fish and Benthic	Y	Y	Y*
DC7_11	Solitary Islands	-30.205060	153.295920	MBLI and Photogram.	Fish and Benthic	Y	Y	Y*
DC7_3	Solitary Islands	-30.212222	153.288333	MBLI and Photogram.	Fish and Benthic	Y	Y	Y*
DC7_5	Solitary Islands	-30.211389	153.285194	MBLI and Photogram.	Fish and Benthic	Y	Y	Y*
DC7_7	Solitary Islands	-30.210080	153.287550	MBLI and Photogram.	Fish and Benthic	Y	Y	Y*
DC7_8	Solitary Islands	-30.208800	153.292220	MBLI and Photogram.	Fish and Benthic	Y	Y	Y*
FIHPZ7	Port Stephens	-32.753235	152.205133	MBLI and Photogram.	Fish and Benthic	Y	Y	Y*
FIHPZ8	Port Stephens	-32.750685	152.207428	MBLI and Photogram.	Fish and Benthic	Y	Y	Y*
FIHPZ9	Port Stephens	-32.752150	152.205680	MBLI and Photogram.	Fish and Benthic	Y	Y	Y*
FISZ1	Port Stephens	-32.753475	152.200298	MBLI and Photogram.	Fish and Benthic	Y	Y	Y*
FISZ3	Port Stephens	-32.752632	152.197292	MBLI and Photogram.	Fish and Benthic	Y	Y	Y*
FISZ4	Port Stephens	-32.753765	152.197265	MBLI and Photogram.	Fish and Benthic	Y	Y	Y*
H4_1_1	Solitary Islands	-30.249290	153.203260	MBLI and Photogram.	Fish and Benthic	Y	Y	Y*
H4_1_2	Solitary Islands	-30.247640	153.205180	MBLI and Photogram.	Fish and Benthic	Y	Y	Y*
H4_1_3	Solitary Islands	-30.245340	153.204830	MBLI and Photogram.	Fish and Benthic	Y	Y	Y*
H4_1_4	Solitary Islands	-30.244050	153.206380	MBLI and Photogram.	Fish and Benthic	Y	Y	Y*
H4_2_1	Solitary Islands	-30.243540	153.202840	MBLI and Photogram.	Fish and Benthic	Y	Y	Y*
H4_2_2	Solitary Islands	-30.240980	153.203390	MBLI and Photogram.	Fish and Benthic	Y	Y	Y*
O2_1_1	Solitary Islands	-30.437770	153.198340	MBLI and Photogram.	Fish and Benthic	Y	Y	Y*
O2_1_2	Solitary Islands	-30.439540	153.196700	MBLI and Photogram.	Fish and Benthic	Y	Y	Y*
O2_1_3	Solitary Islands	-30.439890	153.198910	MBLI and Photogram.	Fish and Benthic	Y	Y	Y*
O2_2_1	Solitary Islands	-30.448830	153.191360	MBLI and Photogram.	Fish and Benthic	Y	Y	Y*
O2_2_2	Solitary Islands	-30.450990	153.189650	MBLI and Photogram.	Fish and Benthic	Y	Y	Y*
O2_2_3	Solitary Islands	-30.452470	153.186720	MBLI and Photogram.	Fish and Benthic	Y	Y	Y*
O2_2_4	Solitary Islands	-30.449740	153.186480	MBLI and Photogram.	Fish and Benthic	Y	Y	Y*
S19_86	Batemans Bay	-35.798100	150.239600	MBLI and Photogram.	Fish and Benthic	Y	Y	Y*
S19_88	Batemans Bay	-35.801004	150.245267	MBLI and Photogram.	Fish and Benthic	Y	Y	Y*
S19_89	Batemans Bay	-35.799010	150.245640	MBLI and Photogram.	Fish and Benthic	Y	Y	Y*
S28_204	Batemans Bay	-35.830340	150.234310	MBLI and Photogram.	Fish and Benthic	Y	Y	Y*
S28_205	Batemans Bay	-35.827020	150.232910	MBLI and Photogram.	Fish and Benthic	Y	Y	Y*
S4_1_1	Solitary Islands	-30.204480	153.226560	MBLI and Photogram.	Fish and Benthic	Y	Y	Y*
S4_1_2	Solitary Islands	-30.202920	153.225300	MBLI and Photogram.	Fish and Benthic	Y	Y	Y*
S4_1_3	Solitary Islands	-30.200740	153.223780	MBLI and Photogram.	Fish and Benthic	Y	Y	Y*
S4_2_1	Solitary Islands	-30.207100	153.219400	MBLI and Photogram.	Fish and Benthic	Y	Y	Y*
S4_2_2	Solitary Islands	-30.207310	153.217120	MBLI and Photogram.	Fish and Benthic	Y	Y	Y*
S4_2_3	Solitary Islands	-30.207660	153.213610	MBLI and Photogram.	Fish and Benthic	Y	Y	Y*
Site3_Box1	Batemans Bay	-35.632346	150.338483	MBLI and Photogram.	Benthic	Y	N	Y*
Site3_Box2	Batemans Bay	-35.632290	150.342855	MBLI and Photogram.	Benthic	Y	N	Y*
Site3_Box3	Batemans Bay	-35.632643	150.347822	MBLI and Photogram.	Benthic	Y	N	Y*
Site4_Box1	Batemans Bay	-35.751203	150.269946	MBLI and Photogram.	Benthic	Y	N	Y*
Site4_Box2	Batemans Bay	-35.752144	150.271688	MBLI and Photogram.	Benthic	Y	N	Y*
Site4_Box3	Batemans Bay	-35.752144	150.273942	MBLI and Photogram.	Benthic	Y	N	Y*
BIHPZ10	Port Stephens	-32.629060	152.300910	MBLI	Fish	N	N	Y
BIHPZ12	Port Stephens	-32.626930	152.298010	MBLI	Fish	N	N	Y
BIHPZ15	Port Stephens	-32.629015	152.301917	MBLI	Fish	N	N	Y
BIHPZ16	Port Stephens	-32.628328	152.299172	MBLI	Fish	N	N	Y
BIHPZ4	Port Stephens	-32.634160	152.306580	MBLI	Fish	N	N	Y
BIHPZ5	Port Stephens	-32.636100	152.306630	MBLI	Fish	N	N	Y
BIHPZ6	Port Stephens	-32.635030	152.304960	MBLI	Fish	N	N	Y
BIHPZ7	Port Stephens	-32.633550	152.303630	MBLI	Fish	N	N	Y
BIHPZ8	Port Stephens	-32.631810	152.303600	MBLI	Fish	N	N	Y

Site	Location	Latitude	Longitude	Bathymetric Data	Biotic Data	Chp 3	Chp 4	Chp. 5
BIHPZ9	Port Stephens	-32.630730	152.301750	MBLI	Fish	N	N	Y
BISZ1	Port Stephens	-32.626300	152.337800	MBLI	Fish	N	N	Y
BISZ2	Port Stephens	-32.627918	152.336192	MBLI	Fish	N	N	Y
BISZ4	Port Stephens	-32.622195	152.338487	MBLI	Fish	N	N	Y
BISZ5	Port Stephens	-32.619388	152.338513	MBLI	Fish	N	N	Y
BISZ6	Port Stephens	-32.617628	152.337462	MBLI	Fish	N	N	Y
BISZ7	Port Stephens	-32.616174	152.337043	MBLI	Fish	N	N	Y
BISZ8	Port Stephens	-32.614702	152.333337	MBLI	Fish	N	N	Y
DC7_10	Solitary Islands	-30.205280	153.292310	MBLI	Fish	N	N	Y
DC7_9	Solitary Islands	-30.207110	153.292690	MBLI	Fish	N	N	Y
DD4_1	Solitary Islands	-30.245453	153.292794	MBLI	Fish	N	N	Y
DD4_2	Solitary Islands	-30.244063	153.294162	MBLI	Fish	N	N	Y
DD4_3	Solitary Islands	-30.239364	153.299650	MBLI	Fish	N	N	Y
DD4_4	Solitary Islands	-30.247900	153.290730	MBLI	Fish	N	N	Y
DD6_1	Solitary Islands	-30.212075	153.322991	MBLI	Fish	N	N	Y
DD6_2	Solitary Islands	-30.210359	153.323640	MBLI	Fish	N	N	Y
DD6_3	Solitary Islands	-30.208685	153.324412	MBLI	Fish	N	N	Y
DD6_4	Solitary Islands	-30.205920	153.325950	MBLI	Fish	N	N	Y
FIHPZ1	Port Stephens	-32.739708	152.207100	MBLI	Fish	N	N	Y
FIHPZ2	Port Stephens	-32.742058	152.208630	MBLI	Fish	N	N	Y
FIHPZ3	Port Stephens	-32.744055	152.209368	MBLI	Fish	N	N	Y
FIHPZ4	Port Stephens	-32.745992	152.207715	MBLI	Fish	N	N	Y
FIHPZ5	Port Stephens	-32.741750	152.207168	MBLI	Fish	N	N	Y
FIHPZ6	Port Stephens	-32.748348	152.208343	MBLI	Fish	N	N	Y
FISZ10	Port Stephens	-32.750552	152.185477	MBLI	Fish	N	N	Y
FISZ12	Port Stephens	-32.753813	152.194697	MBLI	Fish	N	N	Y
FISZ2	Port Stephens	-32.751672	152.198932	MBLI	Fish	N	N	Y
FISZ6	Port Stephens	-32.755773	152.193550	MBLI	Fish	N	N	Y
FISZ7	Port Stephens	-32.756688	152.191090	MBLI	Fish	N	N	Y
FISZ8	Port Stephens	-32.755048	152.190543	MBLI	Fish	N	N	Y
FISZ9	Port Stephens	-32.754787	152.189137	MBLI	Fish	N	N	Y
H4_2_3	Solitary Islands	-30.237880	153.203860	MBLI	Fish	N	N	Y
H4_2_4	Solitary Islands	-30.235530	153.201180	MBLI	Fish	N	N	Y
O2_1_4	Solitary Islands	-30.438220	153.200650	MBLI	Fish	N	N	Y
S16_102	Batemans Bay	-35.755100	150.268800	MBLI	Fish	N	N	Y
S16_103	Batemans Bay	-35.755160	150.266630	MBLI	Fish	N	N	Y
S16_94	Batemans Bay	-35.753370	150.263320	MBLI	Fish	N	N	Y
S16_95	Batemans Bay	-35.754180	150.264920	MBLI	Fish	N	N	Y
S19_93	Batemans Bay	-35.798200	150.241380	MBLI	Fish	N	N	Y
S2_23	Batemans Bay	-35.533540	150.441730	MBLI	Fish	N	N	Y
S2_24	Batemans Bay	-35.532920	150.440190	MBLI	Fish	N	N	Y
S2_25	Batemans Bay	-35.531400	150.439000	MBLI	Fish	N	N	Y
S2_26	Batemans Bay	-35.534410	150.438580	MBLI	Fish	N	N	Y
S23_173	Batemans Bay	-35.967000	150.178500	MBLI	Fish	N	N	Y
S23_174	Batemans Bay	-35.968800	150.178600	MBLI	Fish	N	N	Y
S23_185	Batemans Bay	-35.970600	150.179700	MBLI	Fish	N	N	Y
S23_186	Batemans Bay	-35.970280	150.182180	MBLI	Fish	N	N	Y
S25_151	Batemans Bay	-36.094100	150.158500	MBLI	Fish	N	N	Y
S25_152	Batemans Bay	-36.091200	150.157500	MBLI	Fish	N	N	Y
S25_153	Batemans Bay	-36.090900	150.155300	MBLI	Fish	N	N	Y
S25_154	Batemans Bay	-36.091800	150.153210	MBLI	Fish	N	N	Y
S28_200	Batemans Bay	-35.834500	150.235980	MBLI	Fish	N	N	Y
S28_203	Batemans Bay	-35.832560	150.235890	MBLI	Fish	N	N	Y
S4_1_4	Solitary Islands	-30.198280	153.225320	MBLI	Fish	N	N	Y
S4_2_4	Solitary Islands	-30.207030	153.210430	MBLI	Fish	N	N	Y
S5_39	Batemans Bay	-35.566600	150.392800	MBLI	Fish	N	N	Y
S5_40	Batemans Bay	-35.565880	150.390970	MBLI	Fish	N	N	Y
S5_41	Batemans Bay	-35.565950	150.388590	MBLI	Fish	N	N	Y
S9_159	Batemans Bay	-35.632820	150.337740	MBLI	Fish	N	N	Y
S9_161	Batemans Bay	-35.632800	150.342100	MBLI	Fish	N	N	Y
S9_165	Batemans Bay	-35.633260	150.344670	MBLI	Fish	N	N	Y
S9_166	Batemans Bay	-35.633200	150.347060	MBLI	Fish	N	N	Y

2 Chapter 2 - Review and Meta-analysis of the Importance of Remotely Sensed Habitat Structural Complexity in Marine Ecology

This chapter is already published as: Pygas, D. R., Ferrari, R., & Figueira, W. F. (2020). Review and meta-analysis of the importance of remotely sensed habitat structural complexity in marine ecology. *Estuarine, Coastal and Shelf Science*, 235. https://doi.org/10.1016/j.ecss.2019.106468

2.1 Summary

Habitat structural complexity is a key determinant of the distribution of marine biota. It exerts its influence across broad habitat types and within complex habitats via meditation of several abiotic and biotic processes and the provision of resources such as shelter from prey and water current and a surface for attachment and growth. Recent studies based on remote sensing have examined the role of various measures of complexity over large areas, various communities and biota, though until now there has been no attempt to review and synthesize the findings. This review and meta-analysis of 44 studies developed a standardised rank-based scoring metric ($Rs_{1\text{-}10}$) that enabled meaningful comparisons of the influence of various measures complexity and other predictors across these disparate studies. The main findings were:

- While measures of terrain variability and morphology were important, often in site- and species-specific circumstances, other predictors, including derivatives of hydroacoustic backscatter, abiotic and biotic habitat descriptors, and relative geographic location often outperformed measures of complexity.
- Of note, $Rs_{1\text{-}10}$ identified surface-rugosity, one of the most well-known, utilised and conceptualised measures of complexity, as the poorest performing predictor.
- Explanations for the generally poor performance of measures of complexity included the ability of other predictors to act as broad surrogates of other structuring environmental gradients, the ecological relevance of measures, and whether they capture complexity too broad or specific for the target organism, in addition to the potentially confounding role of spatial extent and resolution.

Having been identified, such considerations provide opportunities for improved design and implementation of the next generation of remote sensing studies with improved potential for the conservation of biodiversity and management of marine resources. In particular,

those based on photogrammetry, which can capture high resolution 3D models of the seafloor over extents far greater than that achievable using *in-situ* diver methods.

2.2 Introduction

The role of habitat structural complexity in the marine environment has received substantial attention. Early studies that measured structural complexity *in-situ* using divers identified strong relationships with marine biota, especially on coral reefs (reviewed by Graham & Nash, 2013). In this review of 140 studies, Graham & Nash, (2013) reported an overall (72% of studies) positive effect of increasing linear-rugosity (one measure of structural complexity) on various fish, invertebrate and coral responses, as well as ecosystem services such as tourism and shoreline protection. Their quantitative meta-analysis using data from 150 sites across the Indo-Pacific and Caribbean indicated a significant positive correlation between linear-rugosity and fish density, fish biomass and coral cover, and a significant negative correlation with algae cover and sea urchin density. However, these, and similar observational and experimental studies that examined the role of structural complexity were restricted in extent and the number of measures of complexity considered, often relying on one measure: refuge availability. Fish studies on coral reefs by far comprise most work undertaken on the influence of structural complexity. Far fewer have been undertaken on algae and invertebrates, though see Margiotta *et al*., (2016) and the density of oyster sprat and the density and size of crabs. It was also important for the settlement and habitat preferences of sponges, corals, and gastropods (Beck, 2000; Carleton & Sammarco, 1987; Russ, 1980).

Previous reviews focused on the structuring role of *in-situ* measures of complexity on coral reef fish communities (Graham & Nash, 2013), the utility of remotely sensed measures and other predictors in mapping of benthic habitat (Brown *et al*., 2011) and identifying coral reef fish-habitat relationships (Mellin *et al*., 2009). None synthesised findings from across a range biota from temperate, sub-tropical and tropical reefs or investigated in detail the differences and similarities in abiotic-biotic relationships among different measures of complexity. We reviewed and conducted a meta-analysis of the current knowledge about the influence of structural complexity on the distribution of marine biota, based on the findings of remote sensing studies. Specifically, we asked how previous studies measured structural complexity in the marine environment, how does the predictive power of these measures compare, what is the influence of spatial extent and resolution and what does this indicate about the underlying ecological mechanisms? Ranking different measures of structural complexity according to their predictive potential via a standardised rank-based

metric enabled an objective comparison across studies with disparate aims and methods. The primary intent is that this meta-analysis will facilitate the efficient and rapid development of future studies using remote sensing to quantify habitat structural complexity.

2.3 Methods

2.3.1 Study Selection

This review examined studies that have:

- Used remote sensing techniques, including hydroacoustic, LIDAR and satellite imagery, to obtain bathymetric data and construct digital elevation models (DEMs) and occasionally Triangular Information Networks (TINs) of the seafloor; and
- Derived one or more measures of structural complexity and used these to predict the distribution of marine biota.

A comprehensive search of the IS Web of Science was undertaken using the following keywords: habitat AND complexity AND structural AND fish OR invertebrate OR alga OR algae. Only studies that met these criteria and were published up to and including 2016 were retained. Other relevant studies cited within these were examined and retained were they met these criteria. Studies included in key previous reviews (Mellin *et al*., 2009; Brown *et al*., 2011; Graham & Nash, 2013) were also examined and included where they met the criteria. A total of 44 studies were reviewed, 36 were examined using response categories and 34 were retained for derivation of the standardised rank score (see below).

2.3.2 Measures of Complexity

Measures of structural complexity and other associated environmental predictors (hereafter referred to as predictors) were placed into broad categories based partly on those provided by Wilson *et al*., (2007a) (**Table 2-1**). Linear-rugosity measured *in-situ* was included only where it was considered alongside other remotely sensed metrics of structural complexity.

2.3.3 Study Focus and Broad Performance

Study focus was explored by categorising studies by biotic group: fish, sessile invertebrates, mobile invertebrates, algae, benthic infauna and mixed (i.e., more than one group). The number and type of predictors (**Figure 2-1**) used across all studies was also examined. Model performance (% variance / deviance explained) among fish, sessile invertebrates and algae (the groups for which a relatively larger number of studies were

Table 2-1 Measures of habitat structural complexity and other associated environmental variables used as predictors of the distribution of marine biota in remote sensing studies included in Section 2.

Predictor	Definition / Description
Habitat Structural Complexity	
Terrain Variability	
Linear-rugosity (LinRug)	Two-dimensional measure of complexity provided by the ratio of convoluted distance to Euclidian distance between two points. Often measured by SCUBA divers *in-situ* using the 'chain and tape' method. The length of chain and chain link provide the spatial extent and resolution of the measure, respectively. Equivalent, virtual methods also exist for DEM and TIN constructs of the seabed derived from remote sensing.
Surface-rugosity (SurRug)	Three-dimensional measure of complexity provided by the ratio of convoluted area to planar area of a DEM or TIN surface. The area provides the spatial extent and DEM pixel or grain size the resolution of the measure. Also known as planar and 3D rugosity.
Bathymetric-range (BathRan)	Maximum minus minimum bathymetry within an area.
Bathymetric-variance (BathVar)	Variability (e.g., standard deviation) of bathymetry values within an area.
Terrain Morphology	
Bathymetric-position-index (BPI)*	Measure of the depth of a location relative to the surrounding area, provides an indication of elevated (+) and (-) depressed terrain features.
Slope (Slope)	Rate of change in bathymetry between a DEM cell and its neighbouring cells.
Slope-of-slope (SloSlo)	Rate of change in slope (analogous to curvature in its simplest form)
Curvature (Curv)	Several related measures that quantify rate of change in slope in various directions. For example, profile (degree of concavity/convexity parallel to the direction of maximum slope) and planar (degree concavity/convexity perpendicular to the direction of maximum slope) curvature. The latter provides a measure of terrain morphology associated with ridges and channels. Various summary measures such as maximum, minimum and mean curvature may be used.
Orientation (Orien)*	Also known as aspect, a measure of the azimuthal direction a location is facing (i.e., direction of greatest slope) expressed in degrees from an arbitrary 0 (usually north).
Other-complexity (OthComp)	These Include: Terrain Ruggedness Index: measure of the local variation in seabed terrain about a central pixel. Reef volume: volume under three-dimensional DEM surface to the minimum Z value for that area that combines Surface Rugosity and elevation, or bathymetry, and accounts for surface variations and differences in elevation (Walker *et al*. 2009). Fractal Dimension: measure of surface complexity between a flat surface and a complete space filling complex surface. Vector ruggedness measure / Terrain Rugosity (TerRug): combination of variation in slope and orientation Categorical: presence of various categories of complexity and discrete geomorphological features (often assessed visually)
Geographic	
Geographic (Geo)	Measures of location on the earth' surface such as geographic coordinates and smaller scale measures of relative location with respect to the proximity of nearby habitats of varying quality / suitability (e.g., distance to sand, reef etc.).
Other	
Bathymetry (Bath)	Bathymetry, or water depth, can act as surrogate for several abiotic variables associated with such as temperature and light availability that may act as direct determinant of biotic distributions related with their physiological tolerances.
Habitat (Hab)	Includes abiotic (e.g., substratum type such as sand or rock) and biotic (e.g.,% coral cover) descriptors obtained from several sources such as direct sampling, visual assessment etc. Includes measures of habitat richness and diversity.
Backscatter (Back)	Provides a direct measure of seafloor 'hardness' and habitat or substratum type (often soft sediment and rock reef) determined from the intensity of the hydroacoustic return signal. The variability (e.g., standard deviation) in return signal also provides a measure of seafloor 'roughness' and terrain variability. A further derivative, Hue Saturation Intensity (HSI), may also be used to accentuate and quantify relatively broader terrain morphological features
Management-zone (ManZon)	Whether the study area or a portion of the study area experiences management actions that may influence the number and type of biota present here. For example, marine protected areas.

*Both these could be considered measures of relative location, similar to geographic measures. However, as they are both associated with the certain physical structural elements of the seafloor, they have been placed within terrain morphology for this review.

available) and among species (e.g., species abundance), group (e.g., family, functional, trophic abundance) and assemblage (e.g., species richness, total abundance, diversity index) response levels were examined using Poisson GLM.

2.3.4 Predictor Performance

The utility of predictors was examined initially by categorising the type of relationship with the response variable as: 1) positive, 2) negative, 3) otherwise significant (direction not reported and significant at $P \leq 0.05$ or retained in final model) and 4) non-significant ($P > 0.05$ or not retained in final model). Non-linear relationships were determined primarily via interpretation of partial dependence plots and were included within otherwise significant.

A standardised rank score ($Rs_{1\text{-}10}$) was developed that provided an objective measure of the relative predictive power of predictors among biotic groups. This enabled meaningful comparisons and the identification of overall patterns otherwise not possible given the various modelling techniques, performance metrics and different numbers and types of predictors used across the studies. The score ranked predictors by their predictive performance and included a standardisation to the total number of predictors considered in an individual model. When the number of predictors ranged from 2 to 10 (as was the case here), it provided 54 individual values corresponding to the 54-total number of predictor / rank position combinations. Importantly, this ensured that scores always reflected the number of predictors ranked more and less important. The potential for bias associated with collinearity in the occurrence of predictors was evaluated using diagnostic checks described below.

To derive ($Rs_{1\text{-}10}$), first, the raw rank score (R) was determined for each predictor in each final model via 1) the relative contribution / importance to species distribution models and regression type analyses, 2) the comparison of correlation coefficients or coefficients of determination, 3) the results of stepwise Multiple Linear Regression model selection or 4) results reported in text or graphics. The standardised rank score (Rs) was calculated by subtracting from R the mean of the rank scores for each model and then dividing by the standard deviation. For ease of interpretation, Rs was scaled from 1 to 10 (10 being most important, 1 the least), where:

$$Rs_{1\text{-}10,} = ((Rs - Rs_{Min}) * 9)) / Rs_{max\text{-}min}) + 1$$

Only studies that included two or more predictors were used to derive $Rs_{1\text{-}10}$ (total of 34 studies). Where predictors were ranked of equal importance (i.e., where the performance measure was equal and where presence / absence of predictors in the final model was

reported but their relative importance was not) $Rs_{1\text{-}10}$ was distributed equally across all predictors. When the relative importance of only an arbitrary number of the most important predictors was reported, the sum of $Rs_{1\text{-}10}$ for the remaining ranks was distributed equally across those predictors not reported. For example, where the relative importance of only the two most important predictors was reported from a five-predictor model, the $Rs_{1\text{-}10}$ for each of the remaining three predictors was the average of the three lowest of a five-predictor model. Predictors not involved with a significant ($P \leq 0.05$) relationship or not included in final models scored zero and counted towards calculation of mean $Rs_{1\text{-}10}$ and std for each predictor. Studies that did not report presence / absence of predictors in the final model were not included in the meta-analysis but were included in the review. $Rs_{1\text{-}10}$ was calculated using information from all taxa (149 models in total), and for fish and sessile invertebrates, those groups that comprised the majority, 93 and 30, respectively, of all models.

Comparison of mean $Rs_{1\text{-}10}$ scores for each predictor provided an indication of their overall relative importance rather than the amount of variation explained. As a diagnostic check of potential bias due to any collinearity in the presence of predictors in models, the phi correlation coefficient of the occurrence of pairs of predictors in models was examined. This provided little evidence of strong correlations between pairs of predictors with divergent Rs scores (i.e., high scoring predictors did not occur consistently alongside those that scored poor, and vice versa). This was evident as low and non-significant ($P > 0.05$) correlations between the strongest and poorest performing predictors. As a further diagnostic check of bias due to a correlation between performance and the total number of predictors considered in each model, the Pearson correlation coefficient between mean $Rs_{1\text{-}10}$ for each predictor and the mean number of predictors in the model was calculated. This did not provide cause for concern ($r = 0.14$, $P = 0.61$).

2.4 Results

2.4.1 Study Focus and Broad Performance

Of the 44 studies reviewed, fish and sessile invertebrate studies were most common (21 studies each), followed by mobile invertebrates (6 studies), algae (4 studies), mixed groups of algae and invertebrates (5 studies) and benthic infauna (1 study) (**Table 2-1**). A wide range of remote sensing, survey and statistical methods, DEM resolutions, spatial scales and response variables were considered across a range of study areas. Nevertheless, some broad groupings were evident. Several fish studies investigated the use of measures of complexity derived from relatively new remote data capture methods (LIDAR

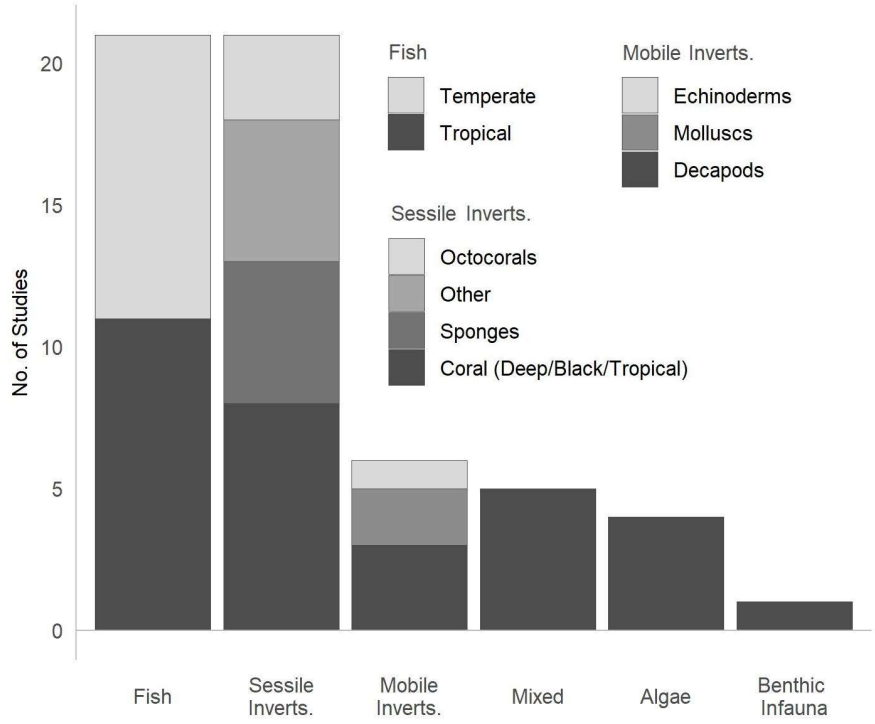

Figure 2-1 Biotic group focus of remote sensing studies that examine the role of habitat structural complexity. Corals include deep/cold water (7 studies) and tropical (1 study) taxa.

imagery from aircraft and satellites) to predict the distribution of coral reef species (Catano *et al*., 2015; Knudby *et al*., 2010, 2011; Kuffner *et al*., 2007; Pittman *et al*., 2009; Pittman & Brown, 2011; Walker *et al*., 2009; Wedding *et al*., 2008; Wedding & Friedlander, 2008). Temperate studies often used hydroacoustic remote sensing, primarily investigating the efficacy of measures derived from multibeam echosounding (MBES) to model the distribution of fish in America (Iampietro *et al*., 2008; Young *et al*., 2010), Europe (Martín-García *et al*., 2013) and Australia (Cameron *et al*., 2014; Coleman *et al*., 2016; Moore *et al*., 2009, 2010). Others examined the distribution of commercial species (Roos *et al*., 2015; Young *et al*., 2010) and / or compared statistical methods.

Sessile invertebrate studies often modelled distributions as part of broad habitat mapping exercises using MBES. These included those on octocorals (sea pens, soft corals, gorgonians) and sponges in Australia (Hill *et al*., 2014; Holmes *et al*., 2008; Rees *et al*., 2014; Woodby *et al*., 2009) and Norway (Gonzalez-Mirelis & Buhl-Mortensen, 2015). Hill *et al*., (2014) and Lucieer *et al*., (2013) investigated the influence of complexity on sponge morphology. Several studies examined the distributions of deep-water corals; the reef building (scleractinian) deep-water corals in the northern pacific (Woodby *et al*., 2009) and northern Atlantic, particularly *Lophelia pertusa* (Guinan *et al*., 2009; Howell *et al*., 2011; Rengstorf *et al*., 2013, 2014). These studies tended to be undertaken over spatial extents

up to 100s km using DEMs of relatively coarse resolution (10s m to 100s m). However, studies on *L. pertusa* and another deep-water coral *Madrepora oculata* by Dolan *et al*., (2008) and the black-coral *Antipathella wollastoni* in the Canary Islands by Martín-García *et al*., (2013) used resolutions of 0.5 m and 5 m, respectively.

Comparatively fewer studies examined algae and mobile invertebrates. These included those on red (e.g., Rhodoliths) and brown (e.g., Ecklonia, Lobophora) algae prevalence (Holmes *et al*., 2008) and % cover (Zavalas *et al*., 2014), prevalence of functional (e.g., canopy, understory) algal groups (Hill *et al*., 2014) in temperate Australia, and red and brown algae prevalence in the Canary Islands (Martín-García *et al*., 2013). Mobile invertebrates examined included commercially important species; lobsters in Ireland (Wilson *et al*., 2007a), Spain (Galparsoro *et al*., 2009) and Australia (Young *et al*., 2016), scallop in Canada (Brown *et al*., 2012), Crinoidea (Hill *et al*., 2014) and abalone in Australia (Jalali *et al*., 2015). A few studies, three Australian (Ierodiaconou *et al*., 2007, 2011; Rattray *et al*., 2009) and one Norwegian (Elvenes *et al*., 2014), examined mixed groups of algae and invertebrates.

Poisson GLM indicated models of algal responses performed best overall, followed by sessile invertebrate and fish, though the number of algae studies and models was low (**Figure 2-2a**). Model performance for species and group level responses was significantly greater than that for assemblage level responses (**Figure 2-2b**).

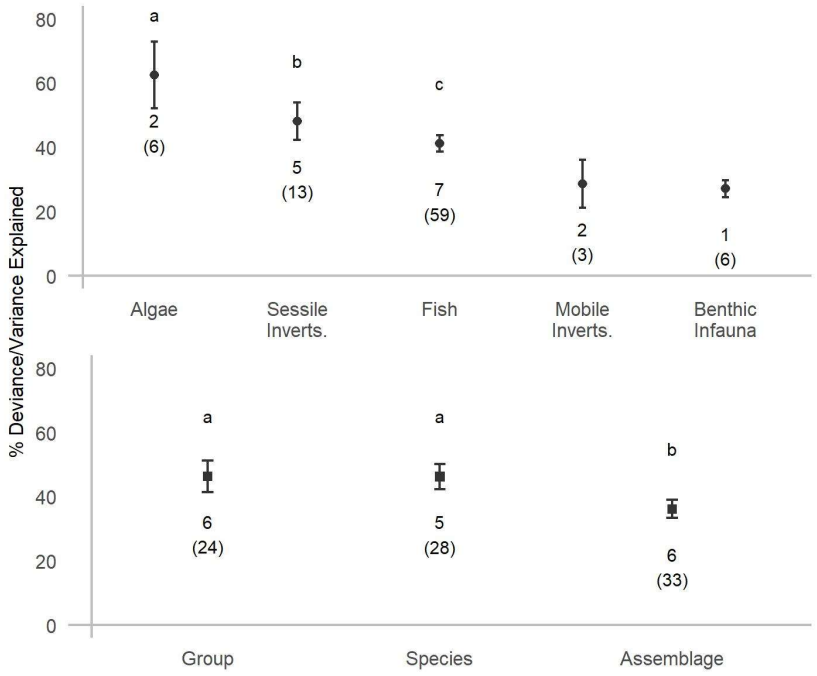

Figure 2-2 Model performance (mean% deviance / variance explained ± SE) a) among biota groups and b) among response levels. Numbers outside and inside parenthesis indicate number of studies and number of models, respectively. Different letters indicate significant differences at P < 0.001. Mobile inverts and benthic infauna were not modelled due to small sample size.

It is noted that most models of species and assemblage level responses were represented by fish: 25 of 28 and 24 of 33 models, respectively. Group level responses were represented relatively evenly by fish, algae and sessile invertebrates. The number and type of predictors varied considerably across studies. Bathymetry was most common followed by the complexity measures surface-rugosity, slope, BPI and orientation (**Figure 2-3**). Predictors were generally well represented across biotic groups, though backscatter was underrepresented in fish studies, and management zone was utilised in a few fish studies only.

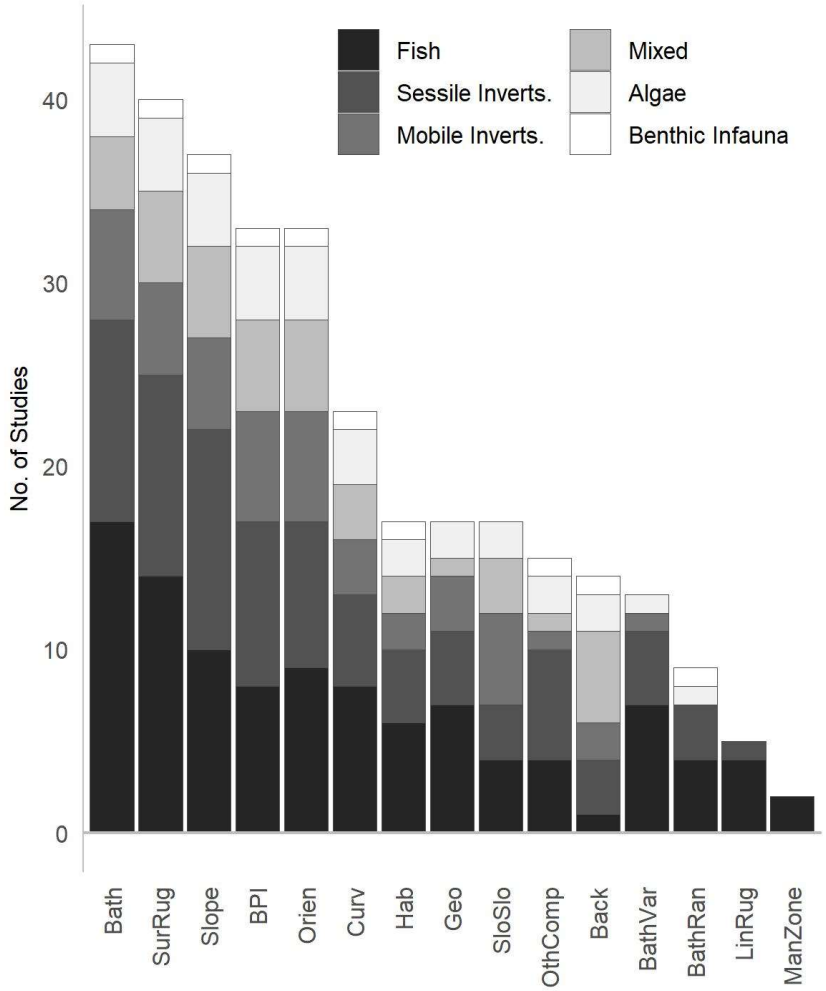

Figure 2-3 Use of measures of complexity and other predictors among taxonomic group. See Table 2-1 for explanation of measures of complexity.

2.4.2 Predictor Performance

$Rs_{1\text{-}10}$ indicated that the predictors linear-rugosity measured *in-situ* and geographic coordinates were the two most important overall (i.e., when using information from all 149 models across all taxonomic groups) and when calculated using models of fish only (**Figure 2-4**). They were also significant/retained in over 90% of models where they were considered (**Figure 2-5**). Geographic predictors (e.g., geographic coordinates and distance to

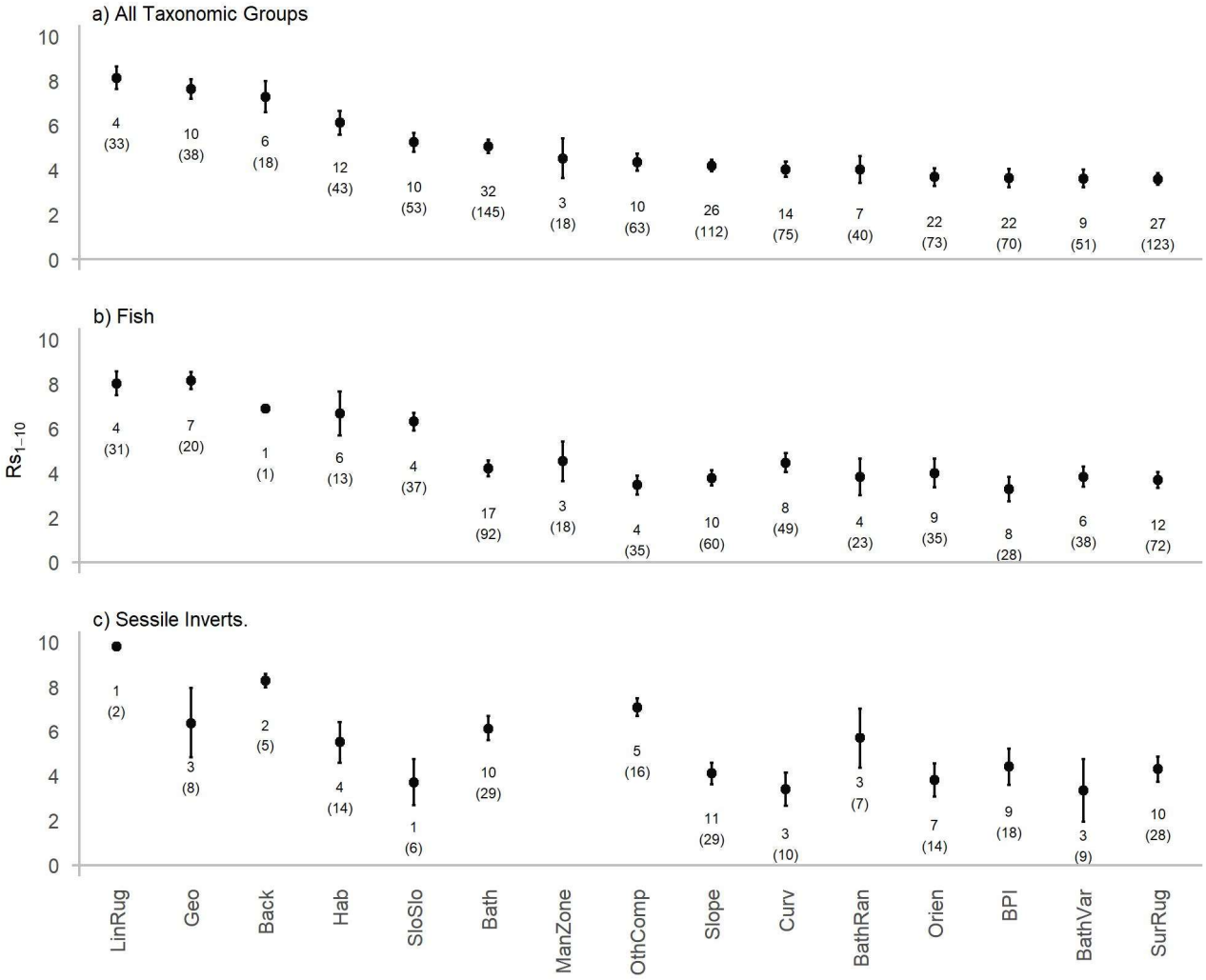

Figure 2-4 Mean standardised rank scores (Rs_{1-10}) (±SE) for predictors for models a) all taxa, b) fish and c) sessile invertebrates. Numbers outside and inside parenthesis indicate number of studies and number of models, respectively. See Table 2-1 for explanation of measures of complexity.

reef/sand) were considered in around one third of studies. Other important predictors included backscatter (and associated derivatives), which was significant / retained in just under 90% models and was third most important overall, the most important for sessile invertebrates and third most for fish (albeit included in one model only). Habitat (significant / retained in 80% models) was relatively important when all models were combined, as was bathymetry (significant / retained in 60% models). Notably, Rs_{1-10} ranked the importance of these predictors above those of all remotely derived measures of complexity (significant / retained in around 45% to 60% models). Slope of slope (retained in 94% models) was the only exception and was ranked above bathymetry when models of all taxa were combined and for models of fish.

Measures of complexity and other predictors, particularly surface-rugosity and 'other' complexity, appeared more likely to be significant / retained in models of sessile

invertebrates than fish (**Figure 2-5**). One possible exception was geographic predictors. The response of sessile invertebrates to increasing slope and surface-rugosity also appeared just as likely associated with a negative as it was a positive relationship, while the response of fish appeared more likely due to positive relationships.

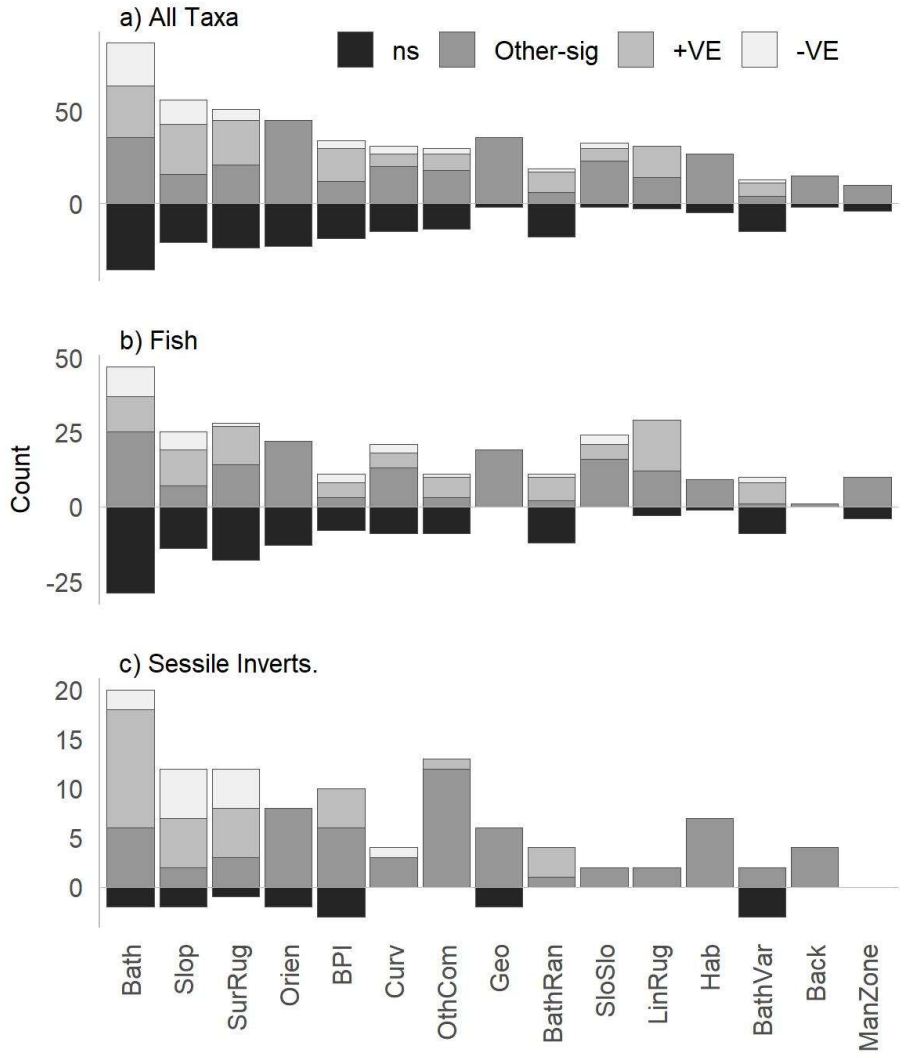

Figure 2-5 **Relationship type (positive, negative, otherwise significant (e.g., significant non-linear relationship or directionality not applicable) and non-significant) reported between predictors and various response variables when a) all models are combined and for models of b) fish and c) sessile invertebrates. Directionality not applicable for orientation, other complexity, geographic, habitat, backscatter and management. See Table 2-1 for explanation of measures of complexity.**

2.5 Discussion

2.5.1 Predictor Performance

2.5.1.1 Geographic Predictors

The importance of geographic predictors was evident in several studies, their predictive power often outweighing that of structural complexity. In their study of Puerto Rican coral reef fish, Pittman & Brown, (2011) found that distance to shelf edge and distance to shoreline were the two most influential predictors (out of a total of seven, including orientation, bathymetry and four remotely sensed measures of complexity) of fish species prevalence. These geographic predictors identified the preference of fish for areas offshore (10 km by 20 km study area) irrespective of reef structural complexity and despite mosaic of habitat types including seagrass, sand and coral reef. The overriding influence of geographic location across the study area also indicated that reefs of equal complexity may not necessarily provide equal habitat suitability. The importance of geographic measures was evident also in several other studies, including distance to reef and blue-throated wrasse (*Notolabrus tetricus*) occurrence in southeast Australia (Monk *et al*., 2011), distance to soft substrate and sediment associated brown garden eel (*Heteroconger longissimus*) prevalence in the Canaries and distance to reef/sand and temperate Australian fish species richness and abundance (Rees *et al*., 2014). In each case, the geographic predictor outperformed one or more measures of complexity. Management zone (e.g., location within or outside a marine protected area), which may also be considered a geographic predictor, was also an important predictor of fish biomass (Wedding *et al*., 2008).

Geographic predictors were also influential for sessile invertebrates, mobile invertebrates and algae, though possibly less so than for fish. Hill *et al*., (2014) found the prevalence of octocorals in southeast Tasmania was explained best by their location (easting and northing coordinates) across the 117 km^2 study area, outperforming several measures of complexity, substratum type, bathymetry and backscatter. Geographic coordinates were also the second largest contributors, after bathymetry, to models of encrusting, understory and canopy algae prevalence and sponge morphological richness. Their importance seemed to reflect the affinity of invertebrates and algae for offshore reef, as well as an algae/invertebrate depth zonation. Prevalence of European lobster (*Homarus gammarus*) on the sand-reef coastline of northern Spain was explained best by distance to rock reef, the most influential of several predictors, followed closely by BPI and slope, reflecting a strong preference for areas closer to rock (Galparsoro *et al*., 2009). Along with slope and bathymetry, distance to sand was one of the three most important predictors of

for mixed algae groups examined by Martín-García *et al*., (2013), reflecting the general affinity of algae for rock substratum. Strong relationships with other invertebrates and algae were, however, less evident. Distance to sand was less influential for filamentous red and *Lobophora* spp. algae and for black-coral prevalence examined by Martín-García *et al*., (2013), where it was outperformed by BPI, bathymetry, and / or surface-rugosity. The apparent limited influence of distance to sand for algae likely reflected their preference for the sediment-rock interface, while the prevalence of black-coral appeared better identified by measures of complexity potentially able to capture its rugose biogenic structure. The importance of distance to soft sediment for fish reported by Rees *et al*., (2014) was also not evident for sessile invertebrates, which appeared associated more with habitat structural complexity captured using bathymetric range. The only exception here was latitude, which was retained in models of the structure of the multivariate assemblages of fish and sessile invertebrates.

The strong predictive performance of geographic predictors appeared related with their efficacy as surrogates of several important environmental gradients and habitat suitability responsible for structuring the distribution of biota over hundreds of metres to several kilometers. Importantly coarse habitat suitability, for example unconsolidated sediment versus rock reef (e.g., the preference of brown garden eel for soft-sediment). They may also provide a surrogate of anthropogenic influence, such as fishing pressure. Predictors that quantify geographic location over distances of several kilometres may also act as surrogates for broad-scale processes independent of habitat type, such as prevailing water current and its effect on food availability and larval recruitment etc. The structuring role of such processes would become increasingly evident over larger spatial scales. Geographic predictors may act as surrogates of several abiotic variables such as bathymetry, temperature, salinity, turbidity etc. that will influence the distribution of biota directly. It is possible also that site attached sessile invertebrates and algae, which appeared somewhat less influenced by such predictors, are influenced more by local processes such as local current velocity and hydrodynamics, which in turn are influenced by structural complexity, rather than any broader scale processes captured by geographic predictors.

2.5.1.2 Habitat

The importance of more direct measures of habitat attributes was evident in several studies. These included categorical and continuous predictors associated with abiotic and biotic habitat / substratum type, abundance and diversity derived from remote sensing and direct sampling. Often, these outperformed measures of complexity. Abiotic and biotic based

habitat categories were relatively strong predictors of coral reef fish richness, diversity and biomass in Fiji (Knudby *et al*., 2011) and backscatter derived substratum categories and octocoral (Gonzalez-Mirelis & Buhl-Mortensen, 2015) and *L. pertusa* (deep-water coral) (Howell *et al*., 2011) prevalence in Norway and the North Atlantic, respectively. Sediment composition from grab sampling was also, perhaps unsurprisingly, a strong predictor of benthic infauna richness and abundance, outperforming several measures of complexity (Huang *et al*., 2014). Importantly, habitat categories may capture variation in habitat structural complexity not captured by remote and *in-situ* methods. Moore *et al*., (2009) found the presence of solid reef and boulders obtained from MBES and towed video (Holmes *et al*., 2008) explained 74% of the deviance in eastern blue grouper (*Achoerodus viridis*) prevalence in southeast Australia, however, surface-rugosity and other measures of complexity were not included in the final model. Similarly, the presence of boulders (same dataset), explained 12.5% of the variation in fish assemblage structure (behind only bathymetry explaining 23%) (Moore *et al*., 2009). Moore *et al*., (2009) found only one of the several measures of complexity, including surface-rugosity, slope, and BPI, was associated with any amount of dissimilarity in assemblage structure, that being bathymetric range explaining 1.4%. This was despite a mosaic of reef, sand-reef and sand habitat of varying complexity and the observation that the sand supported the fewest species of fish. Such results do not necessarily indicate that complexity was not important to fish, just that captured by the measures considered. It is possible the poor predictive power of measures of complexity here may have partly been explained by collinearity with bathymetry, with reef located in shallower near shore areas and soft sediment within deeper areas offshore (Moore *et al*., 2009).

2.5.1.3 Backscatter

Habitat categories are often derived from hydroacoustic backscatter, with backscatter intensity providing a measure of the ‘hardness’ of the seafloor and a surrogate of habitat / substratum type (e.g., sand, reef and boulders). It may also be processed, sometimes with imagery and expert inference, to derive habitat based categorical predictors (Gonzalez-Mirelis & Buhl-Mortensen, 2015; Howell *et al*., 2011). Unprocessed backscatter intensity data also provide a continuous predictor that may better capture variation not captured by broad categories. It outperformed several measures of complexity in the prediction of sponge distribution in Norway (Buhl-Mortensen *et al*., 2009) due to its ability to discriminate amongst various unconsolidated substratum types, and sea scallop (*Placopecten magellanicus*) prevalence across reef and unconsolidated substratum in Canada (Brown *et*

al., 2012). It was also used by Monk *et al*., (2011) to predict blue-throated wrasse prevalence across rock reef in southeast Australia, outperforming some measures of complexity (BPI and orientation) but not others (surface-rugosity).

Standard deviation (std) of backscatter intensity, or substratum 'roughness', may also be used as a direct measure of complexity and terrain variability. It was overall the third most important predictor of algal, sessile and mobile invertebrate prevalence and sponge morphological richness in Tasmania, Australia (Hill *et al*., 2014), outperforming several remotely derived measures of complexity, particularly surface-rugosity, which was a relatively poor predictor. It contributed substantially to models of soft corals, gorgonians and crinoids, reflecting their patchy distribution and preference for 'rough' or complex reef and its associated mediating effect on local hydrology and feeding efficacy of passive filter feeders (Hill *et al*., 2014). Compared with bathymetry and its effect on light availability, complexity measured by std of backscatter was far less important for canopy, encrusting and understory algae groups, suggesting these photosynthetic organisms were less influenced by local hydrodynamics mediated by complexity. This may have explained the relatively less restricted and less patchy distribution predicted for algae and for active filter feeding sponges that are possibly less reliant on local hydrodynamic flows than passive feeders. Overall, (Hill *et al*., 2014) found other measures of structural complexity, including surface-rugosity, slope, and curvature, contributed relatively little to final models. Few other studies included std of backscatter, though it was correlated with sponge genre richness at a depth of 100 m to 600 m in southeast Australia (Schlacher *et al*., 2007).

2.5.1.4 Structural Complexity

According to $Rs_{1\text{-}10}$, measures of terrain variability were overall relatively poor predictors. Notably surface-rugosity, which was the most common measure of complexity utilised and overall the poorest performing of all predictors. In a few instances, surface-rugosity was found influential and was the first or second most important predictor in models of *L. purtusa* relative abundance (Guinan *et al*., 2009) and blacklip abalone (*Haliotis rubra*) (Jalali *et al*., 2015) and *A. wollastoni* (Martín-García *et al*., 2013) prevalence. Its relationship with black-coral appeared due to its ability to distinguish structurally complex biogenic coral structure from surrounding low complexity substratum (mud, sand and gravel) even at a DEM resolution of 5 m. Surface rugosity was also a somewhat important predictor of fish species richness and abundance on reefs of varying complexity (Walker *et al*., 2009) and of biomass across mixed sand-reef in Hawaii (Wedding *et al*., 2008). In these studies, the R^2 value (significant models at $P \leq 0.05$ only) for species richness and abundance (data from

all habitats combined) was 0.16 and 0.19, respectively, and for biomass (averaged across all 4 spatial scales examined) it was 0.47. To place this in some context, in their review of the use of linear-rugosity measured *in-situ* (chain length 3 m to 50 m, link size generally < 1.5 cm) to predict coral reef fish density and biomass, Graham & Nash, (2013) found an overall significant Spearman's rank correlation r of 0.71 (r^2 = 0.50) from 52 observations from 8 studies and 0.80 (r^2 = 0.64) from 56 observations from 5 studies, respectively. Indeed, when linear-rugosity measured *in-situ* was examined alongside remotely derived measures it was often a stronger predictor of various fish community metrics than was complexity derived from remote sensing (Pittman *et al*., 2007, 2009; Walker *et al*., 2009; Wedding *et al*., 2008), though see (Kuffner *et al*., 2007) who reported a generally poor predictive power of *in-situ* and remotely derived measures. The utility of *in-situ* rugosity is almost certainly reflective of a chain link size (i.e., resolution) equivalent to the size of fish and their refuges, much finer than the resolution achievable using remote sensing methods (0.5 m and coarser). On occasion, another measure of terrain variability, bathymetric variability, was relatively important, including the prediction of fish species richness and total abundance (Wedding & Friedlander, 2008) and prevalence (Moore *et al*., 2009).

Similarly, measures of terrain morphology were generally poor predictors except in a few specific circumstances. BPI identified seafloor depressions preferred by *H. gammarus* (Galparsoro *et al*., 2009) and elevations preferred by squat lobster (*Munida* sp.) (Wilson *et al*., 2007a), algae (Holmes *et al*., 2008; Martín-García *et al*., 2013) and *A. wollastoni* (Guinan *et al*., 2009). It appeared less important for other sessile invertebrates and fish, though see Holmes *et al*., (2008) and Moore *et al*., (2009) where it identified preference of ascidians for elevations, and green moray eel (*Gymnothorax prasinus*) for depressions, respectively. The importance of slope was apparent across a broad taxonomic range including algae (Martín-García *et al*., 2013), *L. pertusa* (Guinan *et al*., 2009; Rengstorf *et al*., 2013, 2014), and fish (Wedding & Friedlander, 2008). The related but less commonly utilised measure slope-of-slope was also an important predictor of the distribution of coral reef fish in Puerto Rico (Pittman *et al*., 2009; Pittman & Brown, 2011) and of temperate reef fish (Cameron *et al*., 2014) but less so sessile invertebrates and algae (e.g., Hill *et al*., 2014), in Tasmania. Overall, the response to these two measures was equivocal, with preferences for both flat and sloping terrain evident within each biotic group. Black-corals and deep-water corals appeared associated with sloping terrain, though see (Dolan *et al*., 2008), while the two studies that examined octocorals (Hill *et al*., 2014; Woodby *et al*., 2009) both suggested a preference for flatter terrain. Some fish preferred sloping, e.g., southern hulafish (*Trachinops caudimaculatus*) (Cameron *et al*., 2014) and others flat, e.g., blue-spotted flathead

(*Platycephalus caeruleopunctatus*) (Moore *et al*., 2009) terrain. Mobile invertebrates may also show a preference for both flat, for example rock lobster (*Jasus edwardsii*) (Young *et al*., 2016), and sloping, for example *H. gammarus* (Galparsoro *et al*., 2009), terrain. Constantly sloping, rather than curved, terrain was also associated with greater total fish abundance (Wedding & Friedlander, 2008) and piscivore and grouper biomass (Pittman *et al*., 2009).

Cameron *et al*., (2014) provided strong evidence of the role of another closely related measure, curvature, in this case profile-curvature, across a rocky southeast Tasmanian reef. It was a relatively important predictor of fish species richness and one measure of diversity, with each displaying a preference for concave, and convex, profiles, respectively. Several other fish, including *N. tetricus* preferred flat, rather than curved, profiles as identified by the measure plane morphometric (proportion of cells that do not lie on a concavity / convexity). The performance of channel morphometric (proportion of cells that in a local concavity) also identified the preference of brown-striped leatherjacket (*Meuschenia australis*) for channels. Squat lobster also appeared associated with negative planar-curvature and positive profile-curvature, indicative of channels within convex profiles (Wilson *et al*., 2007a). Orientation, a further morphology measure, was overall the most important predictor of fish distributions by Cameron *et al*., (2014). In this case deviation from east / south was the most important predictor of fish species richness, and abundance of little weed whiting (*Neoodax balteatusl*), *M. australis*, senator wrasse (*Pictilabrus laticlavius*) and *T. caudimaculatus*, out-performing several other measures of complexity. Responses tended to be greater at sheltered north and west (landward) facing sites indicating east and south facing sites exposed to swell and wave energy provided less suitable habitat. Several other, less common, measures of terrain variability and/or morphology were sometimes used with varying success. Fractal-dimension, a measure of rate of increasing complexity with measurement scale, rather than any discrete feature, was a moderately important predictor of *Munida* sp. prevalence (Wilson *et al*., 2007a). Reef volume, which combines surface-rugosity and bathymetry, showed some potential in the prediction of coral reef fish distributions (Walker *et al*., 2009). Vector ruggedness, which combines variation in slope and orientation, was also an important predictor of filamentous red algae prevalence (Martín-García *et al*., 2013).

The structuring role of measures of complexity is likely to a large degree associated with hydrodynamic flows over and around curved and convoluted surfaces. These surface irregularities mediate water movement, enhancing turbulence and providing various biota

shelter from water currents and wave energy. The importance of orientation (e.g., Cameron *et al*., 2014) indicates how the mediation of current and wave energy by habitat structure may be particularly important for fish. Galparsoro *et al*., (2009) also reported lobsters been more active in the lee of ridges, possibly where they are sheltered from prevailing current. Elevated flows over sloping terrain and elevations may also provide more food in the form of suspended particles for sessile filter feeders (e.g., Guinan *et al*., 2009; Holmes *et al*., 2008) and reduce sediment inundation. Variability in current velocity and sheer stress will also influence the suitability of substratum for site attached sessile invertebrates and algae. Slope, orientation and relative height (i.e., BPI) will also affect the level of light irradiance received by photosynthetic biota with implications for the distribution of other organisms. The importance of local-scale complexity may be especially important to non-mobile organisms unable to select their habitat after settlement, possibly explaining the better performance of predictive models, compared with those for fish, as indicated by comparison of model performance and relative proportion of significant relationships reported in this review. As well as providing a greater number and variety of refuges, complex terrain may also be more productive, providing a greater surface area for attachment of algae and sessile invertebrates. It is worth noting also that the utility of some measures may not necessarily be related with such mechanisms, but rather complex biogenic (e.g., *A. wollastoni*) structure directly (Martín-García *et al*., 2013) or broad habitat reference e.g., Moore *et al*., (2009)) and *P. caeruleopunctatus*

2.5.2 Why are measures of complexity often-poor predictors?

2.5.2.1 Other predictors may be more important

Although the importance of hydrodynamic flows in benthic environments would suggest strong relationships between measures of complexity and the distribution of biota, the overall predictive performance of these measures appeared relatively low. There are several potential reasons for this. One is the overriding influence of broader scale environmental gradients for which geographic predictors may act as surrogates (e.g., Pittman & Brown, 2011). The influence of such measures may be most evident when the study area is large and intersects these gradients. The geographic predictors identified by Hill *et al*., (2014) and Pittman & Brown, (2011) were derived over several kilometres of exposed coastline and their importance was likely associated with a range of influential physical oceanographic covariates. The importance of broad-scale geographic predictors may also not be surprising when the distribution of biota is examined over similar spatial extents. Geographic predictors provide a relatively static, easy to quantify surrogate that may indirectly covary with a wide

range of dynamic gradients in environmental conditions including those that are problematic to quantify accurately at appropriate spatial and temporal scales (Pittman & Brown, 2011). As well as their utility as surrogates for abiotic variables including structural complexity, geographic predictors, unlike measures of complexity, are scaleless quantities with applicability regardless of measurement scale. Such generality, however, may make it difficult to identify the specific surrogacy relationships and they are likely to have poor model portability.

2.5.2.2 Variability and specificity in the relationship across biotic groups and taxa

The type of response variable, and whether it is based on the response of several functionally unrelated taxa (e.g., total fish abundance) or the response of individual or groups of related species may also influence model performance. The reduction of several individual responses to a single assemblage level metric may mask otherwise strong relationships at the level of species. The difference in predictive power between assemblage and group/species level responses provides some evidence to support this, though see Wedding & Friedlander, (2008) and Rees *et al*., (2014) where prediction of fish and sessile invertebrate assemblage level responses, respectively, was strong. Coleman *et al*., (2016) postulated that the generally poor relationships between fish metrics and measures of complexity they observed were due to several trophic and functional levels grouped within one response masking otherwise potentially strong relationships. The predominance of wider ranging transient species in the video transects, rather than more cryptic and site-attached species more strongly associated with complexity present at the scales examined, may also have been an influence (Coleman *et al*., 2016). The inclusion of fish species not strongly associated with the substratum may also have explained the generally low predictive power of complexity measured *in-situ* by Sale & Douglas, (1984).

While such considerations may be relevant to all predictors, they are perhaps more so for measures of complexity if associated relationships tend to be species specific. Discreet morphological features of the seafloor may influence some species, but not others. Responses may also be highly site specific, with the strong influence of orientation such as that reported by Cameron *et al*., (2014) likely to occur under only certain geographic and oceanographic conditions (i.e., exposed shores). Lack of a consistent measurement unit in the case of orientation (i.e., deviation from south, deviation from east etc.) and directionality of the structuring influence (e.g., prevailing swell) would also hinder model portability. Such characteristics would be shared by other site-specific predictors such as geographic location and distance to sand / reef. There was also evidence that habitat type may influence the

identification of relationships with complexity. The overall poor correlation between surface-rugosity and fish species richness in Kuffner *et al*., (2007) was attributed to inclusion of only one habitat type (isolated patch reef). Compared with contiguous reef, fish distributions here appeared more affected by stochastic recruitment events rather than post-settlement migration and habitat selection more likely to be influenced by complexity.

2.5.2.3 Threshold, non-linear and interactive effects

Non-linear relationships, threshold effects and interactions between predictors may also hinder the identification of relationships if not accounted for. Statistical methods such as regression trees and GAMs can model such relationships, and when utilised invariably identified non-linearity. For example, a clear threshold effect was evident in the density of threespot damselfish (*Stegastes planifrons*) with surface-rugosity, with a substantial increase following only a slight increase beyond 1 (flat surface) followed by a more gradual increase and eventually a plateauing as it increased further (Pittman *et al*., 2009). Similar responses were seen in this and other reef fish species by Pittman & Brown, (2011) with clear non-linear and threshold effects evident and involving curvature, slope-of-slope, bathymetry and distance to shelf / shore. Of note was a threshold effect evident in coney prevalence, with an abrupt increase approximately 2,000 metres from the shelf edge. Rees *et al*., (2014) also identified such effects with sessile invertebrates, with abundance and richness both increasing with bathymetric range up to 12 m before plateauing. Some studies also indicated an affinity of the response with an intermediate level of the predictor, indicating an optima predictor value. For example, prevalence of *S. planifrons* peaked around 6 km to 8 km offshore and at a slope value of 5 (Pittman & Brown, 2011). Such effects were also evident for temperate reef fish (Cameron *et al*., 2014), sessile invertebrates and algae (Hill *et al*., 2014) and benthic infauna (Huang *et al*., 2014). Interactive effects were also reported by Cameron *et al*., (2014), with greater fish species richness on more southerly facing, higher BPI value reefs, greater diversity at shallower, lower curvature reefs, and more *T. caudimaculatus* on greater curvature, steeper reefs.

The existence of geographical threshold effects may be related to life-history strategies, such as whether a species is a habitat specialist with a critical dependence on a single habitat type, or a generalist capable of using multiple habitat types and geomorphological zones (Pittman & Brown, 2011). They also indicate how a resource, such as any quantified by measures of complexity, may not always be limiting. The consequence of such effects is that failure to capture critical thresholds and thus discrete constraints on habitat suitability and particularly influential ranges of predictor values could result in incorrect conclusions.

Relationships may also be misidentified entirely if a truncated response is not captured. Such findings highlight the importance of using techniques that can model non-linearity and the need to survey across scales that represent the entire range of the predictor variables (Hill *et al*., 2014). Again, such effects would be relevant to all predictors, though in this case it is less clear if relationships involving measures of complexity are more likely to be associated with strong threshold effects and non-linear relationships.

2.5.2.4 Ecological Relevance

The ecological relevance of the specific element of complexity captured by each measure of complexity, and the generality and specificity of measures of terrain variability and morphology, respectively, would also be an important determinant of predictive performance. In their review of the characteristics of habitat complexity in aquatic systems, Tokeshi & Arakaki, (2012) described five 'traits' of habitat structural complexity:

1. Scales of habitat complexity;
2. Diversity of elements;
3. Spatial arrangement of elements;
4. Sizes of elements; and
5. Abundance of elements.

A possible further trait would be the type of element, such as refuge morphology (i.e., its shape and size) and specific coral growth form etc. Together, these traits follow the realisation that habitat structural complexity does not simply encompass the gross abundance of structural elements, but also different characteristics of complex structure. Any structure that results in an increase in the heterogeneity of the physical environment would be considered an element of complexity. Measures of terrain variability such as linear and surface-rugosity are associated primarily with the size and abundance of elements. However, they are not necessarily affected by variation in the diversity or spatial arrangement of elements. A habitat with several depressions (**Figure 2-6a**) would have the same rugosity (linear or otherwise) as a habitat with the same number of identical elevations (**Figure 2-6b**) as would a habitat with half the number of each (**Figure 2-6c**). While rugosity would be identical, the third habitat could be considered to have a greater diversity of elements and, thus, a greater overall total complexity, not reflected in such a measure. This would have ecological relevance, and it is easy to consider how a habitat with both depressions and elevations, and the greater range of niches that this would afford, would likely support a greater number of species. Similarly, measures such as rugosity do not account for the spatial arrangement of elements in a habitat. It would not distinguish between

a habitat where elements are spaced equally throughout the habitat area (**Figure 2-6c**), and a habitat where they were clustered together in one or more groups (**Figure 2-6d**).

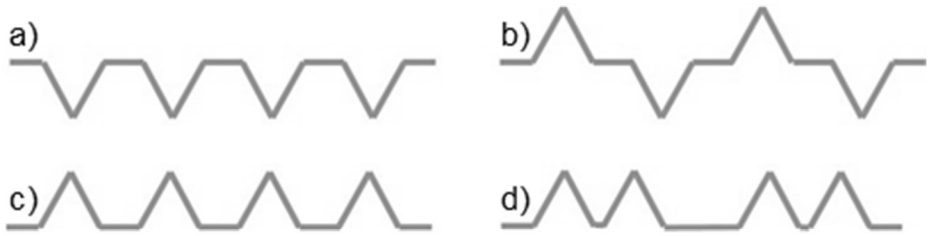

Figure 2-6 The complexity of each of these habitats (a to d) measured using rugosity would be the same, however, they differ in other aspects of complexity including diversity (i.e., a vs c) and spatial arrangement (b vs d) of elements.

Thus, measures of terrain variability provide measures of overall complexity. They account for variability in the size and abundance of elements, but not their type, diversity and spatial arrangement. Each of these elements may or may not be ecologically relevant, and variability in one element may be masked by variability in another. The apparent poor overall predictive power of measures of terrain variability is likely also related to their low specificity, and thus inability to capture discrete and ecologically relevant elements of complexity. The utility of measures of terrain morphology on the other hand, which do quantify discrete and ecologically relevant elements, may be limited by their specificity. Without prior knowledge of elements of complexity relevant to the biota in question, it is likely that several would need to be considered to have a reasonable chance of identifying those of ecological relevance.

2.5.2.5 Role of spatial scale and resolution

The role of scale is likely a further reason why such measures of complexity are often poor predictors. The findings of Hill *et al*., (2014) provide a useful example. In this study, surface-rugosity and other measures of structural complexity derived from a 2 m DEM did not appear to capture ecologically relevant complexity present in the study area. Whereas geographic coordinates and std of backscatter effectively identified reefs for which sessile invertebrate and algae showed affinity. It is possible that the spatial scales (i.e., the DEM resolution and / or spatial extents) from which measures of complexity were derived could not discriminate between relatively complex reef and surrounding unconsolidated sediment. Importantly, while backscatter was gridded to 2 m, std of backscatter intensity may have captured variability in complexity present at sub-2 m resolution. The apparent inability of measures of complexity to discriminate reef from sediment in this study could be due to limited reef complexity at 2 m resolution. For example, if the reef provided refuges on the scale of centimetres to a few 10s of centimetres, but features such caves, overhangs and

boulders on the scale of metres were rare. The specific scale, the first trait of complexity defined by Tokeshi & Arakaki, (2012), is not only a determinant of the predictive power of various measures of complexity, but it also provides important insights in into how organisms respond to their environment.

The generally accepted importance of spatial scale in structuring the response of various biota has led to its consideration in many remote sensing studies examining the role of structural complexity. Several scales are often considered in an exploratory approach, either to help ensure important relationships are captured and improve predictive performance or specifically to identify those of relevance to target biota. On occasion, prior knowledge of the scale over which a species may respond was used to guide study design (e.g., Catano *et al*., 2015; Monk *et al*., 2011). The role of spatial scale has been examined using two methods; either varying the spatial extent or resolution over which measures of complexity are derived, methods 3a and 3b, respectively, in **Table 2-2**. In this context, spatial extent refers to the area associated with calculation of the associated complexity measure, for example, bathymetric range within a 10 m radius. Resolution refers to the grain, pixel, or cell size of the DEM from which such measures are derived. Spatial scale may refer to one or both components. Identification and consideration of the two in multi-scale studies is important, as each may be associated with different structuring mechanisms. A further term, window size, is used often to refer to the area over which these measures are derived, it is usually expressed as the number of DEM cells along one side of a square centered on the cell of interest (e.g., survey point). In such cases it is analogous to resolution.

Table 2-2 Approaches to deriving metrics of complexity from DEMs

Method	Description
1	Studies that derive measures of complexity at the resolution of the DEM using a 3 x 3 cell size moving analysis window (Wilson *et al.* 2007a). This provides a single value for each DEM cell, at a scale equal to the resolution of the DEM. Often used in species distribution modelling where a value of the response variable (e.g., presence / absence or occurrence of a species) is known for individual cells.
2	As for method 1), though values are summarised (e.g., mean, Std) within a certain spatial extent. This may be relevant to the survey methodology or ecology of target species and equal to the fish survey (e.g., transect) area, territory / home range area etc. Otherwise, it may be a more arbitrary area (e.g., expanding radii around the survey point). Alternatively, values may be calculated for each individual cell using a moving spatial extent. Often used for single scale analysis that model a response measured within a discrete area, such as individual sites or transects. Bathymetric range, bathymetric variance and BPI are calculated using this method.
3	Multi-scale studies that consider the role of scale by 3a) varying the spatial extent within which summary (e.g., mean and including BPI) values are derived or 3b) varying the resolution over which terrain variables are derived by keeping the DEM cell size constant and varying the size of the analysis window (e.g., 3 x 3, 9 x 9, 21 x 21 cells), or by varying the resolution of the DEM while keeping the size of the analysis window constant (e.g., 3 x 3 cells).

When considered, spatial extent and resolution were important determinants of predictive performance in each study that had an a-priori aim of investigating the role of

spatial scale (**Table 2-3**). Algae (Holmes *et al*., 2008), sessile invertebrate (Dolan *et al*., 2008; Guinan *et al*., 2009; Rees *et al*., 2014) mobile invertebrate (Galparsoro *et al*., 2009; Jalali *et al*., 2015; Wilson *et al*., 2007a), temperate fish (Moore *et al*., 2009; Purkis *et al*., 2008), and tropical fish (Knudby *et al*., 2010; Pittman *et al*., 2007, 2009; Pittman & Brown, 2011) studies all identified one or more discrete and important scales.

Pittman *et al*., (2009) found the top three predictors of total and trophic group fish biomass to include metrics of complexity averaged within both small (e.g., 15 m and 25 m radii) and large (100 m and 200 m radii) spatial extents. The importance of multiple scales may indicate differing structuring mechanisms, particularly when they are associated with different measures of complexity. Dolan *et al*., (2008) indicated how deep-water corals were more likely to occur on the southwest edges of sediment wave features, as identified by fine resolution BPI and orientation and associated with variability in localised bottom currents, while coarser resolution slope captured larger carbonate mound features that mediate hydrological patterns and influence sedimentation and food supply at broader scales. The relative influence of different predictors of fish (e.g., Coleman *et al*., 2016) and sessile and mobile invertebrates (e.g., Elvenes *et al*., 2014) may also vary with resolution and spatial extent. *H. gammarus* also responded to local variability in slope (captured using a 3 x 3 window and a 5 m DEM), and broader variability in BPI, quantified up to 500 m away (Galparsoro *et al*., 2009). The performance of fine resolution slope was attributed to the provision of shelter by the irregular seafloor and broader BPI the mediation of prevailing hydrodynamics. The same measure quantified over different spatial extents may also capture different ecologically relevant processes, for example BPI and *H. rubra* (Jalali *et al*., 2015). The inclusion of multiple scales may not, however, necessarily lead to the identification of one or more that are particularly important (Kuffner *et al*., 2007; Wedding *et al*., 2008).

Spatial extent may be particularly relevant when it is commensurate with home range size and behavioural characteristics. For example. the three coral reef fish species (*S. planifrons*, blue tang (*Acanthurus coeruleus*) and coney (*Cephalopholis fulva*)) examined by Pittman *et al*., (2009) responded most strongly to complexity averaged within extents of 50 m to 100 m, 15 m to 100 m and 200 m to 300 m, respectively. *S. planifrons* is a territorial fish, with a small home range size of a few metres and affinity for certain coral species (Gratwicke & Speight, 2005a, 2005b; Pittman *et al*., 2009), it also displayed the overall strongest relationship with habitat structural complexity. The home range size of herbivorous *A. coeruleus* on reef crests in the Bahamas was reported at 80 m^2, and up to 300 m^2 at less

Table 2-3 Findings of studies with an a-priori aim of investigating the role of spatial scale (i.e., resolution or spatial extent) on the modelling of the distribution of marine biota using measures of habitat structural complexity. See Table 2-1 for explanation of predictors (measures of complexity).

Study and Method (Table 2-2)	Spatial Extent	Resolution	Predictors	Response and Data Collection Method	Findings
	Radii or length of square (m)	*DEM Resolution (s) (m); Analysis Window: (No. of DEM cells along one side of square)*	*(Those that contributed to final models)*	*Species Richness (SR) Total Abundance (TA) Species Prevalence (SP.) Group Prevalence (GP) Group Abundance (GA) Biomass (Bio) Diversity (Div)*	
Coleman *et al.* (2016) 3b		DEM: 0.5, 1, 2, 5 Analysis window: 3	Orien Bath SurRug Curv	Fish: SR, TA, FD, TL 5 x 50 m^2 video transects Included temporal replication	Overall, metrics derived using 1 m DEM were correlated with the greatest range of fish responses, the same scale over which the fish survey was undertaken in video transects. Generally wide-ranging species identified in video transects, though some cryptic, site attached species identified SR: all four resolutions important, TL and FD only one, TA three. The extent of multicollinearity among measures of complexity increased as the spatial resolution decreased.
Jalali *et al.* (2015) 3a	Radii: 10-50, 50-150	DEM: 5	BPI	*H. rubra*: sp. Commercial fishing data	Small extent BPI contributed more than large extent BPI. Different, non-linear responses were found for each, with no clear pattern overall.
Elvenes *et al.* (2014) 3b		DEM: 50 Analysis window: 3, 9, 21, 49	Orien BPI* Curv SurRug (3 x 3 only) OthComp	Sessile and mobile invertebrate biotope class. Towed video, data pooled to a single point every 200 m	All resolutions were important, though the relative importance of each varied among predictors.
Rees *et al.* (2014) 3a	Radii 15, 50, 75	DEM: 5	Bath BathRan BathyVar BPI	Fish (BRUV) and sessile invertebrate (40 m video transect): SR, TA	Responses best predicted using the largest radii Indicating the importance of complexity over large extents to sessile invertebrates. Fish responses related to bathymetry and distance to habitat only.
Knudby *et al.* (2011) 3a and 3b	Radii: 4-1,000 (10 increments)	DEM: 4	BathVar SurRug	Fish: SR, Bio and Div Average of 3 to 5 x 250 m^2 diver visual transects	Both small and large extents and fine and coarse resolutions appeared important, though relative importance depended on statistical technique. The best performing model (random forests) did not include metrics of complexity derived from smaller extents / finer resolutions.
		DEM: 4 to 1,000 (10 increments) Analysis window: 3	Slope Curv		
Monk *et al.* (2011) 3b	Radii (BPI): 7.5, 22.5, 52.5	DEM: 2.5 Analysis window: 3, 9, 21	Orien SurRug Curv BPI* Bathy	*N. tetricus*: SP 9 x towed video transects, 56 km total, across study area	All three models performed well, though the model based on the larger extent / coarser resolutions performed slightly better. The area of the coarser model (2,756 m^2) was much greater than reported home range sizes (225 to 775 m^2). Variable importance also varied slightly with extent / resolution.
Pittman and Brown (2011) 3a	Radii: 5, 25, 50, 100, 300	DEM: 4	Orien Slope Curv SloSlo Bath	Occurrence of five fish species 100 m^2 diver visual transect	The most important extent varied among species, with no positive allometric scaling relationship evident between body size and extent. Variable model performance across some species suggested some relationship with fish home range size.

Study and Method (Table 2-2)	Spatial Extent	Resolution	Predictors	Response and Data Collection Method	Findings
	Radii or length of square (m)	*DEM Resolution (s) (m); Analysis Window: (No. of DEM cells along one side of square)*	*(Those that contributed to final models)*	*Species Richness (SR) Total Abundance (TA) Species Prevalence (SP.) Group Prevalence (GP) Group Abundance (GA) Biomass (Bio) Diversity (Div)*	
Knudby *et al.* (2010) 3b		DEM: 4 to 300 (12 values) Analysis window: 3 x 3	SurRug Hab	Fish: SR, Bio, Div 5 m radius (78 m^2) diver visual point counts	Overall surface-rugosity measured at the finest resolution was the most important predictor for each response. Surface rugosity at the next finest resolution also had some importance for species richness and diversity, and that at relatively coarse resolutions was also important for biomass
Galparoso *et al.* (2009) 3b	Radii (BPI): 15, 45, 135, 500	DEM: 5 Analysis window: 3, 9, 21	Geo Slope BPI* Bath	*H. gammarus* sp. Lobster pots	Higher resolution model performed best. BPI measured at a coarser resolution was also important.
Guinan *et al.* (2009) 3		DEM: 30, 90 Analysis window: 3	Orien BPI* SurRug Slope	*L. pertusa* mean% cover from video	Fine and coarse resolution predictors both correlated with response, though stronger correlations with coarser resolution measures, this was true for all predictors. Relationships were resolution-dependent.
Moore *et al.* (2009) 3a	Radii: 12.5, 25	DEM: 2 m?	BathRan BPI Slop SurRug Hab	*A. viridis*, *G. prasinus*, *P. caeruleopunctatus*, Australian swell shark (*Cephaloscyllium laticeps*): SP BRUVs	Overall, models based on larger extent provided better predictions using both tree and GAM methods, except for Eastern Blue Grouper, where the smaller extent tree model performed better than the larger, however, this model did not include metrics of complexity. Green moray, blue spotted flathead and Australian swell shark prevalence best predicted by BPI and mean bathymetric range derived using the larger extent. Mean rugosity and slope within 25 m were also important to the prediction of Australian swell shark and blue-spotted flathead, respectively.
Pittman *et al.* (2009) 3a	Radii: 15, 25, 50, 100, 200, 300	DEM: 4 m	Bath BathVar SurRug Slope SloSlo Curv OthCom	Fish: SR, TA, GA, Bio 100 m^2 diver visual transect Coral SR and% cover in 5 x 1 m^2 quadrats	Most important spatial extent varied with species and response variable. Some responses (Inc. SR, Bio and SA, GA) were correlated with variables derived from small and large extents. Overall, response of Herbivores best predicted using 15 m and 25 m radii and Piscivores using 25 to 300 m radii. Mean slope-of-slope in 25 m and 200 m radii was the most important predictor of coral SR and cover, respectively.
Dolan *et al.* (2008) 3b		DEM: 0.5 m, Analysis windows: 3, 9, 17, 33	Slope Orien BPI* Curv FD OthCom (not 3 x 3)	*L. pertusa* and *M. oculata*: SP Video transects at DEM resolution	Predictor importance varied with resolution. Many variables appeared more important when derived at finer resolutions, though slope, FD and orientation measured at coarser resolutions were also important.
Holmes *et al.* (2008) 3a	Radii: 10, 20, 50, 100	DEM: 2 m	BPI BathRan BathVar OthComp	Sessile invertebrate and algae: GP Video transects at DEM resolution	Predictors quantified in small and large spatial extents were important predictors, the relative importance of individual extents varied with biotic group.
Purkis *et al.* (2008) 3a	Radii: 4 to 200, 12 values	DEM: 4 m	BathVar	Fish: SR, TA, GA 5 x 5 m radius (78 m^2) diver visual point counts	Relatively smaller extents (4 m to 20 m radii) most important to SR and TA. No trend when SR partitioned into size, mobility, and functional guilds groups. Radii of 4 m, 8 m and 20 m to 40 m most important to abundance of size groups <20 cm, 21 to 40 cm and 41 to 60 cm, respectively. No indication of relatively important extents for >60 cm fish length.

Study and Method (Table 2-2)	Spatial Extent	Resolution	Predictors	Response and Data Collection Method	Findings
	Radii or length of square (m)	*DEM Resolution (s) (m); Analysis Window: (No. of DEM cells along one side of square)*	*(Those that contributed to final models)*	*Species Richness (SR) Total Abundance (TA) Species Prevalence (SP.) Group Prevalence (GP) Group Abundance (GA) Biomass (Bio) Diversity (Div)*	
					Extents of 4 m and 8 m most important for territorial fish and 40 m for corallivore. Little indication of relatively important extents for mobile fish and algal feeders.
Wedding *et al.* (2008) 3b		DEM: 4, 10, 15, 25 Analysis window: 3	SurRug LinRug (1.3 cm link)	Fish: SR, TA, Bio, Div. 125 m^2 diver visual transect LinRug: TA only	All four resolutions important for SR, TA and Bio. DEM 10 m most important for Div. Linear-rugosity important for all responses, and was also only correlated with surface-rugosity derived from the 4 m DEM. Suggested the coarser resolution DEMs are capturing different, and ecologically relevant, aspects of complexity.
Kuffner *et al.* (2007) 3a	Square: 2, 5, 10	DEM: 1	SurRug LinRug (1 m chain, 1 cm link size)	Fish: SR 7.5 m radius (177 m^2) diver visual point count	Linear-rugosity most correlated, though weakly, with surface-rugosity averaged within the greatest spatial extent, followed by 5 m x 5 m and 2 m x 2 m. Surface rugosity averaged within each of the extents was significantly, though weakly, correlated with SR. That averaged within the 5 m x 5 m extent was a better predictor, though only slightly.
Pittman *et al.* (2007) 3a	Square: 3, 5, 9, 17, 33, 65, 129	DEM: 5	BathVar LinRug (2 x 6 m chain at each transect converted to TIN)	Fish: SR 100 m^2 diver visual transect	Bathymetric range at two smaller extents (3 m x 3 m and 9 m x 9 m) and linear-rugosity at intermediate (17 m x 17 m) and large (129 m x 129 m) extents were retained in the final model. Indicated complexity present at, and well above, the scale of the survey area influenced species richness.
Wilson *et al.* (2007a) 3b	Radii (BPI): 3, 9, 17, 33, 65	DEM: 15 Analysis windows: 3, 9, 17, 33, 65	Orien BPI* Slope SloSlo Curv FD	*Munida* sp. sp. Video transects	Multi-scale model (containing all predictors derived over each resolution, except 65 m x 65 m) performed best, followed by the 17 m x 17 m scale only model, indicating complexity present over small and large extents important.

*BPI derived using Method 3a

complex pavement sites (Semmens *et al*., 2005). *C. fulva* is a larger, wide-ranging Piscivore that would likely prey on fish over larger distances. A similar relationship was found with other species by Pittman & Brown, (2011) and at a trophic level (herbivores and piscivores) by Pittman *et al*., (2009). Purkis *et al*., (2008) also reported that bathymetric range derived over the smallest extents (4 m and 8 m radii) of those examined (4 m to 200 m radii) were most important for territorial species. Failure to identify the spatial extent(s) relevant to each species could hinder or prevent identification of relationships, particularly if the biotic metric included the differencing responses of functionally or trophically dissimilar groups.

A further reason why remote measures of complexity are often poor predictors, at least for fish, is likely to be resolutions (none finer than 0.5 m and the majority larger) are too coarse to adequately capture ecologically relevant components of complexity (e.g., refuges)

commensurate with their body size (Knudby & Ledrew, 2007). Fish species richness and abundance have been shown to be influenced by the number and size of refuges, but these components of complexity would be captured only if the resolution of the associated DEM was commensurate. However, while the relative importance of linear-rugosity derived *in-situ* appears associated with a chain link size (i.e., resolution) commensurate with the size of fish and their refuges, (Wedding *et al*., 2008) provided evidence of how surface-rugosity derived at coarser resolutions captured ecologically relevant complexity not captured by *in-situ* linear-rugosity. Knudby & Ledrew, (2007) also specifically examined how *in-situ* linear-rugosity and fractal dimension derived over various resolutions (0.2 cm, 3.1 cm, 12 cm and 82 cm chain link size) varied across different substrata (sand and rubble) and coral growth forms of various complexity. Each measure changed unpredictably with resolution, indicating these reef structures were too complex for any single measure to provide a comprehensive index of complexity over a range of scales. Resolution may also have a substantial effect on the value of a measure of complexity. Wilson *et al*., (2007a) provided an extreme example and showed how the value of orientation may vary by a full 360 degrees when derived over distances of 10s to 100s of metres. A further consideration is the potential confounding effect of resolution with spatial extent, and how as resolution increases as does spatial extent. As is evident in the findings of studies that have varied spatial extent, area can be an important determinant of species distributions (Kunin, 1998). This is somewhat demonstrated by Monk *et al*., (2011), one of the few studies that examined the role of resolution at a species level (*N. tetricus*). Importantly, both the resolution and extent over which the measures of complexity were derived varied, complicating inferences. Studies that wish to examine the role of resolution may need to keep the spatial extent constant to avoid such complications.

2.6 Conclusion

The wide range of study locations, sampling strategies, statistical approaches, resolutions and spatial extents encountered in the studies examined hindered identification of generalities in the relationship between measures of structural complexity and marine biota. There appeared to be little attempt to standardise methods across studies, nor could this have been expected given the varied objectives, localities and target biota. It was apparent, however, that remotely derived measures of complexity were often outperformed by other associated predictors, many of which appeared associated with components not captured by direct measures of complexity. This was despite the demonstrated importance of structural complexity to marine biota evident in numerous *in-situ* observational and

manipulative experimental studies. While this could suggest that complexity may not be such an important surrogate of species distributions in marine ecosystems; this review identified several studies indicating that when relevant spatial extents and resolutions were considered, structural complexity was a strong predictor of the distribution of marine biota. These examples also provide insight into the environmental variables for which they act as surrogates and the underlying ecological mechanisms. Importantly, close examination of these and studies where measures of complexity have performed poorly suggests why the potential of such measures has yet to be realised fully. This is particularly important in guiding future studies, especially considering the utility of photogrammetry and the opportunity to combine the large coverage of broad-scale remote sensing methods with the fine resolution achievable using *in-situ* methods.

Perhaps the most important consideration is that biota do not respond to all elements of complexity present in their environment, but rather a discrete subset associated with their life history, behaviour, home range size, body size, functional role, trophic level and so on. The measure of complexity and the spatial extent and resolution over which it is derived define the discrete element of complexity that is being quantified. For this to be ecologically relevant, all three of these variables must be so also. Without prior knowledge of the biology and ecology of the biota in question the probability that this specific element of complexity is ecologically relevant is likely to be low. Relationships involving measures of terrain morphology are likely to be species and location specific, limiting model generality and portability, and measures of terrain variability provide a coarser measure of complexity unable to discriminate between discrete elements, potentially limiting their predictive power. Different spatial extents and resolutions may also be related with different structuring mechanisms. Hierarchical, multi-scale approaches will help ensure that the response of biota is measured across a range of scales, thereby identifying those where important relationships are expressed (Pittman & Brown, 2011). This should include consideration of the potential confounding effect of resolution and extent so that a response to the different components of scale may be considered separately. Studies must also consider how grouping potentially dissimilar responses of different species, functional, behavioural and tropic groups may hinder predictive performance at the level of community and mask otherwise strong relationships.

Studies should also aim to measure a response over the entire range of predictor values present in the study area. If not, the unidentified presence of non-linear and threshold effects, themselves key understanding the role of complexity, may at best hinder the

identification of the true relationship, even if the defined element of complexity is ecologically relevant. This will require selection of statistical techniques able to model such relationships. If not considered in the modelling approach, the presence of interactive effects between predictors could also result in the miss-identification of relationships. Key also the inclusion of predictors that capture broad gradients in environmental variables or their surrogates. This is particularly important where the study area is large and where the distribution of biota is likely to be structured by their physiological tolerances to abiotic and biotic variables and patterns in recruitment driven by prevailing hydrological and oceanographic conditions. Such variables may mediate or override the effect of structural complexity (e.g., Kuffner *et al*., 2007; Pittman & Brown, 2011), especially at larger scales. Geographic predictors that describe relative location across the study area, such as latitude, may perform well as surrogates of one or multiple known and unknown environmental variables that may not be readily measured due to technological and cost constraints. They may also provide surrogates of ecologically relevant complexity not captured by the direct, and narrower, measures, as may have been the case in (Hill *et al*., 2014), thereby improving predictive performance and helping to identify measures that could be targeted in future studies.

The utility of one measure of complexity, surface-rugosity, is worthy of attention, as it was both the most common and the poorest performing measure overall, as indicated by the standardized performance metric, $Rs_{1\text{-}10}$, utilised here. It is expected to be one of the most common predictors utilised in photogrammetric studies, partly because it is one of the simpler measures to derive and conceptualise. As well as providing only a coarse measure of complexity it has often been derived over resolutions likely too coarse to capture adequately important components of complexity such as refuges. Surface rugosity captured at resolutions of centimetres and commensurate with the body size of organisms whose habitat is being investigated (Knudby & Ledrew, 2007), achievable using photogrammetry, is expected to provide similar or improved predictive results as that derived *in-situ*. However, there is possibly a limit to the utility of rugosity and other measures of terrain variability imposed by their coarse nature. Whilst the finer resolutions over which they are derived may be commensurate with important, discrete elements of complexity such as refuges, this would not necessarily indicate that these are present. A further avenue for development along with the emergence of photogrammetry would be the development of a second generation of measures of complexity with direct applicability to the marine environment, to supplement those in current use adapted from terrestrial studies. Measures that quantify the number of and type of discrete elements known to directly influence the distribution of biota,

e.g., the number of habitat refuges of a certain size range or benthic sessile biota growth forms could provide especially useful predictors.

Other considerations not considered in detail here include the roles of sampling methodology, particularly survey area, possible temporal variability, and influence of statistical technique on relative performance of predictors. At the very least, studies should aim to standardise methods wherever possible.

3 Chapter 3 - Optimising the Derivation of Habitat Structural Complexity Metrics from Rock reef Environments

3.1 Summary

In marine ecology, habitat structural complexity (structural complexity) is often used as a surrogate of biotic diversity and abundance, yet it is not clear which aspects of structural complexity are the most useful surrogates of biotic assemblages. Different metrics of structural complexity are very often highly correlated with each other, as is the same metric when derived over different resolutions and spatial extents. This often results in large (in this study, over 2,000 potential predictors derived from raster and mesh based bathymetric reconstructions) predictor datasets that hinder most methods of statistical analysis and further complicate identification of important predictors. In this Chapter I aim to identify an optimised and more manageable structural complexity predictor datasets that maximises the amount of unique information retained while minimisng the total number predictors. This will inform subsequent work in this this and other studies that use these predictors to model the abundance of fish and other marine biota. The main findings were:

- Substantial Correlation and variability among structural complexity metrics was identified within the three overlapping and commonly used bathymetric reconstructions (MBLI Raster, AUV Mesh and AUV Raster [AUV Mesh converted to a raster]) over multiple spatial extents and resolutions.
- Successive removal of metrics based on correlations and objective assessment of the sensitivity of metrics to changing spatial extent and resolution identified a reduced predictor dataset of 53 out of 1,980 MBLI Raster predictors, 16 out of 162 AUV Raster predictors and 6 out of 67 AUV Mesh predictor.
- This optimised predictor dataset maximised interpretability whilst minimising potential information loss and was far more suited for common modelling techniques appropriate to the size of typical biotic datasets such as those in **Chapters 4** and **5**.
- Patterns in correlations also uncovered several distinct groupings of common metrics that capture similar information on structural complexity. Such findings further confirm a notable degree of redundancy amongst common metrics and will help guide the selection of suitable metrics in future studies.

3.2 Introduction

Current remote sensing methods using hydroacoustic and Light Detection and Ranging (LIDAR) surveys are able provide broad-scale contiguous digital elevation models (DEMs) of seafloor terrain across a range of coastal, deep offshore, temperate, and tropical marine environments (reviewed in **Section 2**). At present, a substantial variety of metrics of habitat structural complexity have been described and can derived from these DEMs. This includes several originally described in terrestrial environments such as the several terrain analysis algorithms provided by ESRI ArcGIS (Redlands, 2011) and those more specific to marine environments such as the Benthic Terrain Modeler (BTM) toolbox (Walbridge *et al*., 2018). Many of these metrics have been developed to capture variation in topographic structure in terrestrial environments but many studies have also documented how these metrics are also relevant to marine ecology. The ecological relevance and efficacy of these metrics as predictors is due to their ability to act as surrogates of environmental gradients and limiting resources that influence the occurrence and abundance of these biota across landscapes (Guisan & Zimmermann, 2000). The development of metrics based on meshes, and the derivation of traditional raster-based metrics following the conversion of mesh to raster format, is a further source of potential metrics for researchers to consider. Also, for each metric, it is possible to derive a range of summary statistics including the mean, standard deviation (std) and maximum value within an analysis window. Given the importance of considering spatial scale as a key factor in the predictive performance of metrics of structural complexity (Dolan *et al*., 2008; Galparsoro *et al*., 2009; Guinan *et al*., 2009; Holmes *et al*., 2008; Jalali *et al*., 2015; Knudby *et al*., 2010; Moore *et al*., 2009; Pittman *et al*., 2007, 2009; Pittman & Brown, 2011; Purkis *et al*., 2008; Rees *et al*., 2014; Wilson *et al*., 2007b), unless the relevant spatial extent and resolution is known with confidence a priori, then metrics should ideally be derived over a range of extents and resolutions. This will help ensure spatial extents and resolutions with particular importance to the target biota are captured.

While this rapid proliferation of predictor variables improves the ability to capture ecologically relevant information and the performance of models, at the same time the vast number of potential metrics available to researchers can be a substantial hinderance. When associated with the often relatively small (e.g., a few 10s to 100s of data points) biotic datasets this can cause problems for both inferential statistical (such as linear and additive modelling) and machine learning (ML) (such as regression tree) approaches. With such small biotic datasets, the number of available predictors is likely to several times to orders of magnitude larger than the number of observations. For inferential approaches this would

soon result in problems with model fitting and saturated models (no. predictors ≥ biotic observations). Some machine learning approaches can accommodate relatively large numbers of predictors, but at the expense of model and predictor interpretability. Also, there is often an optimum number of predictors that provides the best model performance, beyond which model, including some ML models, performance decreases (i.e., Hughes Phenomenon) (Hughes, 1968). Further, there is often also a large degree of multicollinearity between metrics and between the same metric derived over different resolutions and extents. When not considered, multicollinearity is a serious problem for significance testing and model specification (Blalock, 1963; M. H. Graham, 2003). Statistical approaches that attempt to handle large and multicollinear predictor datasets are available, though they have notable limitations. There may be little oversight of the individual or groups of predicters removed (e.g., automatic predictor removal algorithms based on correlation matrices, which may by chance remove the most easily interpretable predictors) or require substantial transformation of predictors. This latter issue is of particular importance if the goal is inference and ecological understanding of the mechanisms driving species responses. For example, dimensionality reduction techniques such as principal components regression (PCR) handle multi-collinearity by reducing the many predictors to an uncorrelated subset of variables via principal components analysis (PCA) to be used as the basis of regression and other modeling techniques. However, these principal components have no direct ecological relevance, and it is difficult to identify the independent effects of the initial variables, which makes inference problematic (Freckleton, 2011; Graham, 2003). Also, the principal components may not provide the best possible predictors for the response as their derivation only considers the variability of the original predictors, not the response variable (i.e., is unsupervised). Similar techniques such as Partial Least Squares Regression (PLSR) seek to overcome the latter problem by considering variation in the response variable when calculating the principal components (i.e., is supervised). However, as with PCA, the new predictor variables created by PLSR still have no direct ecological relevance. Identification of the most appropriate metrics a-priori is important for the effective and rapid provision of important predictor datasets (Fukunaga *et al*., 2019).

As the number of metrics and the resolution and spatial extents over which they can be derived continue to increase, there will be an ever increasing need to focus metric derivation on those that maximise the unique information quantified from bathymetric reconstructions whilst ensuring predictor datasets are not too large to hinder modelling and inference. Ideally, this would be undertaken prior to statistical analysis to also help avoid some of the limitations inherent in modelling techniques (e.g., PCR, PLSR) that might otherwise be

attempted. As an alternative to the approaches outlined above, a more informed and systematic approach to reducing the size of these predictor datasets is required prior to analysis. The aim of this chapter is to undertake a 'supervised' reduction in the number of potential predictors based on informed choices on the most appropriate metrics to be retained and discarded. This process also provides insight into the relationships between various metrics and their spatial variability on the New South Wales (NSW) coastline that will inform future studies based on the same or similar datasets. The specific aims are to:

1. Inform the future derivation of metrics from three commonly used datasets specifically, and similar datasets in general, by identifying:
   a) Groups of metrics that capture similar information on structural complexity. This will identify where redundancy currently exists and opportunities to streamline metrics derivation whilst maximising information obtained from bathymetric reconstructions.
   b) Discrete components of structural complexity that can be quantified from datasets. This will identify those metrics and associated components of structural complexity that should be considered and quantified from raster and mesh based bathymetric reconstructions.
   c) The sensitivity of metrics to change in spatial scale (spatial extent and resolution). This will identify those metrics that should be derived over multiple extents and / or resolutions to capture the full range of variability in the metric value.
2. Based on the above, identify a reduced predictor dataset that is suitable for modelling of fish abundance using a typical (less than 100 observations) biotic dataset from the NSW coast using common statistical techniques.

3.3 Methods

3.3.1 Approach

The overall approach consisted of:

1. Derivation of several metrics of structural complexity from three types of bathymetric reconstructions commonly used in studies that model the abundance and / or distribution of marine biota. These metrics were derived over a range of spatial scales and resolutions.
2. Examination of the correlative relationships between different metrics derived from the same bathymetric reconstruction. The correlation between the same and different metrics was also examined at varying combinations of spatial extent

and resolution to determine the importance of considering spatial scale during metric derivation.

3. Modelling of metric values as a function of spatial extent and resolution to identify the optimum number of spatial scales to consider when deriving various metrics.
4. Based on correlations and the results of the modelling, identify an optimum predictor dataset that maximise the amount of information on structural complexity captured, whilst minimising the number of metrics and spatial scales that need to be considered.

3.3.2 Bathymetry Reconstructions

Three types of bathymetric reconstructions were available for metric derivation (**Figure 3-1**):

1. Large extent (total 791 km^2 across Solitary Islands, Port Stephens and Batemans Bay) - low resolution (5 m) DEM rasters captured from multibeam echo-sounding (MBES) and light detection ranging (LIDAR) surveys (hereafter referred to as MBLI Raster). MBES data were collected using hydroacoustic surveys of rock reef between 2006 and 2009 (Jordan *et al.*, 2010) (see ref. for further methodology, including detail of data processing, quality and checking and associated accuracy, generally 1 m) and 2018 LIDAR data from surveys undertaken in coastal areas up to approximately 5 km offshore and 35 m deep by the (former) NSW Office of Environment and Heritage (OEH). LIDAR data were collected to Australian standards with vertical accuracy of at least 0.3 m (95% confidence) and horizontal accuracy of at least 0.8 m (95% confidence). Following field collection and processing the MBES (5 m resolution) and LIDAR (2 m resolution) rasters were merged to provide a combined MBLI Raster (5 m resolution) using tools in ESRI ArcGIS (Redlands, 2011). In the case of spatial overlap between the MBES and LIDAR rasters the average depth value was used. It is noted that the spatial overlap between the MBES and LIDAR surveys was limited. The MBES data provided the greatest coverage while the LIDAR dataset was used to supplement the MBES data in areas of shallower coastal water.

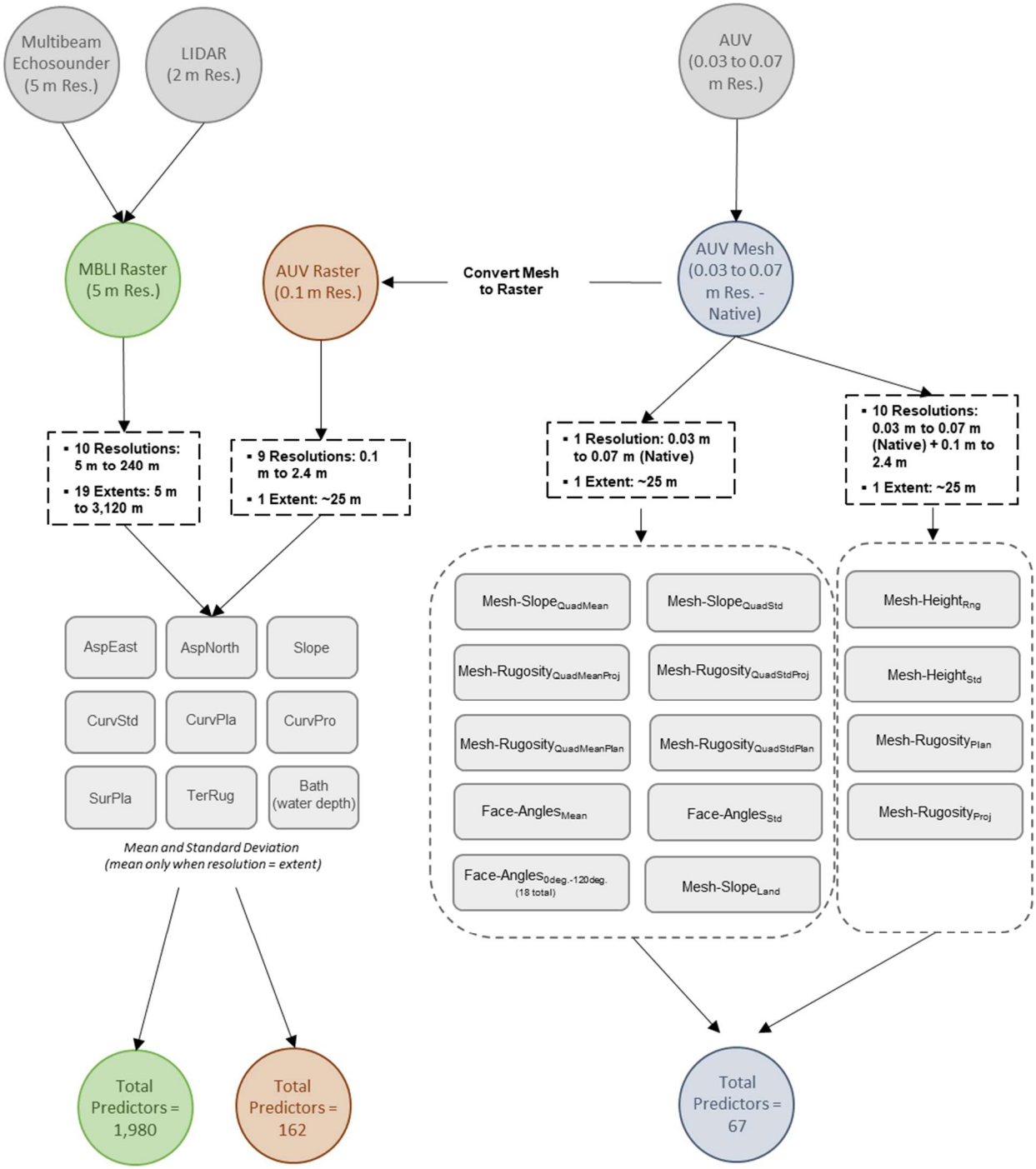

Figure 3-1 **Graphical representation of the three datasets and derived metrics / predictors. For AUV Mesh, the native resolution was the default range of triangle side length (0.03 m to 0.07 m) output from the mesh generation workflow. When converting AUV Mesh to AUV Raster, the finest AUV Raster resolution was set at 0.1 m to ensure creation of a contiguous raster with no missing data.**

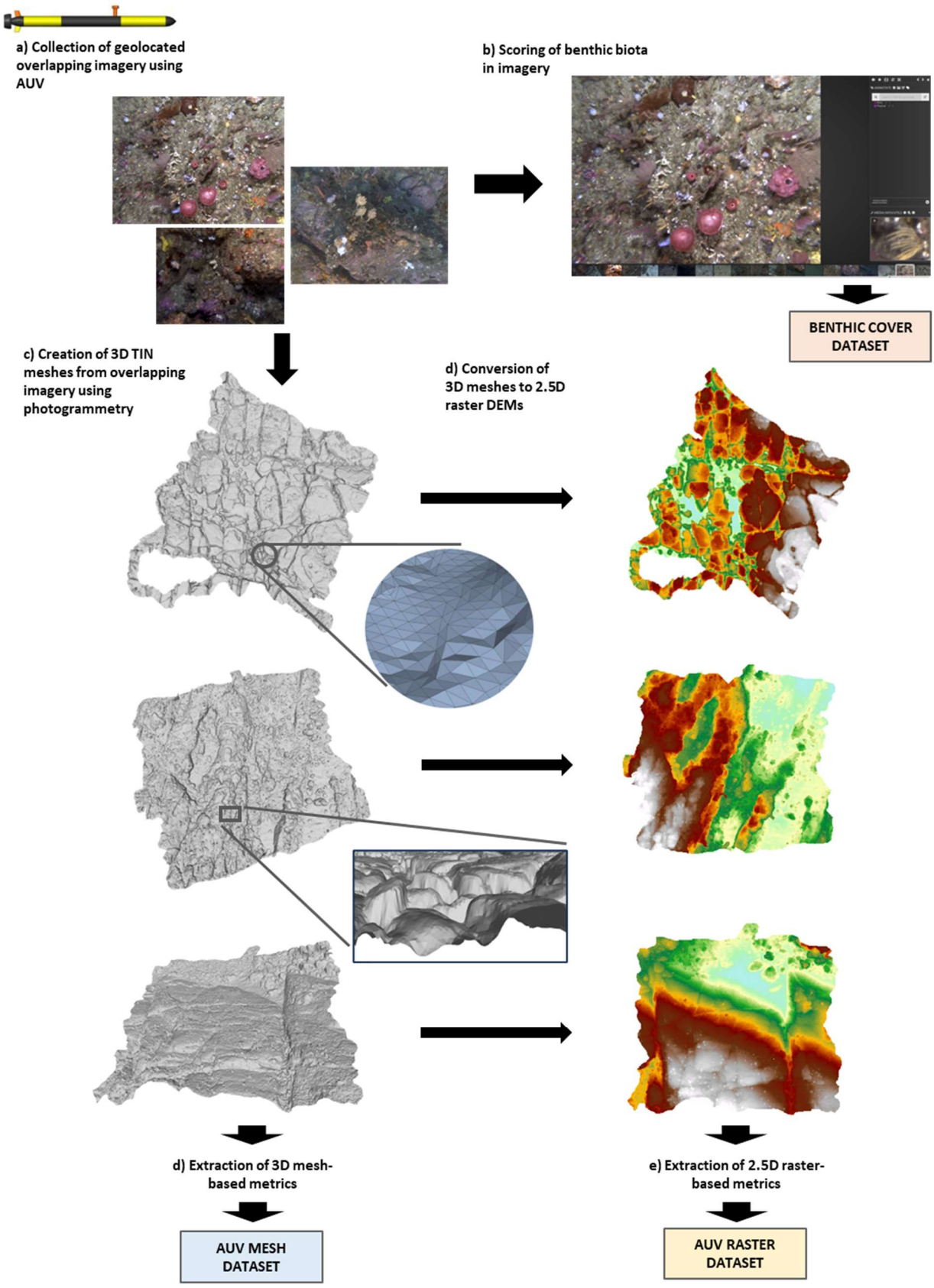

Figure 3-2 Process of deriving AUV Mesh, AUV Raster and benthic cover metrics and predictors from the AUV surveys

2. Small extent (~625 m^2) - high resolution (~0.03 to 0.07 m) TIN meshes derived from automated underwater vehicle (AUV) surveys (hereafter referred to as AUV Meshes). AUV Meshes were derived from the stereo imagery collected using the AUV *Sirus* operated by the Australian Centre for Field Robotics (ACFR), University of Sydney and supported by the Integrated Marine Observing System (IMOS) (Williams *et al*., 2012) (**Figure 3-2**) IMOS is enabled by the National Collaborative Research Infrastructure Strategy (NCRIS). AUV surveys were undertaken in the Solitary Islands from August to September 2012, and Port Stephens and Batemans Bay in November 2012, except for one site (BISZ3) in Port Stephens surveyed in December 2010. The collected stereo images and their geo-locations were used to create the AUV Meshes of approx. 25 m x 25 m (625 m^2) with triangle side length (referred to hereafter as the native mesh resolution) of 0.03 m to 0.07 m (Friedman *et al*., 2012). This was the default mesh resolution output from the mesh generation workflow. The AUV data also included water depth and as data quality check the correlation between the AUV depth data and the MBLI Raster dataset checked with almost identical results (r of >0.99). AUV Meshes were also checked for irregularities in the mesh structure using in-built tools within the Geomagic Control software (3D Systems, Darmstadt, Germany).

3. AUV Meshes converted to raster format (hereafter referred to as AUV Raster). These were the same extent as the AUV meshes but 0.10 m resolution. AUV meshes were converted to raster format using routines in the LiDAR360 software program (GreenValley International, California, USA) to provide AUV Rasters of the same extent as the AUV Meshes but at a resolution of 0.1 m. Raster cell depth values were based on the average depth values of mesh nodes within the cell extent. A resolution of 0.1 m was chosen to ensure creation of a contiguous raster with no missing data from the native mesh resolution (0.03 to 0.07 m). Key differences between the raster and mesh datasets relate to resolution and data format. Raster data provides a 2.5-dimension (2.5D) approximation of the true 3-dimension (3D) structure of the seafloor while the mesh format provides a 3D mesh reconstruction. However, it is noted that the 3D mesh is also an approximation, and whilst it can capture beyond vertical surfaces such as overhangs and caves, deep caves and overhangs would not be fully captured by the more nadir (top-down) rather than oblique camera orientation used for this study. This AUV Raster datas*et al*lowed the derivation of common raster-

based metrics at resolutions finer than that achievable using MBLI Raster. Importantly also, many of these metrics are not, at least at present, able to be easily extracted from mesh-based datasets.

Each of these types of bathymetric reconstructions have been used previously by studies investigating the influence of structural complexity on marine biota (**Section 1.2**).

A total of 49 sites with overlapping MBLI Raster and AUV Mesh / AUV Raster datasets were selected across the three locations covering 740 km of coast and 6 degrees in latitude (**Section 1.5**).

3.3.3 Metrics of Structural Complexity

Bathymetry (water depth), slope (Slope), surface-planar-area (SurPla) (analogous to surface-rugosity but based on the 2D area of best fit and thereby decoupled from slope), terrain-ruggedness (TerRug), two metrics of orientation: aspect-east (AspEast), aspect-north (AspNorth) and three metrics of curvature: standard-curvature (combination of profile-curvature and planar-curvature) (CurvStd), profile-curvature (CurvPro) and planar-curvature (CurvPla), were calculated from MBLI Raster and AUV Rasters using the BTM toolbox (Walbridge *et al*., 2018) (**Table 3-1**). These measures were selected due to their common usage, importance as predictors of the distribution of marine biota (see **Section 2**) and ease of calculation within a GIS environment. Custom scripts (Friedman *et al*., 2012) were used to calculate a total of 31 metrics of structural complexity from the AUV Meshes (**Table 3-2**). Nine mesh metrics were based on slope and surface-rugosity. Two mesh metrics were based on the range in height of the mesh and analogous to bathymetric-range often derived from raster datasets (bathymetric-range was initially derived from the raster datasets in this study but was highly correlated with the std and maximum value of bathymetry and was not included in the detailed analysis presented here). The remaining 20 mesh metrics were specific to mesh datasets and measured the angle between the triangle mesh components (face-angles) and the direction of the z-axis (i.e., vertical upwards). The mean and std of the face-angles across the entire mesh was calculated and their distribution summed within 10 deg. bins from 0 deg. to 180 deg., with the final two bins excluded due to very low counts and variance. The 90 deg. to 180 deg. and greater bins captured overhang, or beyond vertical, surfaces.

Whenever a metric is derived from a dataset it is done so at a specific spatial extent (i.e., window size) and resolution (i.e., cell size or distance between adjacent mesh vertices). Both spatial components contribute to the final metric value and its ecological relevance.

Table 3-1 Metrics of structural complexity derived from raster-based datasets. Mean and SD calculated for each raster-based metric. For further detail see text.

Metric	Description	Resolutions	Extents
MBLI Rasters and AUV Rasters (Mean and std calculated for each metric). Std of metric indicated by -std, e.g., AspEast-std			
Bathymetry (Bath)	Water depth.	MBLI Raster: 5, 10, 20, 30, 40, 60, 80, 120, 160, 240 AUV Raster: 0.1, 0.2, 0.3, 0.4, 0.6, 0.8, 1.2, 1.6, 2.4	MBLI Raster: 5, 10, 20, 30, 40, 60, 80, 120, 160, 240, 360, 480, 600, 960, 1440, 1920, 2400, 2880, 3120 AUV Raster: ~25
Aspect-east (AspEast)	Measure of direction of greatest slope in a west-east direction, east facing = 1 and west facing = -1. .		
Aspect-north (AspNorth)	Measure of direction of greatest slope in a north south direction, with north facing = 1 and south facing = -1		
Slope (Slope)	Rate of change in bathymetry between a DEM cell and its neighboring cells.		
Standard-curvature (CurvStd)	Combines planar and profile-curvature, with 0 indicating a constantly sloping surface with no curvature in any direction. Captures strength and direction of hydrodynamic flows across a surface.		
Planar-curvature (CurvPla)	Curvature evaluated perpendicular to slope. Positive for convex contours (i.e., ridges) (A) and negative for cells with concave (i.e., valleys) (B) contours. A value of zero indicates that the surface is linear (C). 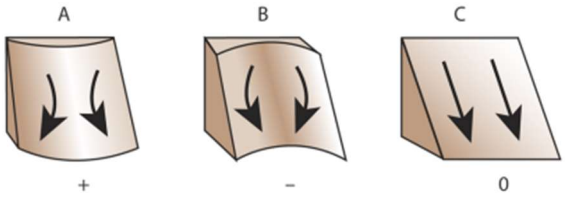 *Image source: ESRI ArcGIS (Redlands, 2011)*		
Profile-curvature (CurvPro)	Curvature evaluated in the direction of (parallel to) greatest slope. Negative for convex (A) surfaces and positive (B) concave surfaces. A value of zero indicates that the surface is linear (C) 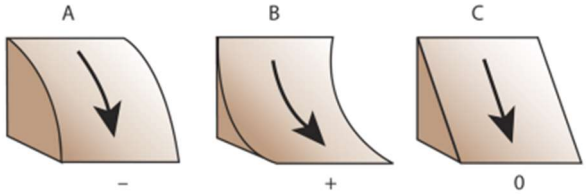 *Image source: ESRI ArcGIS (Redlands, 2011)*		
Surface-planar-area (SurPla)	The ratio of convoluted area to planar area, more commonly known as surface-rugosity. This measure includes a correction for slope based on the plane of best fit.		
Terrain-ruggedness (TurRug)	Measure of the local variation in seabed terrain based on the variability of vectors orthogonal to the plane between raster cells. Captures slope and aspect in one measure that varies between 0 (no variability in terrain) and 1 (complete variation).		
Total MBLI Raster Predictors = 1,980, Total AUV Raster Predictors = 162.			

Therefore, to maximise the potential of identifying ecologically relevant metrics, several combinations of resolutions and / or extents were considered during metric derivation. Each MBLI Raster metric was derived over several resolutions and extents. All AUV Raster and four mesh-based metrics (Mesh-Height$_{Rng}$, Mesh-Height$_{Std}$, Mesh-Rugosity$_{Proj}$ and Mesh-Rugosity$_{Plan}$) were derived over a range of resolutions and the other 27 mesh-based metrics were only derived at the native resolution of the mesh (0.03 m to 0.07 m)). The same approach to metric derivation was undertaken for each of the three datasets, with only minor differences in the procedure depending on whether the dataset was raster (MBLI Raster and AUV Raster) or mesh (AUV Mesh) based, and described below.

Table 3-2 Metrics of structural complexity derived from the mesh-based dataset. For further detail see text.

Metric	Description	Resolutions	Extents
Mesh-Slope$_{Land}$	Overall slope of the mesh surface calculated finding the plane that minimises the perpendicular point-to-plane distances of the mesh vertices using a least squares approach.	0.03 to 0.07 (Native)	~25 (~625 m^2)
Face angle histogram (0-180 by 10 deg: 18 total)* (e.g., Face-Angles$_{10deg.-20deg.}$)	Proportion of the angles (in degrees) between the vertical (z) axis and the slope of each mesh triangle placed within 18 10-deg. bins. A flat surface would have a face angle of zero, while a perfectly vertical one would have an angle of 90		
Face-Angles$_{Mean}$	Mean of the angles (in degrees) between the vertical (z) axis and the slope of each mesh triangle		
Face-Angles$_{Std}$	Standard deviation (Std) of the angles (in degrees) between the vertical (z) axis and the slope of each mesh triangle		
Mesh-Slope$_{QuadMean}$	Mean of slope values within 1 m x 1 m contiguous virtual quadrats placed on the mesh surface		
Mesh-Slope$_{QuadStd}$	Standard deviation of slope values within 1 m x 1 m contiguous virtual quadrats across the mesh surface		
Mesh-Rugosity$_{QuadMeanProj}$	Mean rugosity across 1 m x 1 m contiguous quadrats placed on the mesh surface, using 2D projected area.		
Mesh-Rugosity$_{QuadMeanPlan}$	Mean rugosity across 1 m x 1 m contiguous quadrats placed on the mesh surface, using plane of best fit (plane)		
Mesh-Rugosity$_{QuadStdProj}$	Std of rugosity across 1 m x 1 m contiguous quadrats placed the mesh surface, using 2D projected area.		
Mesh-Rugosity$_{QuadStdPlan}$	Std of rugosity across 1 m x 1 m contiguous quadrats placed the mesh surface, using plane of best fit (plane)		
Mesh-Height$_{Rng}$	Vertical relief, or the maximum – maximum vertex z (depth) value across the whole mesh	0.03 to 0.07 (Native), 0.1, 0.2, 0.3, 0.4, 0.6, 0.8, 1.2, 1.6, 2.4	
Mesh-Height$_{Std}$	Standard deviation in vertex depth values across the whole mesh		
Mesh-Rugosity$_{Proj}$	The ratio between the 3D surface area and the projected area of the x-y plane of the mesh		
Mesh-Rugosity$_{Plan}$	The ratio between the 3D surface area and the projected area of plane of best fit.		
Total AUV Mesh Predictors: 67			

MBLI Rasters were aggregated to cell resolutions (defined by the length of a side of the cell) of 10 m, 20 m, 30 m, 40 m, 60 m, 80 m, 120 m, 160 m and 240 m (**Table 3-3**). Each aggregated raster and the original 5 m resolution raster were converted to new rasters for each metric using BTM and the mean and std of cell values within square analysis windows of increasing extent (16 window sizes of side length 5 m to 3,120 m centered on each fish BRUV sample site) was derived. In cases where the raster cell resolution equaled the window size, only the value of the single raster cell within the window was extracted (this value is hereafter referred to as the mean, albeit only one value was available). The same process was followed for AUV Rasters, except the 0.1 m resolution raster was aggregated to cell resolutions with side lengths of 0.2 m, 0.3 m, 0.4 m, 0.6 m, 0.8 m, 1.2 m, 1.6 m and 2.4 m and the mean and std of metrics calculated over the full extent of the original and aggregated rasters (a window side-length size of approx. 25 m). Due to the large number of

Table 3-3 **Resolutions and extents over which each metric was derived. Numbers in cells indicate the number of metrics derived at that resolution and extent. Blank cells indicate extent x resolution combinations for which metrics were not derived (when resolutions ≥ 10 m were not an even number multiple of the extent).**

a)

MBLI Raster	AUV Raster	AUV Mesh	
		Resolutions 0.10 m to 2.4 m	*Resolution ~0.03-0.07 m*
Bath (mean, SD)	Bath (mean, SD)	$Mesh\text{-}Height_{Rng}$	$Mesh\text{-}Slope_{Land}$
AspEast (mean, SD)	AspEast (mean, SD)	$Mesh\text{-}Height_{Std}$	$Face\text{-}Angles_{xxdeg.\text{-}xxdeg.}$
AspNorth (mean, SD)	AspNorth (mean, SD)	$Mesh\text{-}Rugosity_{Proj}$	$Face\text{-}Angles_{Mean}$
Slope (mean, SD)	Slope (mean, SD)	$Mesh\text{-}Rugosity_{Plan}$	$Face\text{-}Angles_{Std}$
Curv (mean, SD)	Curv (mean, SD)		$Mesh\text{-}Slope_{QuadMean}$
CurvPla (mean, SD)	CurvPla (mean, SD)		$Mesh\text{-}Slope_{QuadStd}$
CurvPro (mean, SD)	CurvPro (mean, SD)		$Mesh\text{-}Rugosity_{QuadMeanProj}$
SurPla (mean, SD)	SurPla (mean, SD)		$Mesh\text{-}Rugosity_{QuadMeanPlan}$
TurRug (mean, SD)	TurRug (mean, SD)		$Mesh\text{-}Rugosity_{QuadStdProj}$
			$Mesh\text{-}Rugosity_{QuadStdPlan}$
			$Mesh\text{-}Height_{Rng}$
			$Mesh\text{-}Height_{Std}$
			$Mesh\text{-}Rugosity_{Proj}$
			$Mesh\text{-}Rugosity_{Plan}$
Total No. of Predictors (Metric x Resolution x Extent)			
		36	*31*
1,980	**162**		**67**

b)

		MBLI Raster			AUV Raster			AUV Mesh															
Resolution (m)	240												9		18		18	18	18	18	18	
	160											9					18		18		18	
	120										9		18		18		18	18	18	18	18	18
	80									9		18			18		18	18	18	18	18	
	60								9		18		18	18	18	18	18	18	18	18	18	18
	40							9		18		18	18		18		18	18	18	18	18	18
	30						9		18		18		18	18	18	18	18	18	18	18	18	18
	20			9				18		18	18	18	18	18	18	18	18	18	18	18	18	18
	10		9	18				18	18	18	18	18	18	18	18	18	18	18	18	18	18	18
	5	9	18	18			18	18	18	18	18	18	18	18	18	18	18	18	18	18	18	18
	2.4				4	18																
	1.6				4	18																
	1.2				4	18																
	0.8				4	18																
	0.6				4	18																
	0.4				4	18																
	0.3				4	18																
	0.2				4	18																
	0.1				4	18																
	0.03-0.07 (native)				31																	
		5	10	20	~25		30	40	60	80	120	160	240	360	480	600	960	1,440	1,920	2,400	2,880	3,120
		Extent (m)																				

resolutions, extents and metrics, this process was automated using the Python Arcpy interface with ArcGIS and custom Python script. It is noted that MBLI Raster metrics were derived only when the resolution was an even number multiple of the window side length (except when extent = resolution). All AUV Mesh metrics were derived at the extent (approximately 625 m^2 or 25 x 25 m) of the entire mesh surface using the native mesh resolution (0.03 m to 0.07 m). Measures of slope and surface-rugosity were derived in contiguous 1 m^2 virtual quadrats (identified here using 'Quad') placed on the mesh surface and the mean and std calculated across the entire 625 m^2 extent. Four metrics (Mesh-$Height_{Rng}$, Mesh-$Height_{Std}$, Mesh-$Rugosity_{Proj}$ and Mesh-$Rugosity_{Plan}$) were also derived from meshes re-sampled to the same resolutions as for the AUV Rasters. Mesh surface-rugosity was also calculated using the projected area of the x-y plane ($_{Proj}$) and the projected area of plane of best fit ($_{Plan}$) to decouple rugosity from slope when it was calculated at each re-sampled resolution across the entire mesh surface and when it was calculated within virtual quadrats at the native resolution.

An important distinction is made here between metrics and predictors. Here, the term metric(s) refers to the measure of structural complexity. For example, surface-planar-area, slope, Face-$Angles_{10\ deg.\ to\ 20\ deg.}$, and including bathymetry. Predictor refers to the metric, plus the resolution and extent over which it was derived. For example, surface-planar-area at 10 m resolution, derived over a spatial extent of 120 m x 120 m. Originally, other summary statistics (range, min and max values within the analysis window) were also calculated for each metric derived from MBLI Raster and AUV Raster. However, only mean and std were retained for further analysis. Preliminary data exploration indicated that these other statistics were highly correlated with the mean, std, and / or were substantially zero inflated (and thus provided little useful information).

3.3.4 Correlations among Metrics

Pearson's correlation coefficient r was calculated for each pair of predictors within each dataset. Correlations between predictors from different datasets were not examined as the intention was to compare the relative performance of each when modelling fish abundance data. Where required, right skewed data was log transformed to achieve an approximate normal distribution (an assumption of calculation of r). Predictors were considered highly correlated when $r \leq -0.7$ or ≥ 0.7. A threshold of $|r|$ 0.7 is a commonly accepted cut-off value that has been shown using simulation to work just as well as other methods designed to reduce multicollinearity beyond which severe distortion of model estimation and subsequent prediction begins to occur (Dormann *et al.*, 2013). Correlations were examined when

resolution and extent was not considered (i.e., all values were included in the calculation of r regardless of the extent and resolution) and separately for each AUV Raster and AUV Mesh resolution. In the case of MBLI Raster (metrics of which were also derived over multiple extents), comparisons were done for each resolution and extent combination. When 70% or more of predictors were highly correlated between metrics, then this was considered a relatively large degree of correlation and one of the two metrics was removed from the dataset based on the following rules:

- Metrics based on mean were retained in favour of those based on Std. Mean values are generally easier to interpret when deriving inference from relationships modelled between predictor and response.
- Metrics were retained in order of the most utilised metric, as identified in Chapter 2.

Due to the large number of face angle bins, these metrics were first reduced to the uncorrelated subset of $\text{Face-Angles}_{20deg\text{-}30deg.}$, $\text{Face-Angles}_{30deg\text{-}40deg.}$, $\text{Face-Angles}_{90deg\text{-}100deg.}$ and $\text{Face-Angles1}_{20deg\text{-}130deg.}$ before further analysis. Preliminary analysis also removed two metrics based on the proportion of mesh angles within $\text{Face-Angles}_{160deg\text{-}170deg.}$ and $\text{Face-Angles}_{170deg\text{-}180deg.}$ due to many zero counts and associated low variance.

3.3.5 Role of Extent and Resolutions

The sensitivity of each retained metric to change in resolution and extent was explored graphically by plotting individual metric values for each resolution (all datasets) and extent (MBLI Raster) over which it was derived. Visual examination of these plots enabled an assessment of relative sensitivity of each metric to changing extent and resolution. Plots with more rapidly changing metric values indicated a greater sensitivity to resolution or extent. Those where the metric value changed relatively little with resolution and extent indicated less sensitivity. This provided some indication of those metrics that may need to be derived over relatively more extents and resolutions to adequately capture variability in metric values those that need only be derived over relatively few resolutions and / or extents.

The optimum number and identity of resolutions and extents required to adequately describe the variability present in metric values was also identified objectively using a model-based approach with metric values modeled as a function of the resolution or extent over which they were derived. This approach was undertaken on the full dataset for each metric from each dataset (i.e., all metric values calculated over all resolutions / extents). For each resolution (all datasets) and extent (MBLI Raster only) a two-level categorical factor was created. The first level identified the metric values derived at that resolution / extent and the

second level the metric values derived at all other extents or resolutions. For example, for the 40 m resolution categorical factor, the first level identified the 40 values (from the 49 total sites) derived at this resolution. The second level identified all remaining values not derived at the 40 m resolution. If the categorical factor based on the 40 m resolution was retained in the final model, it would indicate that metric values derived at 40 m resolution were distinct from values derived from all other resolutions. This resolution would be associated with unique information and accordingly the metric should be derived at this resolution. Metrics may have 0, 1 or several uniquely important resolutions or extents. For example, if both the 40 m resolution factor and 120 m resolution factor were retained, this would indicate the 40 m and 120 m resolutions were each associated with unique information not captured by any other retained or un-retained resolution or extent.

For MBLI metrics, it was not possible to consider extent and resolutions together due to the substantial number of potential candidate models that would have resulted from 115 total combinations of resolution and extent. Thus, separate modelling was undertaken for resolutions and extents. It is noted that during modelling based on resolutions, the extents over which values were derived was not considered, similarly, when modelling using extents, the resolutions over which values were derived were not considered. Also, due to the large number of candidate models that would have resulted from considering all 19 MBLI Raster extents, modelling was undertaken using a subset of 10 extents (beginning at 5 m and including alternate extents up to 3,120 m). The maximum number of extents retained in the modelling for any metric was 9 (see results), which supported the use of a subset of 10 extents.

Overall, for each MBLI Raster metric, a total of 1,023 models were fit for resolutions and a further 1,023 for extents. This represented the total number of unique combinations of 10 extents / resolutions. For AUV Raster metrics a total of 511 models were fit (unique combinations of 9 resolutions). For the four AUV Mesh metrics derived over 10 resolutions, 1,023 models were also fit. Akaike information criterion (AIC) (AIC = 2p – 2LL, where p = the number of unknown parameters and LL the log likelihood of the model) corrected for small sample sizes (AICc) (Hurvich & Tsai, 1989). was used to select the most parsimonious model when model AICc values were 2 or more smaller than the null AICc. The resolutions / extents retained in the most parsimonious model represented the optimum subset of uniquely important resolutions / extents required to adequately explain the variability observed in the metric value. Although none of the remaining extents / resolutions was uniquely important, one was selected as a representative extent or resolution to capture the

variation not explained by the unique extents / resolutions. The median resolution / extent or otherwise the value nearest and greater than the median was selected. In circumstances where none of the candidate models performed better than the null model, this indicated that none the of the extents / resolutions were uniquely important and that any could be selected as representative. Again, the median value was selected in these cases. Metrics that required more uniquely important resolutions / extents to explain variability in their values were considered more sensitive to changing extent / resolution than those required fewer.

3.4 Results

3.4.1 MBLI Raster

3.4.1.1 Metrics

Examination of correlations(where |r| > 0.7 represents highly correlated) among MBLI predictors (**Figure 3-3**) indicated highly positive correlation between slope, surface-plana-area and terrain-ruggedness, and the std of all metrics except those based on orientation (aspect-north and aspect-east), forming a 'complexity grouping'. The only other highly correlated metrics were aspect-east and aspect-east-std, which were highly negatively correlated. It is noted that when correlations were calculated without consideration of extent and resolution (separate figures not presented for brevity), there was a highly positive and highly negative correlation between standard-curvature and each of planar-curvature and profile-curvature, respectively. Also, the high correlation between aspect-east and aspect-east-std was not evident and bathymetry-std was not highly correlated with any other metric. These differences in relationships between metrics depending on the approach to calculating correlations indicate the importance of considering spatial scale when undertaking such comparisons.

Metrics with higher overall correlations (values in **Figure 3-3**) tended to be highly correlated over most or all extent and resolution combinations, for example between bathymetry-std and some other measures of complexity (**Figure 3-4a** to **d**). As overall correlations between pairs of metrics became less extreme, there tended to be more variability in the correlations for each extent x resolution combination. For example, smaller resolutions and extents of aspect-east-std and aspect-east (albeit still highly correlated) were associated with lower individual correlations (**Figure 3-4e**). For metrics that were overall not highly correlated, individual correlations for each extent and resolution combination were more variable, with some extent x resolution combinations highly positive,

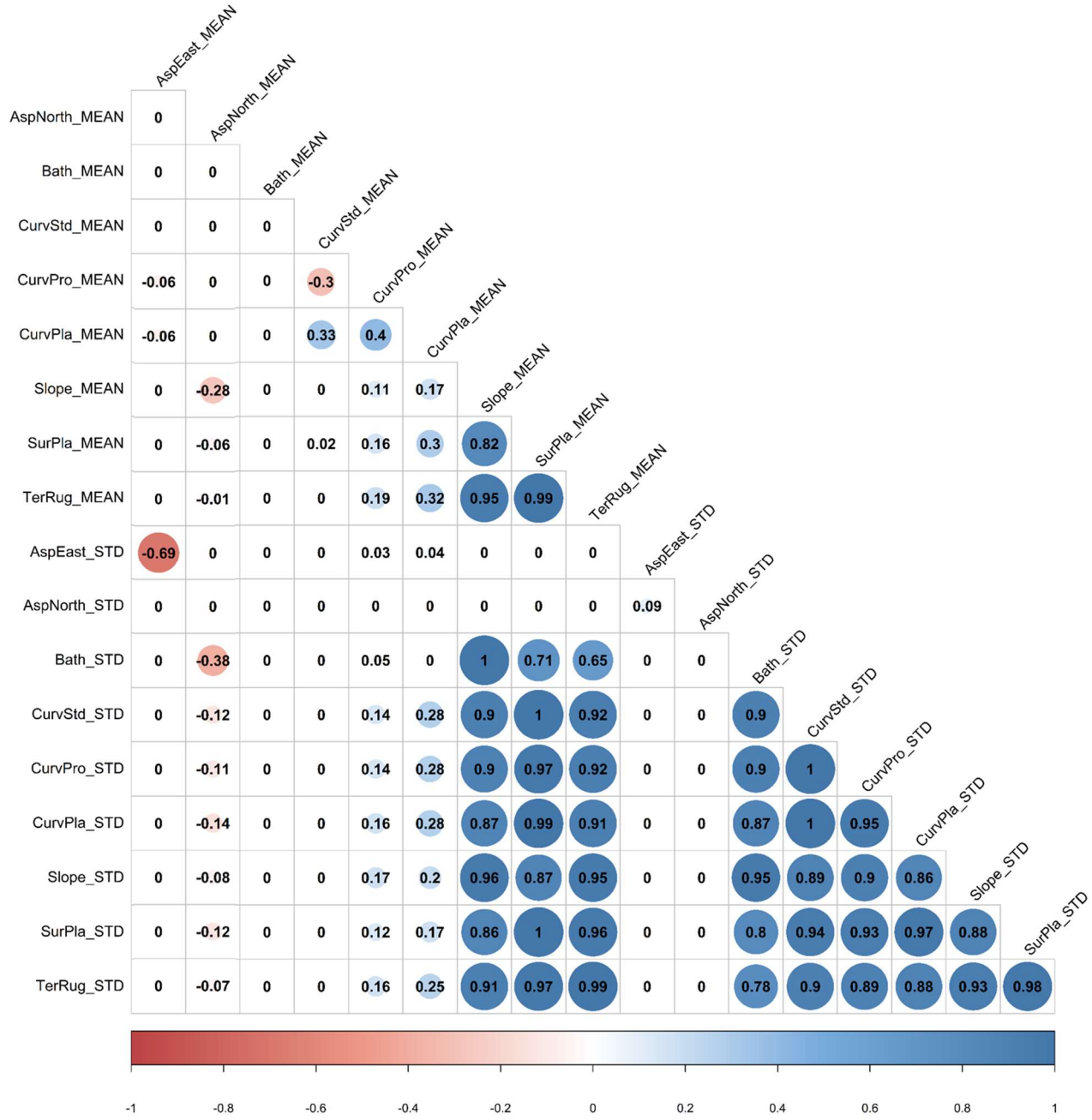

Figure 3-3 **Correlations among MBLI metrics when partitioned among extents and resolutions. Red and blue shading indicates negative and positive correlation, respectively, and the numbers inside the shading the Pearson's correlation coefficient r.**

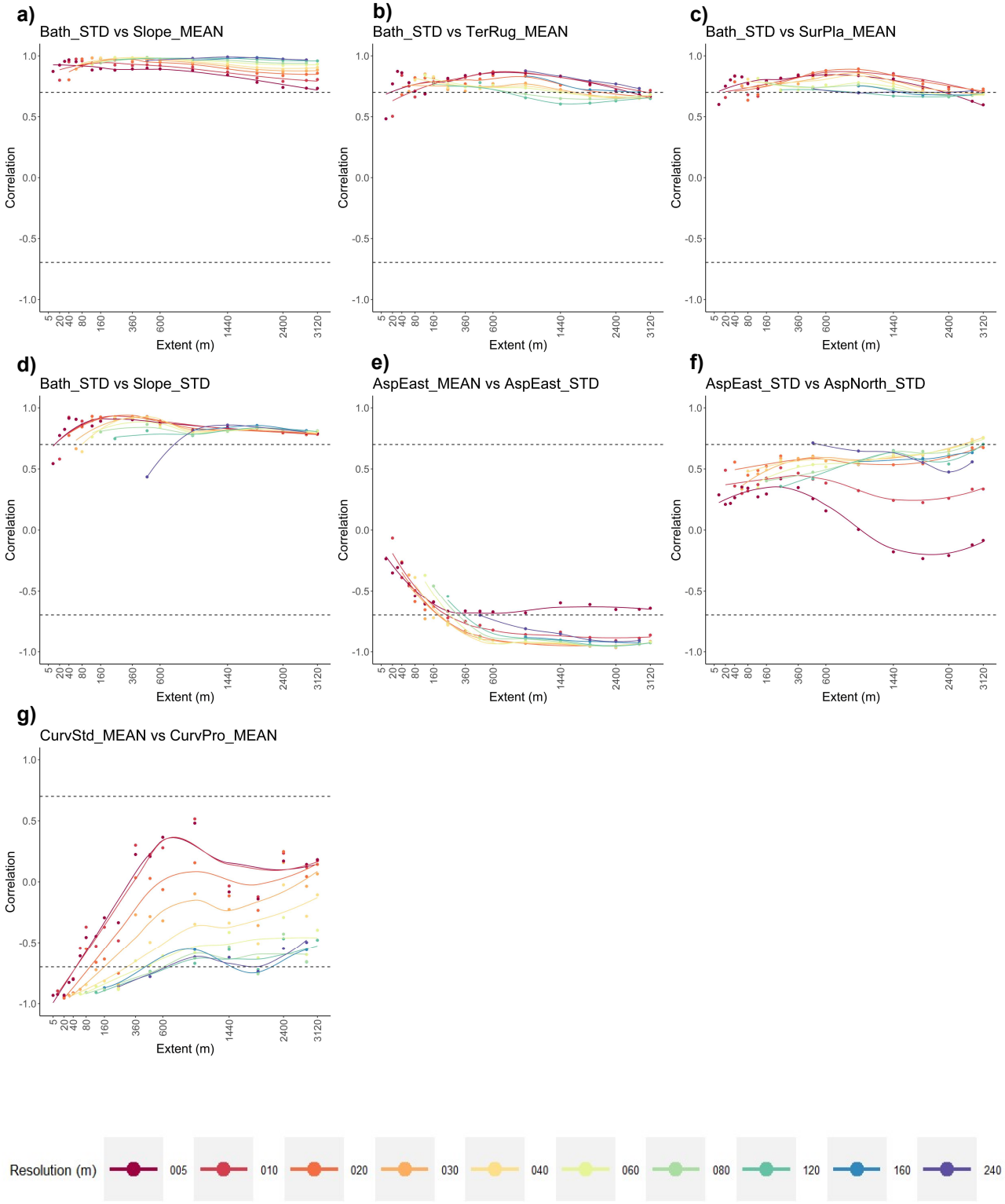

Figure 3-4 **Correlation (r) values (y axis) calculated between pairs of MBLI metrics when extent and resolution (cell side length) was considered. Colours indicate resolutions and x axis the extents. Dots indicate the correlation r value between the metrics for each extent and resolution combination and the lines the fitted locally weighted running line smoother (LOESS).**

for example aspect-east-std and aspect-north-std (**Figure 3-4f**) or highly negative, for example standard-curvature and profile-curvature (**Figure 3-4g**). Thus, for some pairs of metrics, apparent overall correlations would depend on the range and number of resolutions and extents over which they are derived.

In summary, these findings indicated the retention of 8 of the 18 total MBLI Raster derived metrics (**Table 3-4**). Six (aspect-north, bathymetry, standard-curvature, planar-curvature, profile-curvature, and aspect-north-std) that were not correlated with any other, aspect-east that was retained in place of aspect-east-std (mean values are easier to interpret than std in metric values), and surface-planar-area that was retained in favour of all remaining metrics within the '*complexity grouping*' (surface-planar-area is easy to interpret and more commonly utilised than any other metric within this grouping).

Table 3-4 Summary of metric correlations and identity of those metrics that are retained. Coloured shading indicates groups of correlated metrics identified when resolution and extent are considered. Purple and yellow shading represents the AspEast and complexity groupings, respectively. Blank cells indicate where a metric was not retained.

Metric	Correlated with Another Metric (When Considering Ext x Res) (see)	Retained
AspNorth		Yes
Bath		Yes
CurvStd		Yes
CurvPla		Yes
CurvPro		Yes
AspEast	Yes	Yes*
AspEast-std	Yes	
AspNorth-std		Yes
SurPla	Yes	Yes**
Slope	Yes	
TerRug	Yes	
CurvStd-std	Yes	
CurvPla-std	Yes	
CurvPro-std	Yes	
Slope_Std	Yes	
SurPla-std	Yes	
TerRug_Std	Yes	
Bath-std	Yes	

*AspEast retained in favour of std of AspEast, **SurPla retained in favour of all other metrics within the 'complexity grouping' with which it is correlated

3.4.1.2 Extents and Resolutions

Final models of metric values based on resolutions and extents converted to categorical factors were identified using AICc. Models of the eight retained MBLI Raster metrics indicated all except bathymetry required at least two unique extents and resolutions to

adequately explain variability in their values (**Table 3-5**). Overall, there smaller and larger (i.e., more extreme) extents and resolutions tended to be retained in models more often than those in the intermediate range (**Figure 3-5**). The relatively small amount of variation explained by most models would suggest other factors, such as inter-site variability, have a greater influence on metric values than the resolution and extent over which they were derived.

Table 3-5 Final models of MBLI Raster metrics identifying the number and identity of uniquely important resolutions and extents required to explain the optimal proportion of variability in metric values. For each metric, the optimal number of resolutions / extents is equal to those identified by the model terms plus one, where the additional resolution/extent may be any of those not included in the model terms. Res – resolution and Ext = extent over which metrics were derived (m).

Response	Model Terms	Model AICc	null AICc	R^2
Resolutions				
AspEast	Res_005+Res_010+Res_020+Res_030+Res_040+Res_240	4,652.1	5,077.8	0.07
AspNorth	Res_005+Res_010+Res_020+Res_030+Res_240	2,549.6	2,723.5	0.03
Bath	null	40,453.0	40,453.0	0.00
CurvStd	Res_005+Res_010+Res_020	7216.8	7,219.3	0.00
CurvPro	Res_005+Res_010	1,533.6	1,609.0	0.01
CurvPla	Res_005+Res_010+Res_020	-380.0	-157.8	0.04
SurPla	Res_005+Res_010+Res_020+Res_030+Res_040	-57,020.2	-55,107.2	0.29
AspNorth-std	Res_005+Res_010+Res_020+Res_030+Res_040+Res_120+Res_240	-3,885.3	-3,443.4	0.08
Extents				
AspEast	Extent_0005+Extent_0020+Extent_0040+Extent_0160+Extent_2400+ Extent_3120	5,015.1	5,077.8	0.01
AspNorth	Extent_0005+Extent_0020+Extent_0040+Extent_3120	2,677.1	2,723.5	0.01
Bath	Extent_0020+Extent_0040+Extent_2400+Extent_3120	40,431.6	40,453.0	0.00
CurvStd	Extent_0005+Extent_0020+Extent_0040	7,145.5	7,219.3	0.01
CurvPro	Extent_0005+Extent_0020+Extent_0040	1,593.0	1,609.0	0.00
CurvPla	Extent_0005+Extent_0020+Extent_0040+Extent_0080+Extent_2400	-307.8	-157.8	0.03
SurPla	Extent_0005+Extent_0020+Extent_0040+Extent_0080+Extent_0360+ Extent_0600+ Extent_1440+Extent_2400+Extent_3120	-55,443.1	-55,107.2	0.06
AspNorth-std	Extent_0020+Extent_0040+Extent_0080+Extent_0160+Extent_0600+ Extent_1440+ Extent_2400+Extent_3120	-3,818.6	-3,443.4	0.07

Metrics based on orientation (aspect-east, aspect-north and aspect-north-std) and surface-planar-area tended to be most sensitive to change in resolution (5 or more uniquely important resolutions) and those based on curvature less so (2 to 3 uniquely important resolutions). This was partly reflected in the case of extents, with aspect-east, aspect-north-std and surface-planar-area associated with 6 to 9 uniquely important extents. The sensitivity of aspect-north to varying extent was, however, more comparable to bathymetry and those based on curvature, which required 3 to 5 uniquely important extents. Worth

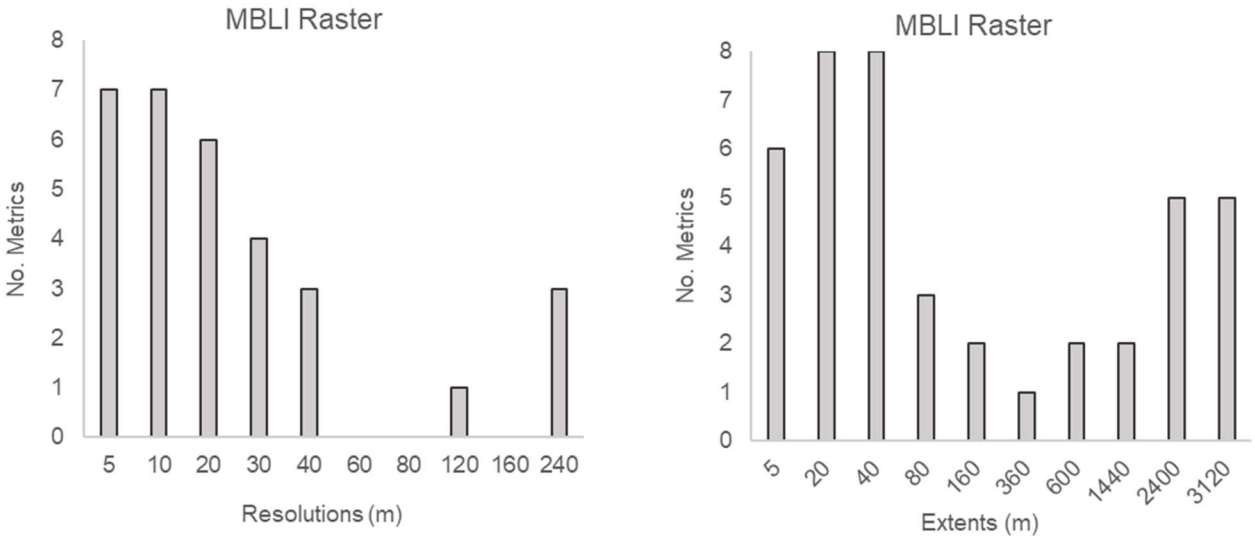

Figure 3-5 Frequency of uniquely important resolutions and extents identified for MBLI metrics

noting is that bathymetry was more sensitive to change in extent (4 unique extents) compared to resolution (0 unique resolutions), and in the case of extents was more sensitive than profile curvature and standard-curvature (3 extents each). For bathymetry, where there was no uniquely important resolution (i.e., no model performed better than the null), indicating that bathymetry may be derived over any resolution and still provide a representative measure.

Aspect-east, aspect-north and aspect-north-std varied relatively greatly depending on the resolution and extent over which they were derived. In the case of resolutions, this was associated with a relatively consistent linear trend in metric values with increasing resolution (**Figure 3-6**). This trend was positive in the case of aspect-east and negative in the case of aspect-north and aspect-north-std. The influence of increasing extent on aspect-east and aspect-north was more complex with evidence of a unimodal pattern between values and changing extent, with maximum and minimum values of aspect-east and aspect-north, respectively, occurring at intermediate values of extent. For aspect-north-std the pattern was relatively linear with greatest values at greater extents. Metrics based on curvature (standard-curvature, profile-curvature, planar-curvature) and surface-planar-area were sensitive to change in resolution and extent occurring over smaller ranges and appeared to plateau and approach an asymptote of 0 as resolution and extent increased. There was an

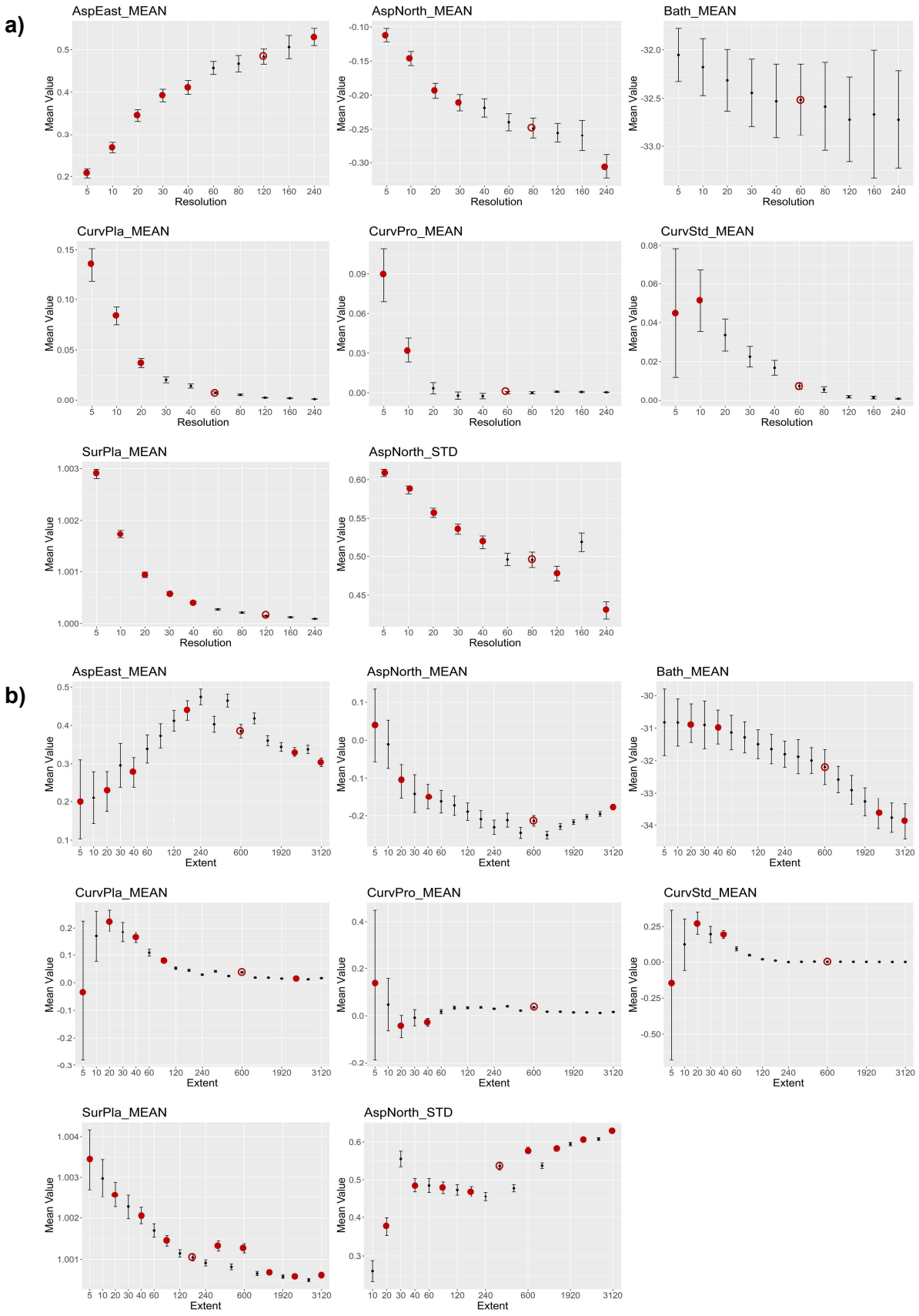

Figure 3-6 **Mean values of metrics derived at a) resolutions and b) extents. Solid red circles indicate the uniquely important resolutions / extents identified by selected parsimonious models. Open red circles indicate the resolution / extent selected to represent all remaining non-uniquely important metrics. Note, only 10 extents were included in the modelling.**

overall relatively weak linear trend for a reduction in bathymetry with increasing resolution and extent. This was more apparent in the case of increasing extents.

It is important to note too that metric values at individual sites could vary substantially with resolution or extent. The change in values of aspect-east and aspect-north as the resolution increased was relatively substantial. For example, the orientation of the seafloor at Site O2_1_2 ranged from directly southerly facing (aspect-east: 0, aspect-north: -1) at 5 m resolution to north-easterly facing (aspect-east: -0.7, aspect-north: 0.8) at 240 m resolution. Similar changes in curvature (planar-curvature, profile-curvature and standard-curvature) were also noted, though these occurred over a narrower and smaller range in resolution. For example, between 5 m and 10 m resolution, the planar-curvature (planar-curvature) at Site DC7_7 changed from -0.8 (concave, or valley like) to 1.5 (convex, or ridge like) and the profile-curvature at H4_2_1 changed from -0.8 (upwardly convex) to 4.6 (upwardly concave). Such changes can have important ecological implications. Changes in aspect-east and aspect-north of such magnitude could be associated with drastically different exposures to wave energy and light available. Such variation in curvature metrics would identify changes between ridges and valleys depending on the resolution / extent, with potentially substantially different hydrodynamic regimes and level of exposure / shelter. Such differences related to the spatial scale over which metrics are derived highlight the importance of considering multiple resolutions and spatial extents. It is also noted that in these comparisons an increase in resolution was accompanied by a comparable increase in the extent of the analysis window (albeit in each case the analysis window consisted of only one cell). A similar pattern was evident for other metrics of curvature and for surface-planar-area, though values were all positive in the case of the latter. Values of bathymetry at an individual site level were relatively consistent.

3.4.2 AUV Raster

3.4.2.1 Metrics

Examination of overall correlations among AUV Raster metrics (**Figure 3-7**) identified highly positive correlations between slope, surface-planar-area, terrain-ruggedness, their std, and standard-curvature-std, planar-curvature-std, profile-curvature-std and bathymetry-std, forming a ‘complexity grouping’. Planar-curvature and profile-curvature were also correlated with each other, but with no other metric. The remaining metrics (aspect-east, aspect-north, bathymetry, and standard-curvature) were uncorrelated with each other and all other metrics. It is noted that not all metrics in the ‘complexity grouping’ were highly correlated with all other metrics in this group. For example, bathymetry-std was correlated

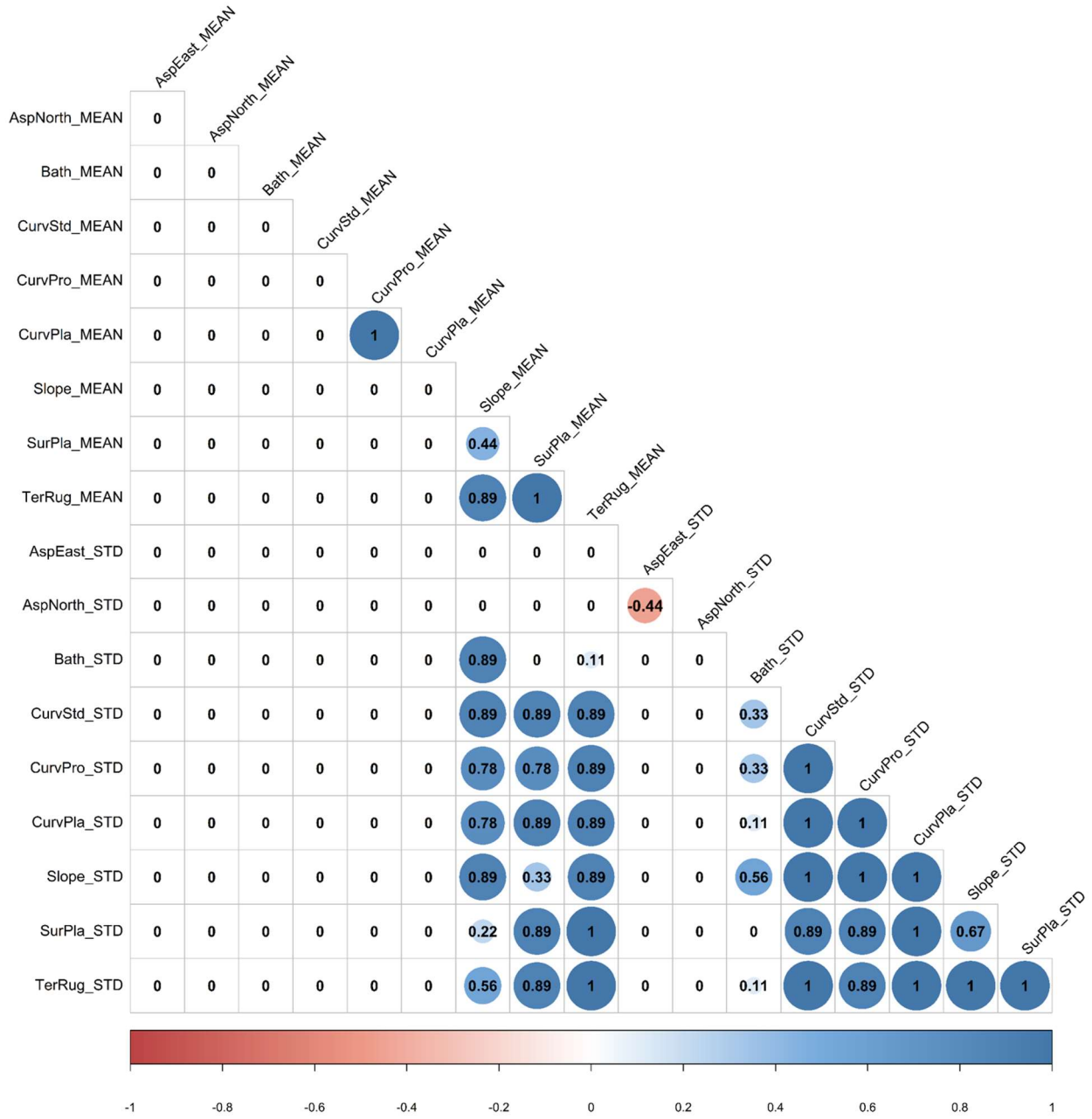

Figure 3-7 Correlations among AUV Raster metrics when partitioned among resolutions. Red and blue shading indicates negative and positive correlation, respectively, and the numbers inside the shading the Pearson's correlation coefficient r.

with slope only. Slope and surface-planar-area were also uncorrelated, whilst, otherwise both correlated to most other metrics within this group. When correlations were calculated without consideration of extent and resolution (separate figures not presented for brevity), planar-curvature. Standard-curvature and profile-curvature were highly correlated with metrics in the '*complexity grouping*'. As was the case with MBLI Raster, this indicates the importance of considering spatial scale (in the case of AUV Raster, the resolution) when undertaking such comparisons.

In summary, these findings indicated the retention of 9 of the total 18 AUV Raster derived metrics (**Table 3-6**). Six (aspect-north, bathymetry, standard-curvature, aspect-east, and aspect-east-std and aspect-north) that were not correlated with any other, planar-curvature that was retained in favour of profile-curvature (either one of these metrics could have been retained), and Slope and surface-planar-area. Although not correlated with each other, slope and surface-planar-area (slope and surface-planar-area are those commonly utilised across comparable studies - **Section 2**), between them they were correlated with all other remaining metrics. This finding is possibly related to the calculating of surface-planar-area accounting for slope, which is undertaken to decouple these two metrics and reduce their correlation.

Table 3-6 Summary of AUV Raster metric correlations and identity of those metrics that are retained (Yes). Green shading indicates the '*curvature grouping*' and blue / red the '*complexity grouping*' (albeit not all pairs of metrics within the 'complexity grouping' were directly highly correlated). Blank cells indicate where a metric was not retained.

Metric	Correlated with Another Metric (When Considering Extent)	Retained?
AspNorth		Yes
Bath		Yes
CurvStd		Yes
CurvPla	Yes	Yes*
CurvPro	Yes	
AspEast		Yes
AspEast-std		Yes
AspNorth-std		Yes
Slope	Yes	Yes**
Slope-std	Yes	
Bath-std	Yes	
TerRug	Yes	
CurvStd-std	Yes	
CurvPla-std	Yes	
CurvPro-std	Yes	
TerRug-std	Yes	
SurPla-std	Yes	
SurPla	Yes	Yes***

*CurvPla retained in favour of CurvPro,**Slope retained in favour of std of Slope and Bath, ***SurPla retained in favour of TerRug and CurvStd-std

3.4.2.2 Extents and Resolutions

Final models of metric values based on resolutions converted to categorical factors were identified using AICc. All metrics except aspect-north and bathymetry required at least one unique resolution to adequately explain variation in their values (**Table 3-7**). For aspect-north and bathymetry, no resolution provided uniquely important information, and any could

be selected to be representative. There was no strong evidence to suggest any trend in the frequency of retention of difference resolutions among the metrics (**Figure 3-8**).

Table 3-7 Final models of AUV Raster metrics identifying important resolutions required to explain the greatest proportion of variability in metric values. Res – resolution over which metrics were derived (m).

Response	Model Terms	Model AICc	null AICc	R^2
AspEast	Res1.6+Res2.4	-267.4	-259.7	0.02
AspNorth	null	-408.0	-408.0	0.00
Bath	null	2,992.1	2,992.1	0.00
CurvStd	Res0.2	-13,003.0	-12,991.1	0.03
CurvPla	Res0.1+Res0.2+Res0.3+Res0.4+ Res0.6	2,808.5	3,437.2	0.76
SurPla	Res0.1+Res0.2+Res0.3+Res0.4+ Res0.6+Res0.8+Res2.4	-2,710.1	-2,122.9	0.74
Slope	Res0.1+Res0.2+Res0.3+Res0.4+ Res0.6+Res0.8+Res2.4	2,441.5	2,901.5	0.65
AspEast-std	Res0.8+Res1.2+Res1.6+Res2.4	-1,195.9	-1,138.5	0.13
AspNorth-std	Res1.6+Res2.4	-1,286.0	-1,267.9	0.04

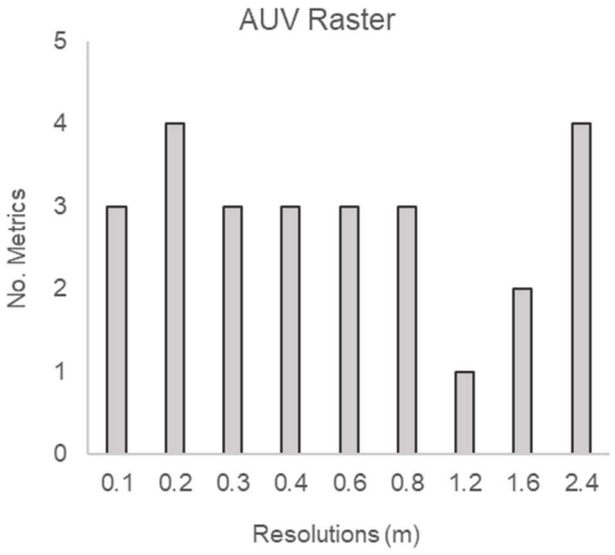

Figure 3-8 Frequency of uniquely important resolutions and extents identified for AUV Raster metrics.

Those metrics most sensitive to change in resolution (planar-curvature, surface-planar-area and slope, requiring 5 to 7 unique resolutions) (**Table 3-7**) also displayed the greatest rate of change in mean values (**Figure 3-8** and **Figure 3-9**). This was associated with a negative linear trend in the case of surface-planar-area and slope. For planar-curvature, values first decreased and then plateaued with an asymptote at 0 with increasing resolution. aspect-north, aspect-north-std and aspect-east-std decreased, whilst aspect-east increased, with increasing resolution. bathymetry did not vary among resolutions. Values of standard-curvature were relatively consistent also, except for a relatively large value corresponding to 0.2 m resolution.

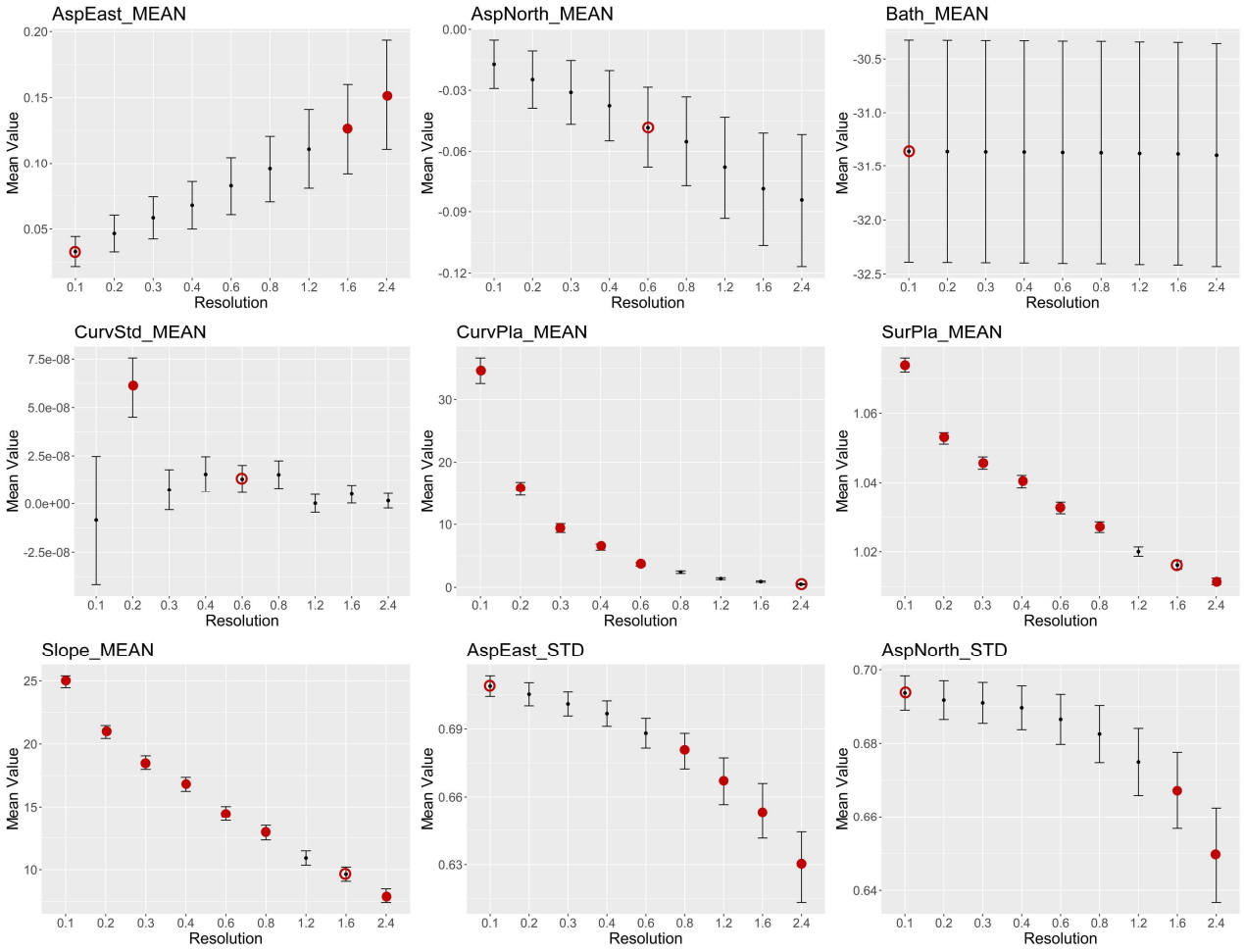

Figure 3-9 Mean values of AUV Raster metrics derived at each resolution. Solid red circles indicate the uniquely important resolutions identified by selected parsimonious models. Open red circles indicate the resolution selected to represent all remaining non-uniquely important metrics.

3.4.3 AUV Mesh

3.4.3.1 Metrics

When derived over the native mesh resolution, all metrics except Face-Angles$_{20deg.-30deg.}$, Face-Angles$_{30deg.-40deg.}$ and Face-Angles$_{120deg.-130deg}$ were highly correlated with at least one other metric, but no one metric was correlated with all other metrics (**Figure 3-10a**). No obvious groupings were initially apparent. However, given that only four metrics (Mesh-Height$_{Rng}$, Mesh-Height$_{Std}$, Mesh-Rugosity$_{Proj}$ and Mesh-Rugosity$_{Plan}$) were derived over multiple resolutions, it was desirable to consider retaining these in the reduced predictor data set. This would allow complexity present at various resolutions to be considered, whilst minimising the number of metrics included in the dataset. Based on this, and considering the need to maximise metric interpretability and minimise the number of different metrics, Mesh-Height$_{Rng}$ and Mesh-Rugosity$_{Plan}$ were selected was being representative of all other metrics (except Face-Angles$_{20deg.-30deg.}$, Face-Angles$_{30deg.-40deg.}$ and Face-Angles$_{120deg.-}$

a)

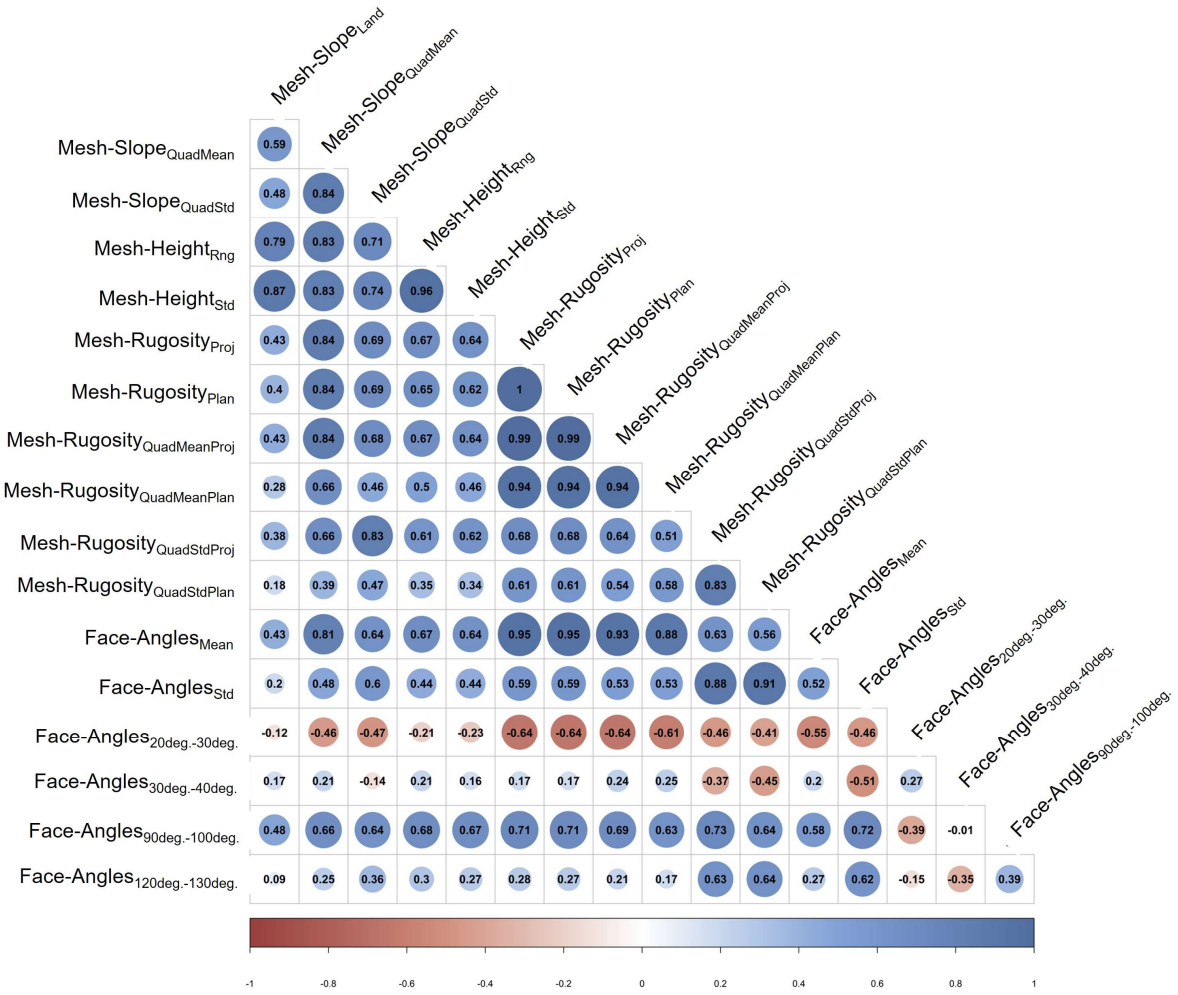

b)

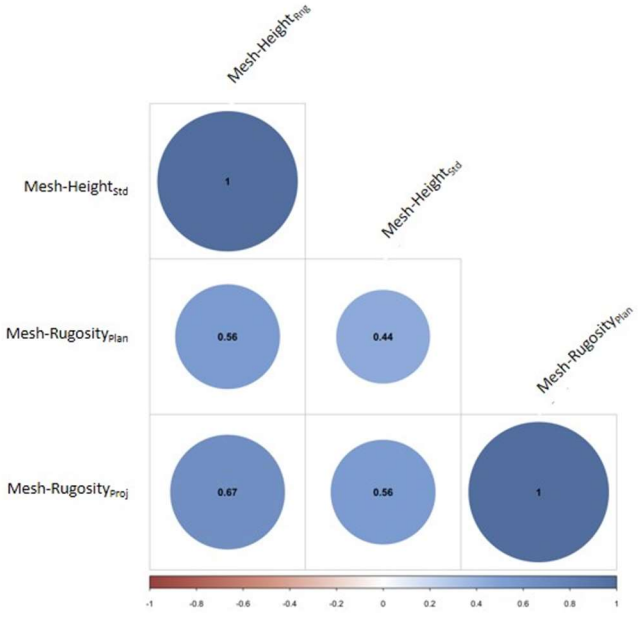

Figure 3-10 Correlations among AUV Mesh metrics a) for all metrics at native resolution and b) for those metrics derived over multiple resolutions. Red and blue shading indicates negative and positive correlation, respectively, and the numbers inside the shading the Pearson's correlation coefficient r.

$_{130deg.}$) (**Table 3-8**). Mesh-Height$_{Rng}$ was highly positively correlated with Mesh-Height$_{Std}$ and metrics based on slope (Mesh-Slope$_{Land}$, Mesh-Slope$_{QuadMean}$ and Mesh-Slope$_{QuadStd}$), forming a '*slope-height grouping*'. Mesh-Rugosity$_{Plan}$, was correlated with all other metrics based on rugosity (Mesh-Rugosity$_{Proj}$, Mesh-Rugosity$_{QuadMeanProj}$, Mesh-Rugosity$_{QuadMeanPlan,}$ Mesh-Rugosity$_{QuadStdProj}$ and Mesh-Rugosity$_{QuadStdPlan}$), and with Face-Angles$_{Mean}$, Face-Angles$_{Std}$ and Face-Angles$_{90deg.-100deg.}$, forming a '*rugosity-face angle*' grouping (Mesh-Height$_{Rng}$ was also highly positively correlated with two of the three slope metrics). Mesh-Height$_{Rng}$ was highly positively correlated with Mesh-Height$_{Std}$ and Mesh-Rugosity$_{Proj}$ was highly positive correlated with Mesh-Rugosity$_{Plan}$ when all resolutions were considered (**Figure 3-10b**). This same pattern was observed for the native resolution (**Figure 3-10a**) and when calculated without consideration of extent and resolution (separate figures not presented for brevity).

Table 3-8 Summary of metric correlations and identity of those metrics that are retained. Coloured shading indicates groups of correlated metrics identified when resolution and extent are considered.

Metric	Correlated with at Least One Other Metric (Overall)	Correlated with Another Metric (When Considering Resolution)	Retained?
Mesh-Height$_{Rng}$	Yes	Yes	Yes
Mesh-Slope$_{Land}$	Yes	na	
Mesh-Height$_{Std}$	Yes	Yes	
Mesh-Slope$_{QuadStd}$	Yes	na	
Mesh-Slope$_{QuadMean}$	Yes	na	
Face-Angles$_{Std}$	Yes	na	
Face-Angles$_{Mean}$	Yes	na	
Mesh-Rugosity$_{QuadStdProj}$	Yes	na	
Mesh-Rugosity$_{QuadStdPlan}$	Yes	na	
Mesh-Rugosity$_{QuadMeanProj}$	Yes	na	
Face-Angles$_{90deg.-100deg.}$	Yes	na	
Mesh-Rugosity$_{QuadMeanPlan}$	Yes	na	
Mesh-Rugosity$_{Proj}$			
Mesh-Rugosity$_{Plan}$	Yes	No	Yes
Face-Angles$_{20deg.-30deg.}$		na	Yes
Face-Angles$_{30deg.-40deg.}$		na	Yes
Face-Angles$_{120deg.-130deg.}$	Yes	na	Yes

3.4.3.2 Extents and Resolutions

For the two retained AUV Mesh metrics derived over multiple resolutions, Mesh-Height$_{Rng}$ and Mesh-Rugosity$_{Plan}$, one and eight, respectively, unique resolutions were required to adequately capture the total variability present in their values (**Table 3-9**). Only a resolution of 2.4 m was retained in both models (**Figure 3-11**). Mesh-Rugosity$_{Plan}$ was far more

sensitive to change in resolution than Mesh-Height$_{Rng}$. with the rate of change with increase resolution around the mean values far more evident for Mesh-Rugosity$_{Plan}$ (**Figure 3-12**).

Table 3-9 Final models of AUV Mesh metrics identifying the number and identity of uniquely important resolutions required to explain the optimal proportion of variability in metric values. For each metric, the optimal number of resolutions is equal to those identified by the model terms plus one, where the additional resolution may be any of those not included in the model terms. Res – resolution over which metrics were derived (m).

Response	Model Terms	Model AICc	null AICc	R^2
Mesh-Height$_{Rng}$	Res2.4	2013.1	2017.9	0.01
Mesh-Rugosity$_{Plan}$	Res0.1+Res0.2+Res0.3+Res0.4+Res0.6+Res0.8+Res2.4+ResNative	-1412.0	-734.4	0.75

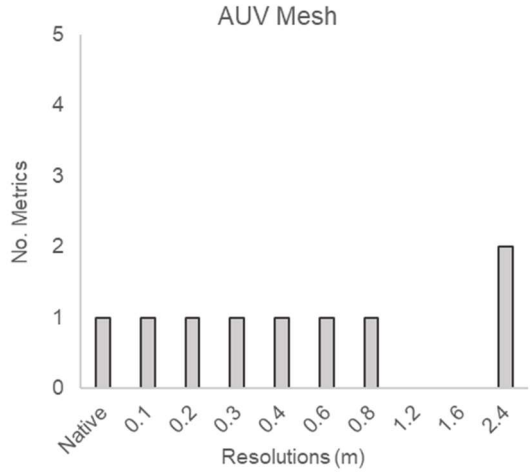

Figure 3-11 Frequency of uniquely important resolutions and extents identified for AUV Mesh metrics.

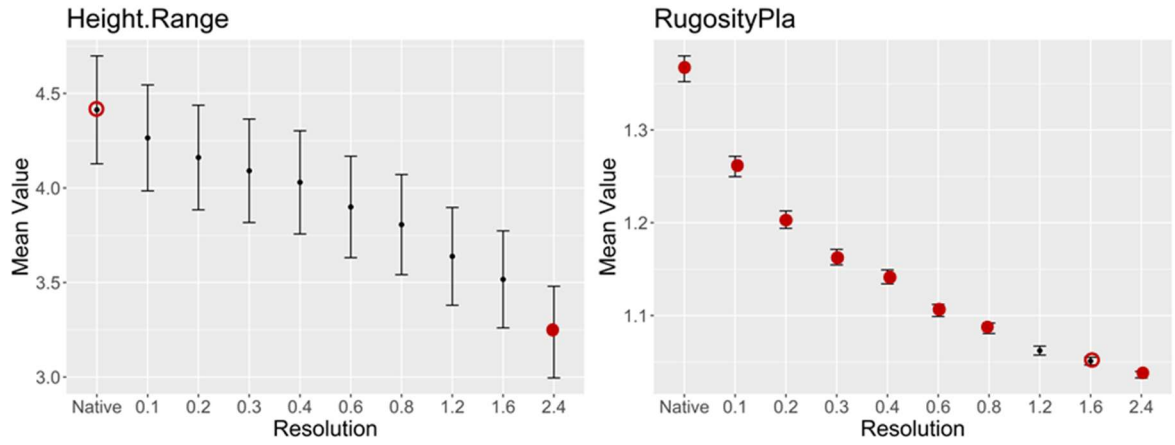

Figure 3-12 Mean values of AUV Raster metrics derived at each resolution. Solid red circles indicate the uniquely important resolutions identified by selected parsimonious models. Open red circles indicate the resolution selected to represent all remaining non-uniquely important metrics.

3.5 Discussion

3.5.1 Relationships Among Metrics

3.5.1.1 Raster-Based

Metrics of structural complexity derived from raster datasets generally correlated well with each other, suggesting many commonly utilised metrics capture very similar components of seafloor physical variability. A key finding of practical importance to researchers was that most metrics based on metric variability (all except variability in orientation) were highly positively correlated with metrics of 'gross complexity' (including slope, surface-planar-area, terrain-ruggedness and the variability in these metrics and variability in curvature metrics). This indicated that the utility of deriving such variability-based metrics is likely limited and that they do not capture any unique information from the bathymetric reconstructions. Thus, the derivation of other and potentially more informative metrics should be prioritised over such metrics. The exception was aspect-north-std and aspect-east-std, albeit the latter was highly correlated with aspect-east. Importantly, there appears to be no other study that has derived variability in metrics of orientation Despite high correlation among metrics of gross complexity, there was evidence of discrete components of structural complexity and individual metrics often captured unique information on structural complexity. Similar findings have been noted in the few previous studies that undertook some exploration of patterns in metrics prior to including them in predictive models. These include comparisons among metrics from multibeam derived rasters from the continental slope 300 m to 500 m of west Ireland (Wilson *et al*., 2007a) and among metrics from photogrammetrically derived rasters of Hawaiian coral reef (Wilson *et al*., 2019). The metric groupings suggested here largely support the groupings suggested by Wilson *et al*., (2007a) and based more on theory rather than empirical examination of correlations (as done here).

The first grouping identified in this Chapter was the largest (by number of metrics) and consisted of several raster metrics capturing 'gross complexity' (i.e., slope, surface-planar-area, terrain-ruggedness, and the variability of these and all other metrics except those based on orientation). This group is equivalent to the 'terrain variability' group identified by (Wilson *et al*., 2007a), within which the author included surface-rugosity, terrain-ruggedness index (TRI) (mean difference between a central pixel value (i.e., depth) and those of its surrounding cells) and two metrics not considered here: fractal dimension (degree of space filling in a surface) and roughness (bathymetric-range). Wilson *et al*., (2007a) did not consider variability in metrics. That this study grouped metrics based on variability in metric

values within the gross complexity grouping is not unexpected, given that as seafloor physical structure becomes increasingly variable, this provides more scope for increased diversity and range in magnitude of discrete elements, such as curvature. What these metrics also have in common is that they capture only a relatively simple measure of the magnitude of complexity using a scaler value of 0 or greater (for example between 0 and 1 for surface-planar-area). Notably (Wilson *et al*., 2007a) did not include slope in their terrain variability groping, though slope was highly correlated with a range of 'gross complexity' metrics in this analysis and should be considered to capture very similar information as other metrics within this grouping. Despite the substantial redundancy evident among several metrics, the finding of distinct groups of metrics indicates that discrete components of terrain variability exist, and that metrics should be carefully selected to account for this.

In addition to 'gross complexity' two other groupings were evident amongst common metrics, a second based on the three metrics of curvature (standard-curvature, planar-curvature and profile-curvature) and a third based on the mean (aspect-north and aspect-east) and variability (aspect-north-std and aspect-east-std) in the two metrics of orientation. These were also recognised as two distinct groups by Wilson *et al*., (2007a). However, compared with metrics of 'gross complexity' individual metrics within these groups were also uncorrelated with each other, the only exception been the correlation between aspect-east and aspect-east-std. Individual curvature and orientation metrics, whilst belonging to the same metric 'family', provide variations of the metric that allow quantification of further distinct information on structural complexity. The absence of any substantial correlation among these metrics should not be unexpected, given they have been developed a-priori to capture specific elements of complexity. Unlike 'gross complexity' measures they also do not just provide a simple scaler measure of magnitude, but also direction, which itself is also associated with different types of complexity. For example, northerly (+1) and southerly (-1) facing surfaces captured by aspect-north and more convex or concave surfaces captured using curvature-based metrics. By design, metrics that quantify discrete elements of complexity are perhaps far less likely to correlate with each other. Orientation and curvature-based metrics were uncorrelated with each other and all other metrics, capture unique information on structural complexity, and should all be considered to maximise the amount of useful information that can be obtain from such datasets.

This divergence between measures of gross complexity and curvature has been noted in other studies previously. Fukunaga *et al*., (2019) undertook a similar study, where raster DEMs were created from photogrammetrically derived meshes and various metrics of

complexity derived using ArcGIS and R packages. However, their study differed in that the extent covered was smaller (90 m^2) and resolution finer (0.01 m) than that produced here. All measures of 'gross complexity' (surface-rugosity, slope, terrain-ruggedness), the two measures of fractal dimension (one each aggregated by a factor of 64 and 128) and viewshed derived by Fukunaga *et al*., (2019) were found to be highly correlated regardless of the method of derivation (ArcGIS or R). The two measures of curvature (profile-curvature and planar-curvature) were uncorrelated with metrics within this group, but were moderately correlated (r 0.64 to 0.69) with slope. Planar-curvature (curvature parallel to the direction of the maximum slope) and profile-curvature (curvature parallel to the direction of the maximum slope) are both likely to have important ecological relevance. Planar-curvature (planar-curvature) captures ridges (positive values) and valleys (negative values). Profile-curvature captures convex (negative values) and concave (positive values) surfaces perpendicular to slope, which are associated with faster and slower, respectively, water velocity along the boundary layer of the benthos. Both will influence the strength and direction of hydrodynamic flow and the types of habitat refuges available to marine biota. The findings of this chapter, which support and extend findings by Fukunaga *et al*., (2019), indicates that these metrics capture discrete and potentially important measures of structural complexity and should be considered separately when quantifying structural complexity.

The third group of metrics, based on orientation also captured unique components of structural complexity. The importance of these metrics as predictors would be at least partly associated with their ability to provide surrogates of environmental gradients such as wave and swell exposure, hydrodynamic flow, and light irradiance (Hill *et al*., 2014). Although measuring such gradients directly may be much less costly, if bathymetric datasets are available the inclusion of orientation metrics represents minimal additional effort. These metrics can also be derived over a range and resolutions thereby capturing a range of local and broader scale variability in hydrodynamic flow, for example, that may be more costly to capture via direct measurement. Variability in measures of orientation is somewhat more difficult to conceptualise but could be thought of as capturing '*orientational diversity*'. Greater values of aspect-north-std would indicate the surface includes a range of northerly and southerly facing surfaces, for instance. Variability in orientation metrics is also unique in that unlike variability in other metrics, they are also uncorrelated with metrics of 'gross complexity'. Thus, they capture a unique component of complexity that should be considered.

Findings from the two raster-based datasets were largely in agreement. Although some differences were noted in correlations between the datasets for each of the three groupings, this most likely represents the single extent considered in the AUV Raster, a limitation of the small footprint size of these higher resolution datasets. In effect, the AUV Raster dataset represents a single sample point compared with the multiple extents included in the MBLI Raster dataset. When combined, however, these two datasets represent several orders of magnitude range in resolutions (0.1 m to 240 m) and extents (5 m to 3,000 m) which is likely to capture the spatial scales considered by almost all ecological and biological studies that derive measures of complexity from bathymetric reconstructions.

The findings of this study relate to abiotic rock reef structure, but many other studies are based on biogenic coral reef. The two known similar studies on coral reef suggest some degree of portability of findings (i.e., findings from one environment could inform those from another). The studies by Fukunaga, *et al*., (2020) and Fukunaga *et al*., (2019) and compared the correlations between surface-rugosity, slope, vector-ruggedness-measure (VRM) (equivalent to terrain-ruggedness), profile-curvature, planar-curvature and fractal dimension at 1 cm, 2 cm, 4 cm, 8 cm, 16 cm and 32 cm resolutions on coral reef. Even over these finer resolutions surface-rugosity, slope and VRM were highly (and positively) correlated with each other, but neither planar-curvature or profile-curvature were correlated. This pattern is the same as that observed in this study, and characteristic of a positively correlated set of 'gross complexity' metrics and uncorrelated curvature-based metrics. Although curvature- and orientation-based metrics were not considered by Fukunaga, *et al*., (2020) and Fukunaga *et al*., (2019), as a minimum, these metrics, and variability in the latter, are likely to provide additional unique information and should be considered when attempting to capture variability in structural complexity. These findings should be applicable to any studies that consider the bathymetric reconstructions of near coastal seafloor of temperate rock reefs and coral reefs. However, whilst findings are comparable between these studies, the number of studies available to make such comparisons is limited. Wherever feasible, further exploration of metric relationships similar to that undertaken by this thesis and other similar studies should be undertaken to further assess the portability of findings. Especially at different geographic locations and depths.

Worth noting also is that bathymetry was not correlated with any of the metrics of complexity considered here indicating structural complexity did not vary consistently with water depth. Water depth is often a strong predictor of biotic distributions and given its ease of measurement should be included in modelling approaches as a rule. Fractal-dimension

was not included here but was reported as highly correlated with several metrics related to gross complexity (slope, surface-planar-area and terrain-ruggedness) by Fukunaga *et al*., (2019). Fractal-dimension is generally more complicated to derive than more common metrics and further study would be required to determine under what circumstances it may be able to provide unique information on structural complexity.

3.5.1.2 Mesh-Based

Metrics derived from AUV Mesh also indicated a relatively large degree of correlation, though distinct groupings were less evident than for raster-based metrics. Examination of correlations between metrics did, however, indicate redundancy among some metrics and instances where the dataset could be reduced whilst minimising information loss. All mesh-based metrics, except those based on individual bins of face-angles, could effectively be explained by two metrics: Mesh-Height$_{Rng}$ and Mesh-Rugosity$_{Plan}$. Mesh-Height$_{Rng}$ and Mesh-Rugosity$_{Plan}$ derived across the entire mesh provided two relatively straightforward to derive metrics (i.e., not requiring virtual quadrats) that together also captured information done so by metrics of slope, and the mean and variability in face-angles. Three bins of face-angles (Face-Angles$_{20deg.-30deg.}$, Face-Angles$_{30deg.-40deg.}$, and Face-Angles$_{120deg.-130deg.}$) were uncorrelated with all other metrics. These provided unique information and were retained also.

The use of x-y plane or the plane of best fit (to decouple rugosity from slope) when calculating rugosity using virtual quadrats made little difference to mean rugosity and its variability among virtual quadrats. As would be expected, rugosity calculated using the plane of best fit was less correlated with measures of slope than when calculated using the x-y plane, though differences in correlations between the 2 ways of calculating 2D area with other metrics were small. Whether rugosity was calculated via virtual quadrats or across the entire mesh model extent also made little difference to rugosity values. In comparison, slope differed depending on whether it was calculated across the whole mesh surface or within virtual quadrats. This was most likely due to the difference in the effective analysis window of these two derivations (approximately 625 m^2 for the entire mesh surface and 1 m^2 for virtual quadrats). All metrics of slope were correlated with the range and variability in height of the mesh surface. However, only the slope in virtual quadrats was correlated with measures of rugosity. (Porter, 2018), who extracted a similar suite of mesh-based metrics though from artificial breakwall structures, also found surface-rugosity calculated using the plane of best fit (Mesh-Rugosity$_{Plan}$) and x-y plane (Mesh-Rugosity$_{Proj}$) to be highly correlated with each other, with slope and with face-angles greater than 90 deg. Also, Mesh-

$Rugosity_{Proj}$ area was more correlated with other metrics, and therefore was dropped from the predictor dataset (as was done in this chapter). Although based on a subset of the data examined in this study, via independent analysis Ferrari, *et al*., (2018) also found rugosity calculated using both methods of calculating the 2D area to be highly correlated. As appears to be the case with raster-based metrics, this points towards findings being portable between environments (though in this case natural vs. artificial rock reef, rather than rock reef vs. biogenic coral reef in the case of raster metrics). How portable findings of mesh-based metric studies on rock reefs are to coral reefs requires further study, though given the similarities in raster and mesh-based studies between environments described here, they would be expected to be similar also.

3.5.2 Spatial Scale

This analysis helped confirm the important role of spatial scale (extent and resolution) in influencing variability in metric values. For MBLI Raster, metrics most sensitive were those based on orientation, followed by those based on 'gross complexity' and curvature. For those based on orientation (aspect-east, aspect-north and aspect-north-std), values varied across the full range of resolutions examined. Curvature and 'gross complexity' metrics were also sensitive but mostly towards the smaller range of resolutions considered. Such sensitivity could be best conceptualised by examining changes at individual sites, where an increase in resolution (albeit coupled with the effect of increasing extent) sometimes resulted in substantial change in the nature of the structural complexity. The change in values of these metrics with increasing extent and resolution observed here equated to an almost 180 deg. change in the orientation of the surface. For example, a 5 m x 5 m area of reef may face directly south, but at a larger 240 m x 240 m scale, the prevailing reef profile may face to the north-east (for example at Site O2_1_2 **Section 3.4.1.2**). Similarly, curvature metrics may capture small ridges situated within larger valleys (e.g., Site DC7_7 **Section 3.4.1.2**). This was comparable to the substantial change in these metrics observed with increasing resolution by (Wilson *et al*., (2007a). Such variability has potential to substantially change habitat suitability. Orientation based metrics (aspect-north and aspect-east) capture important structuring gradients such as swell / wave exposure and light irradiance and have been shown to influence the abundance of fish and other biota on exposed coastlines (Cameron *et al*., 2014; Hill *et al*., 2014). Important resolutions, and, thus, orientations, would depend on a species mobility, behavior, body size and broad biota type (macroalgae, sessile filter feeder, mobile fish species). The magnitude of change in curvature with resolution observed here spans valley- to ridge-like terrain. Given the influence of curvature on

hydrodynamic flow (and, thus, shear stress, availability of particulate food matter, and potentially larval settlement), it is important to consider how this variability in metric values linked to resolution may influence the type and abundance of marine biota. Unless clear a-priori information is available on the spatial scale(s) most relevant to target biota, then studies should consider a range of spatial scales when deriving metrics and using them to model the distribution and abundance of biota. The findings presented here provide a starting point, and, as a minimum, indicate which metrics would be expected to vary the greatest with changing extent and resolution and that would require consideration when choosing what resolution(s) and extent(s) should be included. Otherwise, ecologically important terrain features may not be captured, resulting in poor model performance and predictions.

3.6 Conclusion

This systematic exploration of metric correlations identified substantial redundancy among several commonly used metrics of structural complexity. A subset of 8 of the total 18 MBLI Raster, 9 of the total 18 AUV Raster, and 5 of the 31 AUV Mesh metrics was identified as an optimised metric dataset that maximises the information quantified on structural complexity using a minimum number of metrics. When combined with information the relative sensitivities of each of these metrics to change in extent and resolution (**Figure 3-13**, **Figure 3-14** and **Figure 3-15**), this further minimises the number of predictors to a size suitable for common modelling techniques. Associated distinct groupings of metrics identify opportunities to rationalise metric derivation, particularly among the relatively large number of those that capture ‘gross complexity’. Gross complexity, curvature and orientation metrics, and individual metrics within the latter two groups, are associated with discrete components of structural complexity quantified from bathymetric reconstructions. These components have ecological relevance, and provide surrogates of a range of often otherwise difficult to capture environmental gradients and resources that determine the abundance and distribution of marine biota over local and broad-scales. Mesh-analogues of ‘gross complexity’ were also largely correlated, though novel mesh-based metrics based on face-angles capture unique information on beyond vertical surfaces (i.e., overhangs) that cannot be captured using traditional raster-based metrics. These findings will help guide efficient metric derivation that maximised the amount of information on structural complexity captured from bathymetric reconstructions.

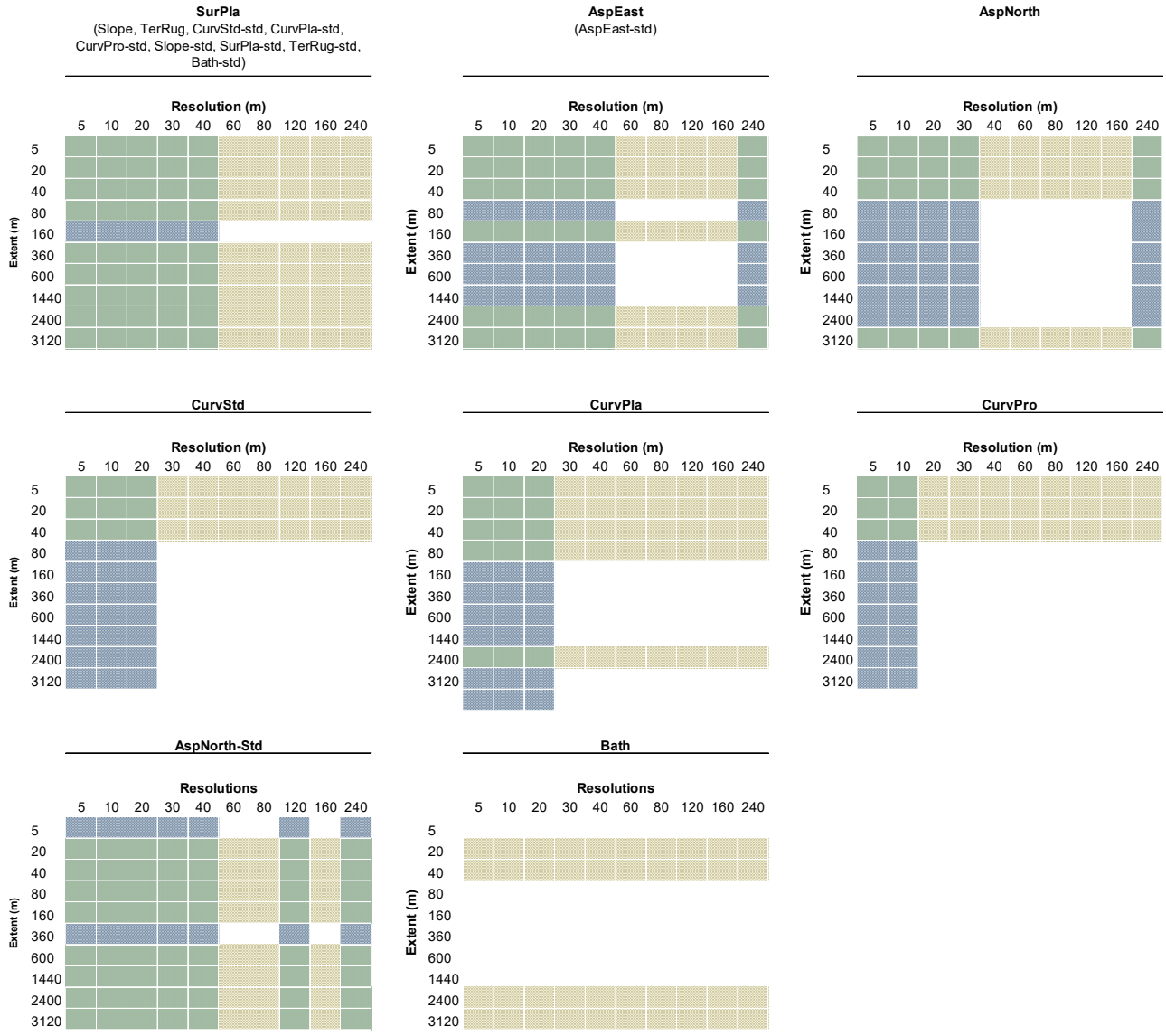

Figure 3-13 Important extents (orange shading) and resolutions (blue shading) identified for each of the MBLI Raster metrics retained (bold type with correlated metrics in brackets) following examination of correlations (green shading indicates important extend and resolution at that scale).

This study also further confirmed the importance of carefully considering spatial scale (resolution and extent) when deriving metrics of structural complexity. For many metrics, a substantial change in values was evident across the range of extents and resolutions considered. In some cases, this was associated with notable changes in the type of feature captured, such as convex vs. concave and northerly vs southerly facing surfaces. If multiple extents and resolutions are not considered when deriving metrics, such variability could result in important relationships with species distributions and ecological mechanisms being misidentified or missed entirely.

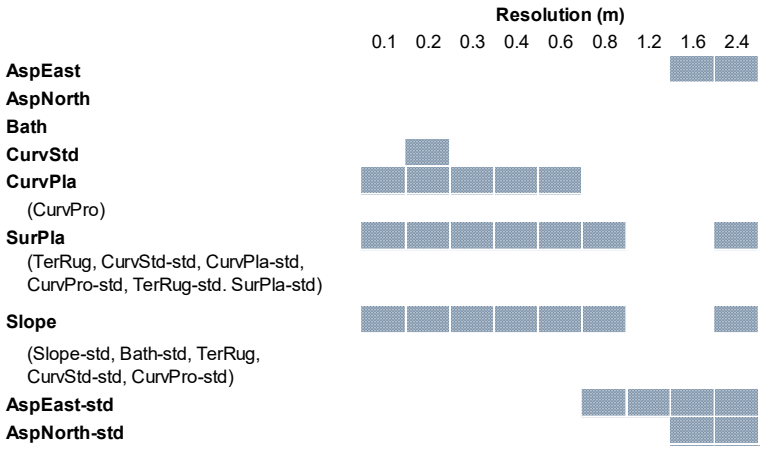

Figure 3-14 Important resolutions (blue shading) identified for each of the AUV Raster metrics retained (bold type with correlated metrics in brackets) following examination of correlations.

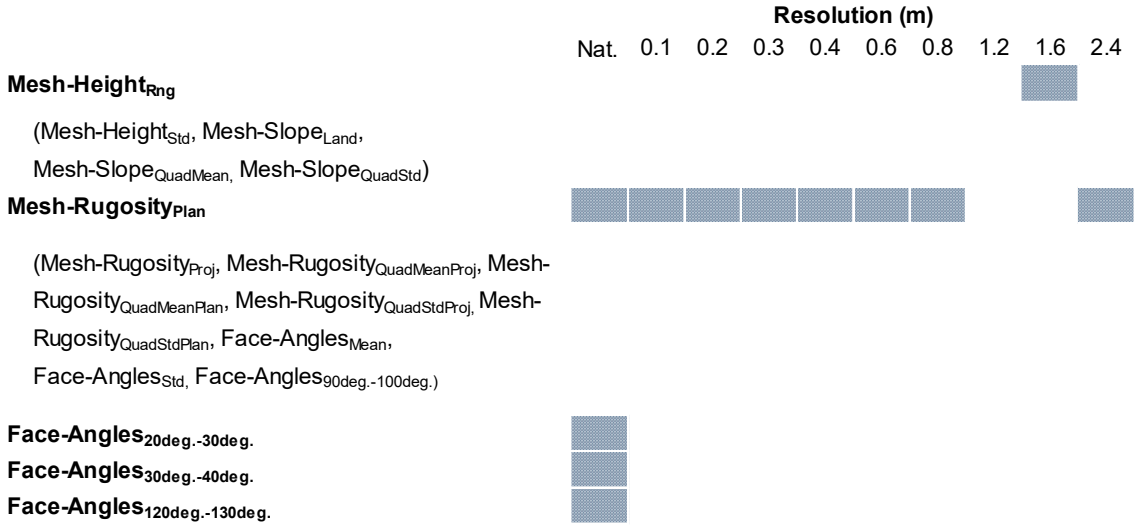

Figure 3-15 Important resolutions (blue shading) identified for each of the AUV Mesh metrics retained (bold type with correlated metrics in brackets) following examination of correlations.

4 Chapter 4 - Synergism of Photogrammetric and Traditional Remote Sensing in Predicting Fish Abundance

4.1 Summary

Metrics of habitat structural complexity are used widely in marine ecology as predictors of species' abundances and distributions. They provide effective surrogates of various environmental gradients and limiting resources that influence species distributions at local and broad-scales. Metrics have mostly been derived from bathymetric reconstructions often captured using 'traditional' remote sensing methods (e.g., multibeam and LIDAR). More recently, photogrammetry has emerged as a technique to capture bathymetric reconstructions and novel metrics at much finer resolutions than traditional methods. However, per unit area, photogrammetric data is far more expensive to collect than traditional methods. Given this, its purported benefits to marine predictive modelling and resource planning must be examined objectively to adequately inform its integration into future studies. Here, I use a suite of metrics from overlapping traditional (multibeam and LIDAR), and photogrammetrically derived bathymetric reconstructions to model the abundance of fish species and trophic-mobility groups at three locations along the southeast coast of Australia. I compare model performance when built on metrics from one and multiple reconstructions to determine which approach best explains variation in fish species and group abundance. The main findings were:

- Combining multibeam / LIDAR and photogrammetric metrics resulted in the best performing model for 20 of the 35 fish species and 9 of the 15 trophic-mobility groups.
- On average, models that combined predictors across two or more datasets predicted 27 % more the variance in fish species abundance compared to models based on a single dataset (combined and single dataset model mean deviance explained of 0.33 (SE: 0.02) and 0.26 (SE: 0.02), respectively). For trophic-mobility groups it was 31 % (combined and single dataset model mean deviance explained of 0.36 (SE: 0.02) and 0.25 (SE: 0.02), respectively).
- Collectively, these findings indicate substantial synergism between traditional and photogrammetric metrics of structural complexity. The findings also provide insights into the ecological and environmental divers of fish abundance and their distributions, and further demonstrate the importance of considering multiple spatial scales when deriving such metrics.

- The importance of traditional methods and metrics should, however, not be overlooked as these provided the best model performance and deviance explained for several species and groups of fish.

4.2 Introduction

Effective management and conservation of marine resources and biodiversity requires accurate information on species distributions and abundance. This information is key to informed establishment of marine use zones including Marine Protected Areas (MPAs) and other interventions aimed at enhancing conservation outcomes and fishery sustainability (Rees *et al*., 2018; Ward *et al*., 1999). Information on species abundance and distribution can be obtained via survey and fishery catch records though such direct methods of biotic data collection often require substantial time and effort. Alternatives use environmental variables to predict distributions in areas where biotic data is unavailable. These methods, such as species distribution models (SDMs), apply relationships identified between overlapping biotic data and their predictors to predict a response in areas where only the predictors exist (Guisan & Thuiller, 2005; Guisan & Zimmermann, 2000). Environmental predictors are generally easy to measure and may include abiotic gradients (e.g., physical and chemical properties of water) that influence species distribution directly according to physiological tolerances (Robinson *et al*., 2017). Metrics of structural complexity derived from digital elevation models (DEMs) of the seafloor provide a notable group of useful predictors. These metrics capture variability in the physical structure of the seafloor and provide surrogates of several important measures of habitat suitability (e.g., refuge availability, hydrodynamic flow, wave exposure). Such measures of habitat suitability are often difficult to measure directly and metrics of structural complexity provide a key linkage between easier to measure physical structure, environmental resources and gradients, and biotic responses.

Structural complexity has received a great degree of attention in marine ecology both as a tool to help predict the distribution of marine biota and to help understand associated ecological and causal abiotic-biotic relationships (see reviews by Brown *et al*., 2012; Pickens *et al*., 2021; Pygas *et al*., 2020). Early observational studies investigated the role of structural complexity measured in-situ in influencing the distribution of fish, either qualitatively using visual assessment of the presence of flat sand, reef, boulders etc. or quantitatively by fitting a metal chain to the contours of the seafloor, known as the ‘chain and tape’ method (e.g., Brokovich *et al*., 2006; Harman *et al*., 2003; Luckhurst & Luckhurst, 1978; Mumby & Wabnitz, 2002) Though see other, less common quantitative methods of measuring structural complexity in-

situ (Dustan *et al*., 2013; Nanami & Nishihira, 2002; Wilson *et al*., 2007b). Several controlled studies also manipulated structural complexity experimentally to help identify causal mechanisms (e.g., Gratwicke & Speight, 2005a; Gregor & Anderson, 2016). The adoption of metrics of structural complexity has taken place alongside the development of marine remote sensing methods such as hydroacoustic multibeam and light detection and ranging (LIDAR) (i.e., traditional methods) used to create bathymetric reconstructions, also known as digital elevation models (DEMs), of the seafloor. This has allowed the role of structural complexity to be explored at vastly greater spatial scales of several kilometers, compared with the several metres generally attainable using *in-situ* methods. These metrics are also a common component of SDMs (see review of over fifty such studies in **Section 2**). Often, the goal of these studies is to improve the outcomes of conservation planning and intervention in addition to improving the understanding of the ecological mechanisms influencing species distributions.

The more recent development of photogrammetry, also known as structure from motion (SfM), provides a further method of obtaining bathymetric reconstructions and metrics. It also has two key differences compared to traditional remote sensing. First, it captures much finer resolutions (centimetre and millimetre) more comparable with the body size of target biota. Second, it captures more realistic mesh-based 3-dimensional (3D) representations of the seafloor, compared to the 2.5D raster-based outputs from traditional remote sensing. Mesh-based reconstructions also allow derivation of novel metrics more relevant to the marine environment, such as those that capture beyond vertical surfaces (e.g., overhangs and caves). It is envisaged such metrics will provide additional and often better performing predictors of marine biota. Indeed, studies have begun to examine the use of photogrammetrically derived metrics as predictors of fish abundance and community composition, with some promising early results. These include using photogrammetric derived metrics to predict fish abundance in the Australian east coast (Ferrari, *et al*., 2018), Caribbean (González-Rivero *et al*., 2017), Philippines (Bayley *et al*., 2019), Hawaii (Fukunaga, Kosaki, *et al*., 2020) the Great Barrier Reef (GBR) (Oakley-Cogan *et al*., 2020) and 1 km deep in the northeast Atlantic (Price *et al*., 2019).

Photogrammetry is, however, not without limitations. Despite advances in camera systems, software and computing power, per unit-area, photogrammetry remains a far more expensive means of obtaining bathymetric reconstructions compared with traditional methods. This is regardless of whether photogrammetry images are collected using diver, Remotely Operated Vehicle (ROV), Automated Underwater Vehicle (AUV) methods.

Although the increasing availability of low cost ROV and AUV platforms will continue to close this gap, the disparity in cost versus coverage between photogrammetric and traditional methods is likely to exist for the foreseeable future. A key question is whether the purported increase in explanatory power associated with finer resolutions and novel metrics is worth the increased cost and smaller spatial coverage associated with photogrammetry and derived metrics. The efficacy of broad-scale metrics derived from traditional remote sensing methods as biotic predictors is well documented (reviewed in **Section 2**). However, the efficacy of local-scale fine-resolution metrics has received less attention. While it might be expected that certain fish, such as benthic, territorial and site attached species, would be responsive to local-scale drivers captured by photogrammetric metrics, they would likely also respond to processes and metrics operating over broad-scales. Presently there is limited if any direct information that would guide future studies on whether using traditional and / or photogrammetric methods and metrics would lead to better model and predictive performance.

The availability of overlapping multibeam / LIDAR (traditional) photogrammetric and derived bathymetric reconstructions and fish data along the NSW coastline provides a unique opportunity to begin examining how photogrammetry may best be integrated with traditional methods. In this study, I derive a suite of common and novel metrics from the three distinct bathymetric reconstructions currently in use in the literature and encompassing traditional, mesh and hybrid (i.e., rasters converted from photogrammetrically derived meshes) approaches. I use these to model fish abundance and compare the predictive performance of each bathymetric reconstruction individually and when combined. I intend that a directed and a-priori approach will provide answers to key emerging questions on the efficacy of photogrammetry and derived metrics as predictors of fish abundance. These answers will help guide future studies that consider the use of photogrammetry, either solely or alongside traditional remote sensing methods, and ultimately improve marine conservation and management interventions. Specifically, I examined the following key questions:

- Do metrics derived from (multibeam / LIDAR) (traditional) or photogrammetric bathymetric reconstructions, or their combination, perform better when predicting fish abundance and is there any synergistic effect of combining traditional and photogrammetric remote sensing methods.

- Can patterns in species responses to metrics be linked with their functional ecological roles and how might these findings advance the integration of these methods for the benefit of future studies and marine management.

4.3 Methods

4.3.1 Study Area

The study area covered a range of temperate rock reef habitats from shallow inshore to deeper offshore reefs along the coast of NSW in southeastern Australia (15 degrees latitude). Sites were situated individually or clustered in groups of up to 5 within a 1 km radius, with a total 40 sites across three locations: The Solitary Islands (25 sites, 17 m to 36 m deep and 0.1 km to 3.4 km offshore), Port Stephens (10 sites, 19 m to 35 m deep and 1.6 km to 6.1 km offshore) and Batemans Bay (5 sites, 25 to 37 m and 3.9 to 11.4 km offshore) (**Section 1.5**). These sites were a subset of those included in **Section 3** with available fish data. Around one quarter (Solitary Islands) to one half (Batemans Bay) of these were in no take zones and the remainder in fished areas.

4.3.2 Bathymetric Data

4.3.2.1 Dataset Acquisition

Bathymetric data were available for each site in three formats: 1) large extent - low resolution (5 m to 240 m) DEM rasters captured from multi-beam echo-sounding (MBES) surveys between 2006 and 2009 and light detection ranging (LIDAR) surveys in 2018 (hereafter referred to as MBLI Rasters or traditional methods), 2) small extent - high resolution (0.03 m to 2.4 m) triangular irregular network (TIN) meshes derived from automated underwater vehicle (AUV) surveys in 2012 (hereafter referred to as AUV Meshes) and 3) the AUV Meshes converted to raster format (hereafter referred to as AUV Rasters), also at small extent – high resolution (0.1 m to 2.4 m). These datasets were collected and processed as described in **Section 3** (**Section 3.3.2**).

4.3.2.2 Metrics of Structural Complexity

The reduced metric dataset identified in **Section 3.4** was used to model fish data in this Chapter. This included the retained metrics and the important extents (MBLI Raster only), and resolutions (all datasets) identified for each. As a further step prior to modeling, highly correlated ($r > 0.7$, $r < -0.7$) predictors (i.e., the metric when derived over a specific resolution and extent) were removed for each metric in turn. A threshold of |r| 0.7 is a commonly accepted cut-off value that has been shown using simulation to work just as well as other

methods designed to reduce multicollinearity beyond which severe problems with model estimation and subsequent prediction begins to occur (Dormann *et al*., 2013). This provided an uncorrelated subset of predictor variables for each metric (**Table 4-1**). Correlations between predictors from different datasets were not examined as the intention was to quantify the predictive performance of each dataset individually.

4.3.3 Fish Data

Fish data were available from baited remote underwater video surveys (BRUVs) undertaken on between one and three occasions across the winters of 2010, 2011 and 2012 at each site (**Appendix 4-1**) by NSW DPI (Fisheries) and the NWS National Parks and Wildlife Service (NPWS). Nineteen of the twenty-five Solitary Islands sites were surveyed in each year with the remaining six in 2012, all 5 Batemans Bay sites were surveyed in 2010 and 2011, and 7 Port Stephens sites sampled in each year, while three were sampled in 2010 and 2012 only. BRUV deployments consisted of a digital video-camera with wide-angle lens (Malcolm *et al*., 2011). Plastic mesh bait bags with 1 kg of mashed pilchard. were attached to the end of a bait-pole at 1.5 m from the lens (Hardinge *et al*., 2013). Deployments were 30 min in duration (Harasti *et al*., 2015; Watson *et al*., 2007) and the maximum count of individuals per species (MaxN) recorded. The field-of-view was standardized to approximately 3 m behind the bait, estimated during analysis by two trained observers. Examination of the data indicated that the majority of species (all but two of the 60 most abundant species) occurred at each location during at least one survey. In total, 114 fish species were represented across the three locations in the dataset (**Appendix 4-2**). The most prevalent of which were snapper (*Chrysophrys auratus*), crimson-banded wrasse (*Notolabrus gymnogenis*) and Maori wrasse (*Ophthalmolepis lineolata*), occurring at 37 of the 40 sites during at least one survey. The four most abundant species were mado (*Atypichthys strigatus*), silver sweep (*Scorpis lineolata*), blackspot goatfish (*Parupeneus spilurus*) and *O. lineolata*, which together accounted for just over half of the total number of individuals observed and 25%, 13%, 8% and 5%, respectively. The 35 species abundances that occurred at 10 or more of the 40 sites were selected for individual analysis. A prevalence of 25% of sites was selected to help ensure confidence around the modelling results and limit the number of responses to a manageable number. Though a widely used method for surveying a range of fish species, BRUVs have some limitations. They may underrepresent fish not attracted to the bait, such as herbivores, as well as small, cryptic and bottom associated fish (Harvey *et al*., 2012).

Table 4-1 Metrics of structural complexity retained for each dataset and used to model fish abundance. Metric values are the mean, except where standard deviation (Std) is identified.

Metric	Description	Resolution(s) (m)	Extent(s) (m)
MBLI Raster			
Bathymetry (Bath)	Water depth.	5	5
Aspect-east (AspEast)	Measure of direction of greatest slope in a west-east direction, east facing = 1 and west facing = -1.	5 240	10, 3120 240
Aspect-north (AspNorth)	Measure of direction of greatest slope in a north south direction, with north facing = 1 and south facing = -1	5 20 30	5 3120 30
Aspect-north-std (AspNorth-std)	Variability in north deviation values	5 10 20 40 240	10 40 40 80 480
Standard-curvature (CurvStd)	Second derivative of the bathymetric reconstruction, or the first derivative of slope. Combines Planar Curvature and Profile Curvature	5 10 60	5 60, 80, 120, 160, 240, 360, 600, 960, 1140, 2400, 3120
Planar-Curvature (CurvPla)	Curvature evaluated perpendicular to slope	5 10 20 60 80	10, 20, 3120 10 240 240, 360, 480, 960, 1920 80
Profile-Curvature (CurvPro)	Curvature evaluated parallel to the slope	5 10 60	5, 40, 60 20, 80, 240, 3120 120, 240, 960, 1920
Surface-planar-area (SurPla)	The ratio of convoluted area to planar area, more commonly known as surface-rugosity. This measure includes a correction for slope based on the plane of best fit.	5 10 20 60 80	5, 10, 20, 3120 10 240 240, 360, 480, 960, 1920 80
AUV Raster			
Bathymetry (Bath)	Water depth.	0.1	~25
Aspect-east (AspEast)	Measure of direction of greatest slope in a west-east direction, east facing = 1 and west facing = -1.	0.1	~25
Aspect-north (AspNorth)	Measure of direction of greatest slope in a north south direction, with north facing = 1 and south facing = -1	0.6	~25
Profile-curvature (CurvPro)		0.2, 0.6	~25
Slope		0.1, 2.4	~25
Planar-curvature (CurvPla)		0.1, 0.6, 2.4	~25
Surface-planar-area (SurPla)		0.1, 2.4	~25
Aspect-east-std		0.1, 2.4	~25
Aspect-north-std		0.1, 2.4	~25
AUV Mesh			
Mesh-Height$_{Rng}$	Vertical relief, or the maximum – maximum z (depth) value from the mesh surface	Native	~25
Mesh-Rugosity$_{Plan}$	The ratio between the 3D surface area and either the 2D projected area or area of plane of best fit (plane)	2.4	~25
Face-Angles$_{20deg.-30deg.}$	Proportion of the angles (in degrees) between the vertical (z) axis and the slope of each mesh triangle within 10-degree bins	Native	~25
Face-Angles$_{30deg.-40deg.}$		Native	~25
Face-Angles$_{120deg.-130deg.}$		Native	~25

Induvial fish abundance data were also summed across functional groups based on trophic level (predator, piscivore, herbivore, planktivore, sediment-infauna-predator) and mobility (midwater, mobile-bottom-dweller, mobile-bottom-dweller-scavenger, sedentary-bottom-dweller) providing a total of 15 functional trophic-mobility groupings. Overall, 99% of all observed individuals represented by 82 species were placed into these functional groupings. All functional groups occurred at each Location except mobile-bottom-dwelling-herbivores, which were absent from Batemans Bay.

Prior to analysis fish data were averaged across all sample years (between 1 and 3) at each site. For most sites (all except the 5 from Batemans Bay) this included sampling in winter of 2012 coinciding with the timing of the AUV surveys in August, September and November of 2012 (except at BISZ3 in December 2010) (**Section 3.3.2**). This would help minimise any effect of annual change in the cover and composition of benthic biota and its associated biogenic physical structure, which would be expected to contribute to overall structural complexity captured by the surveys. Although MBES and LIDAR bathymetric data was collected prior to, and following, respectively, the fish surveys, the coarser resolutions captured by these methods (2 m to 5 m) would be less sensitive to change in coverage and composition of benthic biota.

4.3.4 Data Analysis

4.3.4.1 GAM Modelling

Generalized Additive Modelling (GAM) (Wood, 2011) implemented via the FSSGam package in R (Fisher *et al*. 2018) was used to assess the performance of individual datasets and their combinations when predicting fish abundance. This package facilitates the fitting and comparison of multiple GAM models each based on a complete sub-set of all potential predictor combinations for each response variable of interest. Potential models were fit using predictors from each dataset in isolation and using predictors combined across different datasets. Combined models were those that combined predictors from AUV Mesh and MBLI Rasters, from AUV Mesh and AUV Raster, from AUV Rasters and MBLI Rasters, and from all three datasets. For dataset combinations, only models that contained at least one predictor from each dataset were considered. For example, when all three datasets were combined, each candidate model consisted of one predictor from each of the three datasets. When two datasets were combined, each model consisted either of one predictor from each dataset (total of 2), or one predictor from one dataset and two from the second (total of 3). This allowed individual dataset performance and potential synergistic effects of combining predictors across datasets to be assessed. It is noted that to help prevent spurious results

the full-subsets approach removes potential models built from predictors with a correlation greater than 0.28 r (Fisher *et al*., 2018) This is a further, more conservative threshold beyond which model miss-specification has been shown to occur (Graham, 2003). Predictors with a correlation greater than this value appeared in the potential model combinations but not in the same model. This way, the performance of pairs of predictors with $0.23 < r < 0.70$ could be assessed without substantial risk of model miss-specification. Models were fit using a maximum of 3 predictors (**Table 4-2**). This limited the number of candidate models to a manageable, albeit still large, number, minimised the potential for overfitting and helped ensure final model interpretability, whilst also enabling models using a predictor from each dataset to be included. Attempts using 4 predictors were unsuccessful due to the very large number of candidate models that would be generated (several 10s of thousands of models per response) and exceed computational limits.

Table 4-2 Number of predictors and models used per fish response. For the identity of the predictors see Table 4-1. Only predictors with correlation <0.28 r were included in potential models.

Dataset / Dataset Combination	Number of Predictors Available for Modelling	Number of Predictors Considered in Models	Number of Predictor Combinations / Candidate Models Considered
MBLI Raster	53	1 to 3	11,417
AUV Raster	16	1 to 3	356
AUV Mesh	7*	1 to 3	14
AUV Mesh & AUV Raster	25	2 to 3	777
AUV Mesh & MBLI Raster	60	2 to 3	3,763
AUV Raster & MBLI Raster	69	2 to 3	15,945
AUV Mesh & AUV Raster & MBLI Raster	76	3	2,084

*includes mean bathymetry at 0.2 m resolution from AUV Raster (see text).

To prevent potential bias due to the AUV Mesh datasets not directly providing a measure of bathymetry, which is often an important predictor of fish abundance, the mean bathymetry calculated from the AUV Rasters at 0.1 m resolution (included in the AUV Raster dataset) was combined with the AUV Mesh dataset. This was preferred to removing mean bathymetry from the other datasets as the absence of this important predictor would likely have limited identification of optimal models (preliminary analysis noted that AUV Mesh predictors were often retained in candidate final models alongside bathymetry, when otherwise they would not have been). Further, for combined models mean bathymetry did not count towards the predictor count for each dataset. For example, if bathymetry derived from AUV Raster was included, it was not considered a metric of complexity and a further

AUV Raster based predictor had to be included. This ensured combined models truly represented the contribution of a complexity related metric from each dataset.

Fish responses were fit using a tweedie error distribution appropriate to the continuous abundance data with potential point mass at zero. The dimension of the basis function used to represent the smooth term was set at 3. This was considered appropriate to the biological relationships likely to be encountered, including simple linear and more complex non-linear ecological relationships capturing threshold, asymptotic and parabolic effects, whilst minimising the potential for overfitting, especially with the small sample size (Fisher *et al*., 2018)). GAM was undertaken for each of 50 fish responses (35 species and 15 trophic-mobility groups) % It is noted that GAMs failed to converge for foxfish (*Bodianus frenchii*), and this species was not considered further. Inference was used as the basis of model selection and models were ranked using Akaike information criterion corrected for small sample sizes (AICc) (Hurvich & Tsai, 1989), with candidate final models identified as those with a difference in AICc of 2 or greater and the smaller the AICc for the null model (the random effect of Location). The best performing model for each dataset and combination was identified as that with the smallest AICc and fewest predictors. Of these, that with the smallest AICc and fewest predictors was identified as the overall best performing model, and, thus, identified the overall best performing dataset(s). Where AICc values were within 2 AICc and there was no difference in number of predictors, the best overall model was identified as that which combined the fewest number of datasets.

4.3.4.2 Model Performance

The relative importance score provided for each predictor by the FSSGam function was used to assess the performance of individual metrics, and, thus, different datasets. Scores were calculated for each predictor by summing the model Akaike weights (interpreted as the probability that model is the best model) for all models containing each predictor. To ensure the number of models in which the different predictors are present was uniform (an assumption of using summed model weights to infer variable importance) the number of models included was the minimum number of models in which any one predictor was present (Fisher *et al*., 2018). As a final step, performance of individual predictors was averaged across all extents and resolutions to provide an average performance for each metric. Dataset performance was assessed by comparing the unique (i.e., that explained by the fix component only) deviance explained by final models and by comparing the total number of overall best final models for each dataset and combination. A principal component analysis (PCA) was undertaken to help visualise the relative importance of dataset(s) for different

species. This was based on the deviance explained by the best model for each dataset(s). To highlight relative rather than absolute differences, deviance values were first transformed so that the total deviance explained for each species summed to 1. The performance of different datasets and their combination was also assessed by tallying the number of best performing final models for each species and group provided by each dataset(s) and by comparing the deviance explained by the best performing final models. In these cases results were aggregated separately across species and trophic-mobility groups.

4.3.4.3 Fish-Complexity Relationships

Partial dependence plots (PDP) (Friedman, 2001) of the overall best final model for each fish response were used to help understand the form of relationship between predictor and response variables. PDPs display the marginal effect of each predictor considering the effect of all other predictors and can show how the predictions partially depend on values of the predictors of interest. Visually, this is achieved by plotting the partial residuals against the predictor in question. Partial residuals are the residuals that would be obtained by dropping the predictor concerned from the model. They also serve as a diagnostic check with the partial residuals being evenly spaced around the fitted function in the case of correct model specification. Correct model specification was also checked by examining other residual diagnostic checks including plots of residuals versus fitted values and fitted versus predicted. Semi-variograms were also created using the model residuals to identify any spatial correlation not accounted for by the model. Overall best final models appeared well specified with no obvious evidence of patterns or spatial non-independence in the residuals. Potential exceptions were yellowtail horse mackerel (*Trachurus novaezelandiae*), Günther's butterflyfish (*Chaetodon guentheri*), Australian sawtail (*Prionurus microlepidotus*) and butterfly perch (*Caesioperca lepidoptera*) where there was evidence of heteroskedasticity and spatial non-independence. As such, the modelling results for these three responses should be considered with caution. The model with the best predictive performance for each dataset(s) was examined in detail to provide insight on the metrics and associated resolutions and extents. Four species of commercial, recreational and / or conservation significance were also examined in detail. These were *C. auratus*, grey morwong (*Nemadactylus douglasii*), red morwong (*Cheilodactylus fuscus*), and eastern blue grouper (*Achoerodus viridis*).

4.4 Results

4.4.1 Model Performance

The objective of the comparisons described in this section was to assess the first key question described in **Section 4.2**, that is, which dataset or dataset combination, performs better in explaining variability in fish species and trophic-mobility group abundance. Also, is there evidence of a synergistic effect of combining traditional (MBLI Raster) with photogrammetric (AUV Mesh and AUV Raster) remote sensing methods. The presence of such an effect would be an important finding that would require consideration for similar studies in the future.

Based on comparing the relative importance of individual metrics (**Table 4-1**), MBLI Raster and AUV Raster performed better at explaining variability in fish abundance than AUV Mesh. Aspect-east and profile-curvature from AUV Raster and aspect-east and profile-curvature from MBLI Raster all performed better than the best performing AUV Mesh metric (Face-Angles$_{30deg.-40deg.}$). Bathymetry (water depth) tended to perform better than all metrics of complexity derived from either MBLI Raster, AUV Raster or AUV Mesh. However, bathymetry (albeit derived from the MBLI Raster dataset) was included alongside all datasets to maximise model performance and avoid bias, and thus, did not influence these findings.

Evidence of synergistic effect (i.e., improved predictions when combining predictors across traditional and photogrammetric datasets, compared to each dataset in isolation) was observed for 20 of the 34 species and 9 of the 15 trophic-mobility groups. This was most evident for MBLI Raster and AUV Raster predictors, which when combined provided the overall best performing model of abundance of 17 of the 34 fish species and 7 of the 15 trophic-mobility groups (**Table 4-2a**). The combination of MBLI Raster and AUV Raster also tended to explain more deviance than models based single datasets and other dataset combinations (**Table 4-2b**).

MBLI Raster combined with AUV Mesh also provided the best performing model for 3 species and 1 group and combining all three datasets provided the best model for a further 1 group. For individual species and groups, compared to MBLI Raster alone, the greatest improvement in explained deviance associated with combining MBLI Raster and AUV Raster was observed for yellowfin leatherjacket (*Meuschenia trachylepis*) (0.30 or 250% more explained deviance), *A. strigatus* (0.26 or 69%), predators (0.23 or 143%), *P. spilurus* (0.19 or 111%), sedentary-bottom-dweller-piscivore (0.18 or 75%), midwater-piscivore (0.17

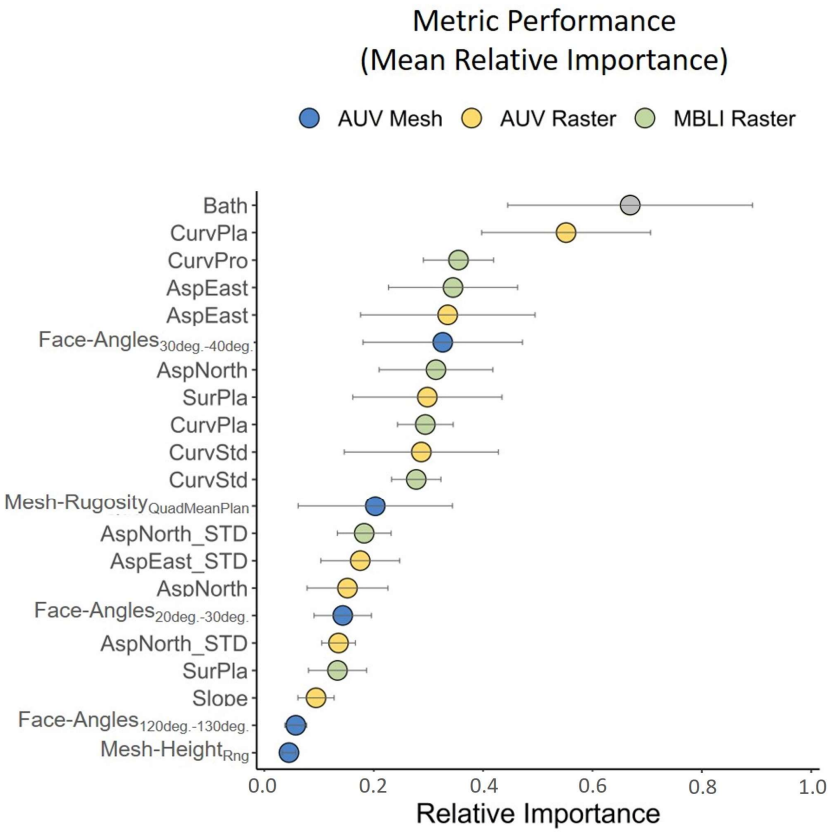

Figure 4-1 **Metric performance based on relative importance. Results are averaged across all extents and resolutions considered for each metric (see Table 4-1) Symbol colours indicate the source of each metric. Bathymetry was sourced from MBLI Raster but was considered separately.**

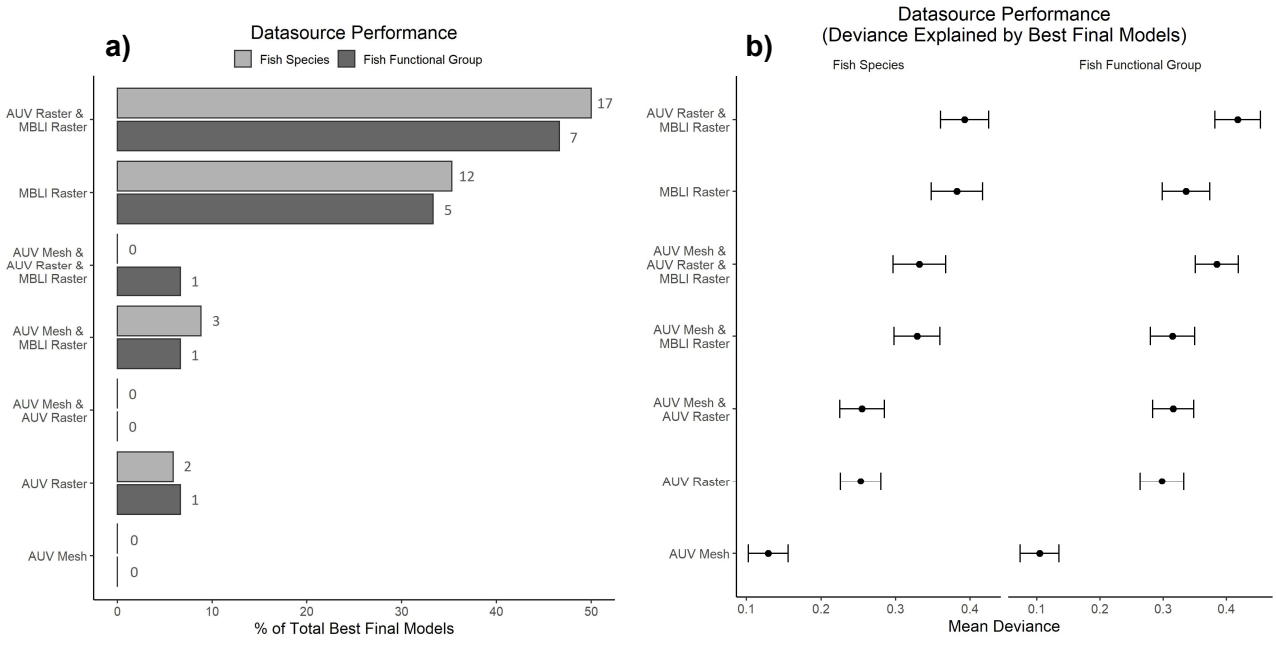

Figure 4-2 **Relative importance of datasets in modelling fish species and functional group abundance determined a) by the rate (numbers above bars indicate number of models) final models were retained in favour of the null model (random effect of location) and b) by the average deviance explained by final models aggregated across all species / groups.**

or 51%) and mobile-bottom-dwelling-predators (0.15% or 86%) (**Figure 4-3** and **Table 4-3**). The increase for the remaining species and groups was more modest (1% to 13%). Other dataset combinations were less likely to be associated with improved performance, though when combined, MBLI Raster and AUV Mesh explained 0.19 (55%) more deviance for midwater-piscivore and 0.09 (18 %) more for *C. picta* compared to MBLI Raster, but a comparable amount (0.20 total explained deviance) to MBLI Raster in the case of *M. scaber*:

The importance of single datasets and traditional methods for some species and groups, however, should not be overlooked. Compared to the next best performing single or combined dataset models, MBLI Raster alone explained 0.09 (22%) more deviance for venus tuskfish (*Choerodon venustus*) and 0.08 (14%) more for sedentary-bottom-dweller-herbivore, though for the remaining 10 species the improvement was modest (<% 0.05). The single dataset model based on AUV Raster also explained modestly more (0.04 or 28%) deviance for blue-striped goatfish (*Upeneichthys lineatus*). However, for eastern talma (*Chelmonops truncatus*) and predators, the better performing AUV Raster based model selected using AICc was associated with around 30 % less deviance explained. This apparent discrepancy between the most parsimonious model (selected using AICc) and predictive performance (in this study measured using deviance explained) was also noted for other species, most notably black reef leatherjacket (*Eubalichthys Bucephalus*) and white-ear (*Parma microlepis*), where the MBLI Raster model selected using AICc also explained less (47% and 31%, respectively) deviance than models based on other dataset(s). Although models selected using AICc would be preferable for inference, competing models based on other datasets / combinations may be preferable for prediction. Such instances would have implications for studies where the aim is to maximise prediction with interpretability of secondary concern.

There was little consistency apparent between the dataset(s) that provided the overall best performing model and the trophic-mobility group to which each species belonged (**Figure 4-4**). Two apparent exceptions were *P. spilurus* and *U. lineatus* (both mobile-bottom-dwelling-scavenger-invertivores), and Sergeant Baker (*Latropiscis purpurissatus*) and eastern red scorpionfish (*Scorpaena cardinalis*) (both sedentary-bottom-dwelling-piscivores), predicted best by models based solely on, or including, AUV Raster. Similarly, there was little evidence of clustering of species from the same trophic-mobility groups in the PCA plot (**Figure 4-5**). Though separation along the x-axis did suggest species / groups towards the left of the PCA were influenced more by MBLI Raster and those to the right more by AUV Raster and AUV Mesh. Those to the right included *P. spilurus*, *U. lineatus,*

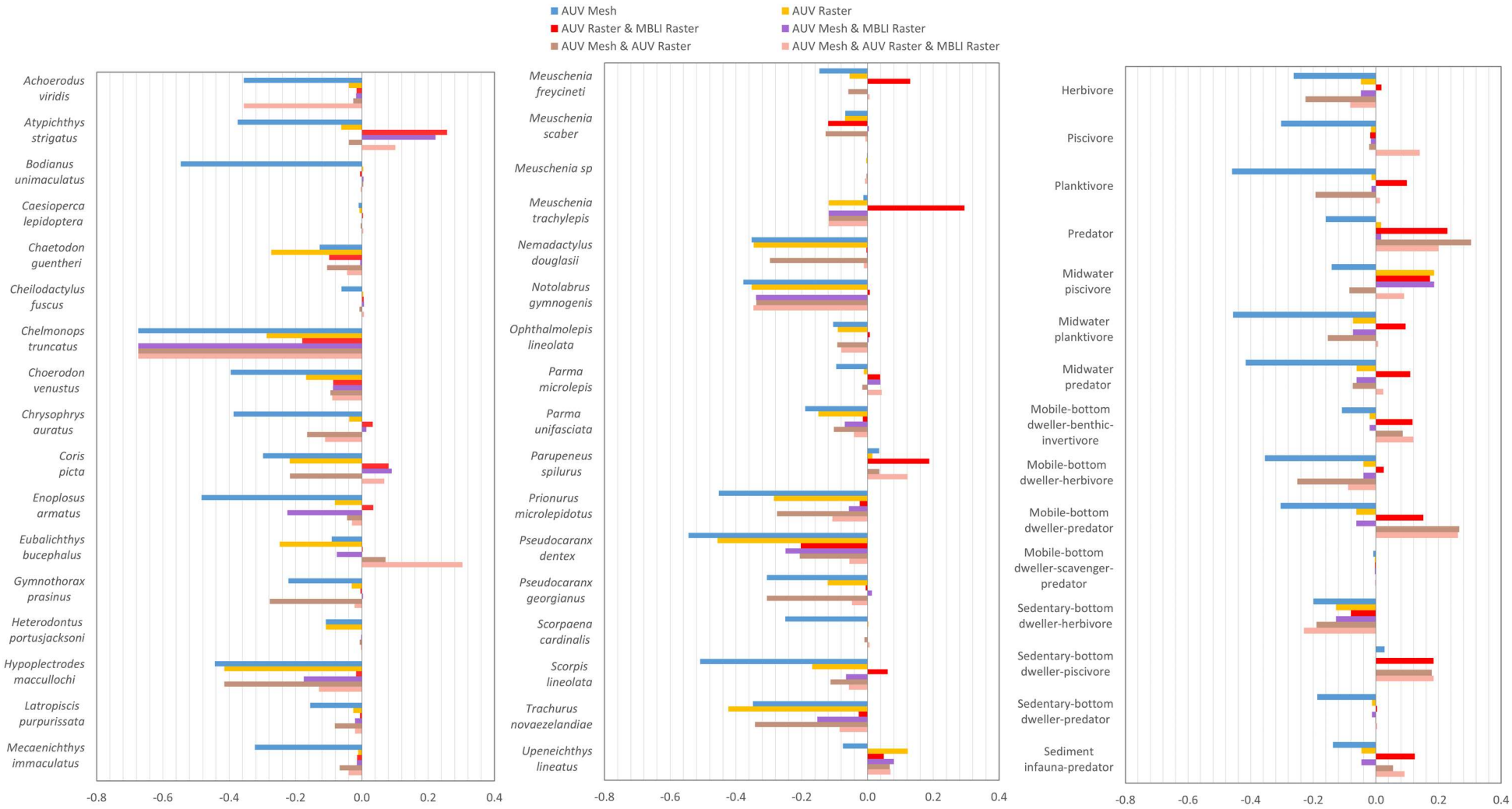

Figure 4-3 **Deviance explained by the best performing model for each dataset (selected using AICc) for fish species and trophic-mobility groups relative to that explained by MBLI Raster. For full final model results see Appendix 4-3. Note that the overall best performing model select using AICc and considering the parsimony principle did not always explain the greatest deviance. Negative and positive x axis labels indicate smaller or greater, respectively, deviance explained by dataset and dataset combinations relative to that explained by MBLI Raster alone.**

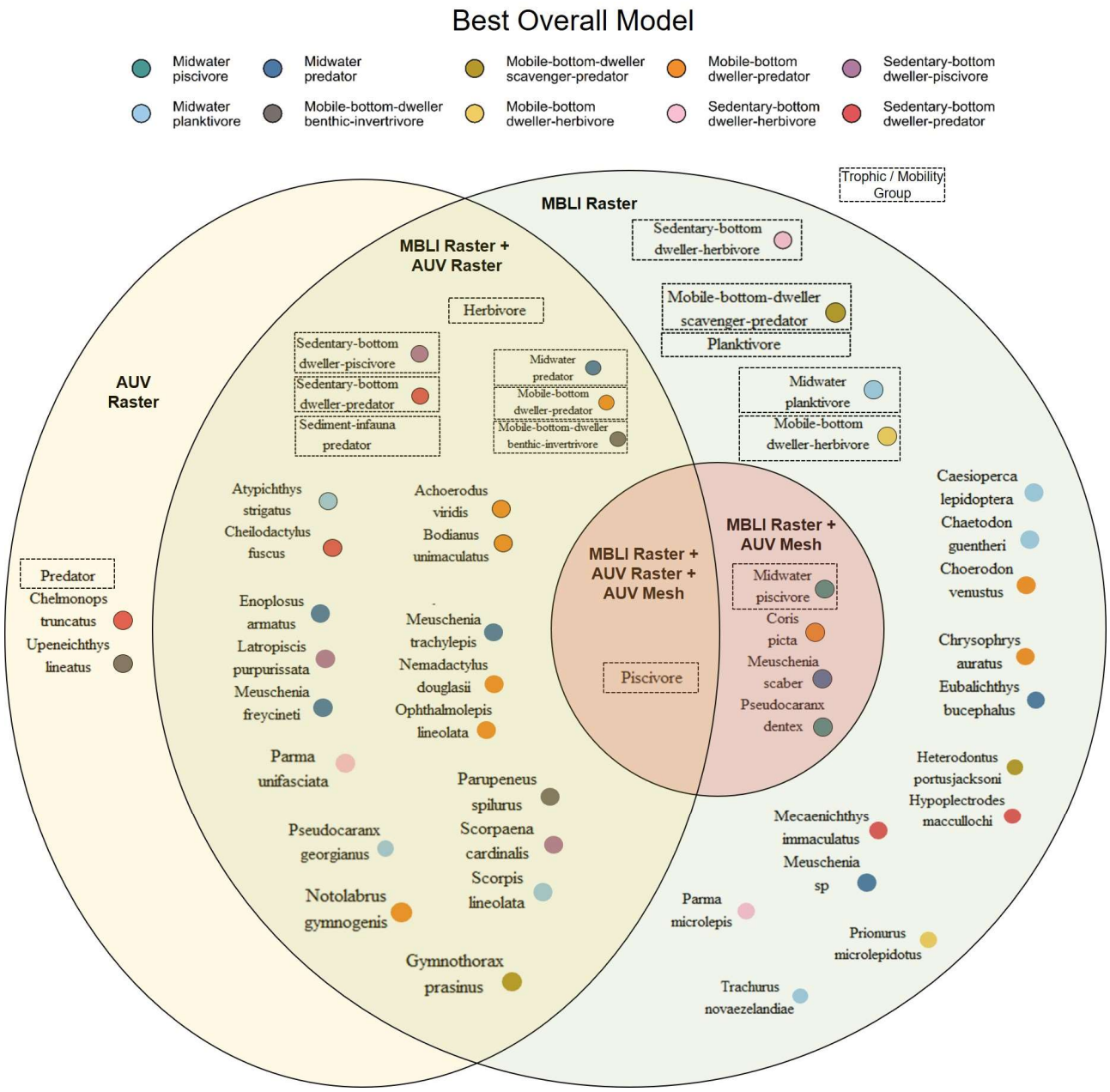

Figure 4-4 Venn diagram identifying the source of predictors included in the overall best performing model of fish species and trophic-mobility group abundance based on model selection using AICc.

L. purpurissatus and *S. cardinalis*, which are all closely bottom-associated with the first two feeding amongst sand patches and the second two ambush piscivores. Port Jackson shark (*Heterodontus portusjacksoni*) and green moray eel (*Gymnothorax prasinus*) (both mobile-bottom-dwelling-scavenger-predators) were located on the left of the PCA, possibly related to the importance of broader-scale structural complexity to these mobile species and captured by MBLI Raster.

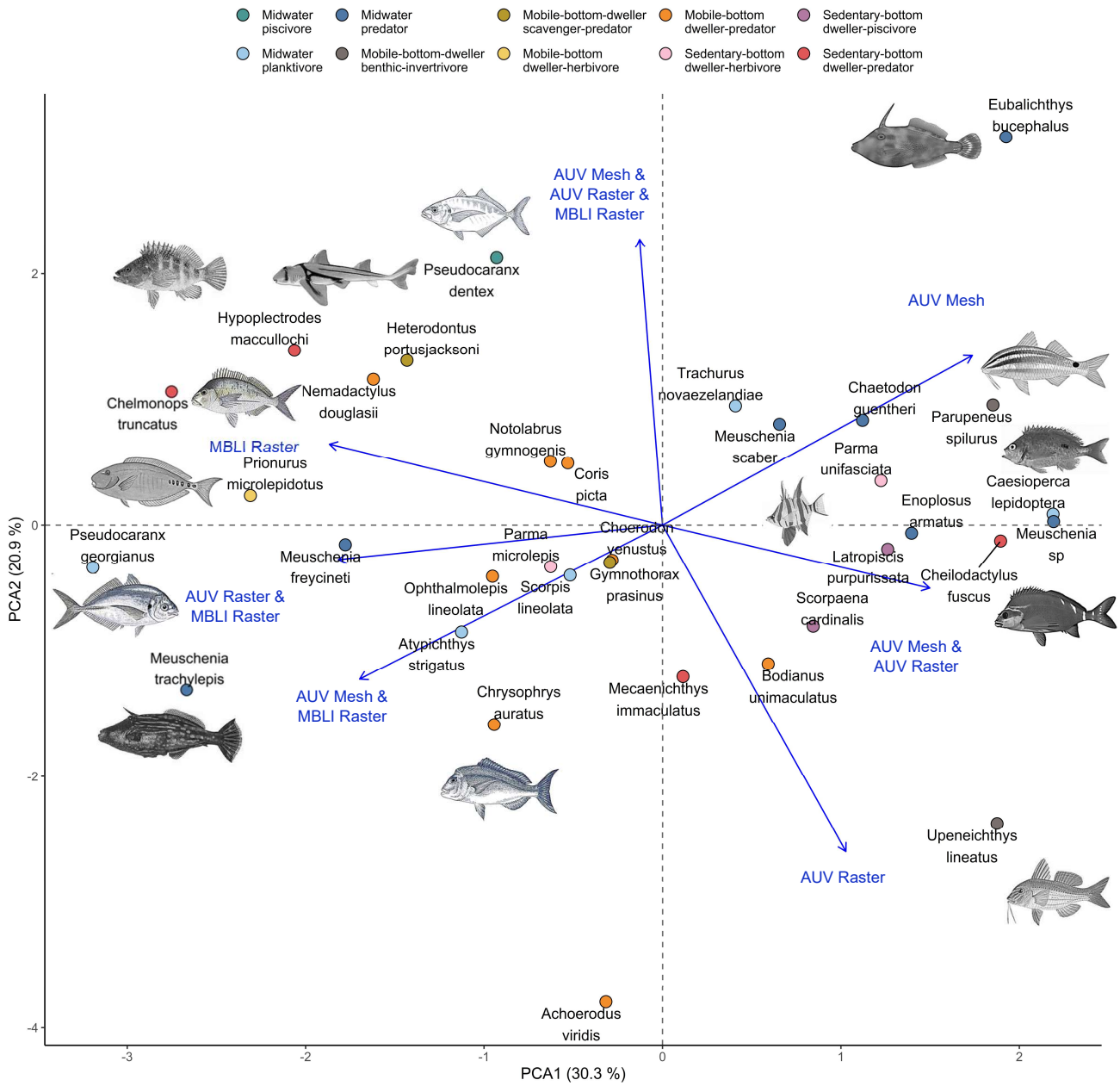

Figure 4-5 PCA based on deviance explained by best final models for each dataset and dataset combination. PCA axis based on deviance values transformed to sum to 1 for each species / groups and then centered. This accentuates relative differences in deviance explained between dataset(s) rather than absolute differences.

4.4.2 Fish-Structural Complexity Relationships

Detailed examination of associations between fish abundance and individual metrics was undertaken for species / groups with the greatest explained deviance by each dataset(s), and species of commercial, recreational or conservation importance (**Table 4-3**) (**Appendix 3-3**). Responses tended to be species / group specific with little consistency in types of metrics retained and the form relationships (i.e., positive, negative, or association with intermediate or extreme predictor values) (**Figure 4-6** and **Figure 4-7**). Most fish were

associated with curvature, though relationships were varied and included a positive relationship with standard-curvature (*N. douglassi*), positive relationship with profile- and planar-curvature (*C. fuscus*), and a negative relationship with standard-, planar- or profile-curvature (*E. armatus*, predators and piscivores), or more complex non-linear relationships with curvature (*T. novaezelandiae*, *C. auratus*, *C. picta* and *E. armatus*).

Table 4-3 Best performing models of fish species / trophic-mobility groups for each dataset and dataset combination indicating the predictor and the resolution (Res.) and extent (window length) (Ext.) over which it was derived. Species targeted (T) by recreational / commercial fishers or of conservation significance (C) also included. Results for all species and groups are provided in Appendix 3-3.

Response	Datasource	Overall Best Final Model	Model AICc	Uni. Dev. Exp.	null AICc	null Dev. Exp.
Fish Species / Trophic-Mobility Group						
Trachurus novaezelandiae	MBLI Raster	CurvPla_Res005xExt3120+ CurvPla_Res060xExt0480+ CurvPro_Res060xExt0120	112.5	0.86	142.9	0.04
Predator	AUV Raster	AspNorth_Res0.6_AUVRaster+ CurvPla_Res0.6_AUVRaster+ CurvStd_Res0.2_AUVRaster	259.6	0.43	285.4	0.29
Enoplosus armatus	AUV Raster & MBLI Raster	AspNorth-std_Res005xExt0010+ CurvPla_Res005xExt0005+ CurvStd_Res0.2_AUVRaster	98.3	0.80	153.8	0.08
Coris picta	AUV Mesh & MBLI Raster	CurvPro_Res060xExt0960+CurvStd_Res010xExt0160+ Mesh-Rugosity$_{Plan}$_Res2.4	54.9	0.60	127.6	0.21
Piscivore	AUV Mesh & AUV Raster & MBLI Raster	AspEast_Res005xExt3120+CurvPla_Res0.6_AUVRaster+ Mesh-Rugosity$_{Plan}$_Res2.4_AUVMesh	119.6	0.55	164.1	0.16
Fish Species – Commercially / Recreational Targeted (T) and of Conservation Significance (C)						
Chrysophrys auratus T	MBLI Raster	CurvPla_Res005xExt0020+CurvPro_Res060xExt0960	157.6	0.39	179.0	0.27
Nemadactylus douglasii T	AUV Raster & MBLI Raster	AspEast_Res0.1_AUVRaster+CurvStd_Res005xExt0005+ CurvStd_Res010xExt0600	50.8	0.49	104.7	0.00
Cheilodactylus fuscus T	AUV Raster & MBLI Raster	AspEast-std_Res0.1_AUVRaster+ CurvPla_Res0.6_AUVRaster+CurvPro_Res005xExt0005	41.5	0.33	200.0	0.11
Achoerodus viridis C	AUV Raster & MBLI Raster	AspEast_Res0.1_AUVRaster+ AspNorth-std_Res240xExt0480+Bath_Res005xExt0005	62.7	0.34	70.1	0.10

Notes: AUV Raster and AUV Mesh metrics were derived over a window side length of approx. 25 m. Null model consists of the intercept and random effect of Location, with the Uni. Dev. Exp. the deviance explained by the fixed effect only.

Responses to rugosity and orientation were also species / group specific. Of the one species (*C. picta*) and one group (piscivores) that responded to rugosity (in both cases Mesh-Rugosity$_{Plan}$) the former was associated with extreme high and low rugosity values and the latter only greater rugosity values. A few species / groups responded to orientation, with predators associated with greater aspect-north (northerly facing surfaces), piscivores smaller aspect-east (westerly facing surfaces) and *N. douglassi* and *A. viridis* greater aspect-east (easterly facing surfaces).

For each species and group, metrics spanned more than one and sometimes several spatial scales with 8 of 9 responding to predictors derived over resolutions and / or extents that differed by 1 to 2 orders of magnitude. This was most notable for piscivores and *N. douglasii*. Piscivores responded to Mesh-Rugosity$_{Plan}$ and planar-curvature derived from AUV Mesh and AUV Raster, respectively, at an extent of ~25 m. Piscivores were also associated with aspect-east derived from MBLI Raster but at a much greater extent of 3,120 m. *N. douglasi* was associated aspect-east derived AUV Raster at an extent of ~25 m, and with greater standard-curvature from MBLI Raster at an extent of 5 m and a much greater extent of 600 m. While the response of *N. douglasi* to the same metric derived over different spatial scales was consistent, this was not the case with all species. *T. novaezelandiae* increased in abundance as planar-curvature increased up to approximately 0.08, regardless of the spatial scale. Beyond this, the increase in abundance plateaued when planar-curvature was derived 60 m resolution and 480 m extent, but when derived at 5 m resolution and 3,120 m extent, abundance dramatically decreased. It is noted that model of *T. novaezelandiae* appeared somewhat miss-specified (**Section 4.3.4.3**), thus findings regarding this species should considered with some caution.

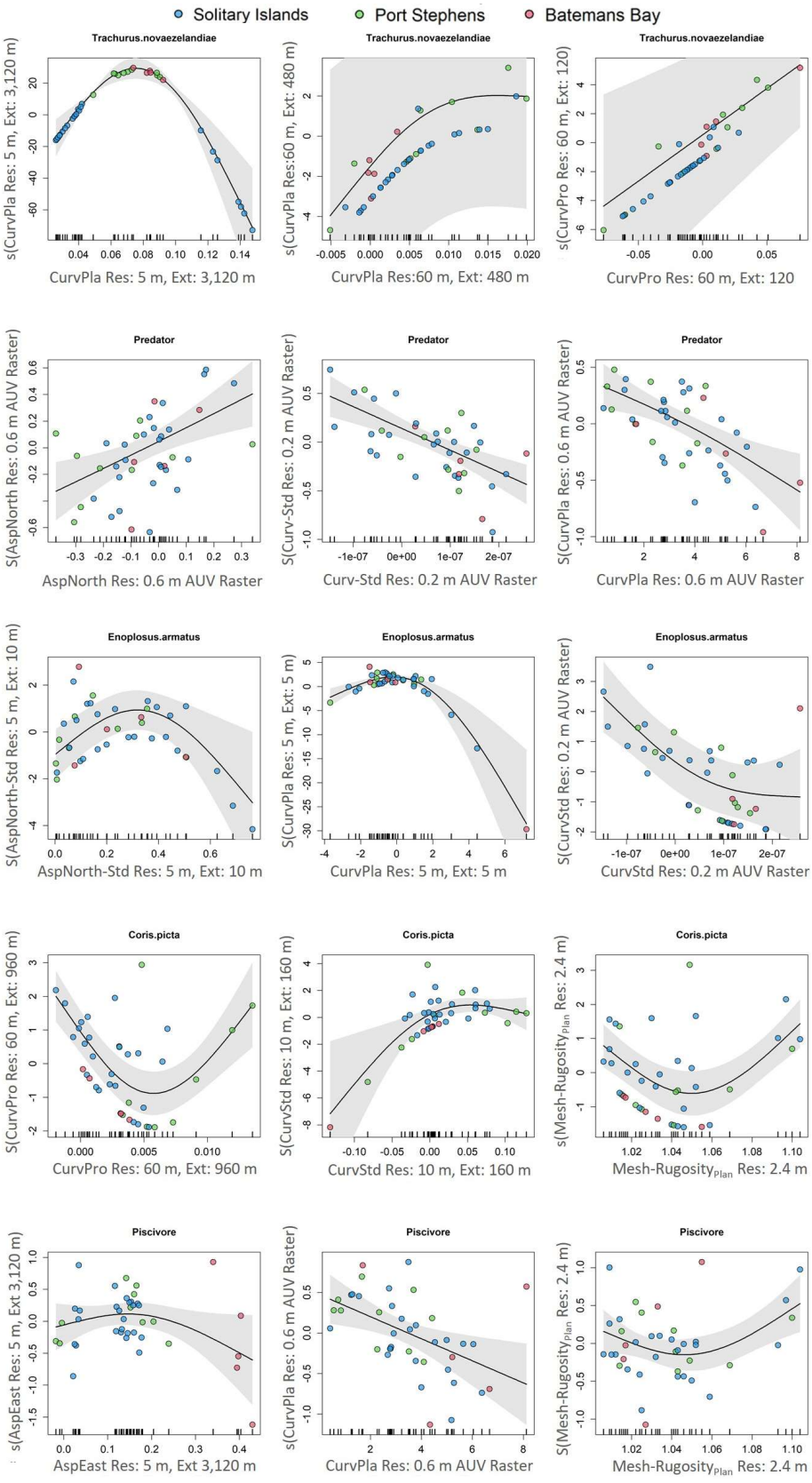

Figure 4-6 Partial dependance plots from best performing GAM models of fish species abundance identifying the marginal effect of the predictor on the response identified as the smooth (s) function of the predictor. Numbers associated with predictors refer to resolution (Res) and extent (Ext) over which the predictor was derived. Circles represent partial residuals coloured by location. Shaded area represents the standard error of the fitted function.

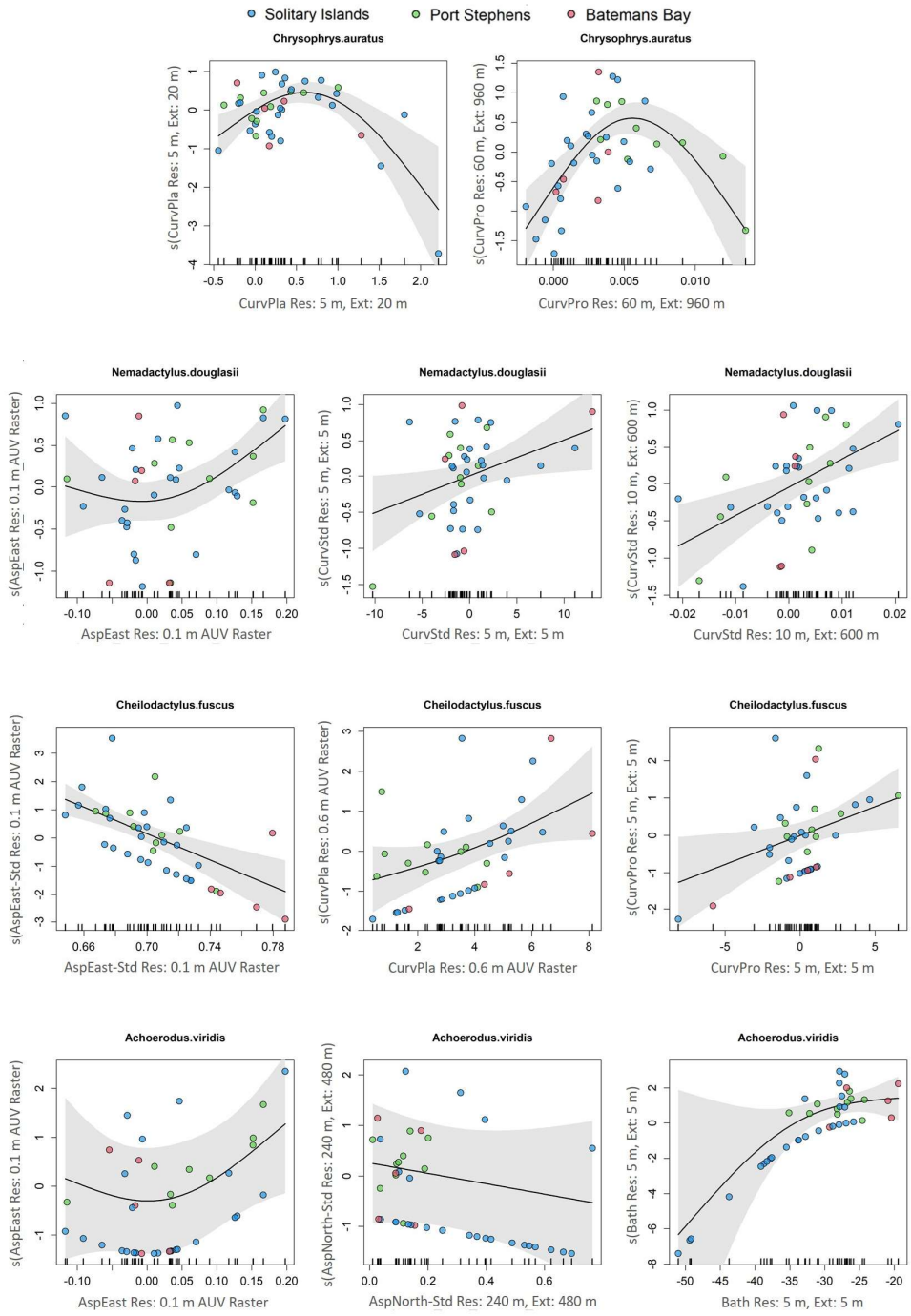

Figure 4-7 Partial dependance plots from best performing GAM models of fish species abundance identifying the marginal effect of the predictor on the response identified as the smooth (s) function of the predictor. Numbers associated with predictors refer to resolution (Res) and extent (Ext) over which the predictor was derived. Circles represent partial residuals coloured by location. Shaded area represents the standard error of the fitted function.

4.5 Discussion

4.5.1 Metric and Dataset Performance

The results here indicated that photogrammetrically derived metrics of structural complexity can substantially improve predictions of fish abundance. However, improvements were sometimes marginal compared to traditional (multibeam / LIDAR) methods. When evident, improved model predictions were largely associated with combining predictors across photogrammetric and traditional methods and were identified for most species (20 of 34) and groups (9 of 15). This confirmed the presence synergism between these approaches, which was a key objective of this study. Improved model performance associated with photogrammetric datasets (AUV Raster and AUV Mesh) was expected given their much finer resolutions (0.1 m to 2.4 m) compared to coarser MBLI Raster (5 m and greater). Finer resolutions would capture variability in structural complexity commensurate with the body size of most marine biota and quantify key features of the seafloor such as refuges from predators, prey and influence on water flow. Variability in biogenic structure associated with sessile biota including sponges, soft corals, ascidians etc. that would influence the distribution of fish directly and indirectly via provision of refuges and in some cases a food source would also be affectively captured by these finer resolutions. Although this study was undertaken on temperate rock reef, it would be expected that photogrammetric datasets would be just, if not more, important on coral reefs. The even more structurally complex biogenic habitat provided by coral and associated with its various growth forms would provide much greater variability in habitat structural complexity at the sub-metre resolution. Together with greater fish diversity on coral reefs, photogrammetry would provide a particularly effective tool for quantifying relationships between fish (and other marine biota) abundance and fine resolution physical habitat structure in this environment.

The better performance of AUV Raster compared to AUV Mesh also suggests the finer resolution afforded by photogrammetry, rather than the novelty of metrics (at least those considered here), is of key importance. However, it is possible this is partly an artefact of the relatively few AUV Mesh metrics included in this study. AUV Raster metrics (the same as derived from MBLI Raster, just at finer resolutions) captured a broad range of complexity types, such as gross complexity, curvature and orientation-based metrics. This compares with the narrower range and fewer overall fewer number of metrics derived from the AUV Mesh, which consisted primarily of those capturing gross complexity and based on rugosity and height range. The exception was those based on Face-Angles, with the proportion

falling between 30 deg. to 40 deg. from vertical performing relatively well overall (7th most important metric of 22). Several other metrics can be derived from meshes, and may have been important predictors if included in this study. This includes metrics of object size distribution in the mesh surface (i.e., does the surface provide objects the size of tennis balls or cars, for example) (Porter, 2018). At present, the extraction of these metrics requires custom scripts, which can limit their accessibility to researchers. Accessibility of novel mesh-based metrics is expected to improve as more user-friendly methods of extraction become available, for example through new R packages developed specifically for use with mesh datasets. If more and easily accessible AUV Mesh metrics had been available for this study, it is likely the performance of the AUV Mesh metric dataset would have at least been comparable to that based on AUV Raster.

The utility of photogrammetrically derived mesh-based predictors has been demonstrated in other studies, albeit none attempted a direct comparison of photogrammetric with traditional methods. Perhaps the earliest was Ferrari, *et al*., (2018) (based on a subset data included in this study), where mesh derived slope and surface-rugosity was a predictor of fish species and functional groups at the Solitary Islands. Mesh derived surface-rugosity and viewshed also predicted coral reef-associated pomacentrid (damselfishes) abundance in the Caribbean (González-Rivero *et al*., 2017a) and surface-rugosity was a predictor fish species richness and total abundance in the Philippines (Bayley *et al*., 2019). Fukunaga, *et al*., (2020) derived traditional metrics from raster based DEMs converted from photogrammetric meshes (equivalent to AUV Raster in this thesis) and found these to be important predictors of fish species richness and abundance of corallivores, herbivores and piscivores, but not planktivores and invertivores, in Hawaii. Outside the tropics, mesh derived surface-rugosity was found to be a predictor of cold-water coral cover and associated fish abundance and benthic community species richness and diversity Price *et al*., (2019). However, not all findings have suggested strong relationships, with Oakley-Cogan *et al*., (2020) not finding relationships between Great Barrier Reef (GBR) herbivorous fish distribution and mesh derived slope, surface-rugosity and refuge-density. Rather, area of turf alga was a more powerful predictor, suggesting structural complexity may not always provide a suitable surrogate of key limiting resources (Oakley-Cogan *et al*., 2020). Habitat descriptors such as turf algae are one of several important variables that could also influence fish distributions. Others include a variety of oceanographic variables such as sea temperature, local and broad scale hydrodynamics including water currents and wave velocity, as well as the spatial configuration of elements of structural complexity (see **Section 2.5.2.4** and Tokeshi & Arakaki, 2012). Variability in habitat and oceanographic

variables would be partly captured by metrics of structural complexity and predictors that capture geographic information, such as latitude or categorical predictors such as location (including in the models in this chapter). However, structural complexity metrics may not always provide adequate surrogates of these important variables, and together with limitations of fish survey methods, such as BRUVs and detection of cryptic species, this would likely explain some of the limited variability in fish abundance explained in this Chapter and in other similar studies.

4.5.2 Behavioral and Ecological Linkages

The second objective of this study was to link dataset(s) performance with fish behavioral and ecological characteristics, thereby describing ecological basis behind observed relationships that could inform future choices on the most informative predictor dataset. The traditional (multibeam / LIDAR) and photogrammetric datasets differed substantially in resolution (0.1 m to 2.4 m for the photogrammetric and 5 m to 240 m for the traditional dataset) and spatial extent (~25 m window side length for the photogrammetric and 5 m to 3,000 m for the traditional dataset). Given this, it was expected seafloor-associated fish species and groups (i.e., fish that are demersal, territorial, less mobile and with high site fidelity and / or small home range sizes) would display strong relationships with photogrammetrically derived metrics that capture fine resolution structural complexity commensurate with the body size, behavior and patterns of movement of these species. Other species / groups more adapted to existence in the water column above the benthos, that are more transient, mobile and / or have larger home ranges were expected to display stronger relationships with the more spatially extensive, albeit coarser resolution, MBLI Raster based metrics. This pattern was observed for some, but not all, species and groups. Planktivore and midwater planktivore groups were predicted best by models based solely on MBLI Raster, which is consistent with previous studies linking planktivores with larger structures and their influence on water flow, recruitment, planktonic food and predatory sighting by prey, (Rilov & Benayahu, 2002; Rilov & Benayahub, 1998; Rountree, 1989; Wilhelmsson *et al*., 1998; Wilhelmsson, *et al*., 2006). Predators, the benthic invertivore *U. lineatus* and the sedentary predator *C. truncatus* were also predicted best solely by AUV Raster, which was also expected given their close association with the seafloor where their prey (benthic infauna and invertebrates) is located. However, it was difficult identify other such links between fish ecology, behaviour, and single dataset performance. Although MBLI Raster performed best for a further 12 species and 4 groups, these species spanned a range

of trophic, mobility and feeding modes including mobile, midwater, sedentary and bottom dwelling species.

A further key finding of this study, and why clearer links between single datasets (i.e., MBLI Raster, AUV Raster and AUV Mesh) and fish trophic and mobility groupings were absent, was the importance of considering multiple spatial scales (resolutions and / or extents). This was particularly the case for species and groups predicted best by combining predictors across photogrammetric and traditional datasets often with vastly different resolutions and extents. Such multi-scale responses to structural complexity mean that, for most species and groups, no single datas*et al*one was likely to provide the best performing model or predictions. It should also be noted that of the 12 species predicted best solely using MBLI Raster, 9 included predictors derived over divergent (an order of magnitude difference) resolutions and / or extents. This further reinforces the importance of considering multiple spatial scales, even within the same dataset. The importance of considering multiple scales when modelling fish abundance agrees with many previous studies (e.g., Knudby *et al*., 2010; Moore *et al*., 2009; Pittman *et al*., 2007; Pittman & Brown, 2011; Purkis *et al*., 2008; Wines *et al*., 2020). Wines *et al*., (2020) was also able to demonstrate the relative importance of various discrete spatial extents when modelling fish abundance off the Victorian coastline. While distinct and sometimes multiple optima of spatial extents were able to be identified, the best predictive performance would likely be achieved if metrics from multiple spatial extent were included in the same model. The importance of considering multiple spatial scales is also not restricted to marine biota, and has also been demonstrated when classifying marine habitats (e.g., Porskamp *et al*., 2018). In this Chapter it was often possible to link the spatial scale of predictors in this study with the ecology and behavior of some species. The commercially / recreationally targeted mobile-bottom-dwelling-predator *C. auratus* displays some site fidelity, though has a relatively large home range size of up to 600,000 m^2 with some individuals traveling up to a few hundred kilometers (Harasti *et al*., 2015). The two MBLI Raster predictors retained in the overall best final model for this species (planar-curvature and profile-curvature) were derived over extents of 400 m^2 for the former and 900,000 m^2 for the latter. This is consistent with a wider ranging mobile species but that also spends some time feeding on seafloor invertebrates. The finding that the sedentary-bottom-dwelling-predator *C. fuscus* was predicted best by AUV Raster and MBLI Raster predictors, but with extent no greater than 625 m^2, could be related to its smaller home range size (1,500 m^2 to 4,000 m^2) and closer association with the seafloor due to seeking refuge amongst boulders (Lockett and Suthers 1998; Lowry and Suthers 1998). This would also be the case for the mobile-bottom-dwelling and territorial *N. gymnogenis*

(predicted best by AUV Raster and MBLI Raster) with a reported home range size of 1,000 m^2 to 2,000 m^2 (Welsford *et al*., 2004), which is consistent with largest extent (6,400 m^2) covered by its associated predictors.

Clear linkages between the spatial scale of important predictors and the home-range size of fish were, however, not always as evident. The abundance of several territorial species with small home ranges sizes, expected to respond most strongly to photogrammetrically derived metrics, also responded to complexity present over areas far larger than their reported home range size. The mobile-bottom-dwelling-predator *A. viridis*, (also of conservation significance) is considered somewhat site attached, at least anecdotally (Curley *et al*., 2013), but was associated with greater aspect-north (possibly related to patterns in food availability associated with northerly facing surfaces and / or some other broad-scale resource) captured over a relatively large area (230,000 m^2). The commercially / recreationally important *N. douglasii* (also a mobile-bottom-dwelling-predator), also responded to metrics derived over a relatively large (360,000 m^2) area. Although responses were not examined in detail here, the mobile-bottom-dwelling ambush predator *G. prasinus* with a home range 1,500 m^2 to 10,000 m^2 (Bassett & Montgomery, 2011), and the mobile-bottom-dwelling *O. lineolata* with a home range size of 1,700 m^2 (Kingsford & Carlson, 2010) both responded to predictors captured at a spatial extent far greater (130,000m^2 for *G. prasinus,* and several times this for *O. lineolata*) than their home range and the area captured here by photogrammetry (625 m^2). Even when a-priori information on a species home range size is available, incorporation of predictors that capture structural complexity well beyond the reported home range may be necessary.

The apparent disparity between reported home range sizes of fish and the often much greater spatial extent of metrics retained in final models is not surprising considering adult fish distributions are a function of several processes operating at different life stages and spatial scales. As well as active habitat selection by adults, many species experience ontogenetic related shifts in habitat usage that would include movements over areas much greater than adult home range, and the area captured by photogrammetry in this study. The importance of MBLI Raster for many species, particularly territorial species with small home range sizes, likely reflects early life history ontogenetic related habitat selection process. This includes species such as *C. auratus* and *A. viridis* where juveniles migrate from estuarine and seagrass nursery habitats to coastal rock reef habitats as they mature (Gillanders & Kingsford, 1998; Leis & Hay, 2004). For *C auratus*, at least, this may be related to habitat, prey and temperature preferences, and possibly also fishing pressure and its

effect on size structure (J. Williams *et al*., 2019). *N. douglasii* (predicted best by combing AUV Raster and MBLI Raster), demonstrate a change in depth usage as they mature, with older individuals tending to be found on deeper reefs. In such cases, early broad-scale habitat selection by migrating fish may exert a comparable or stronger influence on observed adult fish distributions, compared to variability in habitat suitability at local-scales within the adult home range. Other mechanisms operating at early life history stages could also influence the distribution of adult fish. Passive site selection by settling larvae would be influenced by structural complexity mediated hydrodynamic flow. Post settlement predator mediated survival could also influence adult distributions. Such processes would influence species that do not undertake large ontogenetic related migrations. Such a mechanisms could also explain the importance of relatively large extents (3,600,000 m^2) derived from MBLI Raster for the highly site attached and benthic H. maccullochi with a home range size reported as no greater than 12 m^2 (Kingsford & Carlson, 2010). These processes would occur at various spatial scales and would likely be associated with different elements of complexity. All would combine to shape species distributions observed at any one time.

The BRUV fish data used in this study did not include data on fish size, and it is possible a range of fish size and age classes, including adults, sub-adults and juveniles were included in the total fish counts. If such life stages respond differently to structural complexity, combined fish counts may hinder the identification of relationships with fish abundance. Mixed school counts of both juvenile and adult western king wrasse (*Coris auricularis*) and orange-spotted puffer (*Torquigener vicinus*) were postulated as explaining poor abundance model performance in Western Australia (Galaiduk *et al*., 2017). Galaiduk *et al*., (2017) also modelled *C. auratus* abundance separately for juveniles and adults and found each to be associated with different habitats. Adults were associated with deeper, west-facing slopes and juveniles with shallower, east-facing, flatter terrain. Future study site selection should consider the consequence of sampling across different habitats, fish size classes / age and the likelihood for differences in important metrics and forms of relationships among these groups. Otherwise as this could complicate model interpretation. If fish counts could have been partitioned among size classes in this study, then it is possible even stronger relationships between fish abundance, distributions and metrics of structural complexity may have been apparent.

4.5.3 Planning and Management Considerations

Given MBLI Raster was the single best performing dataset, the current large scale and publicly available multibeam / LIDAR dataset (in this study combined to create the MBLI

Raster dataset) of the NSW coastline would be the first, and possibly most suitable, dataset that should be considered for use by researchers and resource managers for modelling and predicting fish abundance and distribution. Indeed, for 8 species and one group, MBLI Raster provided better model quality and greater deviance explained than the photogrammetric datasets and dataset combinations (green highlight in **Table 4-4**).

For 12 species and 10 groups (orange highlight in **Table 4-4)**, photogrammetric metrics alone, or when combined with traditional metrics, provided the best quality model and the greatest explained deviance. These findings provide a relatively strong argument for including photogrammetric metrics when modelling abundance of these fish. However, for 5 of the 12 species and 2 of the 10 groups (light orange highlight in **Table 4-4**), the improvement in deviance explained over MBLI Raster alone was minor (< 5%). If photogrammetric data were unavailable in such cases, the additional cost associated with photogrammetric survey may not justify the relatively small improvement in deviance explained that would be expected.

For the remaining 14 species and 4 groups (blue highlight in **Table 4-4**), the choice of dataset(s) would be more complex and would depend more on the objective of the study. Studies focused more on inference (for example, when interpreting ecological relationships) should select the dataset(s) that provided the best model quality. Studies focused on predictive performance (for example, when informing marine area planning), should select the dataset with the greatest explained deviance. However, for 9 of the 14 species and 1 of the 4 groups the difference in deviance explained between datasets was minor (< 5%) (light blue highlight). In such case, the currently available MBLI Raster would likely provide a suitable predictive dataset, albeit with slightly poorer performance. For the remaining 6 species and 3 groups, there was a greater difference in explained deviance between the best quality model and the model that explained the most deviance. In such cases, the decision on whether to obtain and include photogrammetric metrics would need to consider study objectives (inference versus predictive performance), and if necessary, the additional costs associated with photogrammetric metrics.

In most cases photogrammetric metrics improved models of fish abundance only when incorporated with those from traditional methods. Alone, photogrammetric metrics rarely provided the best models. Importantly this also included AUV Raster, from which the exact metrics were derived as were derived from MBLI Raster. Possibility this reflects the relative importance of drivers of fish abundance operating over coarser resolutions and / or greater extents. It may also be due to the much greater range of spatial extents captured by MBLI

Raster (19) compared to AUV Raster (1). Thus, improved models and predictions may only be achievable for most fish if bathymetric reconstructions and metrics from traditional methods (e.g., MBLI Raster) are available. If they are not, then collection of such datasets would likely take priority, particularly where broad scale spatial planning is required. Importantly also, while the MBLI Raster used in this thesis had a resolution of 5 m, finer resolutions of at least 0.25 m (Ierodiaconou *et al*., 2018) (within the range of AUV Mesh and AUV Raster in this thesis) can be obtained using traditional methods such as MBES. It is possible that some of the improvement in model performance in this thesis associated with including AUV Mesh and / or AUV Raster alongside MBLI Raster could be achieved by using a single traditionally derived bathymetric reconstruction with a resolution comparable to AUV Mesh and AUV Raster (0.1 m to 2.4 m). However, more novel mesh-based metrics, such as face angles beyond vertical, would likely not be able to be derived from such traditional methods.

Table 4-4 Identify of the dataset(s) that would provide the best quality model (identified using AICc) and the greatest predictive performance (identified using dev. Exp.) for each species and group. dataset providing greater predictive performance only identified if this was greater than the best quality model.

Strong evidence for use of traditional metrics. MBLI Raster metrics provided the greatest model quality and Dev. Exp.	Strong evidence for use of photogrammetric metrics. Improved model quality and increase in Dev. Exp. > 5 % compared to MBLI Raster alone.	Minor evidence for use of photogrammetric metrics. Improved model quality but increase in Dev. Exp. < 5 % compared to MBLI Raster alone.	Use of photogrammetric metrics (alone or combined with traditional metrics) strongly dependent on study type (inference or prediction). Large difference (> 5%) in deviance explained between best quality model and alternative model.	Use of photogrammetric metrics (alone or combined with traditional metrics) less dependent on study type (inference or prediction). Small difference (< 5%) in deviance explained between best quality model and alternative model.

Species / Group	Best Quality Model (Identified using AICc)			Alternative Model (When Dev. Exp. > Best Quality Model)		
	Dataset(s)	Dev. Exp	Dev. Exp. Relative to MBLI Raster	Dataset(s)	Dev. Exp	Dev. Exp. Relative to Best Quality Model
Species						
Achoerodus viridis	AUV Raster & MBLI Raster	0.34	-4.4%	MBLI Raster	0.36	4.4%
Atypichthys strigatus	AUV Raster & MBLI Raster	0.63	68.7%			
Bodianus unimaculatus	AUV Raster & MBLI Raster	0.54	-1.1%	AUV Mesh & MBLI Raster	0.55	1.9%
Caesioperca lepidoptera	MBLI Raster	0.56		AUV Mesh & AUV Raster & MBLI Raster	0.57	0.7%
Chaetodon guentheri	MBLI Raster	0.55				
Cheilodactylus fuscus	AUV Raster & MBLI Raster	0.33	1.8%	AUV Mesh & AUV Raster & MBLI Raster	0.33	0.2%
Chelmonops truncatus	AUV Raster	0.39	-42.6%	MBLI Raster	0.67	42.6%
Choerodon venustus	MBLI Raster	0.40				
Chrysophrys auratus	MBLI Raster	0.39		AUV Raster & MBLI Raster	0.42	7.9%
Coris picta	AUV Mesh & MBLI Raster	0.60	17.6%			
Enoplosus armatus	AUV Raster & MBLI Raster	0.80	4.4%			
Eubalichthys bucephalus	MBLI Raster	0.34		AUV Mesh & AUV Raster & MBLI Raster	0.65	46.8%
Gymnothorax prasinus	AUV Raster & MBLI Raster	0.38	-1.1%	AUV Mesh & MBLI Raster	0.39	2.0%
Heterodontus portusjacksoni	MBLI Raster	0.11				
Hypoplectrodes maccullochi	MBLI Raster	0.56				
Latropiscis purpurissatus	AUV Raster & MBLI Raster	0.39	-1.4%	MBLI Raster	0.39	1.4%
Mecaenichthys immaculatus	MBLI Raster	0.32				
Meuschenia freycineti	AUV Raster & MBLI Raster	0.28	88.6%			
Meuschenia scaber	AUV Mesh & MBLI Raster	0.20	1.9%			
Meuschenia sp.	MBLI Raster	0.23				
Meuschenia trachylepis	AUV Raster & MBLI Raster	0.41	249.6%			
Nemadactylus douglasii	AUV Raster & MBLI Raster	0.49	-0.6%	MBLI Raster	0.49	0.6%
Notolabrus gymnogenis	AUV Raster & MBLI Raster	0.60	1.1%			
Ophthalmolepis lineolata	AUV Raster & MBLI Raster	0.19	4.0%			
Parma microlepis	MBLI Raster	0.10		AUV Mesh & AUV Raster & MBLI Raster	0.14	31.1%
Parma unifasciata	AUV Raster & MBLI Raster	0.53	-2.6%	MBLI Raster	0.54	2.6%
Parupeneus spilurus	AUV Raster & MBLI Raster	0.36	110.5%			
Prionurus microlepidotus	MBLI Raster	0.45				
Pseudocaranx dentex	AUV Mesh & MBLI Raster	0.29	-45.8%	MBLI Raster	0.54	45.8
Pseudocaranx georgianus	AUV Raster & MBLI Raster	0.30	-1.7%	AUV Mesh & MBLI Raster	0.32	5.9%
Scorpaena cardinalis	AUV Raster & MBLI Raster	0.30	-0.3%	AUV Mesh & AUV Raster & MBLI Raster	0.30	2.4%
Scorpis lineolata	AUV Raster & MBLI Raster	0.57	12.1%			
Trachurus novaezelandiae	MBLI Raster	0.86				
Upeneichthys lineatus	AUV Raster	0.20	163.6%			

Trophic Mobility Groups						
Herbivore	AUV Raster & MBLI Raster	0.52	3.5%			
Piscivore	AUV Mesh & AUV Raster &	0.55	33.7%			
Planktivore	MBLI Raster	0.46		AUV Raster & MBLI Raster	0.56	17.7%
Predator	AUV Raster	0.43	167.7%	AUV Mesh & AUV Raster	0.46	7.6%
Midwater-piscivore	AUV Mesh & MBLI Raster	0.52	55.0%			
Midwater planktivore	MBLI Raster	0.46		AUV Raster & MBLI Raster	0.55	17.2%
Midwater predator	AUV Raster & MBLI Raster	0.53	26.3%			
Mobile-bottom-dweller-benthic-	AUV Raster & MBLI Raster	0.35	49.4%	AUV Mesh & AUV Raster & MBLI Raster	0.36	0.6%
Mobile-bottom-dweller herbivore	MBLI Raster	0.44		AUV Raster & MBLI Raster	0.46	5.3%
Mobile-bottom-dweller predator	AUV Raster & MBLI Raster	0.46	49.6%	AUV Mesh & AUV Raster	0.57	20.1%
Mobile-bottom-dweller scavenger	MBLI Raster	0.05		AUV Raster	0.05	2.6%
Sedentary-bottom-dweller-	MBLI Raster	0.57				
Sedentary-bottom-dweller	AUV Raster & MBLI Raster	0.43	75.4%	AUV Mesh & AUV Raster & MBLI Raster	0.43	0.0%
Sedentary-bottom-dweller	AUV Raster & MBLI Raster	0.19	2.1%			
Sediment infauna predator	AUV Raster & MBLI Raster	0.39	47.1%			

4.6 Conclusion

Photogrammetrically derived metrics of structural complexity, either alone or when combined with metrics from traditional remote sensing, provided the best performing model of the abundance of 22 of 34 fish species and 10 of 15 trophic-mobility groups considered in this study. In most cases (20 species and 9 groups), combining metrics from photogrammetric and traditional datasets provided the best performing model, indicating a strong synergism of combining different remote sensing methods. The efficacy of photogrammetrically derived metrics in this study appears associated more with their finer resolutions than the more novel mesh-based metrics. However, the number of novel photogrammetric metrics considered here was limited to those based on face-angles. As photogrammetric metrics become more available, they are expected to become increasingly important as predictors of fish abundance and distribution. Photogrammetry, however, is not expected to replace traditional remote sensing methods. Traditional datasets and metrics provide important predictors, and at a relatively lower cost (per unit area). Photogrammetry provides a complementary method of capturing processes that drive variation in fish abundance over small extents and fine-resolutions not achievable using traditional remote sensing methods. Although the incorporation of photogrammetry will depend on associated costs versus the expected improvement in model quality and predictive performance, these findings provide important guidance on the fish species and groups where this novel method is likely to be of most benefit to future studies and management.

4.7 Appendices

Appendix 4-1. BRUV fish survey timing

Survey Year:	2010	2011	2012		2010	2011	2012
Solitary Islands				Batemans Bay			
DC7_1			Y	S19_86	Y	Y	
DC7_11			Y	S19_88	Y	Y	
DC7_3			Y	S19_89	Y	Y	
DC7_5			Y	S28_204	Y	Y	
DC7_7			Y	S28_205	Y	Y	
DC7_8			Y	Port Stephens			
H4_1_1	Y	Y	Y	BIHPZ1	Y	Y	Y
H4_1_2	Y	Y	Y	BIHPZ2	Y		Y
H4_1_3	Y	Y	Y	BIHPZ3	Y	Y	Y
H4_1_4	Y	Y	Y	BISZ3	Y	Y	Y
H4_2_1	Y	Y	Y	FIHPZ7	Y	Y	Y
H4_2_2	Y	Y	Y	FIHPZ8	Y	Y	Y
O2_1_1	Y	Y	Y	FIHPZ9	Y		Y
O2_1_2	Y	Y	Y	FISZ1	Y	Y	Y
O2_1_3	Y	Y	Y	FISZ3	Y		Y
O2_2_1	Y	Y	Y	FISZ4	Y	Y	Y
O2_2_2	Y	Y	Y				
O2_2_3	Y	Y	Y				
O2_2_4	Y	Y	Y				
S4_1_1	Y	Y	Y				
S4_1_2	Y	Y	Y				
S4_1_3	Y	Y	Y				
S4_2_1	Y	Y	Y				
S4_2_2	Y	Y	Y				
S4_2_3	Y	Y	Y				

Appendix 4-2 Fish species and their trophic and mobility groups included in the modelling. Species with prevalence of 20 or more at the 40 sites were modelled separately along with each of the trophic and trophic mobility groups (grey shading). 99% of fish abundance data was placed into functional groupings.

Scientific Name	Trophic Group	Trophic-Mobility Group	Occurrence	Mean Rel. Abun.	Total Abun.
Chrysophrys auratus	Predator	Mobile-bottom-dweller-predator	37	3.03	321
Notolabrus gymnogenis	Predator	Mobile-bottom-dweller-predator	37	1.31	138
Ophthalmolepis lineolata	Predator	Mobile-bottom-dweller-predator	37	3.30	337
Scorpaena cardinalis	Piscivore	Sedentary-bottom-dweller-piscivore	36	1.49	149
Nemadactylus douglasii	Predator	Mobile-bottom-dweller-predator	36	1.11	98
Scorpis lineolate	Planktivore	Midwater-planktivore	34	7.80	830
Gymnothorax prasinus	Predator	Mobile-bottom-dweller-scavenger-predator	34	1.00	103
Hypoplectrodes maccullochi	Predator	Sedentary-bottom-dweller-predator	34	1.20	118
Parupeneus spilurus	Sediment-infauna-	Mobile-bottom-dweller-benthic-invertivore	34	4.75	492
Latropiscis purpurissatus	Predator	Sedentary-bottom-dweller-piscivore	28	0.51	49
Enoplosus armatus	Predator	Midwater-predator	26	1.47	172
Coris picta	Predator	Mobile-bottom-dweller-predator	25	1.02	101
Cheilodactylus fuscus	Predator	Sedentary-bottom-dweller-predator	25	0.45	50
Atypichthys strigatus	Planktivore	Midwater-planktivore	23	14.82	1605
Meuschenia freycineti	Predator	Midwater-predator	22	0.55	50
Parma microlepis	Herbivore	Sedentary-bottom-dweller-herbivore	21	0.45	41
Upeneichthys lineatus	Sediment-infauna-	Mobile-bottom-dweller-benthic-invertivore	21	0.26	24
Prionurus microlepidotus	Herbivore	Mobile-bottom-dweller-herbivore	20	1.24	145
Pseudocaranx georgianus	Planktivore	Midwater-planktivore	19	0.93	87
Achoerodus viridis	Predator	Mobile-bottom-dweller-predator	19	0.35	35
Parma unifasciata	Herbivore	Sedentary-bottom-dweller-herbivore	17	0.61	70
Mecaenichthys immaculatus	Predator	Sedentary-bottom-dweller-predator	17	0.26	27
Choerodon venustus	Predator	Mobile-bottom-dweller-predator	14	0.30	32
Trachurus novaezelandiae	Planktivore	Midwater-planktivore	13	3.07	335
Meuschenia trachylepis	Predator	Midwater-predator	13	0.21	19
Eubalichthys bucephalus	Predator	Midwater-predator	12	0.20	17
Meuschenia scaber	Predator	Midwater-predator	12	0.59	60
Pseudocaranx dentex	Piscivore	Midwater-piscivore	11	0.31	35
Meuschenia sp.	Predator	Midwater-predator	11	0.13	14
Bodianus unimaculatus	Predator	Mobile-bottom-dweller-predator	11	0.24	14
Heterodontus portusjacksoni	Predator	Mobile-bottom-dweller-scavenger-predator	11	0.32	34
Caesioperca lepidoptera	Planktivore	Midwater-planktivore	10	0.20	13
Chaetodon guentheri	Predator	Midwater-predator	10	0.51	57
Bodianus frenchii	Predator	Mobile-bottom-dweller-predator	10	0.12	13
Chelmonops truncatus	Predator	Sedentary-bottom-dweller-predator	10	0.20	16
Chromis hypsilepis	Planktivore	Midwater-planktivore	9	1.46	149
Pseudolabrus guentheri	Predator	Mobile-bottom-dweller-predator	9	0.14	11
Brachaelurus waddi	Predator	Mobile-bottom-dweller-scavenger-predator	9	0.09	11
Austrolabrus maculatus	Predator	Sedentary-bottom-dweller-predator	9	0.10	12
Myliobatis australis	Sediment-infauna-	Midwater-benthic-invertivore	8	0.07	8
Dasyatis brevicaudata	Sediment-infauna-	Mobile-bottom-dweller-benthic-invertivore	8	0.12	14
Acanthistius ocellatus	Piscivore	Sedentary-bottom-dweller-piscivore	7	0.19	18
Rhabdosargus sarba	Predator	Mobile-bottom-dweller-predator	7	1.47	176
Gymnothorax prionodon	Predator	Mobile-bottom-dweller-scavenger-predator	7	0.18	11
Seriola hippos	Piscivore	Midwater-piscivore	6	0.22	20

Scientific Name	Trophic Group	Trophic-Mobility Group	Occurrence	Mean Rel. Abun.	Total Abun.
Seriola lalandi	Piscivore	Midwater-piscivore	6	0.20	9
Trachinops taeniatus	Planktivore	Sedentary-bottom-dweller-planktivore	6	0.52	61
Orectolobus halei	Predator	Mobile-bottom-dweller-scavenger-predator	6	0.07	6
Orectolobus maculatus	Predator	Mobile-bottom-dweller-scavenger-predator	6	0.06	7
Canthigaster callisterna	Predator	Sedentary-bottom-dweller-predator	6	0.06	7
Pictilabrus laticlavius			6	0.10	8
Dinolestes lewini	Piscivore	Midwater-piscivore	5	0.08	8
Anoplocapros inermis	Predator	Midwater-predator	5	0.04	5
Eubalichthys mosaicus	Predator	Midwater-predator	5	0.06	6
Meuschenia venusta	Predator	Midwater-predator	5	0.06	6
Bodianus perditio	Predator	Mobile-bottom-dweller-predator	5	0.07	6
Siganus fuscescens	Herbivore	Mobile-bottom-dweller-herbivore	4	0.06	7
Paracaesio xanthura	Planktivore	Midwater-planktivore	4	0.33	24
Nelusetta ayraud			4	0.07	8
Aplodactylus lophodon	Herbivore	Sedentary-bottom-dweller-herbivore	3	0.31	25
Lotella rhacina	Piscivore	Sedentary-bottom-dweller-piscivore	3	0.05	4
Glaucosoma scapulare			3	0.03	3
Siganus nebulosus			3	0.03	4
Sarda australis	Piscivore	Midwater-piscivore	2	0.05	6
Epinephelus undulatostriatus	Piscivore	Sedentary-bottom-dweller-piscivore	2	0.02	2
Pempheris affinis	Planktivore	Sedentary-bottom-dweller-planktivore	2	0.02	2
Orectolobus ornatus	Predator	Mobile-bottom-dweller-scavenger-predator	2	0.02	2
Hypoplectrodes nigroruber	Predator	Sedentary-bottom-dweller-predator	2	0.04	3
Solegnathus spinosissimus	Predator	Sedentary-bottom-dweller-predator	2	0.05	2
Trygonorrhina fasciata	Sediment-infauna-	Mobile-bottom-dweller-benthic-invertivore	2	0.02	2
Centroberyx affinis			2	0.03	2
Cheilodactylus vestitus			2	0.02	2
Coris sandageri			2	0.02	2
Mustelus antarcticus			2	0.03	2
Notorynchus cepedianus			2	0.04	3
Odax cyanomelas			2	0.04	3
Plectorhinchus flavomaculatus			2	0.02	2
Seriola rivoliana			2	0.02	2
Labroides dimidiatus	Cleaner		1	0.01	1
Caranx sexfasciatus	Piscivore	Midwater-piscivore	1	0.01	1
Atractoscion aequidens	Piscivore	Mobile-bottom-dweller-piscivore	1	0.01	1
Epinephelus daemelii	Piscivore	Sedentary-bottom-dweller-piscivore	1	0.01	1
Epinephelus fasciatus	Piscivore	Sedentary-bottom-dweller-piscivore	1	0.01	1
Pterocaesio digramma	Planktivore	Midwater-planktivore	1	0.14	17
Dicotylichthys punctulatus	Predator	Midwater-predator	1	0.01	1
Meuschenia flavolineata	Predator	Midwater-predator	1	0.03	2
Lutjanus adetii	Predator	Mobile-bottom-dweller-predator	1	0.05	6
Lutjanus russellii	Predator	Mobile-bottom-dweller-predator	1	0.01	1
Chaetodontoplus meredithi	Predator	Sedentary-bottom-dweller-predator	1	0.01	1
Hypoplectrodes annulatus	Predator	Sedentary-bottom-dweller-predator	1	0.02	2
Parapercis ramsayi	Predator	Sedentary-bottom-dweller-predator	1	0.02	2
Parupeneus pleurostigma	Sediment-infauna-	Mobile-bottom-dweller-benthic-invertivore	1	0.01	1
Platycephalus fuscus	Sediment-infauna-	Mobile-bottom-dweller-benthic-invertivore	1	0.03	1

Scientific Name	Trophic Group	Trophic-Mobility Group	Occurrence	Mean Rel. Abun.	Total Abun.
Anampses elegans			1	0.01	1
Apogon sp.			1	0.01	1
Asymbolus analis			1	0.01	1
Chromis flavomaculata			1	0.03	3
Dotalabrus aurantiacus			1	0.01	1
Echeneis naucrates			1	0.01	1
Girella tricuspidata			1	0.19	15
Kyphosus sydneyanus			1	0.01	1
Latridopsis forsteri			1	0.01	1
Microcanthus strigatus			1	0.01	1
Myliobatis hamlyni			1	0.01	1
Notolabrus fucicola			1	0.03	2
Parapercis stricticeps			1	0.01	1
Pseudophycis barbata			1	0.01	1
Sarda sp.			1	0.01	1
Scomber australasicus			1	0.01	1
Seriola dumerili			1	0.03	3
Seriola sp.			1	0.01	1
Upeneus tragula			1	0.01	1
Zeus faber			1	0.03	1
Predator			40	21.01	
Piscivore			39	10.51	
Planktivore			39	20.52	
Herbivore			37	2.20	
Sediment-infauna-predator			39	4.63	
Mobile-bottom-dweller			40	12.17	
Midwater-planktivore			39	27.75	
Midwater-predator			39	3.72	
Mobile-bottom-dweller-benthic-invertivore			39	5.04	
Sedentary-bottom-dweller-piscivore			39	1.83	
Sedentary-bottom-dweller-predator			39	2.64	
Mobile-bottom-dweller scavenger-predator			38	1.66	
Sedentary-bottom-dweller-herbivore			34	1.33	
Midwater-piscivore			22	0.85	
Mobile-bottom-dweller-herbivore			20	1.30	

Appendix 4-3 Overall best final models of fish species and trophic-mobility groups indicating the resolution (Res.), extent (window length) (Ext.) over which metrics were derived. AUV Raster and AUV Mesh metrics were derived over a window length of approx. 25 m.

Species / Group	Dataset(s)	Best Overall Final Model	Fix. Dev. Exp	Fix. + Ran. Dev. Exp
Achoerodus viridis	AUV Raster & MBLI Raster	AspEast_Res0.1_AUVRaster+AspNorth-std_Res240xExt0480+ Bath_Res005xExt0005	0.34	0.44
Atypichthys strigatus	AUV Raster & MBLI Raster	AspEast_Res005xExt0010+CurvPla_Res0.1_AUVRaster+ CurvPro_Res005xExt0060	0.63	0.63
Bodianus unimaculatus	AUV Raster & MBLI Raster	AspEast-std_Res2.4_AUVRaster+Bath_Res0.1_AUVRaster+ CurvStd_Res010xExt0120	0.54	0.77
Caesioperca lepidoptera	MBLI Raster	AspNorth-std_Res020xExt0040+CurvPro_Res060xExt0960	0.56	0.74
Chaetodon guentheri	MBLI Raster	Bath_Res005xExt0005+CurvPro_Res005xExt0040+ CurvStd_Res060xExt1440	0.55	0.90
Cheilodactylus fuscus	AUV Raster & MBLI Raster	AspEast-std_Res0.1_AUVRaster+CurvPla_Res0.6_AUVRaster+ CurvPro_Res005xExt0005	0.33	0.44
Chelmonops truncatus	AUV Raster	AspEast_Res0.1_AUVRaster	0.39	0.39
Choerodon venustus	MBLI Raster	CurvPla_Res005xExt3120+CurvPro_Res010xExt0020	0.40	0.84
Chrysophrys auratus	MBLI Raster	CurvPla_Res005xExt0020+CurvPro_Res060xExt0960	0.39	0.66
Coris picta	AUV Mesh & MBLI Raster	CurvPro_Res060xExt0960+CurvStd_Res010xExt0160+ Mesh-Rugosity$_{QuadMeanPla}$_Res2.4	0.60	0.81
Enoplosus armatus	AUV Raster & MBLI Raster	AspNorth-std_Res005xExt0010+CurvPla_Res005xExt0005+ CurvStd_Res0.2_AUVRaster	0.80	0.88
Eubalichthys bucephalus	MBLI Raster	CurvStd_Res010xExt0360+CurvStd_Res060xExt2400	0.34	0.40
Gymnothorax prasinus	AUV Raster & MBLI Raster	Bath_Res005xExt0005+CurvPla_Res060xExt0360+ CurvPla_Res2.4_AUVRaster	0.38	0.46
Heterodontus portusjacksoni	MBLI Raster	CurvPla_Res005xExt0005+CurvPro_Res060xExt1920+ CurvStd_Res060xExt1440	0.11	1.00
Hypoplectrodes maccullochi	MBLI Raster	CurvPla_Res060xExt1920+CurvPro_Res010xExt0020+ CurvStd_Res010xExt0240	0.56	0.56
Latropiscis purpurissatus	AUV Raster & MBLI Raster	AspEast_Res0.1_AUVRaster+CurvPla_Res060xExt0480+ CurvStd_Res010xExt1920	0.39	0.39
Mecaenichthys immaculatus	MBLI Raster	CurvPro_Res060xExt0960	0.32	0.37
Meuschenia freycineti	AUV Raster & MBLI Raster	AspNorth_Res020xExt3120+CurvPla_Res0.1_AUVRaster+ CurvStd_Res010xExt0600	0.28	0.79
Meuschenia scaber	AUV Mesh & MBLI Raster	CurvPro_Res005xExt0040+CurvPro_Res060xExt0960+ Face-Angles$_{30deg.-40deg.}$ResNative	0.20	0.97
Meuschenia sp.	MBLI Raster	CurvStd_Res060xExt3120	0.23	0.56
Meuschenia trachylepis	AUV Raster & MBLI Raster	Bath_Res0.1_AUVRaster+CurvPro_Res060xExt1920+ CurvStd_Res0.6_AUVRaster	0.41	0.67
Nemadactylus douglasii	AUV Raster & MBLI Raster	AspEast_Res0.1_AUVRaster+CurvStd_Res005xExt0005+ CurvStd_Res010xExt0600	0.49	0.49
Notolabrus gymnogenis	AUV Raster & MBLI Raster	AspNorth-std_Res040xExt0080+Bath_Res005xExt0005+ CurvPla_Res0.1_AUVRaster	0.60	0.65
Ophthalmolepis lineolata	AUV Raster & MBLI Raster	CurvPro_Res010xExt3120+CurvStd_Res060xExt1440+ SurPla_Res0.1_AUVRaster	0.19	0.85
Parma microlepis	MBLI Raster	AspNorth_Res030xExt0030	0.10	0.49
Parma unifasciata	AUV Raster & MBLI Raster	AspEast-std_Res2.4_AUVRaster+Bath_Res0.1_AUVRaster+ CurvPro_Res010xExt3120	0.53	0.70
Parupeneus spilurus	AUV Raster & MBLI Raster	AspNorth-std_Res005xExt0010+CurvPla_Res0.1_AUVRaster+ CurvPro_Res060xExt0960	0.36	0.78

Species / Group	Dataset(s)	Best Overall Final Model	Fix. Dev. Exp	Fix. + Ran. Dev. Exp
Prionurus microlepidotus	MBLI Raster	AspEast_Res240xExt0240+AspNorth_Res020xExt3120+ CurvPro_Res060xExt0120	0.45	0.87
Pseudocaranx dentex	AUV Mesh & MBLI Raster	AspNorth-std_Res005xExt0010+Mesh-$Height_{Rng}$_ResNative	0.29	0.40
Pseudocaranx georgianus	AUV Raster & MBLI Raster	CurvPla_Res0.1_AUVRaster+CurvPla_Res005xExt0020+ CurvStd_Res010xExt0600	0.30	0.83
Scorpaena cardinalis	AUV Raster & MBLI Raster	CurvPla_Res0.1_AUVRaster+CurvPro_Res060xExt0120	0.30	0.52
Scorpis lineolata	AUV Raster & MBLI Raster	CurvPla_Res0.6_AUVRaster+CurvStd_Res010xExt0010+ SurPla_Res005xExt0005	0.57	0.58
Trachurus novaezelandiae	MBLI Raster	CurvPla_Res005xExt3120+CurvPla_Res060xExt0480+ CurvPro_Res060xExt0120	0.86	0.91
Upeneichthys lineatus	AUV Raster	CurvPla_Res0.1_AUVRaster	0.20	0.23
Herbivore	AUV Raster & MBLI Raster	AspEast_Res240xExt0240+AspNorth_Res020xExt3120+ Bath_Res0.1_AUVRaster	0.52	0.62
Midwater-planktivore	MBLI Raster	AspEast_Res240xExt0240+CurvPla_Res005xExt0010+ CurvPro_Res005xExt0060	0.46	0.46
Mobile-bottom-dweller-herbivore	MBLI Raster	AspEast_Res240xExt0240+AspNorth_Res020xExt3120+ CurvPro_Res060xExt0120	0.44	0.87
Mobile-bottom-dweller scavenger-predator	MBLI Raster	AspNorth_Res030xExt0030	0.05	0.44
Planktivore	MBLI Raster	AspEast_Res240xExt0240+CurvPla_Res005xExt0010+ CurvPro_Res005xExt0060	0.46	0.46
Sedentary-bottom-dweller-herbivore	MBLI Raster	Bath_Res005xExt0005+CurvPro_Res010xExt3120+ CurvStd_Res010xExt0360	0.57	0.76
Midwater-piscivore	AUV Mesh & MBLI Raster	CurvStd_Res010xExt0010+CurvStd_Res010xExt1920+ Mesh-$Height_{Rng}$_ResNative	0.52	0.52
Midwater-predator	AUV Raster & MBLI Raster	CurvPla_Res060xExt0480+CurvStd_Res0.2_AUVRaster+ CurvStd_Res010xExt2880	0.53	0.77
Mobile-bottom-dweller Predator	AUV Raster & MBLI Raster	AspNorth-std_Res020xExt0040+CurvPla_Res0.6_AUVRaster+ CurvStd_Res0.2_AUVRaster	0.46	0.60
Mobile-bottom-dweller-benthic-invertivore	AUV Raster & MBLI Raster	AspNorth-std_Res010xExt0040+CurvPla_Res0.1_AUVRaster+ CurvPla_Res060xExt1920	0.35	0.70
Predator	AUV Raster	AspNorth_Res0.6_AUVRaster+CurvPla_Res0.6_AUVRaster+ CurvStd_Res0.2_AUVRaster	0.43	0.72
Sedentary-bottom-dweller-piscivore	AUV Raster & MBLI Raster	CurvPla_Res0.1_AUVRaster+CurvPla_Res0.6_AUVRaster+ CurvStd_Res010xExt2880	0.43	0.63
Sedentary-bottom-dweller-predator	AUV Raster & MBLI Raster	AspEast-std_Res0.1_AUVRaster+CurvPro_Res005xExt0040	0.19	0.26
Piscivore	AUV Mesh & AUV Raster & MBLI Raster	AspEast_Res005xExt3120+CurvPla_Res0.6_AUVRaster+ Mesh-$Rugosity_{QuadMeanPlan}$_Res2.4_AUVMesh	0.55	0.71

5 Chapter 5 - Bridging the Gap Between Photogrammetry and Traditional Remote Sensing Methods to Improve Predictions of Fish Distributions

5.1 Summary

Fine resolution photogrammetric reconstructions of the seafloor, derived metrics of structural complexity and associated descriptors of benthic cover offer great potential for improved understanding of fish-habitat relationships and predictions of fish abundance and distributions. However, the greater cost (per unit area) of photogrammetric compared to traditional remote sensing (here, multibeam and LIDAR or MBLI) data collection is a substantial hinderance to its contribution to marine ecosystem management and ecological research. In this study, I extrapolate relationships between metrics of structural complexity from traditional methods and metrics of structural complexity and benthic cover from photogrammetric surveys (in locations where these datasets overlap) to 'engineer' photogrammetrically derive metrics over areas where only traditionally derived metrics exist. The specific aim is to expand the coverage of overwise local spatial extent photogrammetric metrics over the broad spatial extents typical of traditionally derived metrics, and thereby further improve predictions of fish abundance and distribution for a fraction of the cost of direct photogrammetric data collection. Improved predictions over broad spatial extents and the ability to better identify areas of ecological value would have positive benefits for conservation and management outcomes. The main findings were:

- ''Engineered' photogrammetric and benthic cover metrics were found important contributors to fish species distribution models (SDMs). For 26 of the 50 species / trophic-mobility groups, SDMs based solely or partly on engineered metrics explained more variance than when based solely on MBLI metrics. This included 0.27 (an almost 7-fold increase) increase in deviance explained in fish abundance, including a 0.24 (126%) increase in deviance explained for the recreationally and commercially important snapper (*Chrysophrys auratus*).
- Equally and perhaps more importantly, engineered metrics, but not MBLI metrics, predicted areas of high *C. auratus* abundance on areas of inshore rock reef on the NSW coastline. These areas have potential conservation significance for *C. auratus* and other fish species and should be groundtruthed by further fish surveys.
- Collectively, these findings further confirm the potential contribution of photogrammetry to marine ecological research and describe a method for incorporating derived metrics into broad-scale studies.

- The performance of MBLI metrics, should, however, not be overlooked for several species and groups. Indeed, the availability of MBLI datasets is a prerequisite to the creation of engineered photogrammetric metrics.

5.2 Introduction

The efficacy of photogrammetrically derived metrics of structural complexity as predictors of fish abundance and distribution has been established in several recent studies across coral reefs (Bayley *et al*., 2019; Collins *et al*., 2017; Fukunaga, Kosaki, *et al*., 2020; González-Rivero *et al*., 2017b; Streit *et al*., 2021), temperate rock reefs (Ferrari, Malcolm, Byrne, *et al*., 2018; Monfort *et al*., 2021b; Taylor & Figueira, 2021) and deep cold-water coral reefs (Price *et al*., 2019). The performance of these metrics appears, at least partly, related to their finer millimetre- to centimetre-scale resolutions (Monfort *et al*., 2021b), compared to the coarser resolutions (generally ≥ 0.5 m) of traditional datasets (in this study, multibeam and LIDAR). These finer resolutions better capture important local-scale drivers of fish abundance, for example the density of small habitat refuges and local-scale hydrodynamic sheer stress and viewshed (amount of habitat visible to a fish). Measures of benthic cover from photogrammetrically derived orthorectified image mosaics (orthomosaics) also provide important predictors of fish abundance (Ferrari, *et al*., 2018), as do novel and uniquely mesh-based metrics of habitat structural complexity (Porter, 2018). These metrics allow local-scale drivers of fish abundance to be combined with those operating over much broader scales (e.g., abiotic environmental gradients such as temperature and light availability, and prevailing hydrodynamic flow and its influence on food availability and larval settlement). Resulting improvements to predictions of fish distributions and abundance would have obvious benefits to marine conservation and resource management efforts. For instance, resource planning and establishment of marine protected areas at appropriate broad spatial extents (Elith & Leathwick, 2009; Moore *et al*., 2009).

The expected benefits of photogrammetry are, however, limited by its relatively greater expense (per unit area) of data collection compared to traditional remote sensing methods. Currently, the application of photogrammetry is restricted to relatively small spatial extents rarely greater than 500 m^2 surveyed using divers or snorkelers, for instance 25 m^2 (Chen & Dai, 2021), 10 m^2 (Streit *et al*., 2021), 25 m^2 (Bayley *et al*., 2019), 125 m^2 (Collins *et al*., 2017), 100 m^2 (Taylor & Figueira, 2021) and 90 m^2 (Fukunaga, Kosaki, *et al*., 2020), although AUVs are sometimes used (as is the case for the data in this study). Boat-based and towed camera (e.g., Mizuno *et al*., 2020) platforms and aerial drone (e.g., Casella *et al*., 2022) survey methods are underdevelopment and would enable an increase in survey

extent, albeit with probable reductions in reconstruction resolution. Nevertheless, even with these advances, photogrammetric coverage is very unlikely to approach the broad coverage possible using traditional methods, for example the over 100 km^2 survey extent of Hill *et al*., (2014) and 100s km^2 examined in this thesis. The application of photogrammetry is thus limited to modeling fish abundance on a few relatively small and likely disconnected reef patches. A key challenge is, then, for researchers to find ways of combining the potential improvements in predictive performance afforded by photogrammetric methods with the much broader spatial coverage achievable using traditional methods.

One potential way to address this challenge utilises the often-high correlation observed amongst many structural complexity metrics (e.g., Fukunaga & Burns, 2020, and in Section 3). Usually, this co-linearity is viewed as a hinderance to modelling techniques and the identification of causal relationships between physical habitat structure and fish abundance (Blalock, 1963; Graham, 2003). However, it may be possible to harness this physical feature of natural reef environments to improve predictions of fish abundance and distributions, without the difficulties of collecting photogrammetry data across large spatial extents. Feature engineering is a technique often used as an early step in machine learning (ML) and other modelling approaches to prepare predictor variables prior to model fitting (Verdonck *et al*., 2021). As well as variable scaling, centering and transformations, predictors (or features) may be combined to virtually create (or engineer) entirely new predictors. This can be as simple as using common mathematical operations such as the mean or product of two or more predictors. These engineered predictors are then included alongside, or in place of, the original predictors during model fitting to provide additional predictors that improve model performance (Verdonck *et al*., 2021).

The specific objectives of this study were to:

1. Identify and quantify the best possible predictive relationships between traditional metrics and those derived from AUV surveys (photogrammetric metrics of structural complexity and benthic cover), from areas of reef where overlapping datasets are available;
2. Use the predictive relationships to engineer photogrammetric metrics that would be expected in areas where traditional bathymetric data are available, but where photogrammetric and benthic cover data are not.
3. Incorporate the ‘engineered metrics’ into SDMs to determine:

a. whether they improve model quality and predictions of fish abundance compared with traditional metrics alone.

b. If these SDMs provide new insights about species distributions on NSW coastal reefs.

These steps and outputs are represented graphically in **Figure 5-1**.

5.3 Methods

5.3.1 Approach

In this study, I apply the concept of predictor engineering to engineer photogrammetric metrics of structural complexity and benthic cover, otherwise derived from photogrammetry, using metrics from traditional datasets (here, multibeam and LIDAR). I achieve this by creating predictive models of photogrammetric metrics and benthic cover at sites were these data overlap with traditional datasets. These models are then used to extrapolate photogrammetric metrics and benthic cover in areas where only traditional datasets exist. These 'engineered' metrics are combined traditional metrics in species distribution models (SDM) of fish abundance to provide additional insight into species distributions on the temperate and sub-tropical New South Wales (NSW) coastline of southeastern Australia.

5.3.2 Study Area

The study area consisted of a total of 120 sites across three locations on the NSW coast: The Solitary Islands (40 sites, 17 m to 36 m deep and 0.1 km to 3.4 km offshore), Port Stephens (43 sites, 19 m to 35 m deep and 1.6 km to 6.1 km offshore) and Batemans Bay (37 sites, 25 to 37 m and 3.9 to 11.4 km offshore) (**Figure 1-2**). Overlapping photogrammetry mesh-based models and benthic cover (both derived from the AUV surveys), and traditionally (multibeam and LIDAR) derived raster-based DEMs (MBLI Raster) were available for 49 of these 120 sites (25 from Solitary Islands, 12 from Port Stephens and 12 from Batemans Bay) (MBLI / AUV overlap sites). As described in **Sections 3** and 4, the photogrammetric meshes were also converted to raster DEMs, providing sets of predictors based on mesh (AUV Mesh) and raster (AUV Raster). Fish were also surveyed at these 49 sites. Data from these 49 sites were used to 1) model the relationships between MBLI Raster structural complexity metrics and metrics of structural complexity and benthic cover (**Table 5-1**) from AUV surveys, and 2) using these relationships engineer (predict) AUV Raster / AUV Mesh complexity and benthic cover metrics at the remaining 71 sites with

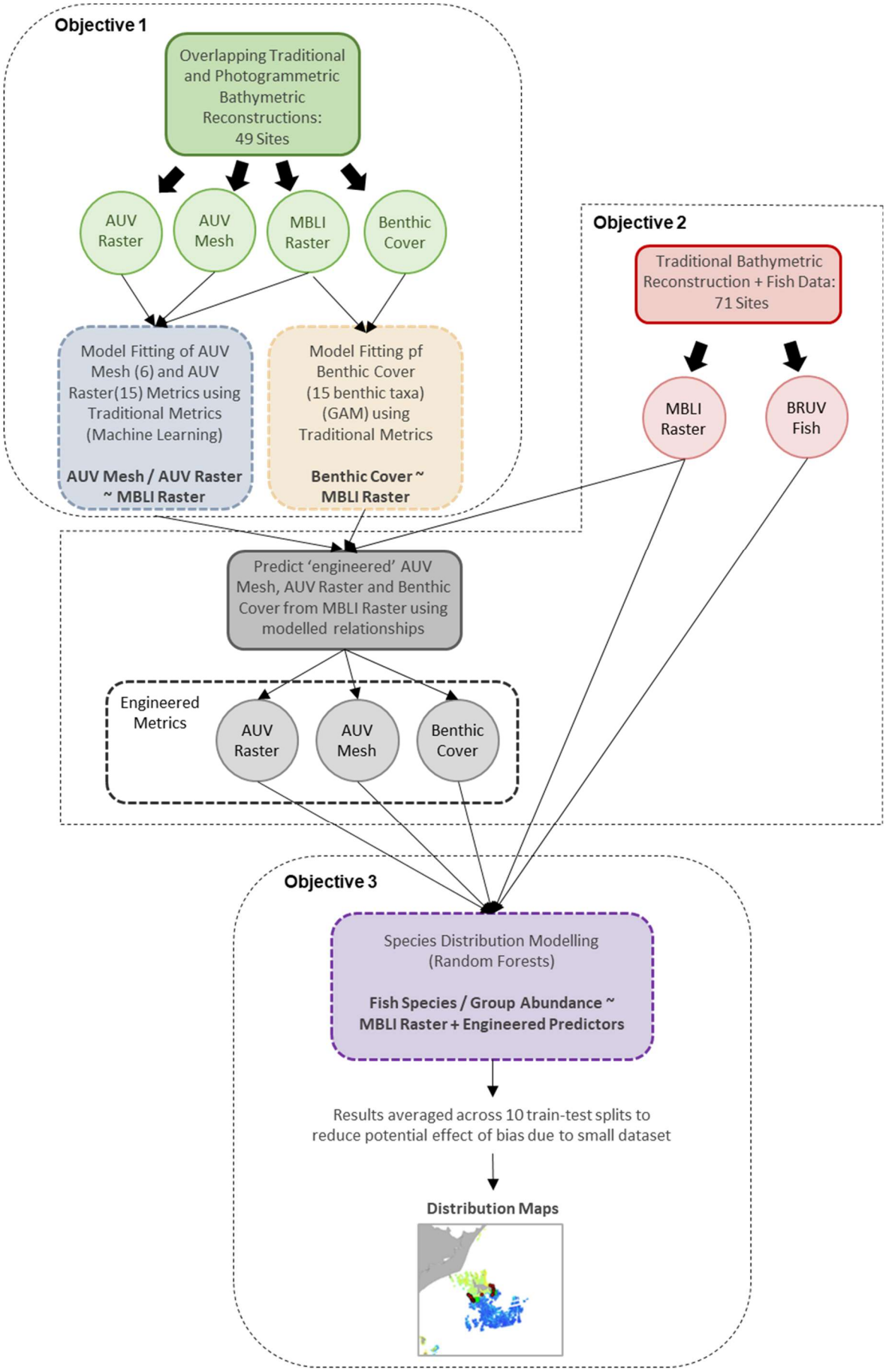

Figure 5-1 Flowchart displaying the key data, steps and outputs of the modelling undertaken in this chapter.

Table 5-1 Metrics (mean value, unless identified as standard deviation = std) of structural complexity and benthic cover included in this study. AUV metrics and benthic cover quantified at an extent of approximately 625 m^2 and MBLI metrics at 900 m^2. Resolution (m) = Res. (m). Native resolution of mesh = 0.03 m to 0.07 m (ResNative).

MBLI Raster	Res. (m)	AUV Raster	Res .(m)	AUV Mesh	Res.(m)	Benthic Cover
Aspect-east (AspEast)	5, 30	Bathymetry (Bath)	0.1	Mesh-Height$_{Rng}$	ResNative	Anemone
Aspect-north (AspNorth)	5, 30	AspEast	0.1	Mesh-Rugosity$_{Plan}$	2.4	Ascidian
Profile-curvature (CurvPro)	5	AspNorth	0.6	Face-Angles$_{20deg.-30deg.}$	ResNative	Branching macroalga
Slope	30	CurvPro	0.2, 0.6	Face-Angles$_{30deg.-40deg.}$	ResNative	Bryozoan
Surface-planar-area (SurPla)	30	Slope	0.1, 2.4	Face-Angles$_{120deg.-130deg.}$	ResNative	Calcareous macroalga
Terrain-ruggedness (TerRug)	30	Planar Curvature (CurvPla)	0.1, 0.6, 2.4			Canopy macroalga
Standard deviation of AspEast (AspEast-std)	5	SurPla	0.1, 2.4			Echinoderms
Standard deviation of AspNorth (AspNorth-std)	5	AspEast-std	0.1, 2.4			Encrusting macroalga
Standard deviation of Bath (Bath-std)	5	AspNorth-std	0.1, 2.4			Filamentous macroalga
Standard deviation of SurPla (SurPla-std)	5					Hydroid
						Macroalga
						Octocoral
						Sponges
						Stony coral
						Turfing macroalga

no AUV surveys. These 71 sites had MBLI Raster data and fish data and are hereafter referred to as the MBLI / fish data overlap sites (15 from Solitary Islands, 30 from Port Stephens and 26 from Batemans Bay). Sites were situated individually or in clusters of up to 5 sites within a 1 km radius.

5.3.3 Bathymetry and Benthic Cover Data

The field acquisition of MBLI Raster, AUV Mesh and AUV Raster datasets and derivation of associated metrics of structural complexity was undertaken as described in **Sections 3.3.2** and **3.3.3**. AUV Raster and AUV Mesh metrics were the uncorrelated subset identified following examination of correlations and model selection using AIC in **Section 3.4**. For the present study, only the MBLI Raster predictors derived over a 30 m window size were selected, which consisted of predictors derived at cell resolutions of 5 x 5 m and 30 x

30 m. A 30 m window size was selected as this was most comparable to the size of the AUV survey extent (window size of approximately 25 x 25 m). The number of MBLI Raster predictors was also reduced by removing those that were highly correlated (r < -0.7 or > 0.7) using a supervised approach (i.e., manual selection of more commonly utilised metrics and of mean in favour of standard deviation (std)).

Benthic cover was derived from images collected during AUV mapping from the 49 overlapping sites in the Solitary Islands (collected 22 to 28 August 2012), Port Stephens (8 to 14 November 2012) and Batemans Bay (27 to 29 November 2012). Collection of these data in winter / early spring helped to reduce seasonal influences (Ferrari, *et al*., 2018) provides detailed description of the data collection and processing of benthic imagery. In summary, full coverage of each approximately 625 m^2 AUV survey typically resulted in approx.15,000 images. From these, 50 spatially balanced images, each covering an area of approx. 2 m^2, were selected using a generalized random tessellated stratified design with the R package spsurvey. Within each image, the taxa present at 25 randomly assigned points were identified and scored into groups using the Collaborative and Annotation Tools for Analysis of Marine Imagery and Video (CATAMI) procedure (Althaus *et al*., 2015), from which data were further grouped into 14 benthic classes: anemone, ascidian, branching macroalga, bryozoan, calcareous macroalga, canopy macroalga, echinoderms, encrusting macroalga, filamentous macroalga, hydroid, macroalga, octocoral, sponges and stony coral. In this study, scores for each group were transformed to presence/absence for each image, which provided a probability of occurrence at each site (no. of images where the benthic cover group was identified / total number of images), providing up to 50 'image trials' per site.

5.3.4 Fish Data

Fish data from the additional 71 sites were collected using baited remote underwater video surveys (BRUVs) undertaken by NSW DPI (Fisheries) and the NWS National Parks and Wildlife Service (NPWS) as described in **Section 3** - **Section 3.3.2**. Importantly, these data provide an independent fish dataset from that presented in **Section 3**, which allowed a separate assessment of the performance of different datasets and metrics. Fish abundance data were available from the Solitary Islands and Port Stephens in winter of 2010, 2011 and 2012, and from Batemans Bay in winter of 2010 and 2011. Fish data were averaged across years at each site and species with a greater than 20% occurrence rate (i.e., present at 14 or more sites) were modelled individually (**Appendix 5-1**). Abundance data from all species regardless of occurrence rate was also summed across functional groups based on trophic

level (predator, piscivore, herbivore, planktivore, sediment-Infauna-predator) and mobility (midwater, mobile-bottom-dweller, mobile-bottom-dweller-scavenger, sedentary-bottom-dweller), providing a total of 15 trophic-mobility groups with a 20% or greater occurrence rate. Most fish species were placed into these groups (representing 98% of total fish abundance). It is worth noting that seven of these groups were dominated numerically by one species (70% or more of the total abundance). Herbivores and sedentary-bottom-dweller-herbivores were dominated by white-ear scalyfin *(Parma microlepis*) (77% and 90% respectively), midwater-piscivores by longfinned pike *(Dinolestes lewini*) (75%), mobile-bottom-dweller-benthic-invertivores and sediment-infauna-predators by blackspot goatfish *(Parupeneus spilurus*) (90% and 90% respectively), mobile-bottom-dweller-herbivores by sawtail surgeonfish *(Prionurus microlepidotus*) (77%), and sedentary-bottom-dweller-planktivores by eastern hulafish *(Trachinops taeiatus*) (70%).

5.3.5 Statistical Methods

5.3.5.1 Engineering Predictors

Generalised Additive Modelling (GAM) and machine learning (ML) were used when engineering AUV Raster and AUV Mesh and benthic cover metrics using all 12 MBLI Raster metrics. These methods also included bathymetry, and easting and northing (capturing geographic location) as other potential important predictors.

The selected ML methods were suitable for modelling continuous AUV Raster and AUV Mesh metrics (Sarker, 2021) and provided a simpler approach to considering various distributions required by Generalised Linear Modeling (GLM) or GAM approaches. Each AUV Raster and AUV Mesh metric was modelled using four ML techniques and the best performing method for each selected. It is difficult to know a-priori which ML method would be most suited to individual response variables, and attempting multiple methods helped maximise overall model performance and variability explained for each individual response. The ML methods attempted were support vector machines (SVMs) based on polynomial (1) and radial (2) kernels, random forests (RFs) (3), and a regularised version of random forest (RFREG) (4) (**Table 5-2**). The best performing ML method for each engineered metric was identified using Root Mean Square Error (RMSE) (the standard deviation of prediction errors), with the lowest RMSE value indicating the best performing model (**Appendix 5-2**). RMSE was preferred as a performance measure as it is in the same units as the response variable, and penalises outliers more than the other commonly used performance measure Mean Absolute Error (MAE). Only the best performing final ML models were considered

Table 5-2 Brief descriptions of the machine learning methods used to model and predict engineered structural complexity predictors.

Technique	Description	Advantages / Disadvantages
Support Vector Machine with polynomial Kernel	Fits a best fit line (or hyperplane in the case of two or more predictors) to the data. Calculates error and loss function differently to simple linear regression with less chance of overfitting. The line / hyperplane is determine only using the closest points rather than the entire dataset. Uses the 'kernel-trick' that allows the algorithm to fit the hyperplane in transformed predictor space and model non-linear relationships. Polynomial kernels are based on derivatives of the predictors.	Robust to noise, large numbers of predictors and overfitting, easy to implement. Can be slow to fit and sensitive to the choice of kernel and hyperparameter values.
Support Vector Machine radial kernel	As above, but the radial kernels provide greater flexibility than derivatives when transforming predictors.	As with all kernels, the radial kernel is not guaranteed to provide the best model fit for all datasets.
Random Forest	Based on many (an ensemble) decision trees each fit on a bootstrap (or bagging) generated subset of the response data and predictors. The final prediction averages the results of the individual trees to improve overall predictive performance. The two primary hyper-parameters are the number of predictors selected in in each subset and the total number of trees in the ensemble.	Suited to capture complex non-linear relationships and interactions. Harder to interpret as there is no single final model.
Regularised Random Forest	As for Random Forest but includes a penalization function (and associated extra hyper-parameter) that retains predictors only if they are associated with a certain reduction in error.	As above, plus generally produces more parsimonious models and is less influenced by correlated predictors. Requires tuning of an additional hyperparameter.

further. Prevalence of benthic cover was modelled using GAM with binomial distribution implemented via the FSSGam package in R (Fisher *et al*., 2018). This package facilitates the fitting and comparison of multiple GAM models each based on a complete sub-set of all potential predictor combinations for each response variable of interest. The best performing model for each benthic cover taxon was selected using AIC corrected for small sample sizes (AICc) (Hurvich & Tsai, 1989) (**Appendix 5-3**). For GAM models, it is noted that to help prevent spurious results the full-subsets approach removes potential models built from predictors with a correlation greater than 0.28 r (Fisher *et al*., 2018). MBLI Predictors with a correlation greater than this value appeared in the potential model combinations but not in the same model.

Following model fitting and selection, the final model for each predictor was used to predict 'engineered' metrics for each of the 71 additional sites where these predictors were unavailable. Further, engineered metrics were also predicted across the entire MBLI Raster bathymetric reconstruction providing a fully contiguous 'engineered' raster surface for each AUV Raster, AUV Mesh and benthic cover metric across the extent of the MBLI Raster datasets. Comparisons of histograms of the predicted AUV Raster and AUV Mesh metric values against the values of the same metrics observed at the 49 sites for which their values were known were also undertaken to help examine predictive performance. This provided little evidence of erroneous ML predictions, with predicted values largely within the ranges observed at each original photogrammetric survey site. A small proportion (around 2% of

values across the entire raster surface) of predicted values of aspect-east and aspect-north were outside the possible ranges of these metrics (< -1 or > 1). In these cases, negative and positive values were converted to -1 or 1, respectively. Similar checks for GAM predictions were not required as the response variable ranged between 0 and 1. Correct GAM specification was also checked by examining residual diagnostic checks including plots of residuals versus fitted values and fitted versus predicted.

To test if engineered predictors generated novel information, rather than providing the same information as the MBLI Raster predictors, correlations between the engineered metrics and the MBLI Raster predictors used to model them were examined. This indicated novel information was created. Only nine of the twenty-one AUV engineered metrics (5 of the 15 AUV Raster and 3 of the 6 AUV Mesh metrics) were highly correlated ($r < -0.7$, $r > 0.7$) with any single MBLI predictor (**Appendix 5-4**). Only 3 of the 15 engineered benthic cover groups were highly correlated with one or more individual MBLI predictor (**Appendix 5-5**). This suggested the engineered predictors did not simply provide the same information done so by the individual MBLI Raster predictors. The contribution of each MBLI predictor to models of AUV Mesh and AUV Raster metrics was quantified via the permutation feature importance method (Altmann *et al*., 2010). This method calculates the increase in the prediction error, or Mean Squared Error (MSE), after permuting the predictor values, with unimportant predictors having little influence on MSE. This routine is not available for SVM techniques and in these cases the model was refit using the random forest technique to provide a measure of variable importance, though predictions were made using the SVM model. For GAM models of benthic cover, the relative importance score provided for each predictor by the FSS GAM function was used to assess the performance of individual predictors. Scores were calculated by summing the model Akaike weights (interpreted as the probability that model is the best model) for all models containing each predictor.

In the case of engineering benthic cover from MBLI Raster predictors, this method differs from the more common method of characterizing benthic habitat using abiotic textural derivates (e.g., MBLI Raster predictors) (e.g., Walbridge *et al*., 2028). Often, the benthic environment is classified into different habitats (e.g., sand, mixed sand-rock, low-relief reef, high-relief reef) using these abiotic predictors. However, in the case of benthic cover in this thesis, this is undertaken using the modelled relationships between benthic cover and the abiotic predictors from where these data overlap. The benthic cover predictors also represent the biological component of the benthic habitat, which is not included in habitat characterisation using such abiotic textural derivatives.

5.3.5.2 Species Distribution Modelling

Individual fish species and trophic-mobility group abundances from the 71 MBLI / fish data overlap sites were modelled using RFs based on the MBLI Raster metrics and the AUV Raster metrics, AUV Mesh metrics and benthic cover engineered from the same MBLI Raster metrics (referred to collectively as engineered predictors). Separate models were fit using each of MBLI Raster, AUV Raster, AUV Mesh, benthic cover, and using all these combined. Prior to fitting, the dataset was randomly split into a 70% training %and 30% test %set. RF models were fit on the training set using leave one out cross validation (LOOCV) to 'tune' the model by identifying the values of hyperparameters ntree (number of trees) and mtry (number of randomly selected predictors per tree) that minimised RMSE. The performance of the trained model was assessed using RMSE when fit on the test dataset. This step assessed potential overfitting and the ability of the model to generalize to data not encountered during model training. Given the relatively small sample size (71 observations) and the associated potential for bias, the train-test split and model fitting was repeated 10 times each using a random train-test data split. Further train-test splits were not undertaken due to the increasing computation time required to undertake model fitting. MSE and R^2 values were averaged across the 10 repeats. Although no formal test was undertaken, it was noted that RMSE and R^2 values were correlated (smaller RMSE = greater R^2). Averaged RMSE was used to rank models based on performance (lower RMSE indicates better performance). Repeating train-test split and model fitting and calculation of mean RMSE and R^2 helped minimise potential bias of individual models and provided more confidence in the assessment of relative performance among models.

To create spatially contiguous maps of predicted fish and fish group distributions, the trained model from each train-test split was used to predict the species abundance across the MBLI Raster extent for each of the Solitary Islands, Port Stephens and Batemans Bay separately. Predicted abundances were then averaged across the 10 splits to provide a single distribution map for each species and group. When engineered predictors outperformed MBLI predictors, further detailed exploration of the performance of individual predictors and predicted distributions was undertaken. For brevity, only maps of the location where the species or group was most abundant were presented (in all but one case, this was Port Stephens). Partial dependency plots (PDP) were used to explore the relationships between fish abundance and important engineered predictors. These plots identify the influence of each predictor on the response while values of all other predictors are kept constant. It is noted that models and PDPs were built using data from all three locations

combined, although distribution maps are presented for individual locations. Principal Component Analysis (PCA) was also used to visualize the relative importance of the AUV Mesh, AUV Raster, benthic cover and MBLI Raster datasets for each species and group using scaled and centered mean R^2 values.

5.4 Results

5.4.1 Predictor Engineering

The best performing ML models based on MBLI Raster metrics explained 8% to 74% of the variance in AUV Mesh and AUV Raster metrics (**Figure 5-2a**). For example, 74 % of the variance observed in the AUV Mesh metric Mesh-$Height_{rng}$ was explained using a ML model built using the nine MBLI Raster metrics. Using the same MBLI Raster metrics, GAM models of benthic cover explained 45% to 87% of the variance in benthic cover (**Figure 5-2b**). MBLI Raster metrics were most important when used to model the same AUV Raster metric, particularly in the case of orientation-based metrics. AUV Raster curvature-based metrics were predicted poorly (the poorest 9 performing AUV Raster metric models included all 6 curvature-based metrics). MBLI Raster curvature metrics also contributed relatively little to models of AUV Mesh and AUV Raster metrics and benthic cover. MBLI Raster derived aspect-east and aspect-north were relatively important for benthic cover, while aspect-north-std and bathymetry-std contributed relatively little to most models of benthic cover.

5.4.2 Species Distribution Models

5.4.2.1 Model Performance

The PCA plots for species (**Figure 5-3**) and trophic-mobility groups (**Figure 5-4**) indicated a clear separation between points along the x axes (PCA1) associated with the overall variance explained by the MBLI vs the engineered predictors. Secondary separation was also evident along the y axes (PCA2) associated with the relative performance of the MBLI Raster predictors versus the engineered predictors (AUV Raster, AUV Mesh and Benthic Cover in blue text). There was no obvious grouping of individual species from similar trophic-mobility groups, though MBLI Raster appeared to be more important for planktivore groups (planktivore, midwater-planktivore, and sedentary-bottom-dwelling-planktivore), with these groups tending to group towards the top of the PCA (**Figure 5-4**).

When averaged across all species and groups, RF models based solely on engineered predictors (AUV Mesh, AUV Raster or benthic cover) or when engineered predictors were combined with MBLI Raster predictors tended to explain more variance (0.18 - 0.25 var. exp.

a)

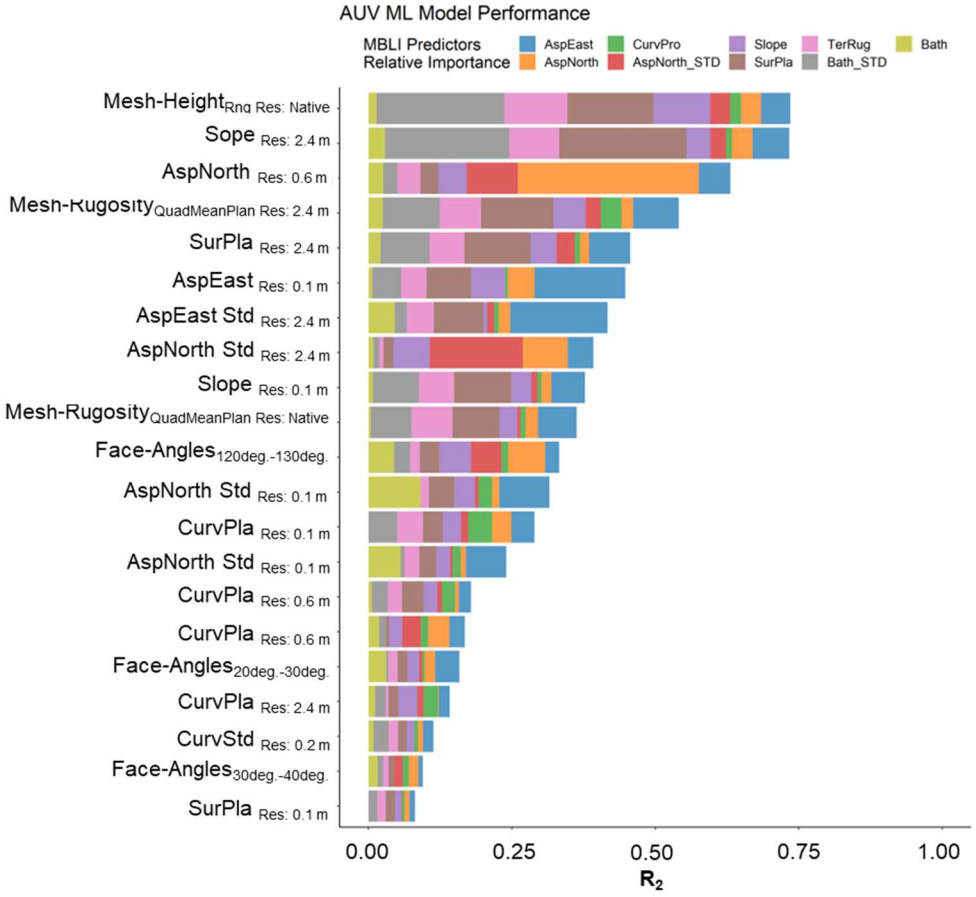

b)

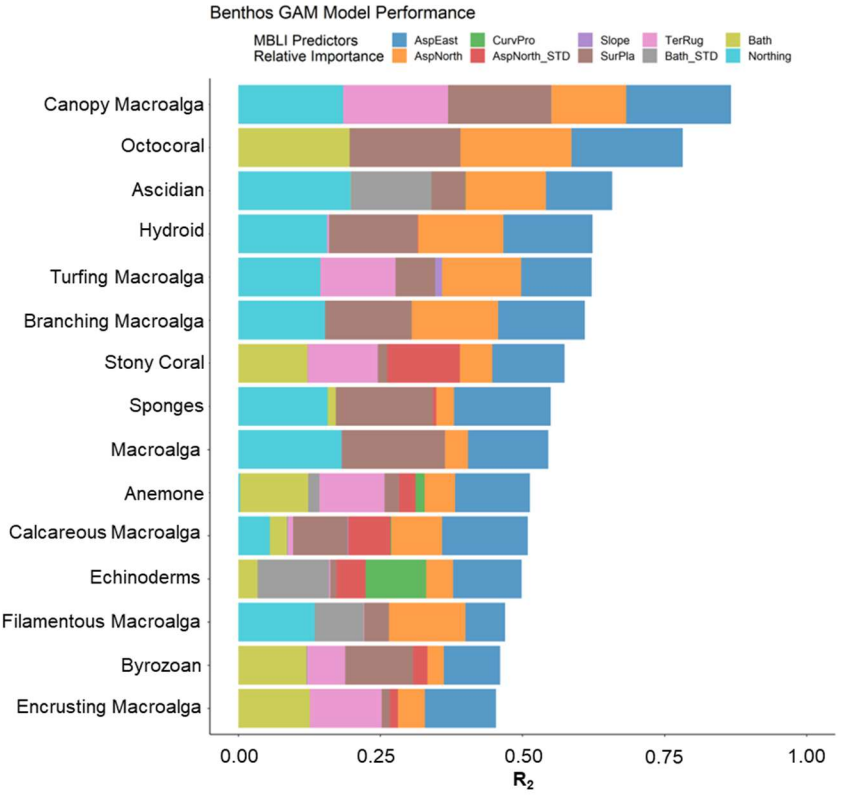

Figure 5-2 **Proportion of variance explained (on x-axis) by a) ML models of AUV metrics (on y-axis) and b) GAM models of benthic cover (i.e., prevalence) (on y-axis) based on MBLI Raster predictors (colours-coded bars). For AspEast and AspNorth, the maximum contribution across the two resolutions considered is presented.**

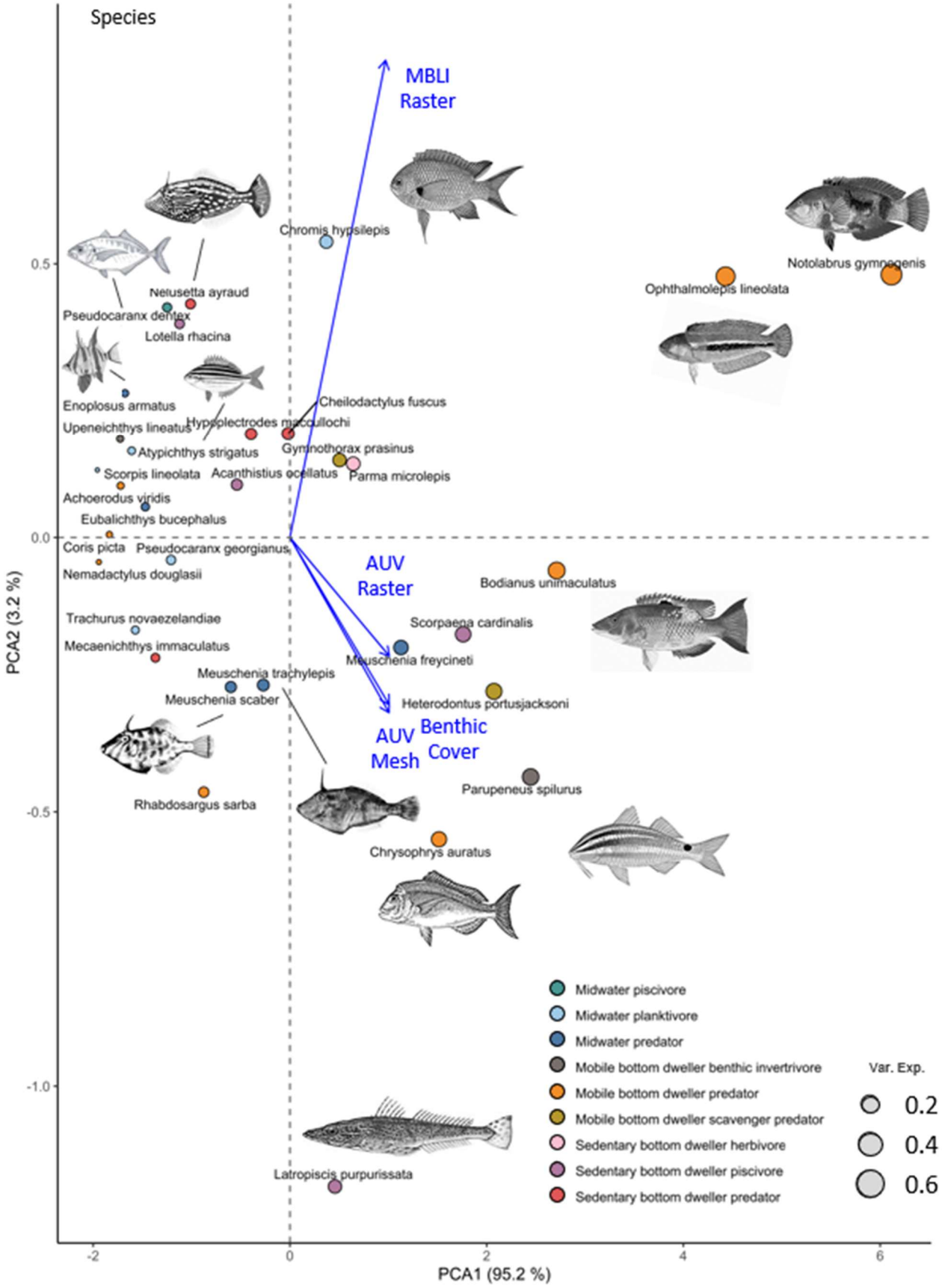

Figure 5-3 **PCA plot based on the variance explained (Var. Exp.) by each set of predictors for fish species. PCA axis based on scaled and centered R2 values averaged across all train-test repeats.**

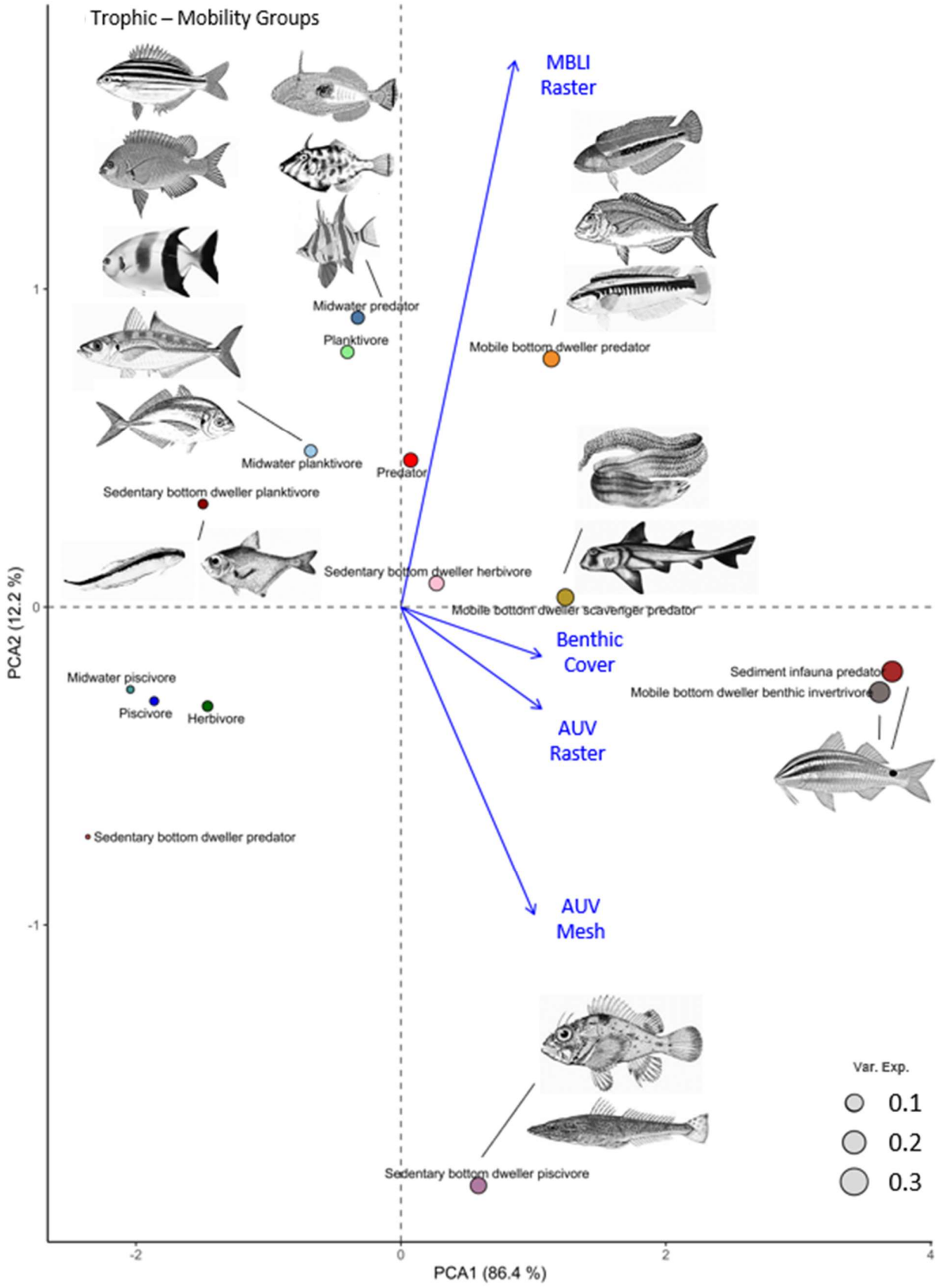

Figure 5-4 **PCA plot based on the variance explained (Var. Exp.) by each set of predictors for fish trophic-mobility groups. PCA axis based on scaled and centered R2 values averaged across all train-test repeats.**

± SE 0.20) in fish abundance than those based solely on the MBLI Raster predictors (0.15 var. exp. ± SE 0.18) (**Figure 5-5**). For individual species and groups, RF models on average explained between 0.3% and 66% of the variation in fish abundance. Of the 50 fish species and groups, variability in the abundance of 26 was best explained by SDMs based solely on or including engineered predictors (**Figure 5-6a-b**). MBLI Raster predictors performed better than all engineered predictors for 7 species and groups, with the remaining 14 species and groups showing mixed results (i.e., MBLI Raster performed better than some, but not all, engineered predictor datasets).

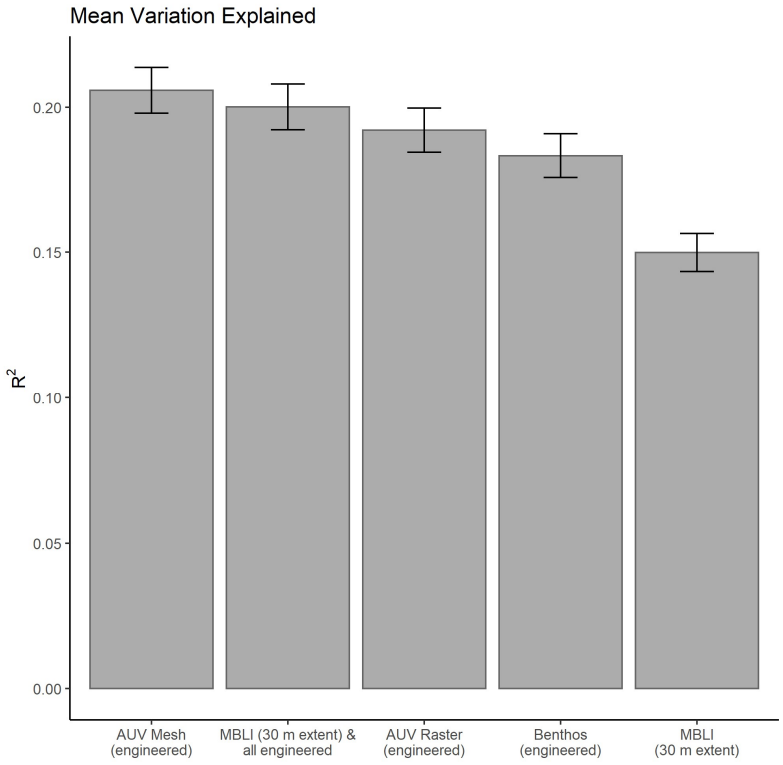

Figure 5-5 Model performance averaged across a) different sets of predictors and b) averaged across species / trophic-mobility groups and c) the difference in variance explained by engineered AUV Raster, AUV Mesh and benthic cover predictions relative to the variance explained by the MBLI Raster predictors.

The greatest improvement in variance explained (R^2 values) by engineered predictors compared to MBLI Raster predictors alone was for Sergeant Baker (*Latropiscis purpurissatus*) (0.27 / 7-fold improvement), snapper (*Chrysophrys auratus*) (0.24 / 126% improvement) and *P. spilurus* (0.20 / 80% improvement). In each case, engineered AUV Mesh predictors provided the best model fit and greatest variance explained. Engineered AUV Raster predictors provided the best fit for yellow-finned leatherjacket (*Meuschenia trachylepis*) and explained 0.11 (110%) more variance than MBLI Raster predictors. For velvet leatherjacket (*Meuschenia scaber*) and crimson banded wrasse (*Notolabrus*

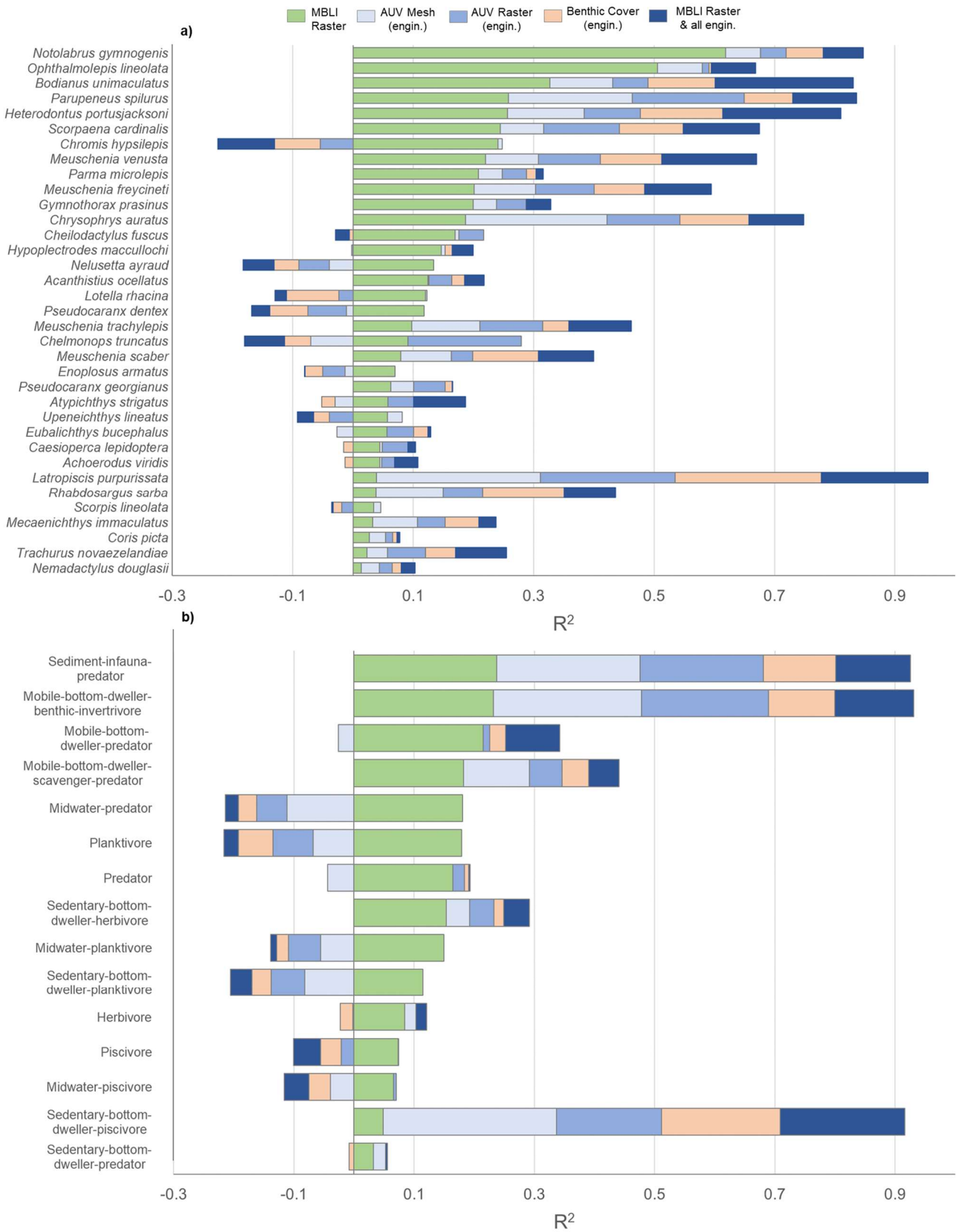

Figure 5-6 **Variance explained my ML models of fish a) species and b) trophic-mobility group abundance. Variance explained by models based on engineered (engin.) AUV Mesh, AUV Raster and Benthic Cover predictors and MBLI Raster & all engineered predictors expressed relative to the variance explained solely using MBLI Raster (green bars). Specie and groups ordered by top to bottom according to variance explained solely using MBLI Raster.**

gymnogenis) benthic cover provided the best model fit and explained 0.10 (125% and 16%, respectively) more variance than MBLI Raster predictors.

For trophic-mobility groups, engineered metrics were most important for mobile bottom dweller-benthic-invertivores, sediment-infauna-predators, and sedentary-bottom-dweller-piscivores, with a 0.25 (109%), 0.24 (100%) and 0.29 (almost 6-fold) improvement in variance explained, respectively, compared to MBLI Raster predictors. Sedentary-bottom-dweller-piscivore consisted mostly of eastern red scorpionfish (*Scorpaena cardinalis*) (48%) and *L. purpurissatus* (27%), however, the other two groups were dominated numerically by *P. spilurus* (80% to 90% of total abundance) (this species was examined individually). A similar but less pronounced improvement in variance explained (0.11 / 61 %) was also observed for mobile-bottom-dweller-scavenger-predator, which consisted primarily of moray eel (*Gymnothorax prasinus*) and Port Jackson shark (*Heterodontus portusjacksoni*), each contributing around 40% of total abundance. For all these groups, AUV Mesh predictors provided the smallest RMSE and the greatest variance explained.

MBLI Raster predictors provided the best model fit and explained more variance than all engineered predictors for white trevally (*Pseudocaranx dentex*), old wife (*Enoplosus armatus*) and Chinaman leatherjacket (*Nelusetta ayraud*), though only marginally and no more than 0.06 (18%, 20%, 42%, respectively). Groups best explained by MBLI Raster predictors (up to 0.11 more variance compared to engineered predictors) included midwater-predators (90% leatherjackets (genera: *Meuschenia* and *Eubalichthys*) and *E. armatus*), planktivores (90% *A. strigatus*, *C. hypsilepis*, *S. lineolate*, *T. novaezelandiae* and *P. georgianus*) and sedentary-bottom-dwelling-planktivores (90% *T. taeniatus* and smallscale bullseye (*Pempheris compressa*)), with a 20%, 50% and 50% improvement in variance explained, respectively.

The best performing models of some species and groups combined engineered and MBLI Raster predictors, suggesting a synergistic effect of combining these methods. This included eastern pigfish (*Bodianus unimaculatus*), *H. portusjacksoni*, *A. Strigatus* and mobile-bottom-dwelling-predators (75% Maori wrasse (*Ophthalmolepis lineolata*), *C. auratus*, and comb wrasse (*Coris picta*), combined), with a 0.12 (27%), 0.06 (15%), 0.05 (50%) and 0.06 (25%), respectively, improvement in variance explained compared to that explained by any single dataset. Other species and groups showed relatively little preference for any set of predictors, with generally small (< 0.05) differences in explained variance.

5.4.2.2 Fish Distributions and Habitat Relationships

At Port Stephens, the better performing engineered predictor based models predicted that *C. auratus* (**Figure 5-7a**, **Figure 5-8a**), *P. spilurus* (**Figure 5-7b**, **Figure 5-8b**), *M. trachylepis* (**Figure 5-7c**, **Figure 5-8c**) and *N. gymnogenis* (**Figure 5-7d**, **Figure 5-8d**) were more abundant on reef inshore of Broughton Island than otherwise predicted by models based solely on MBLI Raster predictors. This was most notable for *C. auratus* and *P. spilurus*, with the AUV Mesh models also predicting greater abundance on the eastern side of the reef inshore of Broughton Island. Although all four species were more abundant at shallower depth, the greater abundance predicted on reef inshore of Broughton Island was far more apparent when using the engineered predictors. Reef inshore of Broughton Island was characterised by greater Mesh-Height$_{Rng}$ (**Appendix 5-6a**) and Mesh-Rugosity$_{Plan}$ (**Appendix 5-6b**), with reef to the east also characterised by greater Face Angles$_{20\ deg.\ to\ 30\ deg.}$ (**Appendix 5-6c**), all of which were associated with greater abundance of *C. auratus* and *P. spilurus*. AUV Mesh models also predicted greater abundance of *C. auratus* on coastal reef southeast of Shark Island, also associated with greater Mesh-Height$_{Rng}$, Mesh-Rugosity$_{Plan}$ and Face Angles$_{20\ deg.\ to\ 30\ deg.}$

The greater abundance of *M. trachylepis* predicted on reef inshore of Broughton Island, was associated with smaller slope (res. 2.4 m) (**Appendix 5-6h**), with which it was negatively correlated, and greater surface-planar-area (res. 2.4 m) in this location (**Appendix 5-6h**), with which it was positively correlated. Although *M. trachylepis* was also positively correlated with surface-planar-area (res. 0.1 m), there was no clear broad-scale pattern in its spatial variability, and it likely contributed only to small scale (individual 30 m cells) variation in abundance. Greater predicted abundance of *N. gymnogenis* inshore of Broughton Island and on coastal reef southwest of Shark Island was associated with greater cover of encrusting algae (**Appendix 5-6n**) and ascidians (**Appendix 5-6o**), and their positive association with abundance. The positive association with filamentous algae (**Appendix 5-6m**) likely contributed more to fine scale variation in *N. gymnogenis* abundance. More mobile-bottom-dwelling-scavenger-predators predicted by AUV Mesh predictors inshore of

Benthic cover models of abundance of *M. scaber* (**Figure 5-7f**, **Figure 5-8f**) and AUV Mesh models of *L. purpurissatus* (**Figure 5-7g**, **Figure 5-8g**) predicted greater abundance on more offshore reef at Port Stephens and the Solitary Islands, respectively. *M. scaber* was associated with lower octocoral and greater encrusting algae cover. *L. purpurissatus* was associated with smaller Mesh-Height$_{Rng}$ and greater Face-Angles$_{30deg.-40deg.}$ and Mesh-Rugosity$_{Plan}$. It is noted that both species were also associated with deeper offshore water,

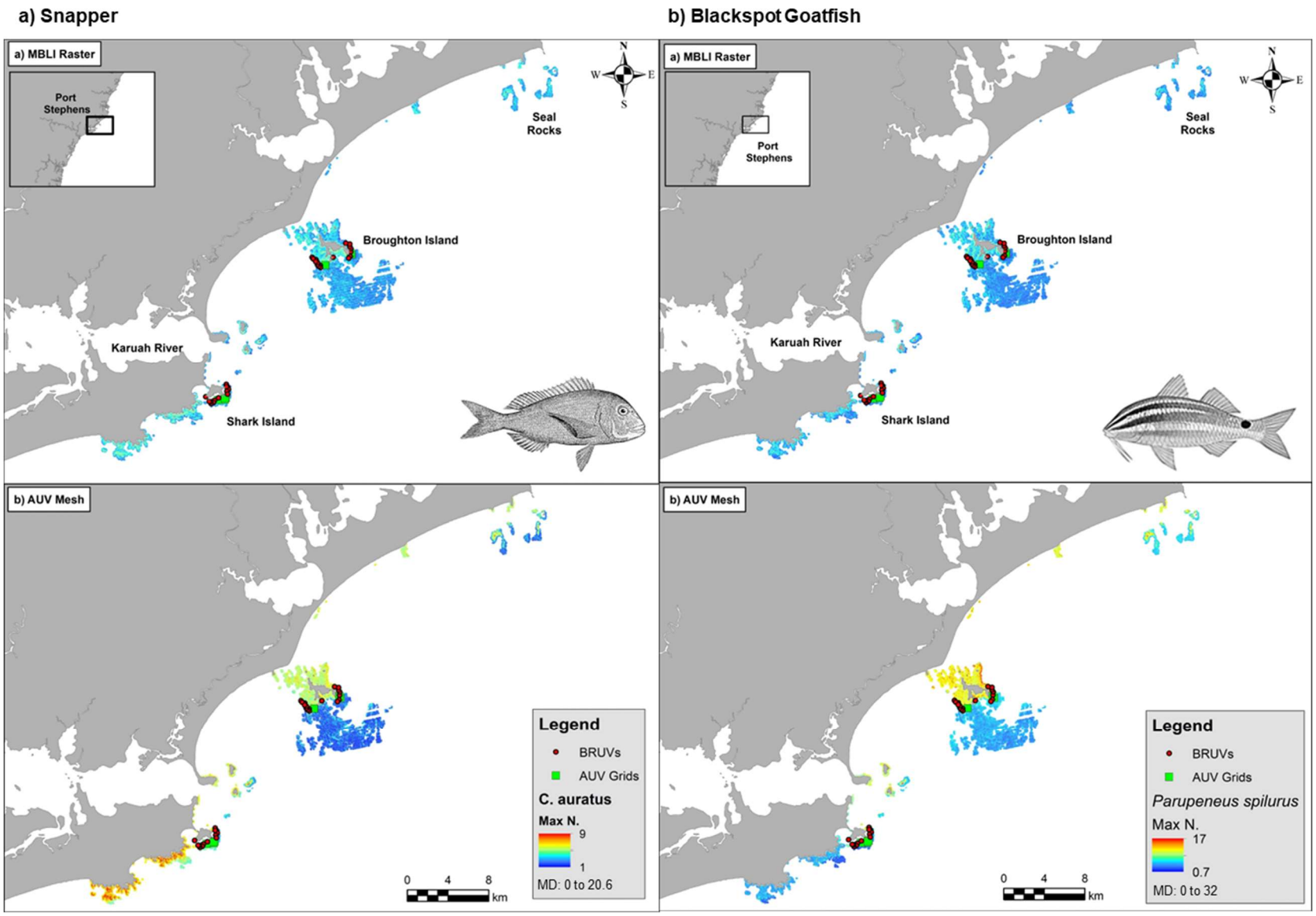

Figure 5-7 **Species distribution models for a) Snapper and b) blackspot goatfish based on MBLI Raster predictors (top) and AUV Mesh (bottom) predictors. Model domain (MD) was the range of abundance values in the fish dataset.**

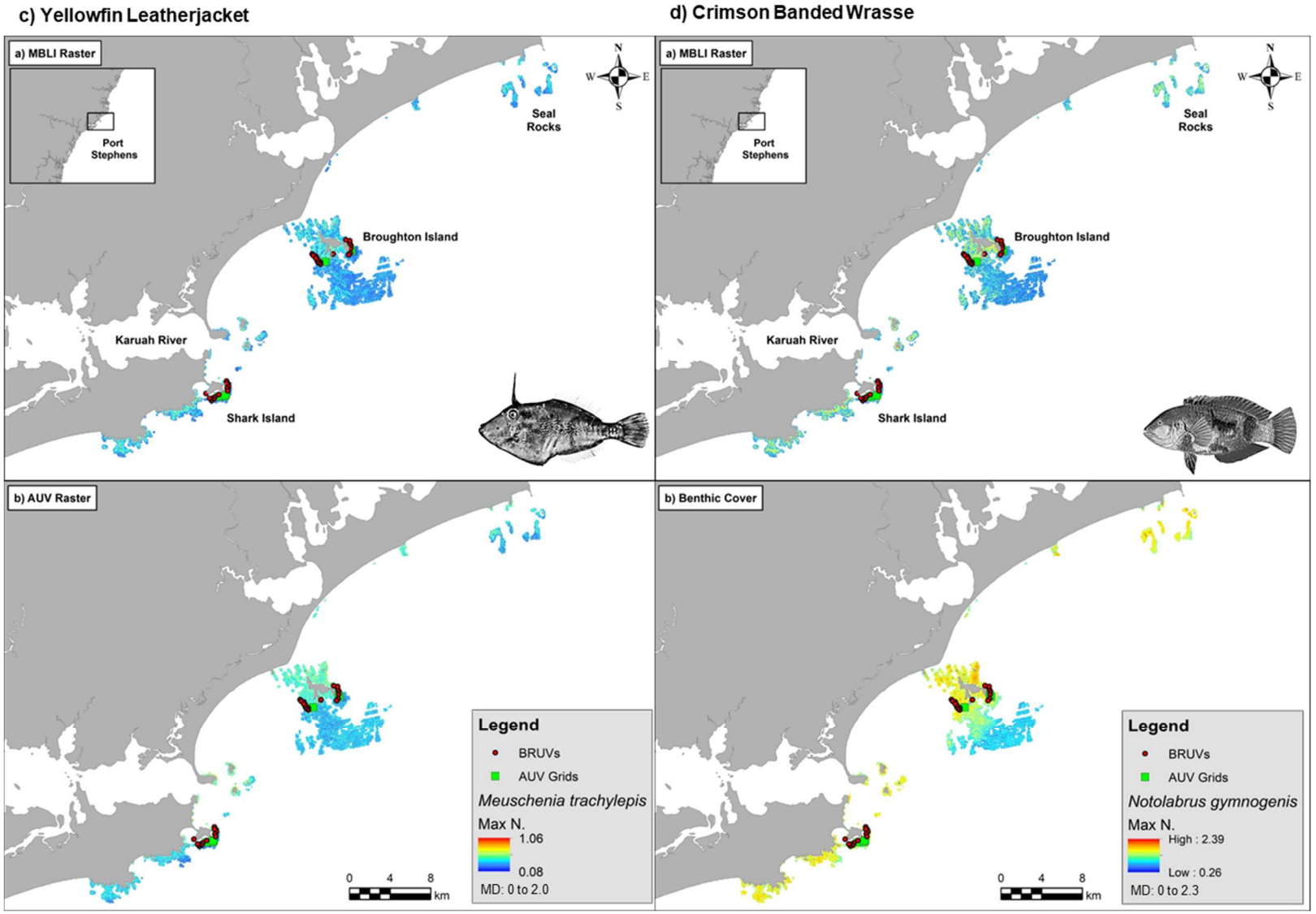

Figure 5-7 continued. Species distribution models for c) Yellowfin Leatherjacket and d) Crimson Banded Wrasse at Port Stephens based on MBLI Raster predictors (top) and AUV Raster and benthic cover (bottom), respectively. Model domain (MD) was the range of abundance values in the fish dataset.

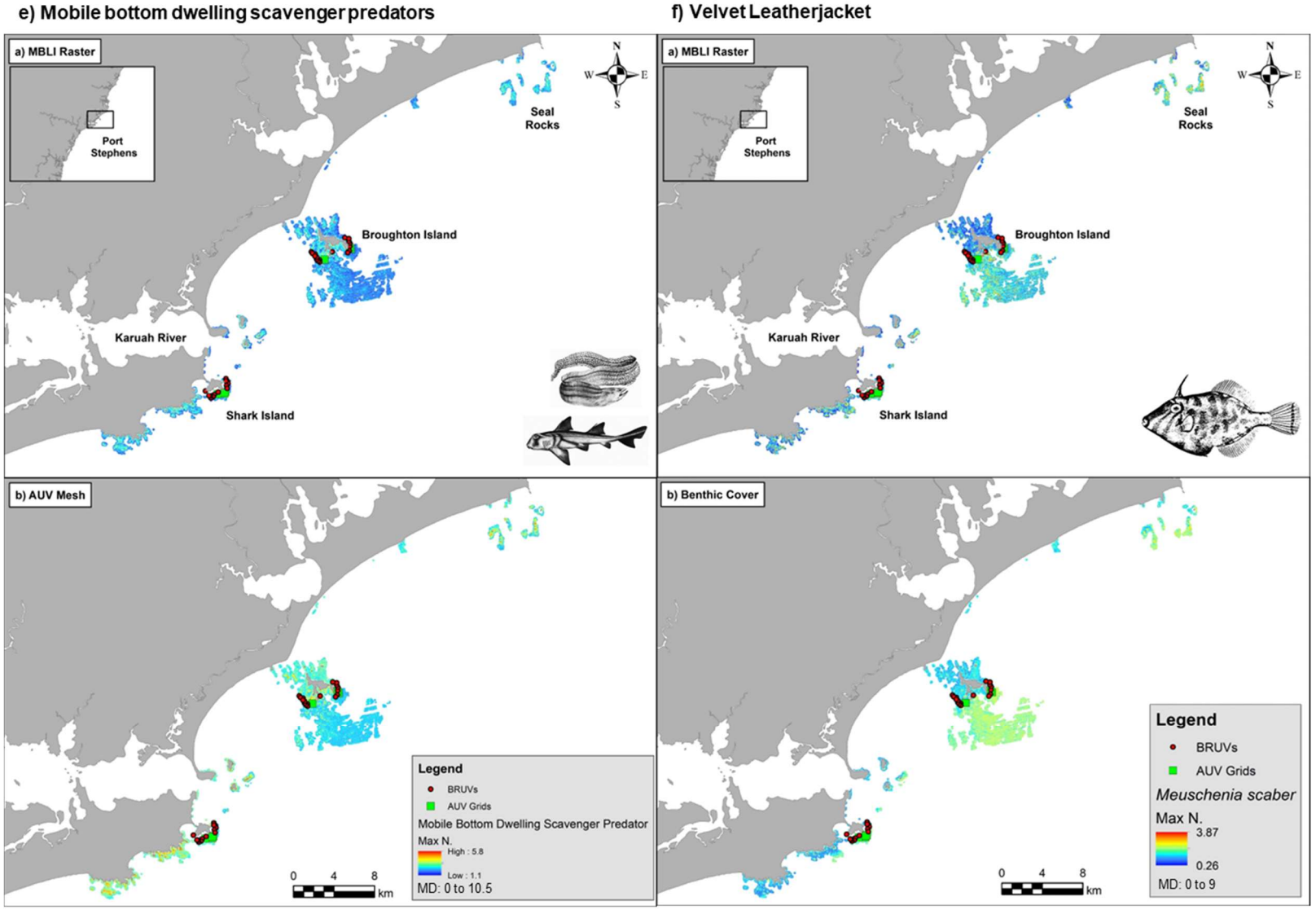

Figure 5-7 continued. Species distribution models for e) mobile-bottom-dwelling-scavenger-predators and f) velvet leatherjacket at Port Stephens based on MBLI Raster predictors (top) and AUV Mesh / benthic cover predictors (bottom). Model domain (MD) was the range of abundance values in the fish dataset.

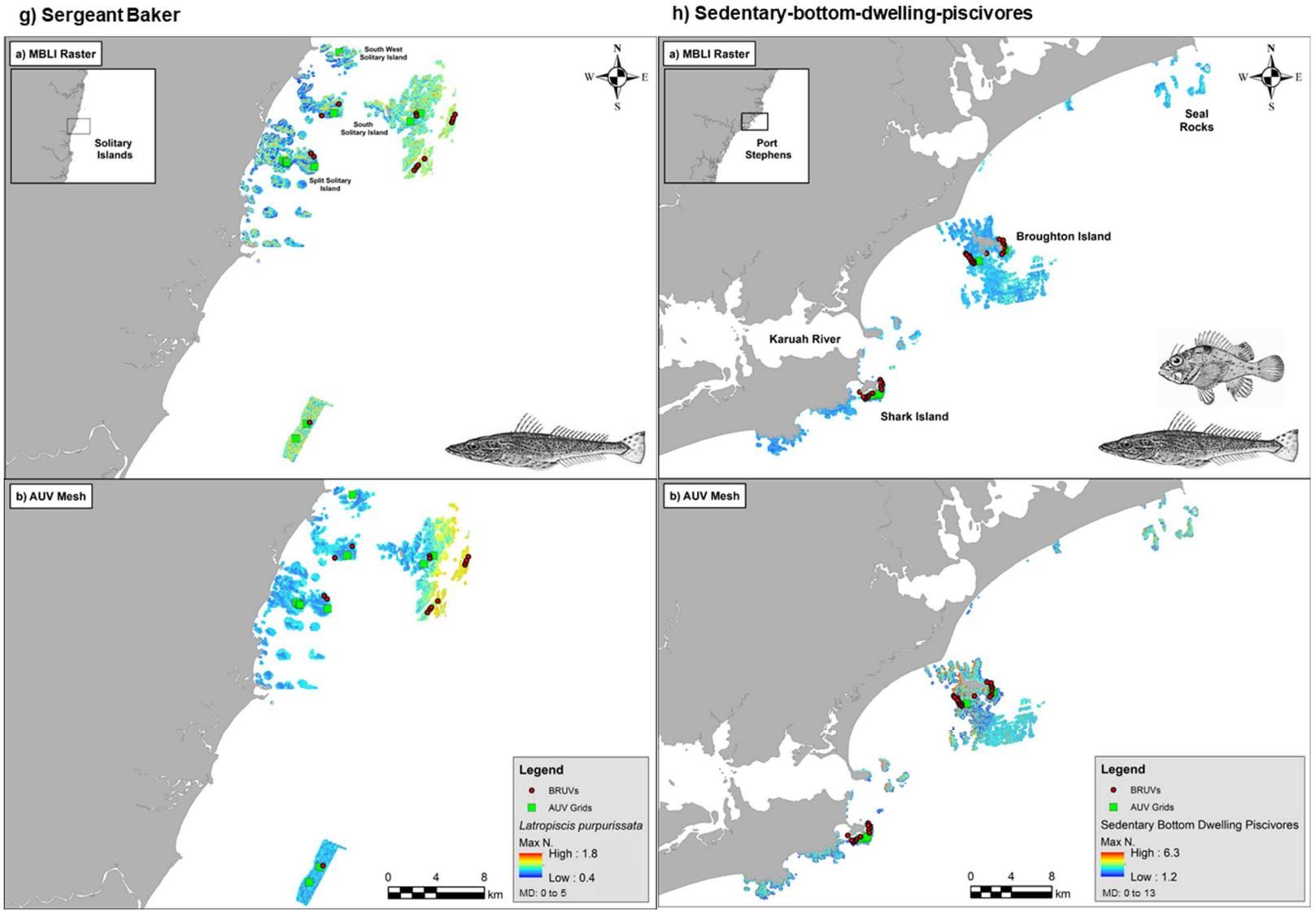

Figure 5-7 continued. Species distribution models for g) Sergeant Baker in the Solitary Islands and sedentary-bottom-dwelling-piscivores at Port Stephens based on MBLI Raster predictors (top) and AUV Mesh predictors (bottom). Model domain (MD) was the range of abundance values in the fish dataset.

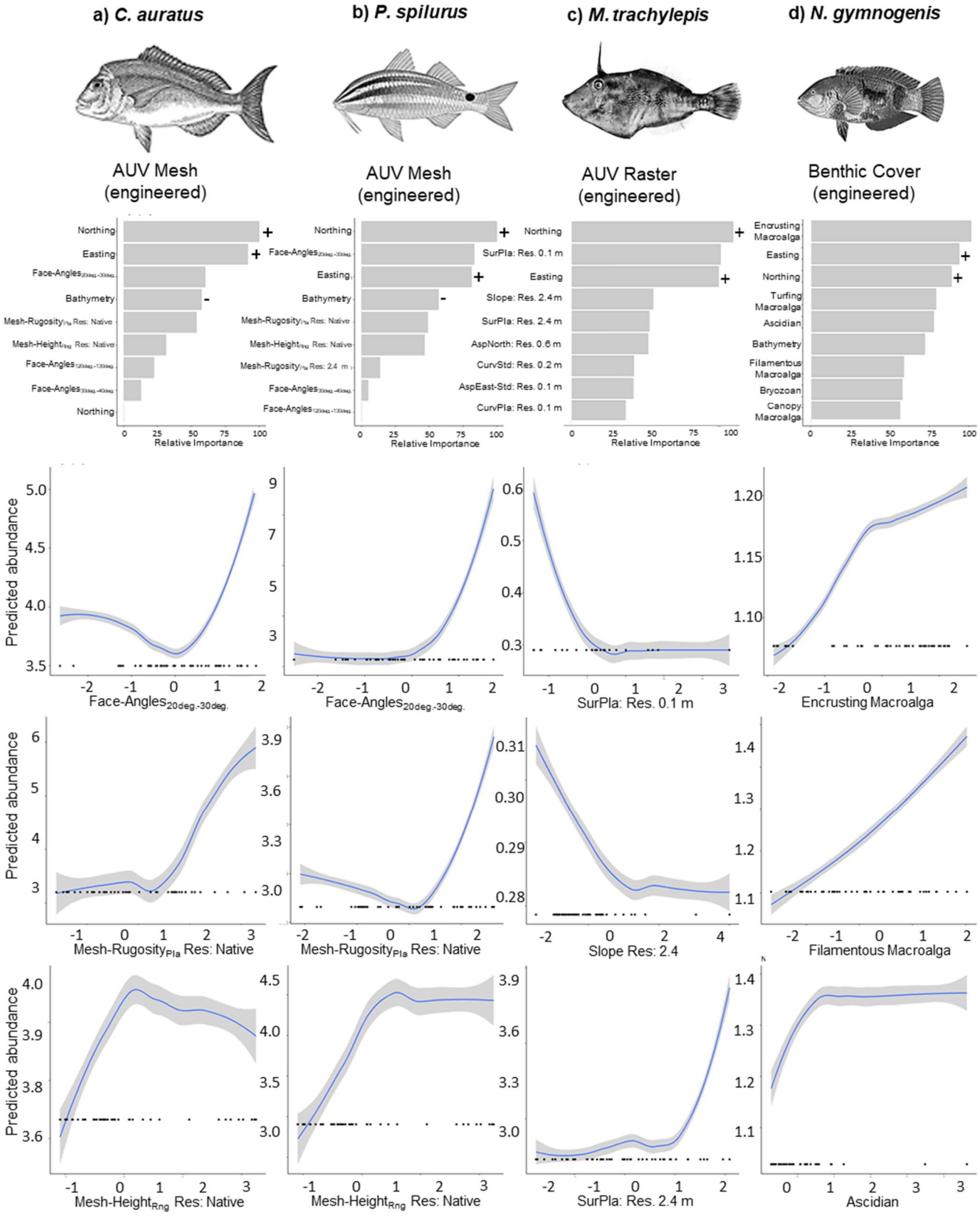

Figure 5-8 **Relative importance of predictors included in random forest models of fish abundance and associated partial dependance plots (PDPs) of the three most important metrics of complexity. Positive and minus signs indicate overall relationships with depth, easting and northing.**

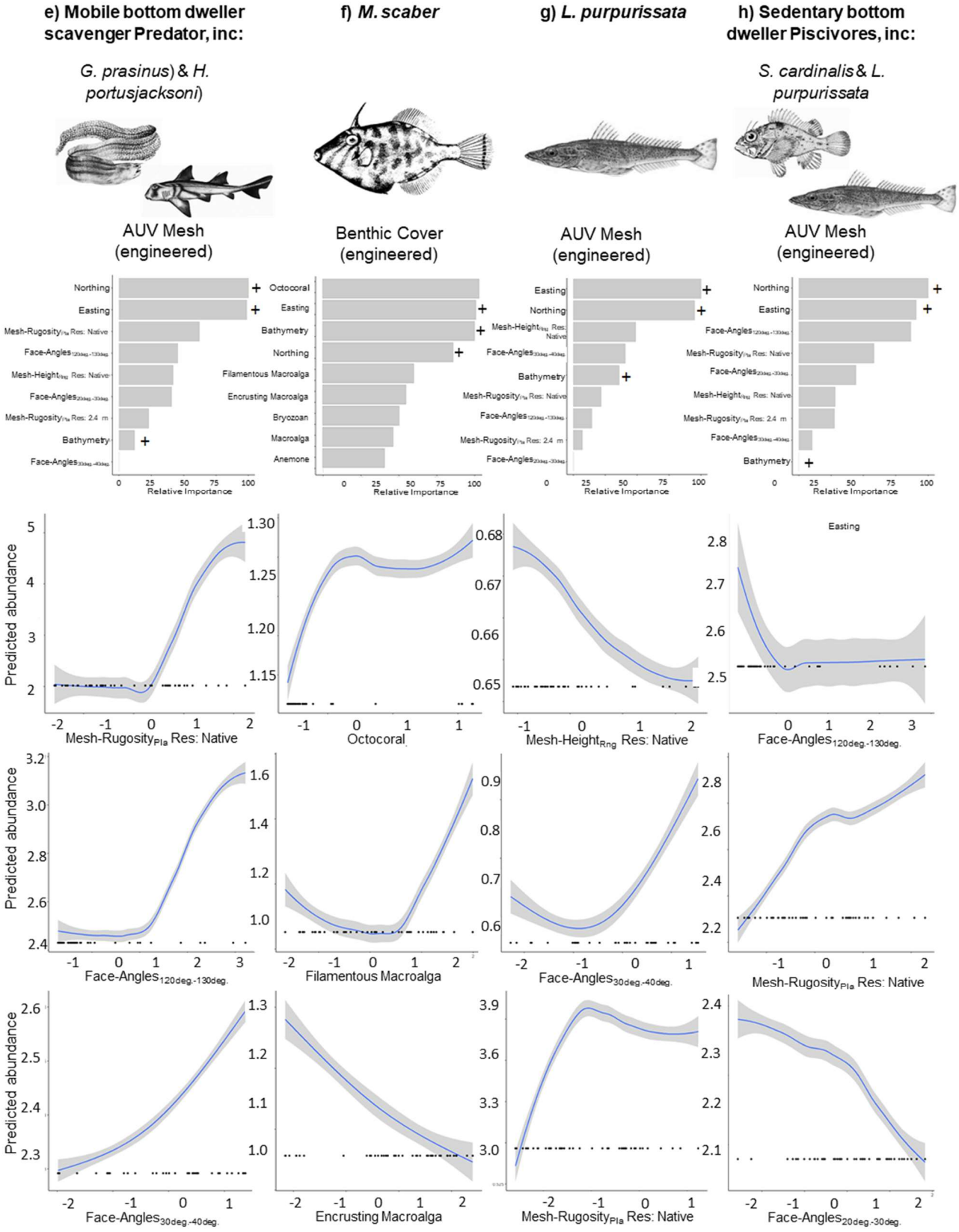

Figure 5-8 **Continued: Relative importance of predictors included in random forest models of fish abundance and associated partial dependance plots (PDPs) of the three most important metrics of complexity. Positive and minus signs indicate overall relationships with depth, easting and northing.**

though for *L. purpurissatus*, the greater abundance offshore appeared more noticeable in AUV Mesh models. Sedentary-bottom-dwelling-piscivores were predicted as more abundant on western facing reef to the north, and to a lesser degree to the south, of Broughton Island (Figure 5-7**h**, **Figure 5-8h**) and mostly likely associated with smaller Face-Angles$_{20deg.-30deg.}$ on this reef (**Appendix 5-6c**).

5.5 Discussion

This study described a novel approach to improving broad-scale predictions of fish species distributions on the NSW coastline using spatially limited photogrammetric data. First, it described a method to derive approximations of photogrammetric metrics using traditionally derived metrics of structural complexity. These 'engineered' metrics were derived across broad spatial extents unobtainable using existing methods and technology. Predictions of the cover of benthic organisms were also obtained using this procedure and provided further contiguous broad-scale predictors of fish abundance. Second, it demonstrated how these engineered predictors can improve predictions of the distribution of several fish species on nearshore rock reef habitats and provide potentially important insights into species distributions that may otherwise have gone unnoticed. Pending ground-truthing of these predictions via further direct fish surveys, these findings and similar procedures have the potential to provide an important contribution to the management and conservation of fish and other marine biota on the NSW coastline.

5.5.1 Predictor Engineering

The variance explained by ML models of AUV Mesh and AUV Raster metrics was variable, though for several metrics (including mesh-based height range and rugosity and raster-based slope and aspect-north) it was relatively large (> 0.50). Unsurprisingly, AUV Raster orientation metrics were predicted best using orientation metrics derived from MBLI Raster. Notably, AUV Raster-based metrics of curvature were both predicted poorly and did not contribute greatly to the prediction of any other metrics. This may reflect the apparent uniqueness of structural complexity captured by these metrics (**Section 3** and Fukunaga & Burns., 2020), and their relatively greater sensitivity to variation in extent and resolution. The difficulty in predicting mesh-based face-angle metrics could also be expected given the inherent differences between the more realistic 3D mesh and simpler 2.5D raster-based bathymetric reconstructions. The relatively large proportion of variation explained by GAM models of benthic cover was comparable, and on occasion slightly greater than, that observed in other similar studies. Those most comparable (in terms of taxa, methods and

location) include the modelling of canopy and encrusting algae, sponge and gorgonian, sea whip and soft coral octocorals of the Tasmanian southeast coast by Hill *et al*., (2014) and sessile invertebrate taxonomic richness, abundance and% cover in Batemans Bay by Rees *et al*., (2014). The variance explained in these studies, between 0.20 and 0.69 for invertebrates, and between 0.19 and 0.69 for algae, was comparable to that explained here. Bathymetry and geographic predictors (e.g., distance to sand / reef) tended to outperform measures of structural complexity in previous studies. In this study, bathymetry was an important contributor to some groups, though metrics of complexity, particularly those based on orientation, were more important in predicting/explaining benthic biota prevalence.

The creation of 'engineered' metrics could be described as 'guiding' modelling approaches towards selecting the most ecologically relevant MBLI Raster predictor(s). Assuming the photogrammetric metrics are themselves ecologically important, as the findings of **Section 3** and of other recent studies (**Section 1**) suggest, such an approach would help identify the best performing models of fish abundance. The concurrent creation of broad-extent photogrammetric predictor datasets, albeit approximations, will go some way to helping solve bottlenecks associated with the lack of resolution in MBLI methods and the prohibitive cost of acquiring broad-scale photogrammetric datasets . Of key importance is that most of the engineered predictors were not highly correlated with the individual MBLI Raster predictors. That is, most engineered predictors were not simply the same MBLI Raster predictors just by another name. Rather, they provide additional ecologically relevant information on structural complexity and benthic biota prevalence not provided directly by the original MBLI Raster predictors. This provides important credence to the process of deriving these predictors in such a way.

Nevertheless, there are some limitations to the method of engineering predictors described here. Curvature-based metrics were generally not predicted well, but that they otherwise appear to capture relatively unique and often ecological important components of structural complexity (**Section 3**, **Section 4**, Fukunaga & Burns, (2020)), is one such limitation. Although engineered predictors often performed well, they would not be expected to provide exact representations of the metrics otherwise obtained via direct photogrammetric survey. For curvature-based and other poorly predicted metrics, there may be no effective substitute to direct survey. A further important consideration is that none of the predictors or modelling undertaken here includes MBLI Raster predictors derived over spatial extents with a window size greater than 30 m side length. If all MBLI Raster metrics had been included, they would require individual calculation for each 30 m x 30 m cell to

create the contiguous predicted raster surfaces for the SDMs. The time required to do this for each of the several 10s thousands of raster cells was prohibitive for this study. However, the inclusion of broader-scale MBLI Raster predictors could have resulted in more realistic engineered predictors and better performing models of fish abundance.

5.5.2 Engineered Predictor Performance

Over half (26 of 47) of the species and groups considered in this study demonstrated a relatively clear preference for engineered predictors over MBLI derived predictors (i.e., all three engineered predictor sets performed better than MBLI Raster predictors). Engineered predictors overall also tended to explain slightly more variance in fish abundance compared to MBLI Raster predictors. These findings support the expectation that photogrammetric metrics can enhance predictions of fish abundance. In this study, mesh-based metrics also generally performed better than those based on benthic cover and (photogrammetrically derived) raster-metrics. This includes mesh-derived metrics analogous to traditional raster-based metrics (e.g., mesh-based rugosity and height range) and novel mesh-based face-angle metrics. Given that all metrics were derived over a similar area (625 m^2 to 900 m^2) this limited any confounding influence of variable spatial extent, suggesting the finer resolutions afforded by photogrammetry was a key contributor to their predictive performance. The overall better performance of AUV Mesh predictors compared AUV Raster predictors also suggests that metrics are more ecologically relevant when derived from mesh surfaces, at least along the coastline of NSW and at the relatively small spatial extent considered here. Engineered benthic cover predictors overall performed poorer than expected given the relatively large amount of variation explained by the models from which they were generated, and given the high efficacy of benthic cover as predictors of fish abundance by Ferrari, *et al*., (2018).

As discussed in Chapter 4, at least part of the better performance of (in the case of Chapter 5, engineered) photogrammetrically derived metrics could be explained by the finer resolutions achievable using this methodology compared to traditionally derived metrics. Thus, using traditional methods that can provide finer resolutions (e.g., 0.1 m to 2.4 m) may be one option to improving predictions in other studies without the need for more costly (per unit area) photogrammetry methods. However, at least part of the better performance of AUV Mesh predictors in this Chapter also appeared associated with deriving them from a mesh-based surface. This was the case for mesh-based metrics for which analogous raster-based metrics were also available (e.g., those based on rugosity) and novel mesh-based metrics for which an analogous raster-based metric was not available (e.g., face angles).

Thus, while finer resolution traditionally-derived bathymetric reconstructions may provide some of improvement in model performance noted for photogrammetrically derived metrics in this study, a more realistic 3D reconstruction from photogrammetry may be required to achieve the best overall performance.

5.5.3 Patterns in Fish Responses

As identified in earlier studies (Cameron *et al*., 2014; Ferrari, Malcolm, Neilson, *et al*., 2018; Monfort *et al*., 2021) the response of fish to metrics of structural complexity is group and species specific. Attempting to identify broad patterns in fish responses to structural complexity metrics was difficult given the often-low explained variance, which hindered the confident identification of relationships with fish abundance. Regardless, some consistent responses of fish could be identified. Most bottom dwellers, particularly sedentary-bottom-dwelling-piscivores (primarily *S. cardinalis* and *L. purpurissatus*), *P. spilurus* (which comprised the majority of mobile-bottom-dwelling-benthic invertivores and sediment-infauna-predators) and mobile-bottom-dwelling-scavenger-predators (primarily *G. prasinus* and *H. portusjacksoni*), were predicted best using engineered AUV Mesh and AUV Raster metrics. All these fish are seafloor-associated, and it is not surprising they were more strongly associated with metrics derived using photogrammetry at finer resolutions (~0.05 m to 2.4 m) than the coarser resolution (5 m and 30 m) MBLI Raster predictors. Metrics derived at these finer resolutions would be expected to capture variability more accurately in structural complexity more commensurate with these fish body sizes, that of their prey and their habitat refugia. Thereby providing important surrogates of refuge density and other components of local-scale habitat suitability, such as hydrodynamic flow and habitat type (for example local variability in low complexity patches of sand and high complexity reef). Thus, these results suggest metrics derived at this spatial extent and resolution are representative of the relevant ecological seascape for these trophic-mobility groups and the species that belong to them.

Planktivore groups (midwater-planktivores, sedentary-bottom-dwelling-planktivores, and all planktivores combined) also displayed a consistent response, with MBLI Raster predictors tending to be most influential. Considering all metrics were derived over comparable spatial extents, this suggests a linkage with the coarser resolution of the MBLI Raster predictors. The importance larger scale components of structural complexity for planktivores been noted previously, with Champion *et al*., (2015) linking changes in artificial reef size on the scales of 10s of meters with density of the midwater-planktivore *A. strigatus*. In this study, *A. strigatus* was best modelled when AUV Mesh and MBLI Raster predictors

were combined, though at group-level midwater-planktivores were modelled best solely using MBLI Raster predictors. Modelling by Champion *et al*., (2015) suggested a complex relationship between *A. strigatus* abundance and reef size, via its influence on the relative availability of fish refuge and foraging area (and thus zooplankton food density). As reef size increased, so did fish refuge availability, but the rate of increase in foraging area and zooplankton density did not keep pace. Other studies have also linked planktivore abundance with large vertical structures, albeit artificial, via the protection these provide from predation and their influence on water flow and associated food availability and recruitment processes (Rilov & Benayahu, 2002; Rilov & Benayahub, 1998; Rountree, 1989; Wilhelmsson, Yahya, *et al*., 2006; Wilhelmsson *et al*., 1998).

In the case of predator-prey interactions, some planktivores and other species that tend to escape predation by schooling or flight, rather than seeking refuge directly within the habitat structure, might be expected to be more response to larger components of structural complexity and how these affect their ability to sight approaching piscivores. Despite being more seafloor associated, sedentary-bottom-dwelling-planktivores were also modeled best using MBLI Raster predictors. Unlike midwater-planktivores, these more seafloor associated species tend to be territorial with small home range sizes, however, the importance of visual field for piscivore sighting has also been documented for such species. Rilov *et al*., (2007) experimentally manipulated the visual field of the sedentary-planktivore bicolor damselfish (*Stegastes partitus*) and found males were associated with areas with greater area of local visual field (viewshed). Although involving a tropical species, and manipulation of viewshed within relatively small scales of 1 metre, this does indicate the importance of visual field to these fish. Viewshed at greater spatial scale would also be important. (González-Rivero *et al*., 2017) found viewshed (captured using photogrammetry) at a scale of 25 m^2 was negatively correlated with the abundance of the sedentary-planktivore blue chromis (*Chromis cyanea*). That is, as the reef became more visually exposed the abundance of *C. cyanea* decreased. Thus, viewshed may influence fish abundance via different mechanisms.

The key role of spatial resolution and extent in mediating structural complexity and fish abundance relationships was evident in this study and worth noting, especially given the relatively narrow resolution range of the engineered predictors. As one example, *M. trachylepis* was associated with greater surface-planar-area at a resolution of 2.4 m but with smaller values of this metric when derived at resolution of 0.1 m. Such divergent responses of species to the same metric derived over different resolutions (and / or spatial scales) appear ubiquitous and was evident in the separate fish dataset in **Section 3**, as well as

several earlier studies (reviewed in **Section 2**). Many metrics, including surface-planar-area, also appeared most sensitive to change in resolution and extent at the smaller end of their ranges (**Section 3.4**). This further reinforces the need to consider multiple spatial extents and resolutions, and probably more so at the smaller end of the range, when using metrics of structural complexity model abundance and distribution of fish (and likely most other marine biota). This study also further confirms the importance of including related predictors bathymetry and geographic location, in this case easting and northing, with or more of these retained in the top three most important predictors of the 8 species and groups examined in detail. This was also noted in the Solitary Islands by Ferrari, *et al*., (2018), with bathymetry and geographic predictors also identified as the most important predictors overall in the meta-analysis in **Section 2**.

5.5.4 Fish Distributions

SDMs based on engineered predictors provided potential key insights into broad-scale fish distributions along the NSW coast that might otherwise have gone unnoticed if only MBLI metrics had been available. Notably the greater abundance of *C. auratus*, *P. spilurus*, *N. gymnogenis*, and to some degree *M. trachylepis*, on reef inshore of Broughton Island, and greater abundance of *C. auratus* on coastal reef southwest of Shark Island stood out. It appears that these areas provide reef of greater fine-scale variability captured better by AUV Mesh metrics than by MBLI Raster metrics that is important to *C. auratus* and *P. spilurus*, both of which are bottom associated. Possibly this is related to greater availability of preferred refuge or feeding habitat. In the case of *M. trachylepis*, AUV Raster appears better able to capture areas of reef that is more rugose at a resolution of 2.4 m, but not 0.1 m, and with reduced slope. Benthic cover, and specifically the greater abundance of macroalgae and ascidians, also appears to be more important for *N. gymnogenis* than are metrics of complexity captured by MBLI Raster, on these areas of reef.

Recently modelling by Rees *et al*., (2021) found that although adult *C. auratus* were more strongly and negatively associated with human population density than bathymetric range and habitat type (e.g., reef, sand, benthic cover), juveniles were more abundant on coastal reef closer to estuaries. If the inshore and coastal reefs provide favorable habitat for *C. auratus* as predicted by the SDMs, they could provide important connectivity between potential nursery habitat within Karuh River estuary and coastal and offshore reef to the north and south. Juvenile *C. auratus* would migrate from estuaries to deeper reef as they mature (Curley *et al*., 2013; Gillanders, 2002; Parsons *et al*., 2014). The presence of suitable coastal reef close to the Karuh River estuary could provide important habitat connectivity

between the estuary and other coastal and deeper reef offshore and reduce the time juveniles spend moving across open areas of sand where they would likely be at greater risk of predation . Pending field validation, these reef areas could be of conservation importance for *C. auratus* and potentially other species such as *P. spilurus*, *N. gymnogenis*, and *M. trachylepis*.

None of the engineered predictors included in the SDMs appeared particularly influential across multiple species or groups. Rather, differences in habitat suitability as indicated by the SDMs were associated with combined effect of multiple metrics of structural complexity and benthic cover. As bathymetry, easting and northing were included in each final model, it is unlikely these explained the differences in model performance and predictions of abundance between the competing models.

5.6 Conclusion

As demonstrated in this chapter, in **Section 4** and in several similar studies on coral reefs (Bayley *et al*., 2019; Collins *et al*., 2017; Fukunaga, Kosaki, *et al*., 2020; González-Rivero *et al*., 2017b; Streit *et al*., 2021) and temperate rock reefs (Ferrari, Malcolm, Byrne, *et al*., 2018; Monfort *et al*., 2021b; Taylor & Figueira, 2021), photogrammetrically derived metrics of structural complexity provide important predictors of the abundance of rock reef and coral associated fish. In this study specifically, approximately 50% of the SDMs of fish species / groups, many of recreational, commercial and / or conservation importance, benefit from the inclusion of these metrics. This has real-world implications for SDMs used to inform management of these fish, spatial prioritisation and MPA re-zoning (Ferrari, *et al*., 2018). These findings support the expected important role of finer resolutions and metrics derived from more realistic 3D mesh-based reconstruction of the seafloor for improving model performance. Finer resolutions and mesh-based metrics appear able to capture ecologically relevant components of structural complexity not captured by traditional remote sensing and associated metrics. As photogrammetric methods continue to mature, additional novel metrics of structural complexity are likely to be identified that can provide further improvement of explanatory models linking structural complexity with fish abundance.

Although photogrammetry provides great potential for exploring local-scale variability in structural complexity and fish abundance, methodological limitations mean that it is unlikely to ever compete with the broad-scales achievable using traditional remote sensing methods. This is likely to represent an ongoing limitation to the application of photogrammetry and a limit to its ability to capture important broad-scale structuring gradients operating over areas

greater than approximately 10,000 m^2. The ability to collect broad-scale finer (< 5 m) resolution bathymetric reconstructions than available for this thesis would likely go some way to achieving some of the improved model performance demonstrated for photogrammetrically derived metrics. However, improved model performance was also partly related to the availability of traditional and novel metrics derived from 3D mesh surfaces. The method of engineering of photogrammetric metrics from broad-scale traditional multibeam datasets as additional broad-extent predictors of fish distributions provide a useful alternative to otherwise prohibitively expensive collection of photogrammetric data across broad spatial extents. In particular, benthic cover, which provides an important predictor of fish abundance, was extrapolated well across large extents using MBLI Raster metrics and provided valuable contribution to models of fish abundance. As demonstrated here, even though these engineered metrics represent approximations of the true values, they improve modelling outcomes and help close the gap between local-scale photogrammetric and the equally important broad-scale traditional remote sensing methods. It is possible also that the inclusion of broad-scale bathymetric reconstructions from satellite data may further improve the extrapolation of such engineered metrics over areas suitable for SDMs and their various uses.

5.7 Appendices

Appendix 5-1 Abundance of fish species and groups considered in this study across all sites. Grey shading indicates species and groups modelled individually. Note, fish counts were averaged across survey years at each site before being summarised across sites.

Species / Group	Sum	Mean	SE	Occ.	Trophic Group	Trophic-mobility Group
Chrysophrys auratus	246.67	3.47	0.47	65	Predator	Mobile-bottom-dweller-predator
Ophthalmolepis lineolata	346.83	4.88	0.42	62	Predator	Mobile-bottom-dweller-predator
Nemadactylus douglasii	83.83	1.18	0.15	61	Predator	Mobile-bottom-dweller-predator
Parma microlepis	71.83	1.01	0.09	58	Herbivore	Sedentary-bottom-dweller-herbivore
Meuschenia freycineti	112.17	1.58	0.19	56	Predator	Midwater-predator
Notolabrus gymnogenis	81.83	1.15	0.10	56	Predator	Mobile-bottom-dweller-predator
Hypoplectrodes maccullochi	67.83	0.96	0.10	54	Predator	Sedentary-bottom-dweller-predator
Scorpis lineolata	407.00	5.73	1.53	52	Planktivore	Midwater-planktivore
Scorpaena cardinalis	74.83	1.05	0.11	49	Piscivore	Sedentary-bottom-dweller-piscivore
Atypichthys strigatus	846.83	11.93	1.95	49	Planktivore	Midwater-planktivore
Gymnothorax prasinus	72.50	1.02	0.14	49	Predator	Mobile-bottom-dweller scavenger-predator
Latropiscis purpurissatus	53.17	0.75	0.12	48	Piscivore	Sedentary-bottom-dweller-piscivore
Heterodontus portusjacksoni	63.00	0.89	0.13	38	Predator	Mobile-bottom-dweller scavenger-predator
Achoerodus viridis	29.50	0.42	0.06	37	Predator	Mobile-bottom-dweller-predator
Pseudocaranx georgianus	119.83	1.69	0.38	36	Planktivore	Midwater-planktivore
Meuschenia scaber	68.50	0.96	0.19	35	Predator	Midwater-predator
Parupeneus spilurus	279.17	3.93	0.76	35	Sediment-infauna-predator	Mobile-bottom-dweller-benthic-invertivore
Enoplosus armatus	53.83	0.76	0.27	34	Predator	Midwater-predator
Upeneichthys lineatus	24.83	0.35	0.05	34	Sediment-infauna-predator	Mobile-bottom-dweller-benthic-invertivore
Cheilodactylus fuscus	27.67	0.39	0.07	33	Predator	Sedentary-bottom-dweller-predator
Trachurus novaezelandiae	307.00	4.32	1.38	25	Planktivore	Midwater-planktivore
Chromis hypsilepis	604.50	8.51	2.55	24	Planktivore	Midwater-planktivore
Coris picta	91.00	1.28	0.55	24	Predator	Mobile-bottom-dweller-predator
Acanthistius ocellatus	21.17	0.30	0.07	23	Piscivore	Sedentary-bottom-dweller-piscivore
Meuschenia trachylepis	21.67	0.31	0.06	23	Predator	Midwater-predator
Bodianus unimaculatus	38.50	0.54	0.14	21	Predator	Mobile-bottom-dweller-predator
Eubalichthys bucephalus	21.50	0.30	0.10	19	Predator	Midwater-predator

Species / Group	Sum	Mean	SE	Occ.	Trophic Group	Trophic-mobility Group
Pseudocaranx dentex	18.67	0.26	0.10	15	Piscivore	Midwater-piscivore
Lotella rhacina	13.67	0.19	0.07	15	Piscivore	Sedentary-bottom-dweller-piscivore
Rhabdosargus sarba	22.50	0.32	0.13	14	Predator	Mobile-bottom-dweller-predator
Mecaenichthys immaculatus	10.83	0.15	0.04	14	Predator	Sedentary-bottom-dweller-predator
Nelusetta ayraud	25.50	0.36	0.12	14	Predator	Sedentary-bottom-dweller-predator
Caesioperca lepidoptera	46.50	0.65	0.33	13	Planktivore	Midwater-planktivore
Meuschenia venusta	12.17	0.17	0.06	13	Predator	Midwater-predator
Gymnothorax prionodon	26.50	0.37	0.12	13	Predator	Mobile-bottom-dweller scavenger-predator
Chelmonops truncatus	34.83	0.49	0.25	13	Predator	Sedentary-bottom-dweller-predator
Eubalichthys mosaicus	7.00	0.10	0.03	12	Predator	Midwater-predator
Brachaelurus waddi	7.00	0.10	0.03	12	Predator	Mobile-bottom-dweller scavenger-predator
Seriola lalandi	15.17	0.21	0.07	11	Piscivore	Midwater-piscivore
Atractoscion aequidens	99.50	1.40	0.50	11	Piscivore	Mobile-bottom-dweller-piscivore
Dasyatis brevicaudata	5.50	0.08	0.02	11	Sediment-infauna-predator	Mobile-bottom-dweller-benthic-invertivore
Epinephelus undulatostriatus	10.17	0.14	0.05	10	Piscivore	Sedentary-bottom-dweller-piscivore
Trachinops taeniatus	71.00	1.00	0.37	10	Planktivore	Sedentary-bottom-dweller-planktivore
Bodianus frenchii	11.17	0.16	0.06	10	Predator	Mobile-bottom-dweller-predator
Pempheris compressa	32.17	0.45	0.34	9	Planktivore	Sedentary-bottom-dweller-planktivore
Meuschenia flavolineata	10.00	0.14	0.05	9	Predator	Midwater-predator
Lutjanus adetii	5.00	0.07	0.03	8	Predator	Mobile-bottom-dweller-predator
Myliobatis australis	4.00	0.06	0.02	8	Sediment-infauna-predator	Midwater benthic invertivore
Prionurus microlepidotus	9.33	0.13	0.09	7	Herbivore	Mobile-bottom-dweller-herbivore
Dinolestes lewini	137.33	1.93	1.80	7	Piscivore	Midwater-piscivore
Sarda australis	4.00	0.06	0.02	7	Piscivore	Midwater-piscivore
Anoplocapros inermis	3.17	0.04	0.02	7	Predator	Midwater-predator
Choerodon venustus	6.00	0.08	0.03	7	Predator	Mobile-bottom-dweller-predator
Lutjanus russellii	4.33	0.06	0.02	7	Predator	Mobile-bottom-dweller-predator
Parma unifasciata	6.00	0.08	0.04	5	Herbivore	Sedentary-bottom-dweller-herbivore
Trygonorrhina fasciata	2.67	0.04	0.02	5	Sediment-infauna-predator	Mobile-bottom-dweller-benthic-invertivore
Aplodactylus lophodon	1.50	0.02	0.01	4	Herbivore	Sedentary-bottom-dweller-herbivore
Orectolobus ornatus	1.50	0.02	0.01	4	Predator	Mobile-bottom-dweller scavenger-predator

Species / Group	Sum	Mean	SE	Occ.	Trophic Group	Trophic-mobility Group
Parapercis ramsayi	39.00	0.55	0.48	4	Predator	Sedentary-bottom-dweller-predator
Pempheris affinis	2.00	0.03	0.02	3	Planktivore	Sedentary-bottom-dweller-planktivore
Chaetodon guentheri	4.00	0.06	0.04	3	Predator	Midwater-predator
Meuschenia sp.	1.67	0.02	0.02	3	Predator	Midwater-predator
Bodianus perditio	1.17	0.02	0.01	3	Predator	Mobile-bottom-dweller-predator
Orectolobus maculatus	1.00	0.01	0.01	3	Predator	Mobile-bottom-dweller scavenger-predator
Hypoplectrodes annulatus	2.00	0.03	0.02	3	Predator	Sedentary-bottom-dweller-predator
Hypoplectrodes nigroruber	2.00	0.03	0.02	3	Predator	Sedentary-bottom-dweller-predator
Siganus fuscescens	1.33	0.02	0.01	2	Herbivore	Mobile-bottom-dweller-herbivore
Seriola hippos	1.33	0.02	0.01	2	Piscivore	Midwater-piscivore
Dicotylichthys punctulatus	1.00	0.01	0.01	2	Predator	Midwater-predator
Pseudolabrus guentheri	1.33	0.02	0.01	2	Predator	Mobile-bottom-dweller-predator
Orectolobus halei	1.00	0.01	0.01	2	Predator	Mobile-bottom-dweller scavenger-predator
Austrolabrus maculatus	1.33	0.02	0.01	2	Predator	Sedentary-bottom-dweller-predator
Canthigaster callisterna	1.67	0.02	0.02	2	Predator	Sedentary-bottom-dweller-predator
Epinephelus fasciatus	0.33	0.00	0.00	1	Piscivore	Sedentary-bottom-dweller-piscivore
Paracaesio xanthura	1.00	0.01	0.01	1	Planktivore	Midwater-planktivore
Solegnathus spinosissimus	1.00	0.01	0.01	1	Predator	Sedentary-bottom-dweller-predator
Predator	1661.83	23.41	1.51	71		
Piscivore	449.33	6.33	1.92	69		
Planktivore	2437.83	34.34	4.55	64		
Midwater-predator	316.67	4.46	0.49	69		
Midwater-planktivore	2332.67	32.85	4.44	64		
Sedentary-bottom-dweller-predator	188.17	2.65	0.53	62		
Mobile-bottom-dweller-scavenger-predator	172.50	2.43	0.23	68		
Sedentary-bottom-dweller-piscivore	173.33	2.44	0.24	66		
Mobile-bottom-dweller-predator	984.50	13.87	1.00	71		
Herbivore	90.00	1.27	0.13	62		
Sedentary-bottom-dweller-Herbivore	79.33	1.12	0.09	62		
Sediment-infauna-predator	316.17	4.45	0.78	56		
Mobile-bottom-dweller-benthic-invertivore	312.17	4.40	0.78	53		

Species / Group	Sum	Mean	SE	Occ.	Trophic Group	Trophic-mobility Group
Midwater-piscivore	176.50	2.49	1.80	35		
Sedentary-bottom-dweller-planktivore	105.17	1.48	0.49	19		

Appendix 5-2 AUV Raster and AUV Mesh metrics modelled from MBLI Raster predictors using ML techniques. Metres (m) after each metric indicate the resolution (Res) over which it was derived. ResNative = native mesh resolution (0.03 m to 0.07 m). All were derived at a spatial extent of 30 m x 30 m. See Table 3-1 for description of each metric.

AUV Mesh / AUV Raster Metric	RMSE	R Squared	ML Technique
Mesh-Height$_{Rng_}$ResNative	1.03	0.74	Regularised Random Forest
Slope_Res2.4m	1.94	0.73	Support Vector Machine Polynomial
AspNorth_Res0.6m	0.09	0.63	Regularised Random Forest
Mesh-Rugosity$_{Pla_Res}$2.4m	0.02	0.54	Support Vector Machine Polynomial
SurPla_Res2.4m	0.00	0.46	Support Vector Machine Radial
AspEast_Res0.1m	0.06	0.45	Support Vector Machine Polynomial
AspEast-std_Res2.4m	0.08	0.42	Regularised Random Forest
AspNorth-std_Res2.4m	0.07	0.39	Regularised Random Forest
Slope_Res0.1m	2.46	0.38	Regularised Random Forest
Mesh-Rugosity$_{Pla}$ ResNative	0.07	0.36	Regularised Random Forest
Face-Angles$_{120deg.-130deg.}$ ResNative	0.00	0.33	Regularised Random Forest
AspEast-std_Res0.1m	0.03	0.32	Regularised Random Forest
CurvPla_Res0.1m	14.54	0.29	Support Vector Machine Polynomial
AspNorth-std_Res0.1m	0.03	0.24	Regularised Random Forest
CurvPla_Res0.6m	1.81	0.18	Support Vector Machine Radial
CurvStd_Res0.6m	0.00	0.17	Regularised Random Forest
Face-Angles$_{20deg.-30deg._}$ResNative	0.02	0.16	Random Forest
CurvPla_Res2.4m	0.47	0.14	Support Vector Machine Polynomial
CurvStd_Res0.2m	0.00	0.11	Regularised Random Forest
Face-Angles$_{30deg.-40deg._}$ResNative	0.02	0.09	Regularised Random Forest
SurPla_Res0.1m	0.01	0.08	Regularised Random Forest

Appendix 5-3 Benthic cover modelled from MBLI Raster predictors using GAM models. Metres (m) after each metric indicate the resolution over which it was derived. All were derived at a spatial extent of 30 m x 30 m.

Benthic Cover	R^2	Final Model
Canopy macroalga	0.87	AspEast_Res30m + AspNorth_Res5m + Northing + SurPla-std_Res5m + TerRug_Res30m
Octocoral	0.78	AspEast_Res30m + AspEast-std_Res5m + AspNorth_Res30m + Bath_Res5m +
Ascidian	0.66	AspEast_Res30m + AspNorth_Res30m + Bath-std_Res5m + Northing
Hydroid	0.62	AspEast_Res30m + AspNorth_Res30m + Northing + SurPla_Res30m + SurPla-std_Res5m
Turfing macroalga	0.62	AspEast_Res5m + AspNorth_Res5m + Northing + SurPla-std_Res5m + TerRug_Res30m
Branching	0.61	AspEast_Res30m + AspEast-std_Res5m + AspNorth_Res5m + Northing + SurPla_Res30m
Stony Coral	0.57	AspEast_Res30m + AspNorth_Res30m + AspNorth-std_Res5m + Bath_Res5m +
Sponges	0.55	AspEast_Res30m + AspEast-std_Res5m + Northing + SurPla_Res30m + SurPla-std_Res5m
Macroalga	0.55	AspEast_Res30m + AspEast-std_Res5m + Northing + SurPla_Res30m + SurPla-std_Res5m
Anemone	0.51	AspEast_Res30m + AspEast-std_Res5m + AspNorth_Res5m + Bath_Res5m +
Calcareous	0.51	AspEast_Res30m + AspEast-std_Res5m + AspNorth-std_Res5m + SurPla_Res30m + SurPla-
Echinoderms	0.50	AspEast_Res5m + AspNorth_Res5m + Bath-std_Res5m + CurvPro_Res5m
Filamentous	0.47	AspEast_Res30m + AspEast-std_Res5m + AspNorth_Res5m + Northing + SurPla_Res30m
Bryozoan	0.46	AspEast_Res5m + AspNorth-std_Res5m + Bath_Res5m + SurPla_Res30m + SurPla-
Encrusting	0.45	AspEast_Res30m + AspEast-std_Res5m + AspNorth_Res30m + Bath_Res5m +

Appendix 5-4 Correlations among engineered AUV predictors and MBLI Raster predictors used to predict them

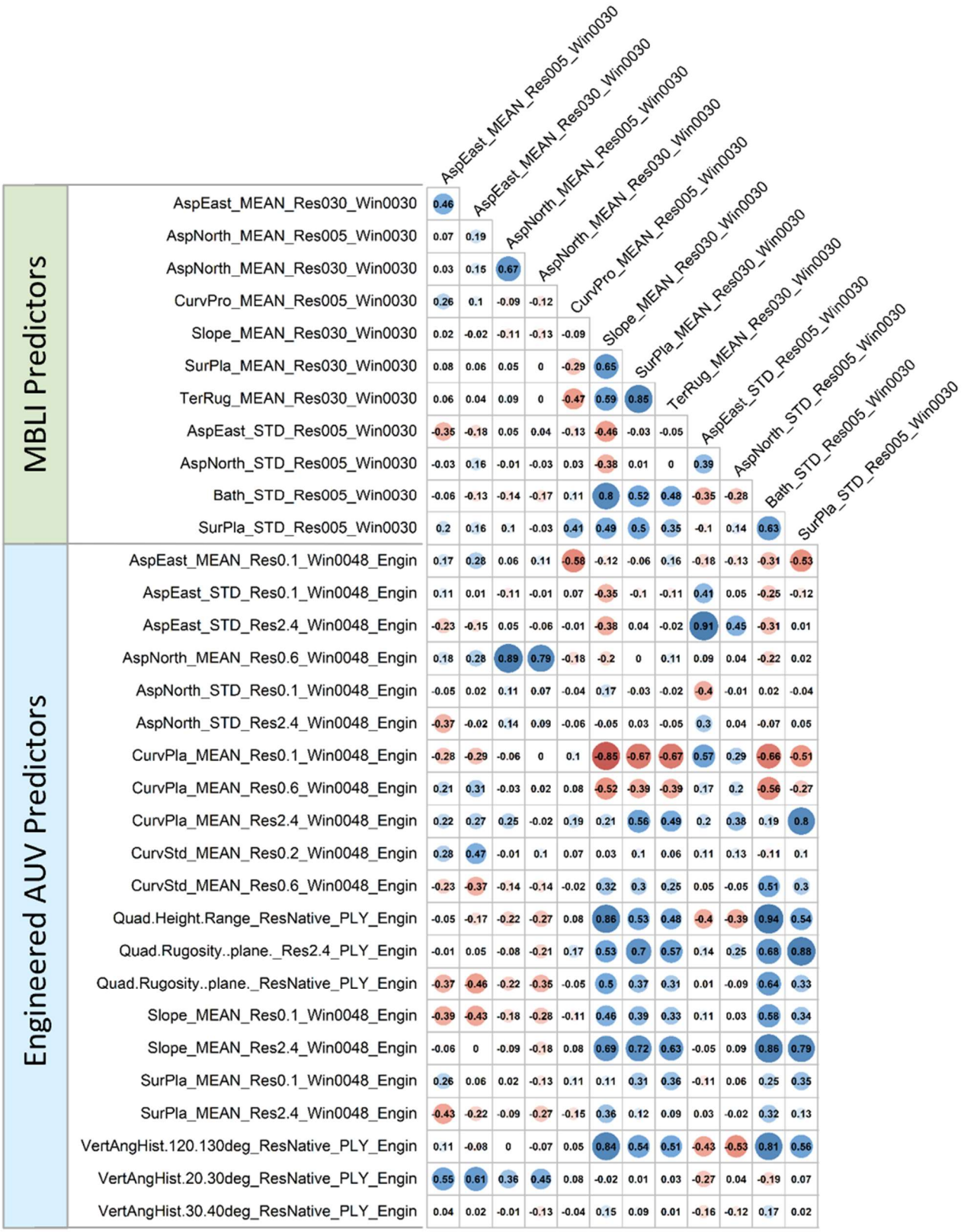

Appendix 5-5 Correlations among engineered benthic cover predictors and MBLI Raster predictors used to predict them

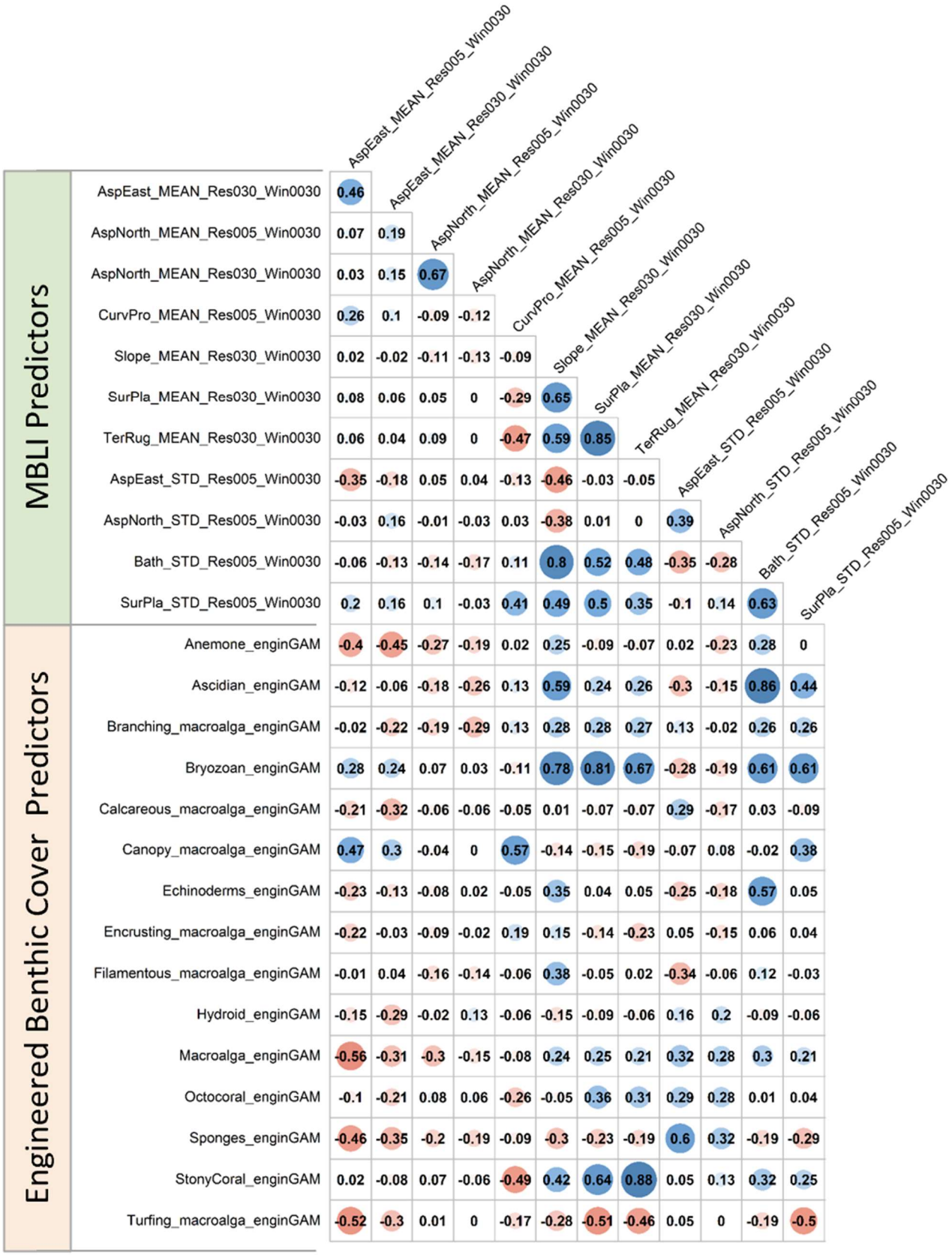

Appendix 5-6 Engineered metrics and benthic cover at a-h and l-o) Port Stephens and l to k) Solitary Islands found to be important predictors in SDMs of fish abundance.

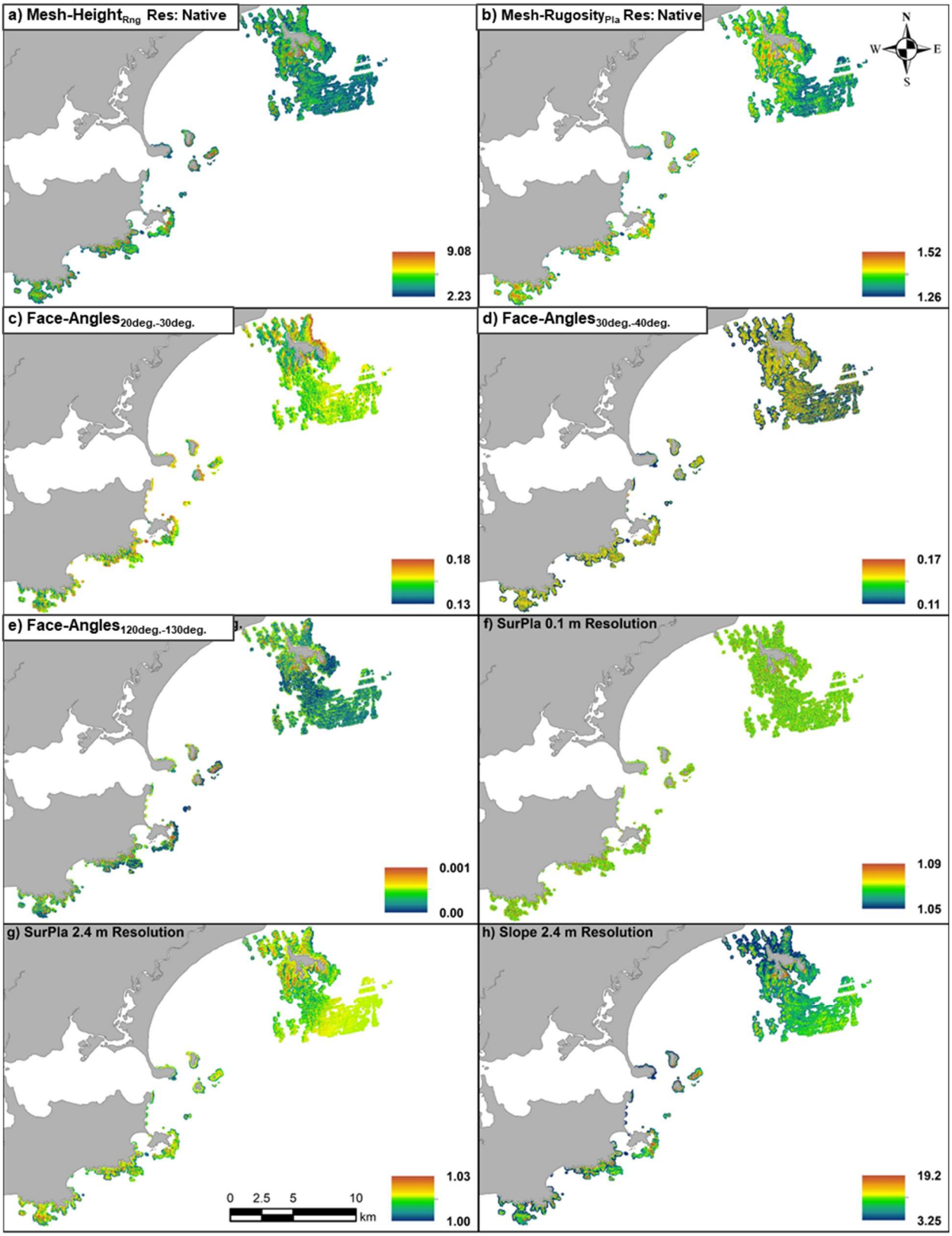

Appendix 5-6 **Continued. Engineered metrics and benthic cover at a-h and l-o) Port Stephens and l to k) Solitary Islands found to be important predictors in SDMs of fish abundance.**

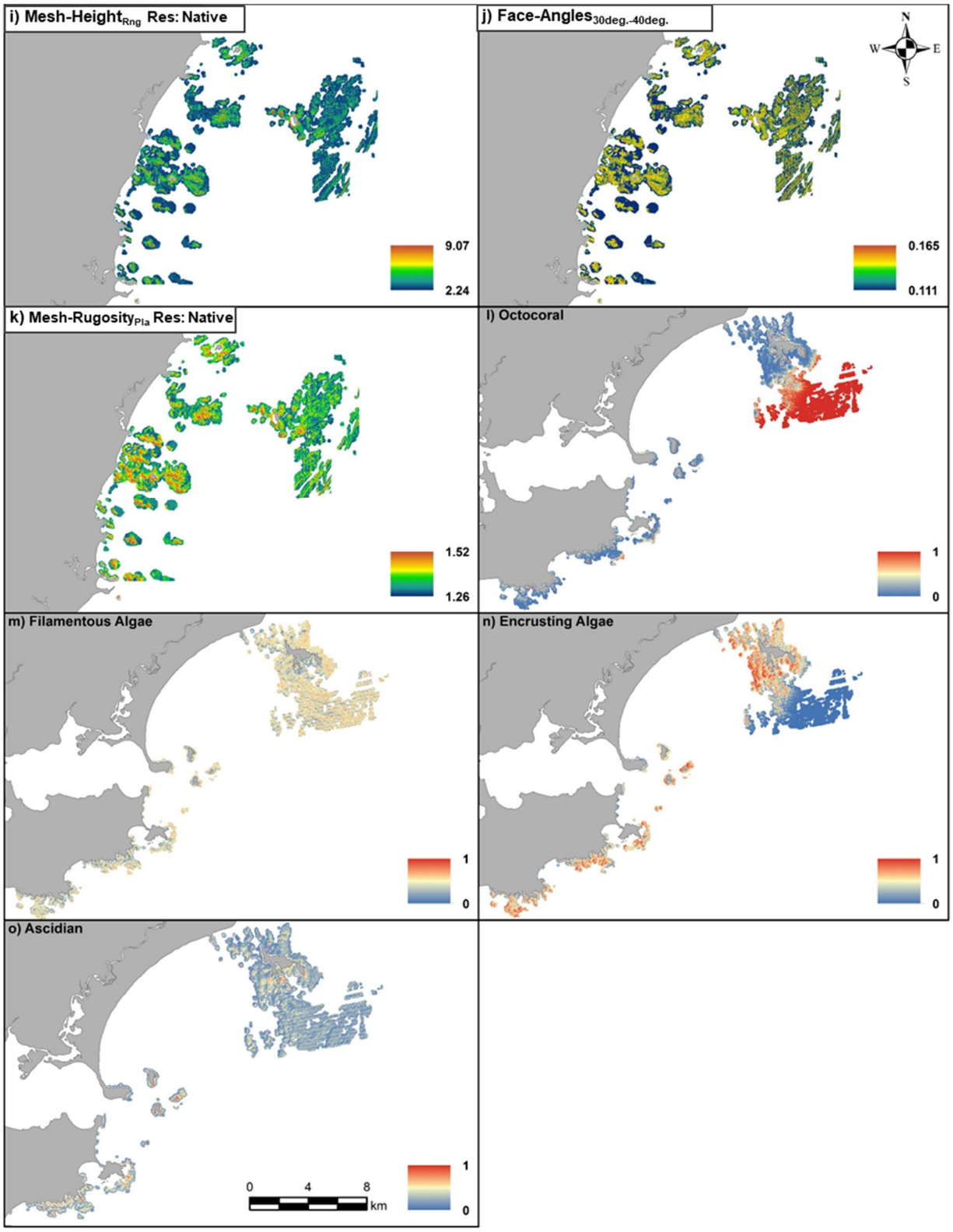

6 Chapter 6 - Overall Discussion

6.1 Summary of Findings

This thesis undertook an objective assessment of the relative performance of traditional (multibeam and LIDAR) and photogrammetrically derived metrics of habitat structural complexity (structural complexity) when predicting the distribution and abundance of temperate reef fish in Eastern Australia. Importantly also, it identified how these various datasets interact, can be combined, and be substituted for each other towards the goal of improving predictions of fish abundance and distribution. Itself, photogrammetry represents several improvements over traditional methods of capturing bathymetric reconstructions, including greater resolution, the capture of more realistic 3D models of the seafloor and associated novel metrics, and the opportunity to capture high resolution benthic imagery during data collection. However, the increased costs (per unit area) associated with photogrammetric data collection relative to traditional methods require that consideration be given to its implementation, if the purported benefits to predictive performance and ecological understanding associated with these improvements justify the additional expense required to obtain them. Addressing this key knowledge gap was the primary aim of this thesis. The findings of this thesis represent the first known attempt to undertake this assessment and inform future marine research, conservation and management studies that use metrics of structural complexity to predict fish abundance and distributions.

Fish species and groups for which photogrammetrically derived metrics perform better than traditionally derived metrics were identified, alongside those where traditional remote sensing and derived metrics provide better predictive performance, and those where combining methods provides better performance than either method in isolation (i.e., a synergistic effect). These findings are supplemented by recommendations on how metric derivation from traditional and photogrammetric datasets can be optimised by minimising the number of metrics required to adequately capture the variability in structural complexity of temperate rock reefs. Importantly, these findings are expected to be relevant to other marine environments where metrics of structural complexity are also a key research tool, particularly coral reefs. This thesis also describes and evaluates a novel approach to deriving approximate photogrammetric metrics from traditional remote sensing methods. Although these metrics do not fully substitute direct photogrammetric survey, they can improve predictive model performance areas where direct photogrammetric survey has not been undertaken. This will allow management and conservation efforts to benefit from some

of the improvements associated with photogrammetric datasets, while minimising the potentially substantial increase in costs associated with their collection over large areas.

6.2 Quantifying structural complexity

Prior to examining the purported benefits and making recommendations regarding the use of photogrammetric metrics, the status of research into the use of traditional remote sensing (multibeam, LIDAR and satellite methods) and derived metrics was reviewed in **Section 2**. The aim of this quantitative literature review and metanalysis was to identify common metrics of structural complexity, their relative predictive performance, and the important factors to consider when deriving these metrics. The review identified the most common metrics currently in use, identified the relative performance of these metrics alongside other common predictors (e.g., habitat type, geographic location) via quantitative meta-analysis, and examined the important role of spatial extent and resolution in mediating the ecological relevance and performance of these metrics. Key findings were that most marine biota to respond to structural complexity captured over multiple discrete spatial scales, indicating important local and broad-scale processes captured by these metrics. Consideration of various spatial scales is thus key to identifying ecologically relevant metrics, especially in the absence of clear a priori information on the relative importance of difference spatial scales to species and groups. Notably also was that surface-rugosity, while the most utilised metric of structural complexity, was on average the worst performing of all metrics. It is suggested that this relates to this metric capturing the total structural complexity present rather than any discrete component with ecological relevance. While total complexity can provide an important surrogate of several biotic and environmental drivers of species abundance, it provides an unreliable measure of more discrete and potentially important seafloor features (such as ridges or valleys). Thus, a variety of metrics that capture different components of structural complexity should be considered in such studies.

In addition to deriving metrics over multiple spatial scales, the number of ways of capturing structural complexity is further expanded by various summary statistics (e.g., mean, variance, min and max values of metrics). While this offers potential for capturing further ecologically important components of complexity, it contributes to increasingly large (relative to typical biotic response sample points) predictor datasets. Different metrics of structural complexity, and the same metric derived over different spatial scales, are often highly correlated with each other. Large and highly correlated datasets are difficult to manage and create problems for many statistical methods. **Section 3** provides one of the

few known (though see Fukunaga & Burns, 2020) attempts to rationalise large predictor datasets of structural complexity a priori. The aim was to identify a reduced predictor dataset that optimises information on structural complexity captured whilst minimising the number of metrics and effort required to capture this information. Metrics were derived from three distinct bathymetric reconstructions:

- Large-extent, coarser-resolution 2.5D rasters from traditional multibeam-echosounder and LIDAR methods (MBLI Raster).
- Small-extent, finer-resolution 3D TIN meshes from photogrammetric surveys undertaken using an AUV (AUV Mesh).
- Small-extent, finer-resolution 2.5D rasters converted from the photogrammetric mesh (AUV Raster).

The findings identified groups of redundant metrics (i.e., strongly correlated with one or more other metrics), those that capture unique components of structural complexity, and those that are particularly sensitive to change in the spatial scale over which they are derived. Together, this provides guidance on the selection of metrics that would maximise the information on physical variability obtained from mesh and raster-based models whilst simultaneously minimising the effort required to derive metrics and the number of predictors to be evaluated. These findings also provide insight into patterns of abiotic variability in the physical structure of temperate rock reefs. Three key groupings were identified among raster based metrics, representing gross complexity (including surface-rugosity, terrain-ruggedness and slope) orientation (the direction the reef is facing identified by aspect-east and aspect-north) and curvature (capturing concave and convex surfaces such as ridges and valleys captured by profile-curvature, planar-curvature and standard curvature) (**Figure 6-1**).

A key finding from this analysis was that ‘gross complexity’ included the variability (std) of bathymetry and all metrics except those based on orientation (aspect-east-std and aspect-north-std). Thus, any one of the ten metrics within this grouping could provide a measure of ‘gross complexity’, substantially reducing the size of predictor dataset and effort required to derive these metrics . Which metric selected to be representative would largely be a choice for researchers, though measures of surface rugosity, such as surface-planar-area, is most utilised, easy to conceptualise and was selected for use when modelling fish abundance in this thesis. The two other uncorrelated groups were based on curvature (standard-curvature, planar-curvature and profile-curvature) and orientation (aspect-north,

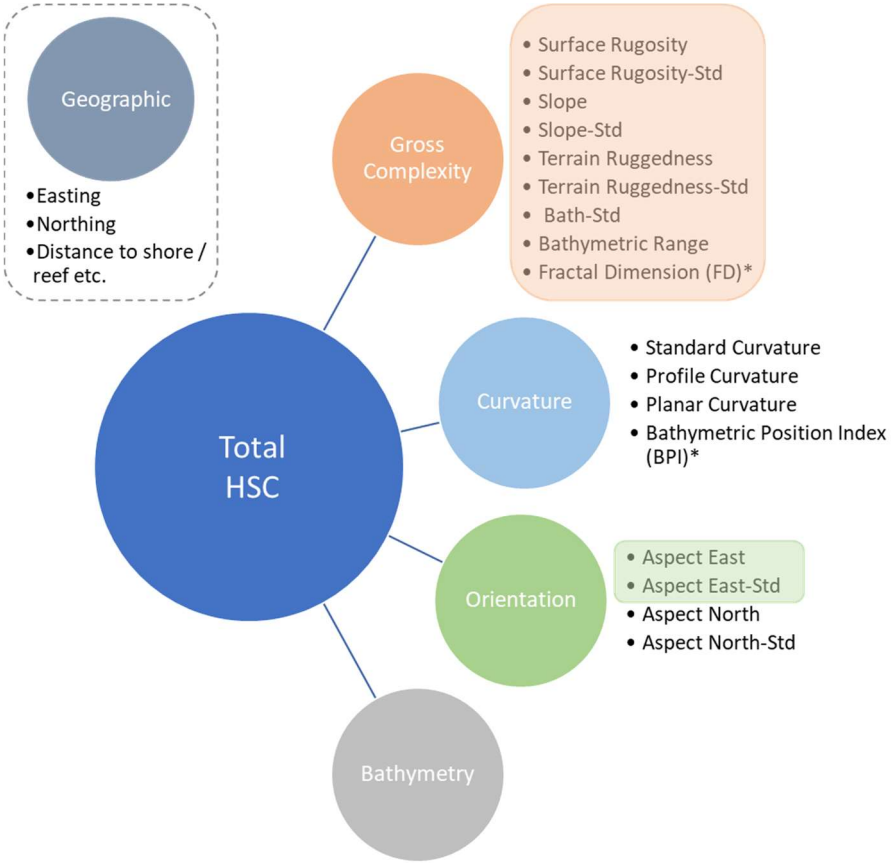

Figure 6-1 Major groups of structural complexity derived from raster-based DEMs. Orange and green shading indicate groups of correlated gross complexity and orientation metrics, respectively. Metrics indicated by * were not included in this thesis but were grouped according to (Wilson *et al.*, 2007a).

aspect-east and their std.). Importantly, individual metrics within the curvature and orientation groups were largely uncorrelated, indicating they too capture discrete components and should be included when quantifying structural complexity.

Although correlations between structural complexity and geographic predictors (e.g., site in **Section 4** and easting and northing in **Section 5**) were not examined, their importance in predictive models supported the findings of the meta-analysis in **Section 2** and reinforced the importance of including such predictors. The underlying surrogacy relationships associated with geographic predictors may be difficult to identify with confidence as they will co-vary with several environmental gradients. The identification of broad-scale structural complexity predictors that can replace these predictors would be desirable, as this would offer some clue as to the environmental gradients / resources. However, it is possible that structural complexity may not be able to provide adequate surrogates for all important environmental gradients, and that geographic predictors (or the underlying environmental gradients themselves) would need to be included to maximise model performance. Though

not strictly a metric of structural complexity, bathymetry should be included as it is often an important predictor regardless of structural complexity (Ferrari, *et al*., 2018; Galaiduk, 2016).

Two other relatively common metrics that were not included here were fractal dimension and bathymetric position index (BPI). Fractal-dimension, conceptualised as the degree of space filling, was found to be highly correlated with rugosity, slope and viewshed derived from rasters, at least when derived from meshes of coral reef with a resolution of 0.01 m to 1.28 m and extent of approximately 150 m^2 (Fukunaga *et al*., 2019). This would suggest fractal dimension could be grouped with other 'gross complexity' metrics, though further examination over a range of resolutions and larger extents would be required to help confirm this. Like other metrics of 'gross complexity' fractal dimension takes values of 0 or greater. BPI provides a measure of the depth of a location relative to its surrounding area, with positive values indicating a peak and negative values a depression. Although not based on empirical data, (Wilson *et al*., 2007a) grouped BPI with curvature metrics. BPI is likely to be correlated with metrics of curvature given the geometric similarities of these metrics. Again, further examination of the correlation over multiple resolutions and extents would be required to confirm this.

Following metric selection, the spatial extent and resolution over which they are derived should also be considered. In this thesis, surface rugosity and aspect-north-std were most sensitive to change in resolution and extent, followed by aspect-east, aspect-north and curvature metrics. Although these findings were from the NSW coastline, similar findings may be evident on other rock reef environments. Regardless, all required more than one extent / resolution to adequately capture the total variability observed in their values. When considering the importance of multiple discrete spatial events noted in **Section 2**, it is not surprising then that the resolution and extent over which metrics are derived can substantially influence the metric value. Indeed, 19 of the 44 studies reviewed in **Section 2** had an a priori aim to investigate the role of spatial extent on the predictive performance of derived metrics. In each case, more than one discrete spatial scale was important. Similar to the identification of redundant metrics, these findings describe how resolution and extent can be selected to obtain the maximum amount of information in structural complexity variability with minimum number of predictors. Multi-scaled approaches such as these will continue to help ensure important species responses across different spatial scales are captured (Pittman & Brown, 2011).

6.3 Performance of Traditional vs Photogrammetry Methods

Chapter 4 (**Section 4**) and Chapter 5 (**Section 5**) used the reduce predictor dataset to model fish abundance on the NSW coastline. The aim of **Section 4** was to identify for which species and groups traditional and / or photogrammetrically derived metrics provide greatest predive performance, potential synergy between these metrics, and, thus, inform future studies considering the use of photogrammetric methods. The primary aim of **Section 5** was to improve predictions of fish abundance and distribution using a novel method to engineer photogrammetric metrics over broad spatial extents. Section 5 also allowed further examination of the relative performance of the three bathymetric reconstructions

The key findings of **Sections 4** and **5** agree and indicate that photogrammetrically derived metrics of structural complexity provide important predictors of fish abundance. Thirty-nine of the 50 best performing models of fish species and group abundance in **Section 4** consisted solely of, or included, photogrammetrically derived metrics (AUV Raster or AUV Mesh) (**Table 6-1**). In **Section 5**, 38 of the 47 models were based solely on, or included, photogrammetrically derived metrics, with a further two best performing models based solely on benthic cover. Clearly, photogrammetrically derived metrics have potential to improve predictions of fish abundance and distributions. A synergistic effect of combining traditional and photogrammetric metrics in models of fish abundance was a further key finding evident in these **Sections**. In **Section 4**, most species (22 of 35) and most groups (8 of 15) were predicted best when models combined predictors from MBLI and photogrammetric (albeit mainly AUV Raster metrics) datasets. A weaker synergistic effect was also evident in **Section 5**, where 11 best performing final models combined MBLI Raster and each of the engineered AUV Raster, AUM Mesh and Benthic Cover datasets appears to be the first objective test of the presence of synergism between predictors from these different datasets, and confirm an effective pathway to improving predictions of species abundances using photogrammetric metrics.

6.4 Fish responses to structural complexity

Whether photogrammetric or traditional metrics are more important for individual species and groups, however, is a more difficult question to answer. The relative importance of different metrics for each individual response will depend on several factors including the species composition (in the case of groups), the spatial extent(s) and resolution(s) considered, habitat (e.g., temperate versus tropical and shallow versus deep areas) and survey timing etc. Any conclusion regarding the relative importance of individual and groups

Table 6-1 **Summary of best models identified for each fish species and groups in Sections 4 and / or 5. The overall response indicates if model performance was best using only MBLI Raster (Obligate MBLI), photogrammetric (AUV Mesh and / or AUV Raster) (Obligate AUV), combined MBLI Raster and photogrammetric (combined) in each Chapter (Combined), combined in Section 4 and either MBLI Raster (Facultative MBLI) or photogrammetric (Facultative AUV) in Section 5, or using MBLI Raster in one chapter but photogrammetric in the other (Divergent).**

Chapter 4 and 5 Scores

MBLI Raster = -1
MBLI Raster & AUV Mesh, AUV Raster and / or Benthic Cover = 0
AUV Mesh, AUV Ratster and / or Benthich Cover = 1

Overall Response (sum of Scores)

Obligate MBLI	Faculative MBLI	Combined	Faculative AUV	Obligate AUV
-2	-1	0	1	2

Divergent (D)
Chapter 4 = MBLI Raster & Chapter 5 = AUV Mesh, AUV Ratster and / or Benthic Cover

Response	Trophic-Mobility Group	Best Model Chapter 4	Best Model Chapter 5	Overall Response
Species				
Acanthistius ocellatus	Sedentary-bottom-dweller-piscivore		1	
Achoerodus viridis	Mobile-bottom-dweller-predator	0	0	0
Atypichthys strigatus	Midwater-planktivore	0	0	0
Bodianus frenchii	Mobile-bottom-dweller-predator	0		
Bodianus unimaculatus	Mobile-bottom-dweller-predator	0	0	0
Caesioperca lepidoptera	Midwater-planktivore	-1		
Chaetodon guentheri	Midwater-predator	-1		
Cheilodactylus fuscus	Sedentary-bottom-dweller-predator	0	1	1
Chromis hypsilepis	Midwater-planktivore		1	
Chelmonops truncatus	Sedentary-bottom-dweller-predator	1		
Choerodon venustus	Mobile-bottom-dweller-predator	-1		
Chrysophrys auratus	Mobile-bottom-dweller-predator	-1	1	D
Coris picta	Mobile-bottom-dweller-predator	0	1	1
Enoplosus armatus	Midwater-predator	0	-1	-1
Eubalichthys bucephalus	Midwater-predator	-1	1	D
Gymnothorax prasinus	Mobile-bottom-dweller scavenger-predator	0	1	1
Heterodontus portusjacksoni	Mobile-bottom-dweller scavenger-predator	-1	0	-1
Hypoplectrodes maccullochi	Sedentary-bottom-dweller-predator	-1	0	-1
Latropiscis purpurissatus	Sedentary-bottom-dweller-piscivore	0	1	1
Lotella rhacina	Sedentary-bottom-dweller-piscivore		1	
Mecaenichthys immaculatus	Sedentary-bottom-dweller-predator	-1	1	D
Meuschenia freycineti	Midwater-predator	0	0	0
Meuschenia scaber	Midwater-predator	0	1	1
Meuschenia sp.	Midwater-predator	-1	1	D
Meuschenia trachylepis	Midwater-predator	0		
Nelusetta ayraud	Sedentary-bottom-dweller-predator		-1	
Nemadactylus douglasii	Mobile-bottom-dweller-predator	0	1	1
Notolabrus gymnogenis	Mobile-bottom-dweller-predator	0	0	0
Ophthalmolepis lineolata	Mobile-bottom-dweller-predator	0	1	1
Parma microlepis	Sedentary-bottom-dweller-herbivore	-1	1	D
Parma unifasciata	Sedentary-bottom-dweller-herbivore	0		
Parupeneus spilurus	Mobile-bottom-dweller-benthic-invertivore	0	1	1
Prionurus microlepidotus	Mobile-bottom-dweller-herbivore	-1		
Pseudocaranx dentex	Midwater-piscivore	0	-1	-1
Pseudocaranx georgianus	Midwater-planktivore	0	1	1
Radioargons sarba	Mobile-bottom-dweller-predator		1	
Scorpaena cardinalis	Sedentary-bottom-dweller-piscivore	0	0	0
Scorpis lineolata	Midwater-planktivore	0	1	1
Trachurus novaezelandiae	Midwater-planktivore	-1	0	-1
Upeneichthys lineatus	Mobile-bottom-dweller-benthic-invertivore	1	1	2
Trophic-Mobility Groups				
Herbivore		0	1	1
Piscivore		0	1	1
Planktivore		-1	-1	-2
Predator		1	1	2
Sediment-infauna-predator		0	1	1
Midwater-piscivore		0	1	1
Midwater-planktivore		-1	-1	-2
Midwater-predator		0	-1	-1
Mobile-bottom-dweller-benthic-invertivore		0	1	1
Mobile-bottom-dweller-herbivore		-1		
Mobile-bottom-dweller-predator		0	0	0
Mobile-bottom-dweller scavenger-predator		-1	1	D
Sedentary-bottom-dweller-herbivore		-1	0	-1
Sedentary-bottom-dweller-piscivore		0	1	1
Sedentary-bottom-dweller-planktivore			-1	-1
Sedentary-bottom-dweller-predator		0	1	1

of metrics would need to be qualified by these (and several other known and likely unknown) factors. Any site-specific findings would also limit model portability so that findings for the same species and group may vary somewhat among different studies. Despite this, when examined together, the findings **Sections 4** and **5** allow some tentative observations on patterns between individual species and group responses to be made that can be linked with the knowledge of species ecology and behaviour.

A small number of species and groups displayed consistent responses, with the abundance of *U. lineatus* and predators predicted best solely by photogrammetric metrics derived over local extents at relatively fine resolutions (≤ 2.4 m) (i.e., Obligate AUV) (**Table 6-2**). These finer resolutions (0.05 m to 2.4 m) are far more commensurate with the level of seafloor complexity typical of the feeding habitat of *U. lineatus*, which typically could consist of a mixed reef-sand habitat mosaic, compared to the coarser resolutions provided by MBLI Raster predictors (5 m to 240 m). Finer resolutions are also commensurate with the biogenic physical structure provide by sessile epifauna and mobile invertebrates consumed by predators and amongst which these predatory fish may also seek refuge from piscivores. Thus, in these cases, photogrammetric metrics are likely providing surrogates for benthic food and refuge availability, which would be important predictors of the abundance of predatory fish.

Planktivores and midwater planktivores also displayed a consistent response and were predicted best solely using MBLI Raster predictors in **Sections** 4 and 5 (i.e., Obligate MBLI), with MBLI Raster predictors at local (30 m window size) and broad (> 30 m window size) extents important (at least in **Section 4**, as broader > 30 m window size predictors were not included in **Section 5**). Although sedentary bottom dweller planktivores were not examined in **Section 4** due to low abundance in that dataset, this group was predicted best solely using MBLI Raster predictors in **Section 5**. Thus, for planktivore groups, the most important dataset appears to be the broad extent and coarser resolution MBLI Raster dataset. This finding could initially be surprising given planktivores are often prey for piscivores, and could have been expected to respond more strongly to finer resolution photogrammetric metrics that capture refuges from piscivores. However, the findings here and in other similar studies generally agree, and suggest these fish respond more strongly to variability in broad-scale, coarser resolution metrics such as those provided by MBLI Raster. Planktivores feed higher in the water column than predators, where broader scale predictors derived over coarser resolutions and the larger structures they capture appear more important for influencing water flow, recruitment, planktonic food and predatory sighting by prey, which have been

Table 6-2 Summary of the form of responses of fish species and groups to metrics of structural complexity in Sections 4 and 5. Only species and groups that provided the best performing models and that were examined in detail in each chapter are presented. Responses consist of preference for positive (Pos.), negative (Neg.), intermediate (Int.) and extreme (Ext.) values of the metric.

Datasource	Metric	Res. (m) x Ext. (m)	*Chrysophrys auratus*	*Nemadactylus douglasii*	*Chelodactylus fuscus*	*Achoerodus viridis*	*Trachurus novaezelandiae*	*Enoplosus armatus*	*Coris picta*	*Parupeneus spilurus*	*Meuschenia trachylepis*	*Notolabrus gymnogenis*	*Meuschenia scaber*	*Latropiscis purpurissata*	Predator	Piscivore	Mobile bottom dweller scavenger predator	Sedentary bottom dweller piscivores
Chapter 4																		
MBLI Raster	AspEast	Res005_Ext3120														Int.		
MBLI Raster	AspNorth	Res240_Ext0480				Neg.												
MBLI Raster	AspNorth_Std	Res005_Ext0010						Int.										
MBLI Raster	CurvPla	Res005_Ext0020	Int.															
MBLI Raster	CurvPla	Res005_Ext0005						Int.										
MBLI Raster	CurvPla	Res005_Ext3120					Int.											
MBLI Raster	CurvPla	Res060_Ext0480					Pos.											
MBLI Raster	CurvPro	Res005_Ext0005			Pos.													
MBLI Raster	CurvPro	Res060_Ext0960	Int.						Ext.									
MBLI Raster	CurvPro	Res060_Ext0120					Pos.											
MBLI Raster	CurvStd	Res005_Ext0005		Pos.														
MBLI Raster	CurvStd	Res010_Ext0160							Int.									
MBLI Raster	CurvStd	Res010_Ext0600		Pos.														
AUV Raster	AspEast	Res0.1		Pos.		Pos.												
AUV Raster	AspEast_Std	Res0.1			Neg.													
AUV Raster	AspNorth	Res0.6													Pos.			
AUV Raster	CurvPla	Res0.6			Pos.										Neg.	Neg.		
AUV Raster	CurvStd	Res0.2						Neg.							Neg.			
AUV Mesh	Quad Rugosity Plane	Res2.4							Ext.							Ext.		
Chapter 5																		
AUV Mesh	Face Angles 20.30 deg.	ResNative	Pos.							Pos.								Neg.
AUV Mesh	Face Angles 30.40 deg.	ResNative												Pos.				
AUV Mesh	Face Angles 120.130 deg.	ResNative															Pos.	Neg.
AUV Mesh	Quad rugosity plane	ResNative	Pos.							Pos.				Pos.			Pos.	Pos.
AUV Mesh	Quad height range	ResNative	Int.							Pos.				Neg.				
AUV Raster	SurPla Res0.1	Res0.1									Neg.							
AUV Raster	Slope Res2.4	Res2.4									Neg.							
AUV Raster	SurPla Res2.4	Res2.4									Pos.							
Benthic Cover	Encrusting macroalgae											Pos.	Neg.					
Benthic Cover	Filamentous macroalgae											Pos.	Neg.					
Benthic Cover	Ascidian											Pos.						
Benthic Cover	Octocoral												Pos.					

linked with planktivore abundance (**Section 5** and Rilov & Benayahu, 2002; Rilov & Benayahub, 1998; Rountree, 1989; Wilhelmsson, Yahya, *et al*., 2006; Wilhelmsson *et al*., 1998).

Similar findings regarding planktivores were also identified by Ferrari, Malcolm, Byrne, *et al*., (2018) based on a subset of the Solitary Islands data presented in **Section 4**), where predator, piscivore and sediment infauna predator groups responded more strongly (explaining 10% to 17% of total variance in abundance) to AUV Mesh metrics (capturing

surface-rugosity and slope) than did planktivores (where AUV Mesh metrics explained only 1% of total variance). Notably also, as it was based on a separate fish dataset collected using a different method (visual census) from different locations (Botany Bay and Port Kembla in NSW), (Porter, 2018) found midwater planktivore and demersal planktivore abundance was positively related more to the presence of larger objects (approx. 14 m^3 and 0.2 m^3, respectively) than was the abundance of midwater piscivores (object size 0.03 m^3) and demersal herbivores and predators (object size 0.003 m^3). Porter, (2018) also observed planktivorous pempherids (Bullseye) sheltering amongst overhanging features in the 0.03 m^3 to 0.2 m^3 size range at both rock reef and artificial breakwall habitats. In each case, fish abundance increased with a greater proportion of total structural complexity in the landscape belonging to that object size class. Together, these findings provide convincing evidence that planktivores, including demersal and site attached species, respond more strongly to variation in larger scale components of structural complexity. Also, that this appears at least partly due to the greater provision of shelter from piscivores afforded by larger objects. Such findings are also supported by studies identifying the importance of viewshed for planktivorous damselfish, albeit with both positive (Rilov *et al*., 2007) and negative (González-Rivero *et al*., 2017a) effects on abundance.

For some other species and groups, there were relatively distinct preferences for different datasets between **Sections 4** and **Sections 5** (those identified as Divergent in **Table 6-1**). In all 6 cases (5 species and 1 group), this was associated with a preference for MBLI Raster predictors in **Section 4** and AUV Mesh or AUV Raster predictors in **Section 5**. This included one species (*C. auratus*) where the Section 4 MBLI Raster predictors spanned local and broad extents and for three (*M. immaculatus*, *M. trachylepis* and *Meuschenia* sp.) they included only broad extents. This would suggest that 1) broad-scale predictors are more important for these fish than local-scale fine resolution photogrammetric predictors, but that 2) at local scales, finer resolution photogrammetric metrics become more important than coarser resolution MBLI raster metrics. This second point is also supported by the finding that local-scale fine resolution photogrammetric predictors (AUV Mesh and AUV Raster) more often were retained in the best performing models in **Section 5** when broad-scale MBLI Raster predictors were not considered. For the remaining two (*Parma microlepis* and mobile bottom dweller scavenger predator), the MBLI Raster predictors in **Section 4** were based only on the local extent (in each case AspNorth resolution 30 m and extent 30 m), suggesting broader extent MBLI Raster predictors and associated environmental gradients / resources were less important. It is unclear why *Parma microlepis* and mobile bottom

dweller scavenger Predator did not also display a preference for local extent MBLI Raster predictors in **Section 5**. Possibly, this reflected the different datasets examined.

For the 6 species (*Achoerodus viridis*, *Atypichthys strigatus*, *Bodianus unimaculatus*, *Meuschenia freycineti*, *Notolabrus gymnogenis* and *Scorpaena cardinalis*) and one group (mobile bottom dweller predator) where the best performing models in **Section 4** and **Section 5** combined predictors across MBLI and photogrammetric dataset, this provided strong evidence of the presence of synergistic effects of including predictors across different datasets. Importantly for each, at least one MBLI predictor in **Section 4** was derived over a broad extent, indicating the importance of broad extent coarse resolution and local extent fine resolution predictors for each species and group. Clear patterns of preference were less evident for the remaining species and groups. These included the 10 species and 7 groups that were predicted best by photogrammetric metrics (AUV Mesh, AUV Raster) or benthic cover in **Section 5** but by models that combined photogrammetric with MBLI raster metrics in **Section 4** (Facultative AUV). It also included the 5 species and 2 groups predicted best solely using MBLI Raster metrics in **Section 5** but combined models in **Section 4**, or using combined models in **Section 5** and solely MBLI Raster metrics in **Section 4** (Facultative MBLI).

Although not a metric of structural complexity, benthic cover (albeit 'engineered') was found to be the most important dataset for only two species (*Meuschenia scaber* and *Rhabdosargus sarba*) in **Section 5**. Benthic cover also contributed to the best final models of a further 9 species and 2 groups. Various benthic cover predictors were found to be important contributors to final models of total fish abundance and abundance of piscivores, predators, herbivores and planktivores by Ferrari, Malcolm, Byrne, *et al*., (2018) based on a subset of the data from the Solitary Islands presented in **Section 4**, often outperforming metrics of structural complexity derived from the AUV Mesh surface. Why benthic cover appears less important in **Section 5** is unclear. It was perhaps related to the use of 'engineered' predictors of benthic cover in **Section 5**, though abiotic models of benthic cover used to derive the engineered metrics performed relatively well and generally explained 50% to 80% total variance observed in benthic cover. It is possible that if direct measures of benthic cover had been included, these would been more effective predictors of fish abundance than the engineered benthic cover predictors. However, obtaining these data across such broad extents would be impractical given the costs involved.

Fish groups were included as response variables in this thesis as they have potential to simplify the application of study findings by researchers and resource managers. The

relatively consistent response of planktivores and predators, at least, to structural complexity does support the consideration of these groups of fish, at least. However, it is important to note that individual species within groups will not necessarily follow the same pattern observed by the group to which they belong. This was the case when the group level preference for different datasets was relatively consistent (Obligate AUV or Obligate MBLI) or otherwise differed between Sections 4 and 5. For example, of the 6 Planktivore species with sufficient abundance to model separately (all of which were midwater-planktivores), none indicated a consistent preference for MBLI Raster predictors between **Sections** 4 and 5 and none would have been identified 'Obligate MBLI'. Only two (*Caesioperca lepidoptera* and *Trachurus novaezelandiae*) displayed a strong preference for MBLI Raster, and in these cases only in **Section 4** (neither was modelled individually in **Section 5** due to low abundance in that dataset). Similarly, none of the species within the Obligate AUV group (predators) would individually be considered Obligate AUV. Rather, best performing model in each chapter combed predictors across different datasets (i.e., they displayed a Combined, or strong synergistic, response), or they were associated with a Facultative MBLI, Facultative AUV or Divergent response. Grouping species into groups based on their trophic, feeding and behavioural characteristics appears to result in an emergent response at the group level that differs from individual species responses. While such groupings may be useful to research and conservation practitioners when considering broad groups, they should not replace consideration of response at individual species levels particularly when a species may be of conservation or economic interest.

Only limited comparison of the form and direction of the response fish abundance to individual predictors between **Sections 4** and **5** was possible. This was due to different species being included in the best final models in each chapter (only these were examined in detail). The one exception, *Chrysophrys auratus*, was included in the best final model in both Sections / Chapters, though different predictors were retained in each model (**Table 6-2**). The response of most species and groups to structural complexity metrics appears varied, with responses to metrics within the same final model including positive and negative responses and / or preferences for intermediate or extreme metric values. Only two species and one group displayed consistent responses to metrics within the same structural complexity metric grouping (i.e., complexity, curvature or orientation), and then only in either **Section 4** or **5**. These were *Nemadactylus douglasii*, *Parupeneus spilurus* and mobile bottom dwelling scavenger predators, all of which were consistently positively correlated with measures of curvature and / or complexity.

6.5 Limitations and Further Research

Key thesis limitations and associated opportunities for further research are:

- **Relatively coarse resolution (5 m) of the traditional bathymetric dataset.** While the 5 m resolution of the MBLI Raster dataset in this thesis was typical of that used in the wider research area, much finer resolutions are currently achievable on the order of 10s of centimetres (e.g., Ierodiaconou *et al*., 2018). Such resolutions are comparable with the resolution of photogrammetrically derived bathymetric reconstructions, including those used in this thesis (AUV Mesh and AUV Raster, resolutions from around 0.05 m to 2.4 m). Thus, some of the improved fish abundance and distribution model performance attributed to photogrammetrically derived metrics in this thesis may be obtained by use of finer resolution and broader-extent traditional methods of deriving bathymetric reconstructions. Further research should examine the potential for these finer resolution traditional methods to improve predictions of fish and other marine biota. Such research will also help identify whether greater resolutions and / or novel photogrammetrically derived metrics are the source of improved predictive performance.
- **Portability of findings.** This thesis was undertaken using available data from the NSW coastline where strong patterns in the relationships between metrics of structural complexity and between fish and structural complexity were identified. Comparison of the findings with previous similar studies identified some trends across rock and / or coral reefs, including common groupings of related metrics and similar responses of fish groups, including planktivores, to specific components of structural complexity. The availability of similar studies with which to make such comparisons is. however, limited, and only tentative conclusions on the portability of the findings from the NSW coastline to other rock reefs, coral reefs, and other geographic locations can be made. Wherever possible, future similar studies should attempt some comparison of relationships among metrics, including consideration of spatial scale, and report the findings. As the size and spatial coverage of this dataset grows, more confident conclusions regarding how representative the NSW coastline is of other reefs and other geographic locations can be made.
- **Other drivers of variability in fish abundance and distribution.** Other key variables known or likely to contribute to variability in fish abundance and distribution but that were not considered directly in this thesis include the spatial configuration of elements of complexity (Tokeshi & Arakaki, 2012) and temporal variability in fish

assemblages (e.g., Wines *et al*., 2020). Temporal variability was not considered in this thesis as not all sites were sampled in all years. Where possible these factors should be considered in future studies to maximise the explained variability in fish (and other marine biota) abundance. A key next step in the use of metrics of structural complexity to explain ecological patterns is the development of new metrics that are able to capture the density and spatial arrangement of key discrete elements of complexity, such as habitat refuges. The skillsets required to develop such metrics often sit outside the core experience of ecological scientists, requiring collaboration among ecologists, spatial scientists and computer programmers.

6.6 Conclusions and Recommendations

Quantifying structural complexity: There is a plethora of metrics available to researchers, capturing a variety of components of seafloor physical structure across a range of spatial extents and resolutions. These are often also highly colinear and sometimes difficult to conceptualise. This represents a substantial potential hindrance to researchers associated with data management and analysis limits the effective use of structural complexity as predictors of the abundance and distribution of marine biota. The identification here of where this collinearity exists, where it does not, and of resulting groupings of related metrics of structural complexity provides a rationalization that will go some way to resolving these hinderances by reducing the degree of redundancy among common metrics. Not all metrics capture unique components of structural complexity, nor that all respond to varying spatial extent and resolution in the same way. The substantial collinearity between metrics of ‘gross complexity’ indicates that choosing a standard metric to represent this component of structural complexity would allow the greatest reduction in predictor dataset size for the smallest potential degree of information loss. Surface rugosity, an easy to conceptualise and very commonly utilised metric (as identified in **Section 2**) appears the most likely candidate for such a standard metric. In most circumstances, inclusion of this metric would remove the need to include those based on slope, terrain-ruggedness, and the variability in these and most other metrics, except those based on orientation, representing a substantial reduction in the work associated with handling these metrics. There is less scope for reducing the number of metrics within the curvature and orientation groupings as metrics within these groups are generally also uncorrelated with each other. However, this does indicate that these groups and individual metrics should be included as predictors as each is likely to capture a unique component of structural complexity.

Purported Benefits of Photogrammetric Metrics: The findings of **Sections 4** and **5** clearly demonstrate the potential for photogrammetry and derived metrics of structural complexity to improve predictions of the abundance and distribution of fish on the NSW coastline. This includes circumstances where AUV Raster or AUV Mesh-based metrics performed better than those derived from traditional methods (MBLI Raster), but in many cases also where models that combined metrics across these traditional and photogrammetric datasets performed better than models based on either dataset in isolation. This synergistic effect of combing metrics almost certainly reflects the presence of important resources and environmental gradients that exist over multiple spatial scales that combine to influence species abundance and distributions at any given location. This provides the first known extensive and objective assessment of the relative performance of these datasets in predicting the abundance and distribution of any marine biota. However, whilst photogrammetric metrics are important, and in some cases more so than traditional metrics, they do not replace the need for broad-scale traditional metrics derived over much broader scales. Rather, photogrammetric and traditional methods and associated metrics are complimentary and should both be considered as potential predictors wherever available. This is expected to remain the case for the foreseeable future, and if or when methods of capturing photogrammetric data over broad spatial extents become available. For species and groups where the use of photogrammetric metrics (solely or alongside traditionally derived metrics) was shown in this thesis to improve predictions of abundance / distribution, researchers would be able undertaken their own cost-benefit analysis based on their specific circumstances and study objectives.

Integrating Photogrammetric and Traditional Methods: Whilst photogrammetric metrics are likely to be associated with improved predictions of species abundance and distribution, and should be included alongside traditional methods and datasets wherever possible, this may not always be feasible due to the expense associated with their collection. Where photogrammetry surveys are undertaken, these will typically be restricted to smaller extents, restricting their ability to inform larger scale studies and models required for effective marine resource management and conservation. In the absence of broad-scale photogrammetric data collection, the ‘engineering’ of photogrammetric metrics using MBLI Raster metrics described here provides an achievable and effective alternative to direct photogrammetric data collection. These engineered metrics were shown useful predictors of fish abundance and distribution, and provide a way for future studies to capture some of this enhanced predictive performance without the otherwise prohibitive cost of deriving these predictive directly from effort intensive photogrammetric survey.

Insights into Fish Ecology and Distributions: Overall, and as noted earlier and in many other similar studies, fish responses to different datasets (MBLI Raster vs AUV Mesh vs AUV Raster) were largely species specific. Generalisations in responses among species from within trophic-mobility groups were also difficult to identify, which made it difficult to suggest preferred approaches for most groups of fish. Planktivore groups and predators provided exceptions and responded more strongly to traditionally and photogrammetrically derived metrics, respectively. Regardless of how fish adults or juvenile fish may actively respond to structural complexity within their home range, observed distributions and abundance would likely be a function of environmental gradients and resources operating outside of this range. Even benthic species with small home range sizes would mostly have pelagic larval stages with drift and settlement of larvae influenced by local and broad-scale hydrodynamic flow itself influenced by structural complexity. Ontogenetic migration and associated habitat selection, and how habitat suitability is captured by broad-scale predictors would also be important. In these circumstances, it would be harder to link predictive performance with a species ecology and behavior, at least that associated with adult fish, which would more likely be confidently identified by observers. A key consideration here is that in this thesis, and possibly in most other similar studies, it is adult fish that are observed and that findings may be somewhat skewed towards the ecology and behaviors, and habitat selection of adults. Different fish survey methods may also not be the best method for surveying all species and groups, for example BRUVs baited with pilchards may not be the best method for surveying herbivorous fish.

Overall, the greater understanding of the influence of metrics of structural complexity on fish ecology and better methods of obtaining these metrics provided by this thesis provide several key improvements to fish SDMs, spatial prioritisation and management. This work provides much greater understanding of structural complexity, the relationships among metrics, the discrete categories they represent, and how metrics vary with resolution and spatial extent. Researchers and managers no longer need to derive and handle thousands of highly correlated metrics but rather can concentrate on a few key metrics that best capture variability in this important driver of fish abundance and distribution. Relationships between species / groups of fish, specific components of structural complexity important spatial scales are now also better understood. For fish ecologists, this allows enhanced inference and prediction of fish abundance and distribution, but also further confirms the importance of considering structural complexity and its different components. Just as important is the realisation that the question for ecologists is less whether photogrammetric or traditionally derived metrics perform better, but rather how to incorporate both given the synergistic effect

of combining these metrics demonstrated for most species and groups in this Thesis. One option is to use smaller-extent photogrammetric reconstructions within much larger-extent reconstructions from traditional remote sensing methods, as done in **Section 4**. A further option is to combine these methods by engineering photogrammetric metrics from traditional metrics, as done in **Section 5**. Such a method is probably the only way of accessing the improved predictive performance associated with photogrammetric metrics over the broad-spatial scales required by spatial prioritisation and marine-use planning. Collectively, these improvements substantially advance the field of remote sensing of marine environments and ecosystems, spatial science and marine ecology.

7 References

Almany, G. R. (2004a). Does increased habitat complexity reduce predation and competition in coral reef fish assemblages? *Oikos*, *106*(2), 275–284. https://doi.org/10.1111/j.0030-1299.2004.13193.x

Almany, G. R. (2004b). Differential effects of habitat complexity, predators and competitors on abundance of juvenile and adult coral reef fishes. *Oecologia*, *141*(1), 105–113. https://doi.org/10.1007/s00442-004-1617-0

Althaus, F., Hill, N., Ferrari, R., Edwards, L., Przeslawski, R., Schönberg, C. H. L., Stuart-Smith, R., Barrett, N., Edgar, G., Colquhoun, J., Tran, M., Jordan, A., Rees, T., & Gowlett-Holmes, K. (2015). A standardised vocabulary for identifying benthic biota and substrata from underwater imagery: The CATAMI classification scheme. *PLoS ONE*, *10*(10). https://doi.org/10.1371/journal.pone.0141039

Altmann, A., Toloşi, L., Sander, O., & Lengauer, T. (2010). Permutation importance: A corrected feature importance measure. *Bioinformatics*, *26*(10), 1340–1347. https://doi.org/10.1093/bioinformatics/btq134

Anderson, T. J., Syms, C., Roberts, D. A., & Howard, D. F. (2009). Multi-scale fish-habitat associations and the use of habitat surrogates to predict the organisation and abundance of deep-water fish assemblages. *Journal of Experimental Marine Biology and Ecology*, *379*(1–2), 34–42. https://doi.org/10.1016/j.jembe.2009.07.033

Aston, E. A., Duce, S., Hoey, A. S., & Ferrari, R. (2022). A Protocol for Extracting Structural Metrics From 3D Reconstructions of Corals. *Frontiers in Marine Science*, *9*. https://doi.org/10.3389/fmars.2022.854395

Bassett, D., & Montgomery, J. (2011). Home range use and movement patterns of the yellow moray eel Gymnothorax prasinus. *Journal of Fish Biology*, *79*(2), 520–525. https://doi.org/10.1111/j.1095-8649.2011.03018.x

Bayley, D. T. I., Mogg, A. O. M., Purvis, A., & Koldewey, H. J. (2019). Evaluating the efficacy of small-scale marine protected areas for preserving reef health: A case study applying emerging monitoring technology. *Aquatic Conservation: Marine and Freshwater Ecosystems*, *29*(12), 2026–2044. https://doi.org/10.1002/aqc.3215

Beck, M. W. (2000). Separating the elements of habitat structure: independent effects of habitat complexity and structural components on rocky intertidal gastropods. In *Journal of Experimental Marine Biology and Ecology* (Vol. 249). www.elsevier.nl/locate/jembe

Bell, J. J., & Barnes, D. K. A. (2000). The influences of bathymetry and flow regime upon the morphology of sublittoral sponge communities. *Journal of the Marine Biological Association of the United Kingdom*, *80*(4), 707–718. https://doi.org/10.1017/S0025315400002538

Bhargava, N., Bhargava, R., & Singh Tanwar, P. (2013). Triangulated Irregular Network Model from Mass Points. In *International Journal of Advanced Computer Research*.

Blalock, H. M. (1963). CORRELATED INDEPENDENT VARIABLES: THE PROBLEM OF MULTICOLLINEARITY. *Social Forces*, *42*, 233–237.

Brokovich, E., Baranes, A., & Goren, M. (2006). Habitat structure determines coral reef fish assemblages at the northern tip of the Red Sea. *Ecological Indicators*, *6*(3), 494–507. https://doi.org/10.1016/j.ecolind.2005.07.002

Brown, C. J., Sameoto, J. A., & Smith, S. J. (2012). Multiple methods, maps, and management applications: Purpose made seafloor maps in support of ocean management. *Journal of Sea Research*, *72*, 1–13. https://doi.org/10.1016/j.seares.2012.04.009

Brown, C. J., Smith, S. J., Lawton, P., & Anderson, J. T. (2011). Benthic habitat mapping: A review of progress towards improved understanding of the spatial ecology of the seafloor using acoustic techniques. *Estuarine, Coastal and Shelf Science*, *92*(3), 502–520. https://doi.org/10.1016/j.ecss.2011.02.007

Buhl-Mortensen, P., Dolan, M., Buhl-Mortensen Mortensen, L., Buhl-Mortensen, P., & Buhl-Mortensen, L. (2009). Prediction of benthic biotopes on a Norwegian offshore bank using a combination of multivariate analysis and GIS classification. *International Council for the Exploration of the Sea*, *66*, 2026–2032. http://icesjms.oxfordjournals.org/

Calders, K., Adams, J., Armston, J., Bartholomeus, H., Bauwens, S., Bentley, L. P., Chave, J., Danson, F. M., Demol, M., Disney, M., Gaulton, R., Krishna Moorthy, S. M., Levick, S. R., Saarinen, N., Schaaf, C., Stovall, A., Terryn, L., Wilkes, P., & Verbeeck, H. (2020). Terrestrial laser scanning in forest ecology: Expanding the horizon. In *Remote Sensing of Environment* (Vol. 251). Elsevier Inc. https://doi.org/10.1016/j.rse.2020.112102

Cameron, M. J., Lucieer, V., Barrett, N. S., Johnson, C. R., & Edgar, G. J. (2014). Understanding community-habitat associations of temperate reef fishes using fine-resolution bathymetric measures of physical structure. *Marine Ecology Progress Series*, *506*, 213–229. https://doi.org/10.3354/meps10788

Carleton, J. H., & Sammarco, P. W. (1987). Effects of substratum irregularity on success of coral settlement: quantification by comparative geomorphological techniques. In B*ulletin of Marine Science* (Vol. 40, Issue 1).

Carlot, J., Rovère, A., Casella, E., Harris, D., Grellet-Muñoz, C., Chancerelle, Y., Dormy, E., Hedouin, L., & Parravicini, V. (2020). Community composition predicts photogrammetry-based structural complexity on coral reefs. *Coral Reefs*, *39*(4), 967–975. https://doi.org/10.1007/s00338-020-01916-8

Casella, E., Lewin, P., Ghilardi, M., Rovere, A., & Bejarano, S. (2022). Assessing the relative accuracy of coral heights reconstructed from drones and structure from motion photogrammetry on coral reefs. In *Coral Reefs*. Springer Science and Business Media Deutschland GmbH. https://doi.org/10.1007/s00338-022-02244-9

Catano, L. B., Gunn, B. K., Kelley, M. C., & Burkepile, D. E. (2015). Predation risk, resource quality, and reef structural complexity shape territoriality in a coral reef herbivore. *PLoS ONE*, *10*(2). https://doi.org/10.1371/journal.pone.0118764

Champion, C., Suthers, I. M., & Smith, J. A. (2015). Zooplanktivory is a key process for fish production on a coastal artificial reef. *Marine Ecology Progress Series*, *541*, 1–14. https://doi.org/10.3354/meps11529

Chen, G. K., & Dai, C. F. (2021). Using 3D photogrammetry to quantify the subtle differences of coral reefs under the impacts of marine activities. *Marine Pollution Bulletin*, *173*. https://doi.org/10.1016/j.marpolbul.2021.113032

Coleman, M. A., Ingleton, T., Millar, R. B., Davies, P. L., Jordan, A., & Kelaher, B. P. (2016). Remotely sensed habitat variables are poor surrogates for functional traits of rock reef fish assemblages. *Environmental Conservation*, *43*(4), 368–375. https://doi.org/10.1017/S0376892916000205

Collins, D. L., Langlois, T. J., Bond, T., Holmes, T. H., Harvey, E. S., Fisher, R., & McLean, D. L. (2017). A novel stereo-video method to investigate fish–habitat relationships. *Methods in Ecology and Evolution*, *8*(1), 116–125. https://doi.org/10.1111/2041-210X.12650

Combs, I. R., Studivan, M. S., Eckert, R. J., & Voss, J. D. (2021). Quantifying impacts of stony coral tissue loss disease on corals in Southeast Florida through surveys and 3D photogrammetry. In *PLoS ONE* (Vol. 16, Issue 6 June). Public Library of Science. https://doi.org/10.1371/journal.pone.0252593

Curley, B. G., Jordan, A. R., Figueira, W. F., & Valenzuela, V. C. (2013). A review of the biology and ecology of key fishes targeted by coastal fisheries in south-east Australia: Identifying critical knowledge gaps required to improve spatial management. In *Reviews in Fish Biology and Fisheries* (Vol. 23, Issue 4, pp. 435–458). https://doi.org/10.1007/s11160-013-9309-7

Davies, A. B., & Asner, G. P. (2014). Advances in animal ecology from 3D-LiDAR ecosystem mapping. In *Trends in Ecology and Evolution* (Vol. 29, Issue 12, pp. 681–691). Elsevier Ltd. https://doi.org/10.1016/j.tree.2014.10.005

Dolan, M. F. J., Grehan, A. J., Guinan, J. C., & Brown, C. (2008). Modelling the local distribution of cold-water corals in relation to bathymetric variables: Adding spatial context to deep-sea video data. *Deep-Sea Research Part I: Oceanographic Research Papers*, *55*(11), 1564–1579. https://doi.org/10.1016/j.dsr.2008.06.010

Dormann, C. F., Elith, J., Bacher, S., Buchmann, C., Carl, G., Carré, G., Marquéz, J. R. G., Gruber, B., Lafourcade, B., Leitão, P. J., Münkemüller, T., Mcclean, C., Osborne, P. E., Reineking, B., Schröder, B., Skidmore, A. K., Zurell, D., & Lautenbach, S. (2013). Collinearity: A review of methods to deal with it and a simulation study evaluating their performance. *Ecography*, *36*(1), 27–46. https://doi.org/10.1111/j.1600-0587.2012.07348.x

Dustan, P., Doherty, O., & Pardede, S. (2013). Digital Reef Rugosity Estimates Coral Reef Habitat Complexity. *PLoS ONE*, *8*(2). https://doi.org/10.1371/journal.pone.0057386

Elith, J., & Leathwick, J. R. (2009). Species distribution models: Ecological explanation and prediction across space and time. *Annual Review of Ecology, Evolution, and Systematics*, *40*, 677–697. https://doi.org/10.1146/annurev.ecolsys.110308.120159

Elvenes, S., Dolan, M. F. J., Buhl-Mortensen, P., & Bellec, V. K. (2014). An evaluation of compiled single-beam bathymetry data as a basis for regional sediment and biotope mapping. *ICES Journal of Marine Science*, *71*(4), 867–881. https://doi.org/10.1093/icesjms/fst154

Ferrari, R., Figueira, W. F., Pratchett, M. S., Boube, T., Adam, A., Kobelkowsky-Vidrio, T., Doo, S. S., Atwood, T. B., & Byrne, M. (2017). 3D photogrammetry quantifies growth and external erosion of individual coral colonies and skeletons. *Scientific Reports*, *7*(1). https://doi.org/10.1038/s41598-017-16408-z

Ferrari, R., Leon, J. X., Davies, A. J., Burns, J. H. R., Sandin, S. A., Figueira, W. F., & Gonzalez-Rivero, M. (2022). Editorial: Advances in 3D Habitat Mapping of Marine Ecosystem Ecology and Conservation. In *Frontiers in Marine Science* (Vol. 8). Frontiers Media S.A. https://doi.org/10.3389/fmars.2021.827430

Ferrari, R., Malcolm, H., Neilson, J., Lucieer, V., Jordan, A., Ingleton, T., Figueira, W., Johnstone, N., & Hill, N. (2018). Integrating distribution models and habitat classification maps into marine protected area planning. *Estuarine, Coastal and Shelf Science*, *212*, 40–50. https://doi.org/10.1016/j.ecss.2018.06.015

Ferrari, R., Marzinelli, E. M., Ayroza, C. R., Jordan, A., Figueira, W. F., Byrne, M., Malcolm, H. A., Williams, S. B., & Steinberg, P. D. (2018). Large-scale assessment of benthic communities

across multiple marine protected areas using an autonomous underwater vehicle. *PLoS ONE*, *13*(3). https://doi.org/10.1371/journal.pone.0193711

Ferrari, R., McKinnon, D., He, H., Smith, R. N., Corke, P., González-Rivero, M., Mumby, P. J., & Upcroft, B. (2016a). Quantifying multiscale habitat structural complexity: A cost-effective framework for underwater 3D modelling. *Remote Sensing*, *8*(2). https://doi.org/10.3390/rs8020113

Ferrari, R., McKinnon, D., He, H., Smith, R. N., Corke, P., González-Rivero, M., Mumby, P. J., & Upcroft, B. (2016b). Quantifying multiscale habitat structural complexity: A cost-effective framework for underwater 3D modelling. *Remote Sensing*, *8*(2). https://doi.org/10.3390/rs8020113

Ferrari, Renata., Malcolm, Hamish. A., Byrne, Maria., Friedman, Ariell., Williams, Stefan. B., Schultz, Arthur., Jordan, Alan. R., & Figueira, Will. F. (2018). Habitat structural complexity metrics improve predictions of fish abundance and distribution. *Ecography*, *41*(7), 1077–1091. https://doi.org/10.1111/ecog.02580

Figueira, W., Ferrari, R., Weatherby, E., Porter, A., Hawes, S., & Byrne, M. (2015). Accuracy and precision of habitat structural complexity metrics derived from underwater photogrammetry. *Remote Sensing*, *7*(12), 16883–16900. https://doi.org/10.3390/rs71215859

Fisher, R., Wilson, S. K., Sin, T. M., Lee, A. C., & Langlois, T. J. (2018). A simple function for full-subsets multiple regression in ecology with R. *Ecology and Evolution*, *8*(12), 6104–6113. https://doi.org/10.1002/ece3.4134

Freckleton, R. P. (2011). Dealing with collinearity in behavioural and ecological data: Model averaging and the problems of measurement error. *Behavioral Ecology and Sociobiology*, *65*(1), 91–101. https://doi.org/10.1007/s00265-010-1045-6

Friedman, A., Pizarro, O., Williams, S. B., & Johnson-Roberson, M. (2012). Multi-Scale Measures of Rugosity, Slope and Aspect from Benthic Stereo Image Reconstructions. *PLoS ONE*, *7*(12). https://doi.org/10.1371/journal.pone.0050440

Friedman, J. H. (2001). Greedy function approximation: A gradient boosting machine. *The Annals of Statistics*, *29*(5), 1189–1232.

Fukunaga, A., Burns, J. H. R., Pascoe, K. H., & Kosaki, K. (2020). Associations between benthic cover and habitat complexity metrics obtained from 3D reconstruction of coral reefs at different resolutions. *Remote Sensing*, *12*(6). https://doi.org/10.3390/rs12061011

Fukunaga, Atsuko., Burns, J. H. R., Craig, B. K., & Kosaki, R. K. (2019). Integrating three-dimensional benthic habitat characterization techniques into ecological monitoring of coral reefs. *Journal of Marine Science and Engineering*, *7*(2). https://doi.org/10.3390/jmse7020027

Fukunaga, Atsuko., & John H. R. Burns. (2020). Metrics of coral reef structural complexity extracted from 3D mesh models and digital elevation models. *Remote Sensing*, *12*(17). https://doi.org/10.3390/RS12172676

Fukunaga, Atsuko., Kosaki, Randall. K., Pascoe, Kailey. H., & Burns, John. H. R. (2020). Fish assemblage structure in the northwestern Hawaiian islands is associated with the architectural complexity of coral-reef habitats. *Diversity*, *12*(11), 1–19. https://doi.org/10.3390/d12110430

Galaiduk, R. (2016). I*ncorporating fish size-classes into species distribution models* [PhD Thesis]. Curtin University.

Galaiduk, R., Radford, B. T., Saunders, B. J., Newman, S. J., & Harvey, E. S. (2017). Characterizing ontogenetic habitat shifts in marine fishes: advancing nascent methods for marine spatial management. In *Source: Ecological Applications* (Vol. 27, Issue 6).

Galparsoro, I., Borja, Á., Bald, J., Liria, P., & Chust, G. (2009). Predicting suitable habitat for the European lobster (Homarus gammarus), on the Basque continental shelf (Bay of Biscay), using Ecological-Niche Factor Analysis. *Ecological Modelling*, *220*(4), 556–567. https://doi.org/10.1016/j.ecolmodel.2008.11.003

Gillanders, B. M. (2002). Connectivity between juvenile and adult fish populations: Do adults remain near their recruitment estuaries? *Marine Ecology Progress Series*, *240*, 215–223. https://doi.org/10.3354/meps240215

Gillanders, B. M., & Kingsford, M. K. (1998). Influence of habitat on abundance and size structure of a large temperate-reef fish, Achoerodus viridis (Pisces: Labridae). *Marine Biology*, *132*, 503–514.

Gonzalez-Mirelis, G., & Buhl-Mortensen, P. (2015). Modelling benthic habitats and biotopes off the coast of Norway to support spatial management. *Ecological Informatics*, *30*, 284–292. https://doi.org/10.1016/j.ecoinf.2015.06.005

González-Rivero, M., Harborne, A. R., Herrera-Reveles, A., Bozec, Y. M., Rogers, A., Friedman, A., Ganase, A., & Hoegh-Guldberg, O. (2017a). Linking fishes to multiple metrics of coral reef structural complexity using three-dimensional technology. *Scientific Reports*, *7*(1). https://doi.org/10.1038/s41598-017-14272-5

González-Rivero, M., Harborne, A. R., Herrera-Reveles, A., Bozec, Y. M., Rogers, A., Friedman, A., Ganase, A., & Hoegh-Guldberg, O. (2017b). Linking fishes to multiple metrics of coral reef structural complexity using three-dimensional technology. *Scientific Reports*, *7*(1). https://doi.org/10.1038/s41598-017-14272-5

Graham, M. H. (2003). Confronting Multicollinearity in Ecological Multiple Regression. *Ecology*, *84*(11), 2809–2815.

Graham, N. A. , & Nash, K. L. (2013). The importance of structural complexity in coral reef ecosystems. *Coral Reefs*, *32*(2), 315–326. https://doi.org/10.1007/s00338-012-0984-y

Gratwicke, A. N. B., & Speight, D. M. R. (2005a). Effects of habitat complexity on Caribbean marine fish assemblages. *Marine Ecology Progress Series*, *292*, 301–310.

Gratwicke, A. N. B., & Speight, D. M. R. (2005b). The relationship between fish species richness, abundance and habitat complexity in a range of shallow tropical marine habitats. *Journal of Fish Biology*, *66*, 650–667. https://doi.org/10.1111/j.1095-8649.2005.00629.x

Gregor, C. A., & Anderson, T. W. (2016). Relative importance of habitat attributes to predation risk in a temperate reef fish. *Environmental Biology of Fishes*, *99*(6–7), 539–556. https://doi.org/10.1007/s10641-016-0496-7

Guinan, J., Grehan, A. J., Dolan, M. F. J., & Brown, C. (2009). Quantifying relationships between video observations of cold-water coral cover and seafloor features in Rockall Trough, west of Ireland. *Marine Ecology Progress Series*, *375*, 125–138. https://doi.org/10.3354/meps07739

Guisan, A., & Thuiller, W. (2005). Predicting species distribution: Offering more than simple habitat models. In *Ecology Letters* (Vol. 8, Issue 9, pp. 993–1009). https://doi.org/10.1111/j.1461-0248.2005.00792.x

Guisan, A., & Zimmermann, N. E. (2000). Predictive habitat distribution models in ecology. In *Ecological Modelling* (Vol. 135). www.elsevier.com/locate/ecolmodel

Harasti, D., Lee, K. A., Gallen, C., Hughes, J. M., & Stewart, J. (2015). Movements, home range and site fidelity of snapper (Chrysophrys auratus) within a temperate marine protected area. *PLoS ONE*, *10*(11). https://doi.org/10.1371/journal.pone.0142454

Harborne, A. R., Mumby, P. J., & Ferrari, R. (2012). The effectiveness of different meso-scale rugosity metrics for predicting intra-habitat variation in coral-reef fish assemblages. *Environmental Biology of Fishes*, *94*(2), 431–442. https://doi.org/10.1007/s10641-011-9956-2

Harborne, A. R., Mumby, P. J., Kennedy, E. v., & Ferrari, R. (2011). Biotic and multi-scale abiotic controls of habitat quality: Their effect on coral-reef fishes. *Marine Ecology Progress Series*, *437*, 201–214. https://doi.org/10.3354/meps09280

Hardinge, J., Harvey, E. S., Saunders, B. J., & Newman, S. J. (2013). A little bait goes a long way: The influence of bait quantity on a temperate fish assemblage sampled using stereo-BRUVs. *Journal of Experimental Marine Biology and Ecology*, *449*, 250–260. https://doi.org/10.1016/j.jembe.2013.09.018

Harman, N., Harvey, E. S., & Kendrick, G. A. (2003). Differences in fish assemblages from different reef habitats at Hamelin Bay, south-western Australia. *Marine and Freshwater Research*, *54*(2), 177–184. https://doi.org/10.1071/MF02040

Harvey, E., Newman, S. J., Mclean, D., Cappo, M., Meeuwig, J., & Skepper, C. L. (2012). Comparison of the relative efficiencies of stereo-BRUVs and traps for sampling tropical continental shelf demersal fishes. *Fisheries Research*, 125-126, 108-120. https://doi.org/10.1016/j.fishres.2012.01.026

Helmholz, P., Long, J., Munsie, T., & Belton, D. (2016). Accuracy assessment of go pro hero 3 (Black) camera in underwater environment. *International Archives of the Photogrammetry, Remote Sensing and Spatial Information Sciences - ISPRS Archives*, *41*, 477–483. https://doi.org/10.5194/isprsarchives-XLI-B5-477-2016

Hill, N. A., Lucieer, V., Barrett, N. S., Anderson, T. J., & Williams, S. B. (2014). Filling the gaps: Predicting the distribution of temperate reef biota using high resolution biological and acoustic data. *Estuarine, Coastal and Shelf Science*, *147*, 137–147. https://doi.org/10.1016/j.ecss.2014.05.019

Hirst, A. J. (2008). Surrogate measures for assessing cryptic faunal biodiversity on macroalgal-dominated subtidal reefs. *Biological Conservation*, *141*(1), 211–220. https://doi.org/10.1016/j.biocon.2007.09.025

Hixon, M. A., & Beets, J. P. (1993). Predation, Prey Refuges, and the Structure of Coral-Reef Fish Assemblages. In *Source: Ecological Monographs* (Vol. 63, Issue 1). http://www.jstor.orgURL:http://www.jstor.org/stable/2937124

Holmes, K. W., van Niel, K. P., Radford, B., Kendrick, G. A., & Grove, S. L. (2008). Modelling distribution of marine benthos from hydroacoustics and underwater video. *Continental Shelf Research*, *28*(14), 1800–1810. https://doi.org/10.1016/j.csr.2008.04.016

Howell, K. L., Holt, R., Endrino, I. P., & Stewart, H. (2011). When the species is also a habitat: Comparing the predictively modelled distributions of *Lophelia pertusa* and the reef habitat it forms. *Biological Conservation*, *144*(11), 2656–2665. https://doi.org/10.1016/j.biocon.2011.07.025

Huang, Z., McArthur, M., Przeslawski, R., Siwabessy, J., Nichol, S., & Brooke, B. (2014). Predictive mapping of soft-bottom benthic biodiversity using a surrogacy approach. *Marine and Freshwater Research*, *65*(5), 409–424. https://doi.org/10.1071/MF13104

Hughes, G. F. (1968). On the mean accuracy of statistical pattern recognizers. *IEEE Trans. Inf. Theory*, *14*, 55–63.

Hurvich, C. M., & Tsai, C.-L. (1989). Regression and time series model selection in small samples. *Biometrika*, *76*(2), 297–307.

Iampietro, P. J., Young, M. A., & Kvitek, R. G. (2008). Multivariate prediction of rockfish habitat suitability in Cordell Bank National Marine sanctuary and Del Monte Shalebeds, California, USA. *Marine Geodesy*, *31*(4), 359–371. https://doi.org/10.1080/01490410802466900

Ierodiaconou, D., Burq, S., Reston, M., & Laurenson, L. (2007). Marine benthic habitat mapping using multibeam data, georeferenced video and image classification techniques in Victoria, Australia. *Journal of Spatial Science*, *52*(1), 93–104. https://doi.org/10.1080/14498596.2007.9635105

Ierodiaconou, D., Monk, J., Rattray, A., Laurenson, L., & Versace, V. L. (2011). Comparison of automated classification techniques for predicting benthic biological communities using hydroacoustics and video observations. *Continental Shelf Research*, *31*(2 SUPPL.). https://doi.org/10.1016/j.csr.2010.01.012

Ierodiaconou, D., Schimel, A. C. G., Kennedy, D., Monk, J., Gaylard, G., Young, M., Diesing, M., & Rattray, A. (2018). Combining pixel and object based image analysis of ultra-high resolution multibeam bathymetry and backscatter for habitat mapping in shallow marine waters. *Marine Geophysical Research*, *39*(1–2), 271–288. https://doi.org/10.1007/s11001-017-9338-z

Jalali, M. A., Ierodiaconou, D., Monk, J., Gorfine, H., & Rattray, A. (2015). Predictive mapping of abalone fishing grounds using remotely-sensed LiDAR and commercial catch data. *Fisheries Research*, *169*, 26–36. https://doi.org/10.1016/j.fishres.2015.04.009

Jennings, S., Boullc2, D. P., & Polunin', N. V. C. (1996). Habitat correlates of the distribution and biomass of Seychelles' reef fishes. In *Environmental Biology of Fishes* (Vol. 46). Kluwer Academic Publishers.

Johnson-Roberson, M., Pizarro, O., Williams, S. B., & Mahon, I. (2010). Generation and visualization of large-scale three-dimensional reconstructions from underwater robotic surveys. *Journal of Field Robotics*, *27*(1), 21–51. https://doi.org/10.1002/rob.20324

Jordan, A., Davies, P., Ingleton, T., Foulsham, E., Neilson, J., & Pritchard, T. (2010). *Seabed habitat mapping of the continental shelf of NSW This report was compiled*. www.environment.nsw.gov.au

Kerry, J. T., & Bellwood, D. R. (2015). The functional role of tabular structures for large reef fishes: avoiding predators or solar irradiance? *Coral Reefs*, *34*(2), 693–702. https://doi.org/10.1007/s00338-015-1275-1

Kingsford, M. J., & Carlson, I. J. (2010). Patterns of distribution and movement of fishes, *Ophthalmolepis lineolata* and *Hypoplectrodes maccullochi*, on temperate rock reefs of southeastern Australia. *Environmental Biology of Fishes*, *88*(2), 105–118. https://doi.org/10.1007/s10641-010-9621-1

Knudby, A., & Ledrew, E. (2007). Measuring Structural Complexity on Coral Reefs. *Proceedings of the American Academy of Underwater Sciences*.

Knudby, A., LeDrew, E., & Brenning, A. (2010). Predictive mapping of reef fish species richness, diversity and biomass in Zanzibar using IKONOS imagery and machine-learning techniques. *Remote Sensing of Environment*, *114*(6), 1230–1241. https://doi.org/10.1016/j.rse.2010.01.007

Knudby, A., LeDrew, E., & Newman, C. (2007). Progress in the use of remote sensing for coral reef biodiversity studies. *Progress in Physical Geography*, *31*(4), 421–434. https://doi.org/10.1177/0309133307081292

Knudby, A., Roelfsema, C., Lyons, M., Phinn, S., & Jupiter, S. (2011). Mapping fish community variables by Integrating field and satellite data, object-based image analysis and modeling in a traditional Fijian fisheries management area. *Remote Sensing*, *3*(3), 460–483. https://doi.org/10.3390/rs3030460

Komyakova, V., Munday, P. L., & Jones, G. P. (2013). Relative importance of coral cover, habitat complexity and diversity in determining the structure of reef fish communities. *PLoS ONE*, *8*(12). https://doi.org/10.1371/journal.pone.0083178

Kuffner, I. B., Brock, J. C., Grober-Dunsmore, R., Bonito, V. E., Hickey, T. D., & Wright, C. W. (2007). Relationships between reef fish communities and remotely sensed rugosity measurements in Biscayne National Park, Florida, USA. *Environmental Biology of Fishes*, *78*(1), 71–82. https://doi.org/10.1007/s10641-006-9078-4

Kunin, W. E. (1998). Extrapolating Species Abundance Across Spatial Scales. In *Source: Science, New Series* (Vol. 281, Issue 5382)

Lazarus, M., & Belmaker, J. (2021). A review of seascape complexity indices and their performance in coral and rock reefs. *Methods in Ecology and Evolution*, *12*(4), 681–695. https://doi.org/10.1111/2041-210X.13557

Leis, J. M., & Hay, A. C. (2004). Larval development of *Achoerodus viridis* (Pisces: Labridae), the Australian eastern blue groper. *Ichthyological Research*, *51*(1), 46–51. https://doi.org/10.1007/s10228-003-0192-4

Lingo, M. E., & Szedlmayer, S. T. (2006). The influence of habitat complexity on reef fish communities in the northeastern Gulf of Mexico. *Environmental Biology of Fishes*, *76*(1), 71–80. https://doi.org/10.1007/s10641-006-9009-4

Lucieer, V., Hill, N. A., Barrett, N. S., & Nichol, S. (2013). Do marine substrates “look” and “sound” the same? Supervised classification of multibeam acoustic data using autonomous underwater vehicle images. *Estuarine, Coastal and Shelf Science*, *117*, 94–106. https://doi.org/10.1016/j.ecss.2012.11.001

Luckhurst, E., & Luckhurst, K. (1978). Analysis of the Influence of Substrate Variables on Coral Reef Fish Communities. In *Marine Biology* (Vol. 49).

Macarthur, R. H., & Macarthur, J. W. (1961). *On Bird Species Diversity* (Vol. 42, Issue 3).

Malcolm, H. A., Jordan, A., & Smith, S. D. A. (2011). Testing a depth-based Habitat Classification System against reef fish assemblage patterns in a subtropical marine park. *Aquatic Conservation: Marine and Freshwater Ecosystems*, *21*(2), 173–185. https://doi.org/10.1002/aqc.1165

Margiotta, A. M., Shervette, V. R., Hadley, N. H., Plante, C. J., & Wilber, D. H. (2016). Species-specific responses of resident crabs to vertical habitat complexity on intertidal oyster reefs. *Journal of Experimental Marine Biology and Ecology*, *477*, 7–13. https://doi.org/10.1016/j.jembe.2016.01.007

Martín-García, L., González-Lorenzo, G., Brito-Izquierdo, I. T., & Barquín-Diez, J. (2013). Use of topographic predictors for macrobenthic community mapping in the Marine Reserve of La Palma (Canary Islands, Spain). *Ecological Modelling*, *263*, 19–31. https://doi.org/10.1016/j.ecolmodel.2013.04.005

McArthur, M. A., Brooke, B. P., Przeslawski, R., Ryan, D. A., Lucieer, V. L., Nichol, S., McCallum, A. W., Mellin, C., Cresswell, I. D., & Radke, L. C. (2010). On the use of abiotic surrogates to describe marine benthic biodiversity. *Estuarine, Coastal and Shelf Science*, *88*(1), 21–32. https://doi.org/10.1016/j.ecss.2010.03.003

Mccormick, M. I. (1994). *Comparison of field methods for measuring surface topography and their associations with a tropical reef fish assemblage* (Vol. 112).

Mellin, C., Andréfouët, S., Kulbicki, M., Dalleau, M., & Vigliola, L. (2009). Remote sensing and fish-habitat relationships in coral reef ecosystems: Review and pathways for multi-scale hierarchical research. *Marine Pollution Bulletin*, *58*(1), 11–19. https://doi.org/10.1016/j.marpolbul.2008.10.010

Mellin, C., Andréfouët, S., & Ponton, D. (2007). Spatial predictability of juvenile fish species richness and abundance in a coral reef environment. *Coral Reefs*, *26*(4), 895–907. https://doi.org/10.1007/s00338-007-0281-3

Mizuno, K., Terayama, K., Hagino, S., Tabeta, S., Sakamoto, S., Ogawa, T., Sugimoto, K., & Fukami, H. (2020). An efficient coral survey method based on a large-scale 3-D structure model obtained by Speedy Sea Scanner and U-Net segmentation. *Scientific Reports*, *10*(1). https://doi.org/10.1038/s41598-020-69400-5

Monfort, T., Cheminée, A., Bianchimani, O., Drap, P., Puzenat, A., & Thibaut, T. (2021a). The Three-Dimensional Structure of Mediterranean Shallow Rock reefs: Use of Photogrammetry-Based Descriptors to Assess Its Influence on Associated Teleost Assemblages. *Frontiers in Marine Science*, *8*. https://doi.org/10.3389/fmars.2021.639309

Monfort, T., Cheminée, A., Bianchimani, O., Drap, P., Puzenat, A., & Thibaut, T. (2021b). The Three-Dimensional Structure of Mediterranean Shallow Rock reefs: Use of Photogrammetry-Based Descriptors to Assess Its Influence on Associated Teleost Assemblages. *Frontiers in Marine Science*, *8*. https://doi.org/10.3389/fmars.2021.639309

Monk, J., Ierodiaconou, D., Bellgrove, A., Harvey, E., & Laurenson, L. (2011). Remotely sensed hydroacoustics and observation data for predicting fish habitat suitability. *Continental Shelf Research*, *31*(2 SUPPL.). https://doi.org/10.1016/j.csr.2010.02.012

Moore, C. H., Harvey, E. S., Van, K. P., Moore, N., Harvey, C. H., Niel, V., Moore, C. H., & Harvey, E. S. (2009). Spatial prediction of demersal fish distributions: enhancing our understanding of species-environment relationships. *ICES Journal of Marine Science*, *66*, 2068–2075. https://academic.oup.com/icesjms/article/66/9/2068/727082

Moore, C. H., Harvey, E. S., & van Niel, K. (2010). The application of predicted habitat models to investigate the spatial ecology of demersal fish assemblages. *Marine Biology*, *157*(12), 2717–2729. https://doi.org/10.1007/s00227-010-1531-4

Moravec, H. P., & Elfes, A. (1985). High resolution maps from wide angle sonar. *Proceedings - IEEE International Conference on Robotics and Automation*, 116–121. https://doi.org/10.1109/ROBOT.1985.1087316

Mumby, P. J., & Wabnitz, C. C. C. (2002). Spatial patterns of aggression, territory size, and harem size in five sympatric Caribbean parrotfish species. In *Environmental Biology of Fishes* (Vol. 63).

Murdoch, W. W., Evans, F. C., & Peterson, C. H. (1972). *Diversity and Pattern in Plants and Insects* (Vol. 53, Issue 5).

Nanami, A., & Nishihira, M. (2002). The structures and dynamics of fish communities in an Okinawan coral reef: effects of coral-based habitat structures at sites with rocky and sandy sea bottoms. In *Environmental Biology of Fishes* (Vol. 63).

Newman, S. P., Meesters, E. H., Dryden, C. S., Williams, S. M., Sanchez, C., Mumby, P. J., & Polunin, N. V. C. (2015). Reef flattening effects on total richness and species responses in the Caribbean. *Journal of Animal Ecology*, *84*(6), 1678–1689. https://doi.org/10.1111/1365-2656.12429

Oakley-Cogan, A., Tebbett, S. B., & Bellwood, D. R. (2020). Habitat zonation on coral reefs: Structural complexity, nutritional resources and herbivorous fish distributions. *PLoS ONE*, *15*(6). https://doi.org/10.1371/journal.pone.0233498

Olinger, L. K., Scott, A. R., McMurray, S. E., & Pawlik, J. R. (2019). Growth estimates of Caribbean reef sponges on a shipwreck using 3D photogrammetry. *Scientific Reports*, *9*(1). https://doi.org/10.1038/s41598-019-54681-2

Parravicini, V., Rovere, A., Donato, M., Morri, C., & Bianchi, C. N. (2006). A method to measure three-dimensional substratum rugosity for ecological studies: an example from the date-mussel fishery desertification in the north-western Mediterranean. In *Journal of the Marine Biological Association of the United Kingdom* (Vol. 86).

Parsons, D. M., Sim-Smith, C., Cryer, M., Francis, M., Hartill, B., Jones, E., le Port, A., Lowe, M., McKenzie, J., Morrison, M., Paul, L., Radford, C., Ross, P., Spong, K., Trnski, T., Usmar, N., Walsh, C., & Zeldis, J. (2014). Snapper (Chrysophrys auratus): A review of life history and key vulnerabilities in New Zealand. In *New Zealand Journal of Marine and Freshwater Research* (Vol. 48, Issue 2, pp. 256–283). Taylor and Francis Ltd. https://doi.org/10.1080/00288330.2014.892013

Pianka, E. R. (1967). On Lizard Species Diversity: North American Flatland Deserts. In *Source: Ecology* (Vol. 48, Issue 3).

Pickens, B. A., Carroll, R., Schirripa, M. J., Forrestal, F., Friedland, K. D., & Taylor, J. C. (2021). A systematic review of spatial habitat associations and modeling of marine fish distribution: A guide to predictors, methods, and knowledge gaps. *PLoS ONE*, *16*(5 May). https://doi.org/10.1371/journal.pone.0251818

Pittman, S. J., & Brown, K. A. (2011). Multi-scale approach for predicting fish species distributions across coral reef seascapes. *PLoS ONE*, *6*(5). https://doi.org/10.1371/journal.pone.0020583

Pittman, S. J., Christensen, J. D., Caldow, C., Menza, C., & Monaco, M. E. (2007). Predictive mapping of fish species richness across shallow-water seascapes in the Caribbean. *Ecological Modelling*, *204*(1–2), 9–21. https://doi.org/10.1016/j.ecolmodel.2006.12.017

Pittman, S. J., Costa, B. M., & Battista, T. A. (2009). Using lidar bathymetry and boosted regression trees to predict the diversity and abundance of fish and corals. *Journal of Coastal Research*, *SPECIAL ISSUE 53*, 27–38. https://doi.org/10.2112/SI53-004.1

Porskamp, P., Rattray, A., Young, M., & Ierodiaconou, D. (2018). Multiscale and hierarchical classification for benthic habitat mapping. Geosciences (Switzerland), 8(4). https://doi.org/10.3390/geosciences8040119

Porter, A. G. (2018). *Habitat structural complexity in the 21st century: measurement, fish responses and why it matters*. University of Sydney.

Price, D. M., Robert, K., Callaway, A., lo Iacono, C., Hall, R. A., & Huvenne, V. A. I. (2019a). Using 3D photogrammetry from ROV video to quantify cold-water coral reef structural complexity

and investigate its influence on biodiversity and community assemblage. *Coral Reefs*, *38*(5), 1007–1021. https://doi.org/10.1007/s00338-019-01827-3

Price, D. M., Robert, K., Callaway, A., lo Iacono, C., Hall, R. A., & Huvenne, V. A. I. (2019b). Using 3D photogrammetry from ROV video to quantify cold-water coral reef structural complexity and investigate its influence on biodiversity and community assemblage. *Coral Reefs*, *38*(5), 1007–1021. https://doi.org/10.1007/s00338-019-01827-3

Purkis, S. J., Graham, N. A. J., & Riegl, B. M. (2008). Predictability of reef fish diversity and abundance using remote sensing data in Diego Garcia (Chagos Archipelago). *Coral Reefs*, *27*(1), 167–178. https://doi.org/10.1007/s00338-007-0306-y

Pygas, D. R., Ferrari, R., & Figueira, W. F. (2020). Review and meta-analysis of the importance of remotely sensed habitat structural complexity in marine ecology. *Estuarine, Coastal and Shelf Science*, *235*. https://doi.org/10.1016/j.ecss.2019.106468

Randlkofer, B., Obermaier, E., Casas, J., & Meiners, T. (2010). Connectivity counts: Disentangling effects of vegetation structure elements on the searching movement of a parasitoid. *Ecological Entomology*, *35*(4), 446–455. https://doi.org/10.1111/j.1365-2311.2010.01200.x

Rattray, A., Ierodiaconou, D., Laurenson, L., Burq, S., & Reston, M. (2009). Hydro-acoustic remote sensing of benthic biological communities on the shallow Southeast Australian continental shelf. *Estuarine, Coastal and Shelf Science*, *84*(2), 237–245. https://doi.org/10.1016/j.ecss.2009.06.023

Redlands, C. (2011). *ArcGIS Desktop: Release 10.* ESRI.

Rees, M. J., Jordan, A., Price, O. F., Coleman, M. A., & Davis, A. R. (2014). Abiotic surrogates for temperate rock reef biodiversity: Implications for marine protected areas. *Diversity and Distributions*, *20*(3), 284–296. https://doi.org/10.1111/ddi.12134

Rees, M. J., Knott, N. A., Hing, M. L., Hammond, M., Williams, J., Neilson, J., Swadling, D. S., & Jordan, A. (2021). Habitat and humans predict the distribution of juvenile and adult snapper (Sparidae: *Chrysophrys auratus*) along Australia's most populated coastline. *Estuarine, Coastal and Shelf Science*, *257*. https://doi.org/10.1016/j.ecss.2021.107397

Rees, M. J., Knott, N. A., Neilson, J., Linklater, M., Osterloh, I., Jordan, A., & Davis, A. R. (2018). Accounting for habitat structural complexity improves the assessment of performance in no-take marine reserves. *Biological Conservation*, *224*, 100–110. https://doi.org/10.1016/j.biocon.2018.04.040

Rengstorf, A. M., Mohn, C., Brown, C., Wisz, M. S., & Grehan, A. J. (2014). Predicting the distribution of deep-sea vulnerable marine ecosystems using high-resolution data: Considerations and novel approaches. *Deep-Sea Research Part I: Oceanographic Research Papers*, *93*, 72–82. https://doi.org/10.1016/j.dsr.2014.07.007

Rengstorf, A. M., Yesson, C., Brown, C., & Grehan, A. J. (2013). High-resolution habitat suitability modelling can improve conservation of vulnerable marine ecosystems in the deep sea. *Journal of Biogeography*, *40*(9), 1702–1714. https://doi.org/10.1111/jbi.12123

Rilov, G., & Benayahu, Y. (2002). Rehabilitation of coral reef-fish communities: the importance of artificial-reef relief to recruitment rates. In *Bulletin of marine science* (Vol. 70, Issue 1).

Rilov, G., & Benayahub, Y. (1998). Vertical Artificial Structures as an Alternative Habitat for Coral Reef Fishes in Disturbed Environments. In *Marine Environmental Research* (Vol. 45, Issue 415).

Rilov, G., Figueira, W. F., Lyman, S. J., & Crowder, L. B. (2007). Complex habitats may not always benefit prey: Linking visual field with reef fish behavior and distribution. *Marine Ecology Progress Series*, *329*, 225–238. https://doi.org/10.3354/meps329225

Risk, M. (1972). Fish Diversity on a Coral Reef in the Virgin Islands. *Atoll Research Bulletin*, *153*, 1–4.

Roberts, Callum. M., & Ormond, Rupert. F. G. (1987). *Habitat complexity and coral reef fish diversity and abundance on Red Sea fringing reefs* (Vol. 41).

Robertson, D. R., & Sheldon, J. M. (1979). Competitive interactions and the availability of sleeping sites for a diurnal coral reef fish. In *mar. Biol. Ecol* (Vol. 40).

Robinson, N. M., Nelson, W. A., Costello, M. J., Sutherland, J. E., & Lundquist, C. J. (2017). A systematic review of marine-based Species Distribution Models (SDMs) with recommendations for best practice. In *Frontiers in Marine Science* (Vol. 4, Issue DEC). Frontiers Media S. A. https://doi.org/10.3389/fmars.2017.00421

Roos, N. C., Carvalho, A. R., Lopes, P. F. M., & Pennino, M. G. (2015). Modeling sensitive parrotfish (Labridae: Scarini) habitats along the Brazilian coast. *Marine Environmental Research*, *110*, 92–100. https://doi.org/10.1016/j.marenvres.2015.08.005

Rosenzweig, M. L., & Winakur, J. (1969). Population Ecology of Desert Rodent Communities: Habitats and Environmental Complexity. In *Source: Ecology* (Vol. 50, Issue 4).

Roth, R. R. (1976). *Spatial Heterogeneity and Bird Species Diversity* (Vol. 57, Issue 4).

Rountree, R. A. (1989). Association of Fishes with Fish Aggregation Devices: Effects of Structure Size on Fish Abundance. *Bulletin of Marine Science*, *44*(2), 960–972.

Russ, G. , R. (1980). Effects of predation by fishes, competition, and structural complexity of the substratum on the establishment of a marine epifaunal community. *Journal of Experimental Marine Biology and Ecology*, *42*, 55–69.

Sale, P. F., & Douglas, W. A. (1984). Temporal Variability in the Community Structure of Fish on Coral Patch Reefs and the Relation of Community Structure to Reef Structure. In *Source: Ecology* (Vol. 65, Issue 2). http://www.jstor.orgURL:http://www.jstor.org/stable/1941404

Sarker, I. H. (2021). Machine Learning: Algorithms, Real-World Applications and Research Directions. In *SN Computer Science* (Vol. 2, Issue 3). Springer. https://doi.org/10.1007/s42979-021-00592-x

Schlacher, T. A., Schlacher-Hoenlinger, M. A., Williams, A., Althaus, F., Hooper, J. N. A., & Kloser, R. (2007). Richness and distribution of sponge megabenthos in continental margin canyons off southeastern Australia. *Marine Ecology Progress Series*, *340*, 73–88.

Semmens, B. X., Brumbaugh, D. R., & Drew, J. A. (2005). Interpreting space use and behavior of blue tang, Acanthurus coeruleus, in the context of habitat, density, and intra-specific interactions. *Environmental Biology of Fishes*, *74*(1), 99–107. https://doi.org/10.1007/s10641-005-6467-z

Storlazzi, C. D., Dartnell, P., Hatcher, G. A., & Gibbs, A. E. (2016). End of the chain? Rugosity and fine-scale bathymetry from existing underwater digital imagery using structure-from-motion (SfM) technology. *Coral Reefs*, *35*(3), 889–894. https://doi.org/10.1007/s00338-016-1462-8

Streit, R. P., Hemingson, C. R., Cumming, G. S., & Bellwood, D. R. (2021). How flexible are habitat specialists? Short-term space use in obligate coral-dwelling damselfishes. *Reviews in Fish Biology and Fisheries*, *31*(2), 381–398. https://doi.org/10.1007/s11160-021-09646-y

Taylor, T., & Figueira, W. F. (2021). Assessing the role of competitive processes in mediating the range expansions of tropical vagrant fish. *Marine Ecology*, *42*(2). https://doi.org/10.1111/maec.12644

Tokeshi, M., & Arakaki, S. (2012). Habitat complexity in aquatic systems: Fractals and beyond. In *Hydrobiologia* (Vol. 685, Issue 1, pp. 27–47). https://doi.org/10.1007/s10750-011-0832-z

Urbina-Barreto, I., Chiroleu, F., Pinel, R., Fréchon, L., Mahamadaly, V., Elise, S., Kulbicki, M., Quod, J. P., Dutrieux, E., Garnier, R., Henrich Bruggemann, J., Penin, L., & Adjeroud, M. (2021). Quantifying the shelter capacity of coral reefs using photogrammetric 3D modeling: From colonies to reefscapes. *Ecological Indicators*, *121*. https://doi.org/10.1016/j.ecolind.2020.107151

Verdonck, T., Baesens, B., Óskarsdóttir, M., & vanden Broucke, S. (2021). Special issue on feature engineering editorial. In *Machine Learning*. Springer. https://doi.org/10.1007/s10994-021-06042-2

Walbridge, S., Slocum, N., Pobuda, M., & Esri, D. J. W. (2018). *Unified Geomorphological Analysis Workflows with Benthic Terrain Modeler*. https://doi.org/10.6084/m9.figshare.5946463

Walker, B. K., Jordan, L. K. B., & Spieler, R. E. (2009). Relationship of reef fish assemblages and topographic complexity on southeastern Florida coral reef habitats. *Journal of Coastal Research*, *SPECIAL ISSUE 53*, 39–48. https://doi.org/10.2112/SI53-005.1

Ward, T. J., Vanderklift, M. A., Nicholls, A. O., & Kenchington, R. A. (1999). Selecting Marine Reserves Using Habitats And Species Assemblages As Surrogates For Biological Diversity. In *Ecological Applications* (Vol. 9, Issue 2).

Watson, D. L., Harvey, E. S., Kendrick, G. A., Nardi, K., & Anderson, M. J. (2007). Protection from fishing alters the species composition of fish assemblages in a temperate-tropical transition zone. *Marine Biology*, *152*(5), 1197–1206. https://doi.org/10.1007/s00227-007-0767-0

Wedding, L. M., & Friedlander, A. (2008). Determining the influence of seascape structure on coral reef fishes in Hawaii using a geospatial approach. *Marine Geodesy*, *31*(4), 246–266. https://doi.org/10.1080/01490410802466504

Wedding, L. M., Friedlander, A. M., McGranaghan, M., Yost, R. S., & Monaco, M. E. (2008). Using bathymetric lidar to define nearshore benthic habitat complexity: Implications for management of reef fish assemblages in Hawaii. *Remote Sensing of Environment*, *112*(11), 4159–4165. https://doi.org/10.1016/j.rse.2008.01.025

Welsford, D. C., Jordan, A. R., & Smolenski, A. J. (2004). Description and genetic identification of the early life-stages of *Notolabrus fucicola* and N. tetricus from Tasmanian waters, Australia, with notes on their newly-settled juveniles. *New Zealand Journal of Marine and Freshwater Research*, *38*(2), 267–277. https://doi.org/10.1080/00288330.2004.9517236

Wilhelmsson, D., Malm, T., & Öhman, M. C. (2006). The influence of offshore windpower on demersal fish. *ICES Journal of Marine Science*, *63*(5), 775–784. https://doi.org/10.1016/j.icesjms.2006.02.001

Wilhelmsson, D., Yahya, S. A. S., & Öhman, M. C. (2006). Effects of high-relief structures on cold temperate fish assemblages: A field experiment. *Marine Biology Research*, *2*(2), 136–147. https://doi.org/10.1080/17451000600684359

Wilhelmsson, Dan., Öhman, Marcus. C., Ståhl, Henrik., & Shlesinger, Yechiam. (1998). *Artificial Reefs and Dive Tourism in Eilat, Israel* (Vol. 27, Issue 8).

Williams, J., Jordan, A., Harasti, D., Davies, P., & Ingleton, T. (2019). Taking a deeper look: Quantifying the differences in fish assemblages between shallow and mesophotic temperate rock reefs. *PLoS ONE*, *14*(3). https://doi.org/10.1371/journal.pone.0206778

Williams, S. B., Pizarro, O. R., Jakuba, M. v., Johnson, C. R., Barrett, N. S., Babcock, R. C., Kendrick, G. A., Steinberg, P. D., Heyward, A. J., Doherty, P. J., Mahon, I., Johnson-Roberson, M., Steinberg, D., & Friedman, A. (2012). Monitoring of benthic reference sites: Using an autonomous underwater vehicle. *IEEE Robotics and Automation Magazine*, *19*(1), 73–84. https://doi.org/10.1109/MRA.2011.2181772

Wilson, M. F. J., O'Connell, B., Brown, C., Guinan, J. C., & Grehan, A. J. (2019). Integrating three-dimensional benthic habitat characterization techniques into ecological monitoring of coral reefs. *Journal of Marine Science and Engineering*, *7*(2). https://doi.org/10.3390/jmse7020027

Wilson, M., O'Connell, B., & Brown, C. (2007a). Multiscale terrain analysis of multibeam bathymetry data for habitat mapping on the continental slope. *Marine Geodesy*, *30*(1–2), 3–35. https://doi.org/10.1080/01490410701295962

Wilson, S. K., Graham, N. A. J., & Polunin, N. V. C. (2007b). Appraisal of visual assessments of habitat complexity and benthic composition on coral reefs. *Marine Biology*, *151*(3), 1069–1076. https://doi.org/10.1007/s00227-006-0538-3

Wines SL, Young MA, Zavalas R, Logan JM, Tinkler P, Ierodiaconou D (2020) Accounting for spatial scale and temporal variation in fish-habitat analyses using baited remote underwater video stations (BRUVS). Mar Ecol Prog Ser 640:171-187. https://doi.org/10.3354/meps13292

Wood, S. N. (2011). Fast stable restricted maximum likelihood and marginal likelihood estimation of semiparametric generalized linear models. *Journal of the Royal Statistical Society. Series B (Statistical Methodology)*, *73*(1), 3–36. https://www.jstor.org/stable/41057423?seq=1&cid=pdf-

Woodby, D., Carlile, D., & Hulbert, L. (2009). Predictive modeling of coral distribution in the central Aleutian Islands, USA. *Marine Ecology Progress Series*, *397*, 227–240. https://doi.org/10.3354/meps08358

Young, M. A., Iampietro, P. J., Kvitek, R. G., & Garza, C. D. (2010). Multivariate bathymetry-derived generalized linear model accurately predicts rockfish distribution on Cordell Bank, California, USA. *Marine Ecology Progress Series*, *415*, 247–261. https://doi.org/10.3354/meps08760

Young, M. A., Ierodiaconou, D., Edmunds, M., Hulands, L., & Schimel, A. C. G. (2016). Accounting for habitat and seafloor structure characteristics on southern rock lobster (Jasus edwardsii) assessment in a small marine reserve. *Marine Biology*, *163*(6). https://doi.org/10.1007/s00227-016-2914-y

Zavalas, R., Ierodiaconou Daniel, D., Ryan, D., Rattray, A., & Monk, J. (2014). Habitat classification of temperate marine macroalgal communities using bathymetric LiDAR. *Remote Sensing*, *6*(3), 2154–2175. https://doi.org/10.3390/rs6032154